

93

IMPLEMENTING A 50x50 GRAVITY FIELD MODEL IN AN ORBIT DETERMINATION SYSTEM

by

Daniel John Fonte, Jr.

B.S. Astronautical Engineering
United States Air Force Academy
(1991)

SUBMITTED TO THE DEPARTMENT OF
AERONAUTICS AND ASTRONAUTICS IN PARTIAL
FULFILLMENT OF THE REQUIREMENTS FOR THE
DEGREE OF

MASTER OF SCIENCE

at the

MASSACHUSETTS INSTITUTE OF TECHNOLOGY

June 1993

© Daniel John Fonte, Jr.

Signature of Author _____
Department of Aeronautics and Astronautics
June 1993

Certified by _____
Dr. Ronald J. Proulx
Thesis Supervisor, CSDL

Certified by _____
Dr. Paul J. Cefola
Thesis Supervisor, CSDL
Lecturer, Department of Aeronautics and Astronautics

Accepted by _____
Professor Harold Y. Wachman
Chairman, Departmental Graduate Committee

IMPLEMENTING A 50x50 GRAVITY FIELD MODEL IN AN ORBIT DETERMINATION SYSTEM

by

Daniel John Fonte, Jr.

Submitted to the Department of Aeronautics and Astronautics
on May 7, 1993 in partial fulfillment of the
requirements for the Degree of Master of Science

ABSTRACT

The Kepler problem treats the earth as if it is a spherical body of uniform density. In actuality, the earth's shape deviates from a sphere in terms of latitude (described by zonal harmonics), longitude (sectorial harmonics), and combinations of both latitude and longitude (tesseral harmonics). Operational Orbit Determination (OD) systems in the 1960's focused on the effects of the first few zonal harmonics since (1) they represented the dominant terms of the geopotential perturbation, (2) they were well known, and (3) the use of a limited number of harmonics greatly simplified the perturbation theory used. The demand for increasingly accurate modeling of a satellite's motion, combined with an increase in knowledge of the geopotential and an advancement in computer technology, led to the inclusion of tesseral harmonics. The Draper Laboratory version of the Goddard Trajectory Determination System (R&D GTDS), one operational OD system, can currently implement up to a 21x21 gravity field model in its Cowell and Semianalytic Satellite Theory (SST) orbit generators. This thesis investigates the extension of R&D GTDS to include a 50x50 gravity field model in the Cowell and SST orbit generators. This extension would require code modifications in the following environments to support the various operational versions of R&D GTDS: IBM, VAX, Sun Workstation, and Silicon Graphics. In each of these environments, the Legendre polynomials, associated Legendre polynomials, Jacobi polynomials, Hansen coefficients, and harmonic coefficients must be investigated to determine if (1) overflow/underflow boundaries would be violated in computations or (2) a loss of accuracy would occur in computations of high degree and order. This investigation will determine whether normalized or un-normalized components of the potential must be used.

Thesis Supervisor: Dr. Ronald J. Proulx
Title: Technical Staff Engineer, The Charles Stark Draper Laboratory, Inc.

Thesis Supervisor: Dr. Paul J. Cefola
Title: Lecturer, Department of Aeronautics and Astronautics
Program Manager, The Charles Stark Draper Laboratory, Inc.

[This page intentionally left blank.]

Acknowledgements

My thanks is extended to many: Paul Cefola, for (1) ensuring I got here and (2) ensuring I got out of here. You taught me about space programs and how to always look at things from a positive perspective. Wayne McClain, for teaching me astrodynamics and about business life, in general. You were always willing to lend a hand and to lead me out of the land of the lost and confused. Ron Proulx, for being my partner in the trenches of GTDS. You gave me numerous tips concerning the handling of large software systems. David Carter, Rick Metzinger, Mark Slutsky, Moshe Cohen, and Jay Portnoy, your discussions on all topics ranging from GTDS, estimation, mathematics, physics, propulsion, to thesis preparation all added to the knowledge I captured here. Linda Leonard, for keeping the VAX raring to go. Roger Medeiros, for your generous support as group leader. John Sweeney and Joan Chiffer, for giving me the opportunity and handling countless administrative issues. My friends at Draper, you all know first hand what this is about. Keith Mertz, Diane Kim, and Hermann Rufenacht, for contributing to my knowledge about space systems. Dick Farrar, for providing TRACE results. Girish Patel (NASA GSFC) and Carl Wagner (NOAA), for sending the gravity models. Lee Myers (CSC), for updates to GTDS databases and TRAMP related discussions. My family, Stacey, and God, for unlimited support and encouragement.

This thesis was prepared at The Charles Stark Draper Laboratory, Inc., with support from the Canadian Space Agency and Spar Aerospace Limited under Spar Aerospace Purchase Order 302163 and the RADARSAT Flight Dynamics Program (Contract S.700067).

Publication of this thesis does not constitute approval by The Charles Stark Draper Laboratory, Inc., or the Massachusetts Institute of Technology of the findings or conclusions contained herein. It is published for the exchange and stimulation of ideas.

I hereby assign my copyright of this thesis to The Charles Stark Draper Laboratory, Inc., Cambridge, Massachusetts.

—
Daniel John Fonte, Jr., Lt., USAF

Permission is hereby granted by The Charles Stark Draper Laboratory, Inc., to the Massachusetts Institute of Technology to reproduce any or all of this thesis.

[This page intentionally left blank.]

Contents

Chapter 1 Introduction	19
1.1 Background.....	19
1.2 Thesis Overview	29
Chapter 2 Mathematical Techniques	32
2.1 Non-Spherical Earth Gravitational Attraction.....	32
2.1.1 Geopotential and Spherical Harmonics.....	33
2.1.2 Zonal Harmonics (order $m = 0$).....	48
2.1.3 Tesseral Harmonics (order $m \neq 0$).....	57
2.2 Perturbation Techniques.....	62
2.2.1 Cowell Mathematical Techniques	65
2.2.2 Variation of Parameters (VOP).....	68
2.2.2.1 Lagrange's VOP Equations	75
2.2.2.2 Gauss' VOP Equations	78
2.2.3 Implementation of VOP Formulations with Numerical Methods.....	82
2.3 Semianalytic Methods	82
2.3.1 Semianalytic Equations of Motion and the Generalized Method of Averaging	83
2.3.2 Semianalytic Propagators and Orbit Determination	96
Chapter 3 Stability Testing	99
3.1 Background.....	99
3.2 Cowell Truth Model Description and Test Set-Up	101

3.3	Cowell Testing for 50x50 Fields.....	105
3.4	Stability Testing for Semianalytic Theory.....	109
3.4.1	Jacobi Polynomial Stability Testing	110
3.4.2	Hansen Coefficient Stability Testing	117
Chapter 4	Draper R&D GTDS Description.....	125
4.1	Chapter Introduction.....	125
4.1.1	GTDS Overview	125
4.1.2	GTDS Developmental History	128
4.2	R&D GTDS Functionality Associated to Gravity Modeling.....	132
4.2.1	Numerical Theories.....	133
4.2.2	Analytical Theories	134
4.2.3	Semianalytical Theory.....	134
4.2.4	Gravity-Related Input Processing.....	140
4.2.5	Gravity-Related Database Maintenance.....	145
4.3	Code Related Changes for 50x50 Gravity Field Models.....	148
4.3.1	WRITHARM Replacement, DANWHARM.FOR.....	151
4.3.2	Changes Shared by Cowell and Semianalytic Theory.....	160
4.3.2.1	HRMCF.CMN	160
4.3.2.2	GEOVAR.CMN.....	165
4.3.2.3	LEGPOL.CMN.....	168
4.3.2.4	FRCBD.FOR	168
4.3.2.5	SETDAF.FOR.....	169
4.3.2.6	Harmonic Coefficient READ Logic	169
4.3.2.7	LUMPCS.CMN.....	172
4.3.2.8	CSBLNK.CMN.....	173

4.3.3	Changes Unique to the Semianalytic Theory (SST).....	175
4.3.3.1	ANAV1.CMN.....	176
4.3.3.2	AVEPOT.CMN.....	178
4.3.3.3	GRAVITY.CMN.....	179
4.3.3.4	MDWRK.CMN.....	180
4.3.3.5	NUKES.CMN.....	181
4.3.3.6	PTSDAT.CMN.....	182
4.3.3.7	SPREAL.CMN.....	183
4.3.3.8	SPZONB.CMN.....	187
4.3.3.9	TESS.CMN.....	190
4.3.3.10	TSRES.CMN.....	192
4.3.4	Summary of Modifications to GTDS.....	193
4.3.5	Modifications to "Original" GTDS.....	208
Chapter 5	50x50 Gravity Field Model Results.....	211
5.1	Chapter Introduction.....	211
5.2	Validation of Report Function.....	213
5.3	Unit Testing of Cowell Accelerations.....	215
5.4	Testing of the Cowell Orbit Generator.....	219
5.5	Testing of Cowell Differential Correction.....	225
5.6	Testing of the Semianalytic Orbit Generator.....	228
5.7	Impact of 50x50 Gravity Models in Orbit Determination.....	235
Chapter 6	Conclusions / Future Work.....	243
6.1	Summary.....	243
6.2	Conclusions.....	246
6.3	Future Work.....	246

Appendix A Element Sets	251
A.1 Background.....	251
A.2 Classical Orbital Elements.....	251
A.3 Equinoctial Element Set	255
Appendix B HWIRE Listing.....	257
B.1 Description.....	257
Appendix C Output Plots.....	281
C.1 Description.....	281
Appendix D Additional Software Tree Plots.....	297
D.1 Background.....	297
Appendix E Software Tools	303
E.1 Background.....	303
References	305

List of Figures

Figure 2.1	Zonal Harmonics / Equipotential Surfaces	52
Figure 2.2	Zonal Harmonics.....	53
Figure 2.3	Nodal Regression	54
Figure 2.4	Apsidal Line Precession.....	54
Figure 2.5	Sectorial Harmonics	61
Figure 2.6	Tesseral Harmonics.....	61
Figure 4.1	Tree Structure of GTDS Developmental History.....	129
Figure 4.2	Routines Associated to the Averaged Orbit Generator.....	136
Figure 4.3	Routines Associated to the Short-Periodic Orbit Generator.....	137
Figure 4.4	J ₂ /M-Daily Coupling Short Periodic (SPJ2MD) Software Tree.....	138
Figure 4.5	Tesseral M-Daily Short Periodic (SPMDLY) Software Tree	138
Figure 4.6	Tesseral Linear Combination Short Periodic (SPTCESS) Software Tree.....	139
Figure 4.7	Zonal Short Periodic (SPZONL) Software Tree	139
Figure 4.8	Zonal Short Periodic Software Tree for Routines Under ZONGEN.....	140
Figure 4.9	Sample GTDS Card Deck to Fit Semianalytic Theory to Cowell Theory.....	142
Figure 4.10	EARTHFLD_GEM10B_21BY21_NORREC.DAT	147
Figure 4.11	CHANGES CMS Library.....	149
Figure 4.12	Form for Original File Containing GEMT3 Class Harmonic Coefficients	154
Figure 4.13	GCSU2.FOR Code Diagram	154
Figure 4.14	DANWHARM.FOR Code Diagram.....	156
Figure 4.15	OUTPUT_TEXT_GEMT3_50BY50.DAT - Before Execution	157
Figure 4.16	OUTPUT_TEXT_GEMT3_50BY50.DAT - After Execution	158

Figure 4.17	DATA_STATEMENTS_GEMT3_50BY50.DAT.....	159
Figure 4.18	CS Replacement Example.....	164
Figure 4.19	"Old" Harmonic Coefficient READ Logic	170
Figure 4.20	New Harmonic Coefficient READ Statement.....	171
Figure 4.21	Blank Common, Version 1	173
Figure 4.22	Blank Common, Version 2	173
Figure 4.23	ANAV1 Definition	176
Figure 4.24	GRAVITY Variables.....	180
Figure 4.25	NUKESBD.FOR, Original GTDS.....	182
Figure 4.26	NUKES.CMN, Modified GTDS	182
Figure 4.27	DIMENSION Statements for SPREAL	185
Figure 4.28	SPZONB in Original GTDS	187
Figure 5.1	Directory System for Testing	213
Figure 5.2	Sample Input Deck to Validate Report Function THEISIS_REPORT.GTDS.....	214
Figure 5.3	Standard Cowell Input Deck Format LANDSAT 4.....	215
Figure 5.4	GTDS/TRACE Input Deck Format GEMT3 Harmonic Coefficients	221
Figure 5.5	Radial Error Between TRACE and GTDS 11 Day Arc, Cowell 50x50 GEMT3.....	223
Figure 5.6	Cross-Track Error Between TRACE and GTDS 11 Day Arc, Cowell 50x50 GEMT3.....	224
Figure 5.7	Along-Track Error Between TRACE and GTDS 11 Day Arc, Cowell 50x50 GEMT3.....	225
Figure 5.8	Standard Cowell Differential Correction Input Deck Format RADARSAT	226

Figure 5.9	50x50 GEMT3 Cowell Differential Correction First Three Days.....	227
Figure 5.10	50x50 GEMT3 Cowell Differential Correction Last Two Days	227
Figure 5.11	Standard Semianalytic Input Deck Format LANDSAT 4.....	228
Figure 5.12	GTDS Card Deck to Fit Semianalytic Theory to Cowell Theory 50x50 GEMT3	233
Figure 5.13	Two Day 50x50 GEMT3 Fit of Semianalytic Theory to Cowell Theory.....	234
Figure 5.14	Two Day 21x21 GEMT3 Fit of Semianalytic Theory to Cowell Theory, Un-Modified Old GTDS.....	234
Figure 5.15	Two Day 21x21 GEMT3 Fit of Semianalytic Theory to Cowell Theory, Modified Old GTDS.....	234
Figure 5.16	200 Day Fit of 21x21 GEMT3 AOG to 50x50 GEMT3 AOG.....	237
Figure 5.17	200 Day GEMT3 Fit of 21x21 AOG to 50x50 AOG	238
Figure A.1	Classical Orbital Elements.....	253
Figure C.1	Recap of Figure 5.17	281
Figure D.1	Software Tree for Routines Under ECSUM1	297
Figure D.2	Software Tree for Routines Under ECSUM2	298
Figure D.3	Software Tree for Routines Under ECSUM3	298
Figure D.4	Software Tree for Routines Under SNGESM.....	299
Figure D.5	Software Tree for Routines Under TERM.....	299
Figure D.6	Software Tree for Routines Under EVESM1.....	300
Figure D.7	Software Tree for Routines Under EVESM2.....	300
Figure D.8	Software Tree for Routines Under ODESM1.....	301
Figure D.9	Software Tree for Routines Under ODESM2.....	301

[This page intentionally left blank.]

List of Tables

Table 1.1	Harmonic Conditions.....	21
Table 1.2	Maximum M-Daily Errors.....	24
Table 1.3	Tesseral Harmonic Effects Beyond 21x21 Fields.....	27
Table 1.4	Current Numerical Boundaries for Computer Systems.....	28
Table 2.1	Inclination Function Values.....	40
Table 2.2	Eccentricity Function Values.....	41
Table 2.3	Normalized GEMT3 Zonal Harmonic Coefficient Values.....	50
Table 3.1	Un-Normalized Polynomial Validation GTDS vs. Lundberg Truth.....	103
Table 3.2	Initial Condition Summary.....	104
Table 3.3	Cowell Acceleration Validation GTDS vs. Lundberg Truth (21x21 GEM10B).....	104
Table 3.4	Un-Normalized Polynomial Validation GTDS Emulation vs. Actual GTDS.....	107
Table 3.5	Cowell Acceleration Validation GTDS Emulation vs. Actual GTDS (21x21 GEM10B).....	107
Table 3.6	Un-Normalized Polynomial Validation GTDS Emulation vs. Lundberg Truth.....	108
Table 3.7	Cowell Acceleration Validation GTDS Emulation vs. Lundberg Truth (50x50 GEMT3).....	108
Table 3.8	Maximum Jacobi Polynomial Relative Errors	114
Table 3.9	Jacobi Polynomial Relative Error Distribution.....	115
Table 3.10	Jacobi Polynomials for Maximum Relative Errors.....	116
Table 3.11	Maximum Hansen Coefficient Relative Errors	121

Table 3.12	Hansen Coefficients for Maximum Relative Errors.....	121
Table 3.13	Hansen Coefficients with the Minimum Number of Significant Digits of Decimal Accuracy.....	122
Table 4.1	Analytical Theories in GTDS Associated to the Gravity Model	134
Table 4.2	Earth Gravity Models, Original GTDS NEW_EARTHFLD.DAT	145
Table 4.3	Additional Earth Gravity Models, Modified GTDS DAN_POTENTIAL.DAT.....	146
Table 4.4	Distribution of Bytes for FRN 8	151
Table 4.5	Distribution of Bytes for FRN 47	152
Table 4.6	ANAV1 Variables.....	177
Table 4.7	AVEPOT Variables	178
Table 4.8	MDWRK Variables.....	180
Table 4.9	PTSDAT Variables.....	182
Table 4.10	SPREAL Variables.....	184
Table 4.11	SPZONB Variables.....	188
Table 4.12	TESS Variables.....	190
Table 4.13	TSRES Variables.....	192
Table 4.14	Summary of Modifications to Original GTDS.....	193
Table 4.15	Summary of New Routines Added to GTDS.....	204
Table 4.16	Summary of Actions to Increase Limits of Gravity Field Model Beyond 50x50.....	207
Table 5.1	Cowell Acceleration Validation New GTDS vs. Lundberg Truth (21x21 GEM10B).....	216
Table 5.2	Cowell Acceleration Validation New GTDS vs. Lundberg Truth (21x21 GEMT3)	217

Table 5.3	Cowell Acceleration Validation New GTDS vs. Lundberg Truth (25x25 GEMT3)	217
Table 5.4	Cowell Acceleration Validation New GTDS vs. Lundberg Truth (30x30 GEMT3)	217
Table 5.5	Cowell Acceleration Validation New GTDS vs. Lundberg Truth (50x50 GEMT3)	218
Table 5.6	Cowell Orbit Generator Validation Old GTDS vs. New GTDS (21x21 GEM10B).....	219
Table 5.7	Cowell Orbit Generator Validation Old GTDS vs. New GTDS (21x21 GEMT3)	220
Table 5.8	Semianalytic Orbit Generator Validation Old GTDS vs. New GTDS (2x0 GEMT3)	229
Table 5.9	Semianalytic Orbit Generator Validation Old GTDS vs. New GTDS (21x0 GEMT3).....	230
Table 5.10	Semianalytic Orbit Generator Validation Old GTDS vs. New GTDS (2x2 GEMT3)	230
Table 5.11	Semianalytic Orbit Generator Validation Old GTDS vs. New GTDS (8x8 GEMT3)	230
Table 5.12	Semianalytic Orbit Generator Validation Un-Modified Old GTDS vs. New GTDS (21x21 GEMT3).....	231
Table 5.13	Semianalytic Orbit Generator Validation Modified Old GTDS vs. New GTDS (21x21 GEMT3).....	231
Table A.1	Keplerian Elements	253
Table A.2	Semimajor Axis and Eccentricity Ranges for Orbits	254
Table A.3	Equinoctial Elements.....	256
Table E.1	Software Tools Developed For Thesis	303

[This page intentionally left blank.]

Chapter 1

Introduction

1.1 Background

The Kepler problem treats the earth as if it is a spherical body with uniform density. Even though this treatment serves to provide an adequate approximation or "first guess" of a satellite's motion, the contributions of perturbations have been neglected. The major perturbations which cause a satellite to deviate from Kepler motion are the non-spherical gravitational effects of the earth, atmospheric drag, solar radiation pressure, third-body gravitational effects, and thrust. Dominant among these perturbations for near-earth satellites are the non-spherical earth contributions. In actuality, the earth is not spherical and does not possess an uniform distribution of density as is assumed in the Kepler problem. These irregularities contribute secular, long-period, and short-period variations to a satellite's motion. Secular variations imply that an element would either increase or decrease monotonically from initial values. On the other hand, periodic variations produce element values which oscillate about the initial element values; long-period variations arise due to the presence of sinusoidal terms with arguments containing the slowly varying elements, while short-period variations arise from sinusoidal terms with the fast element in the argument. The following expression is an hypothetical example of how each of these variations add up to the total variance in an element, c [22]:

$$c = c_0 + c_{\text{sec}} t + A \sin(\omega) + B \cos(M + \omega) \quad (1.1)$$

where t is time, A and B are coefficients, ω is the argument of perigee (the slow variable) and M is the mean anomaly (the fast variable). The first term is the initial condition; the second term is the secular variation; and the third and fourth terms are the long-period and short-period variations, respectively. Note that short-period variations can arise from sinusoidal terms of linear combinations of both fast elements and slowly varying elements. Again, it only matters that the fast element is present.

The geopotential, the potential function derived to model the effects of the non-spherical earth, describes deviations from two-body symmetry in terms of latitude (described by zonal harmonics), longitude (sectorial harmonics), and combinations of both latitude and longitude (tesseral harmonics). One common form of the geopotential involves spherical harmonics [26]:

$$\psi = -\frac{\mu}{r} \left[1 + \sum_{n=2}^{\infty} \sum_{m=0}^n \left(\frac{R_e}{r} \right)^n P_{n,m}(\sin \phi) (C_{n,m} \cos m\lambda + S_{n,m} \sin m\lambda) \right] \quad (1.2)$$

where

μ is the gravitational parameter

R_e is the mean equatorial radius of the earth

r is the distance of the satellite from the origin of the coordinate system
reference frame

$P_{n,m}(x)$ is an associated Legendre polynomial of degree n , order m , and
argument x

ϕ is the satellite's latitude measured relative to the coordinate system
reference frame

$C_{n,m}$, $S_{n,m}$ are the spherical harmonic coefficients which are determined
empirically for a given body

λ the body-fixed longitude of the satellite (measured positive eastward from the Greenwich Meridian)

The zonal harmonics, sectorial harmonics, and tesseral harmonics imbedded within this expression can be identified with the conditions established in Table 1.1:

Table 1.1 Harmonic Conditions

Zonal Harmonics	Sectorial Harmonics	Tesseral Harmonics
$m = 0$	$n = m$	$n \neq m$
	$m \neq 0$	$m \neq 0$

Orbit Determination (OD) systems in the 1960's used truncated versions of this potential which incorporated only the first few zonal harmonics. A geopotential representation of this form was used for several reasons: (1) this "zonal" form of the potential represented a greatly simplified version of the "full" potential; (2) the zonal harmonics represented the dominant contributions of the non-spherical earth perturbation; hence, this form would capture the dominant contributions to the motion; and (3) limited empirical data was available for the harmonic coefficients; therefore, "full" potential representations would have insufficient data for complete implementation.

In order to understand the first reason entirely, the distinction between general and special perturbation techniques needs to be explained. Initially, two methods were available to account for the effects of perturbations--special and general perturbation techniques. Special perturbation methods deal with a direct numerical integration of the equations of motion to include the perturbing accelerations [2]. For example, Cowell methods augment the two-body equation of motion with the various perturbing accelerations. Integration of

this augmented equation of motion produces a satellite's velocity and position--a velocity and position which account for the various perturbations acting on the satellite. Chapter 2 will describe Cowell Methods and their use in an orbit determination (OD) system.

Special perturbation techniques are not limited solely to the propagation of position and velocity vectors. The Lagrangian and Gaussian VOP equations provide sets of expressions which determine how the orbital elements are affected by the various perturbations. The orbital element rates of change resulting from the VOP equations can be integrated over a desired time period in a special perturbation fashion to determine updated orbital elements which have been corrected for the applicable perturbations. Wright [65] presents an high precision application of VOP for definitive geocentric orbits.

With special perturbation techniques, multiple time steps and force evaluations are needed to "step" from a given set of initial conditions to a final solution which "describes" a satellite's motion throughout an orbit. If the initial conditions are changed or altered, new evaluations must be made at each of the various time steps. Therefore, each solution is unique to a given set of initial conditions. For applications in which a large amount of satellite ephemerides must be determined, special perturbation techniques have the potential to consume large amounts of precious computation time in order to step through all of the various orbits. In addition, small time steps are needed to accurately model a satellite's motion. Generally, the time step for integration is 1/5 to 1/10 of the smallest wavelength included in the dynamics which, for short-period contributions, can be restrictive. The increased number of steps which accompany these small time steps add to round-off and truncation error, as well as serving to further increase the computation time of special perturbation techniques. To summarize, special perturbation techniques provide a classic trade-off between computation time and result accuracy.

General perturbation techniques, on the other hand, do not use multiple time steps to transfer from a set of initial conditions to a final solution. Rather, general perturbation techniques provide analytical formulae which are used to predict a satellite's motion usually with the aid of series approximations to model the effects of the various perturbations. A set of specified initial conditions can be inserted into the analytic expressions to directly determine the perturbed motion of the satellite. If the motion of a new (different) satellite is to be determined, the corresponding initial conditions are inserted into the analytic expressions to compute results; multiple time steps are not needed each time the motion of a new (different) satellite is to be determined. For this reason, general perturbation techniques are computationally more efficient than special perturbation techniques. However, it classically has been difficult and time consuming to derive the closed form analytic expressions characteristic of general perturbation techniques. Furthermore, the length of the closed form expressions (if they can be determined) can potentially strain the storage requirements or computation time of the computer involved. As a result, truncated or simplified models have been used, which serve to degrade the accuracy of the results.

Since special perturbation techniques were computationally demanding, computer technology was not as advanced in the early 1960's as it is today, and few early space missions were dedicated to expanding the knowledge of the harmonic coefficients, initial OD systems were based upon general perturbation techniques. These techniques, which were designed to achieve the maximum computational efficiency with moderate prediction accuracy [1], incorporated the use of simplified "zonal" forms of the potential. What resulted were OD systems that were operational, but of limited accuracy due to the simplifying assumptions inherent in the general perturbation methods. The Simplified General Perturbation (SGP) theory utilized by NORAD is one such OD system. This system was optimized for low-eccentricity and non-equatorial orbits [29]. The theory includes the zonal harmonics J_2 and J_3 , secular and long-periodic terms truncated to the

square of the eccentricity $O(e^2)$, and a few selected short-period terms from the Aeronutronic Complete First-Order General Perturbations theory (AGP; SGP is a truncated form of AGP).

As time progressed, an increase in knowledge of the potential was accompanied by an increase in computer technology and an expanded knowledge of the harmonic coefficients. Faster computers with larger storage capacities permitted the numerical integration required by special perturbation techniques. By the late 1960's, OD systems began to incorporate tesseral harmonics of low degree and order with the use of special perturbation techniques. For low-altitude satellites, it was shown that short-period tesseral harmonics terms contribute errors in the 100-200 m range for degree and order up to three [12]. Tesseral m-dailies, which result as a special case of the tesseral harmonics, were shown to produce the following additional effects on low-altitude satellites for low degree and order combinations [12]:

Table 1.2 Maximum M-Daily Errors

Harmonic	Radial (m)	Cross-Track (m)	In-Track (m)
J _{2,2}	---	260	790
J _{3,1}	300	---	600
J _{3,2}	65	---	130
J _{3,3}	75	---	150
J _{4,1}	---	225	590
J _{4,2}	---	90	270
J _{4,3}	---	75	210
J _{4,4}	---	40	100

Obviously, the effects of tesseral harmonics were proven to be significant and in need of consideration. Gaposchkin [25] and Cefola [9] confirm that 8x8 and 16x16 gravity field models (zonal and tesseral harmonics through degree and order 8 and 16) became widely used in orbit determination algorithms.

Knowledge of the potential continued to increase, particularly of the effects contributed by higher degree zonal and tesseral harmonic terms. To summarize [12], it was found that higher degree zonal terms (J_6 through J_{18}) could cause positional errors on the order of 500 m or 1000 m after just 10 revolutions of a 16 rev/day satellite. Tesseral resonance terms, additional special case terms stemming from the tesseral harmonics, could also contribute errors of this size. Therefore, work in the 1970's expanded OD systems to include 21x21 class gravity field models.

In a similar fashion, the knowledge of harmonic coefficients increased. As was stated earlier in this chapter, limited empirical data was available for the harmonic coefficients in the 1960's. This limited amount of data can be accredited to a lack of technical knowledge and resources dedicated to study the earth's gravitational force. From the 1970's through the 1990's, resources were dedicated and technology was developed in an attempt to refine the harmonic coefficients, which are determined through an analysis of large numbers of diverse types of observations. From these observations, large numerical systems of equations are built, permitting a simultaneous solution of several thousand unknowns (depending on the desired number of coefficients) [35,37]. Classically, the observations were collected from satellite tracking data. More recently, however, the observations have been collected from combinations of satellite tracking, satellite altimeter, and surface gravimetric data.

As the size of gravity fields increased, it was noticed that values for the harmonic coefficients become smaller in magnitude with increasing degree and order. In order to avoid ill-conditioned values for computation purposes, normalized coefficients became readily available. These normalized coefficients, when combined with other normalized components of the potential, produce results which are consistent with analogous un-normalized values. Of particular interest are the harmonic coefficients of the Goddard Earth Model (GEM) T3 generation. The collection of normalized coefficients in these models are complete through degree and order 50.

This thesis focuses on updating Draper Laboratory's version of the Goddard Trajectory Determination System (R&D GTDS) to implement 50x50 gravity field models in its Cowell and Semianalytic Satellite Theory (SST) orbit generators. This modification would greatly improve R&D GTDS's capability to model the effects of the non-spherical earth perturbation upon a satellite's motion. The motivation to provide this expanded field stems from specific accuracy goals established for space applications. For example, a scientific mission may be designed to observe the surface wind and wave structure over the oceans [62]. A mission of this type would require very accurate knowledge of the satellite's position. It is also important to consider satellites which are in low altitude, repeat-groundtrack type orbits. Satellites of this type encounter significant tesseral harmonic effects for degree and order combinations beyond the 21x21 field capability. Studies for ERS-1 show the following contributions of over 5 meters [62] (refer to table at top of next page):

Table 1.3 Tesseral Harmonic Effects Beyond 21x21 Fields

n	m	Radial (m)	Cross-Track (m)	Along-Track (m)
23	15	0.2	1.0	9.4
30	29	0.3	1.5	23.4
34	29	0.1	0.4	5.5
36	29	0.1	0.3	5.4
43	43	0.2	1.2	200.2
44	43	1.8	0.1	7.7
45	43	0.4	1.9	319.2

The values for the order m represented in this table indicate tesseral resonance contributions in that they are approximate multiples of the $14 \frac{1}{3}$ rev/day rate for ERS-1 (more detail on tesseral resonance will be given in Chapter 2). The 50x50 gravity field model would capture these effects and, therefore, be useful in meeting accuracy goals.

In addition, the more exacting results stemming from the 50x50 gravity field model would serve to ensure that the dominant error source in an orbit determination system would not stem from the non-spherical earth perturbation. In this manner, theory is driven to be more accurate than observations, which enhances the differential correction process. Other advantages of using larger gravity field models can be studied with the addition of this capability to the software.

Inherent in the task of expanding the gravity field model is determining the stability of various components of the potential that are utilized for computational purposes within R&D GTDS. In the Cowell orbit generator, the Legendre polynomials, associated

Legendre polynomials, and harmonic coefficients must be analyzed. When investigating terms of the potential beyond the current, un-normalized 21x21 field capability, values for the polynomials are quite large, while values for the coefficients are small. Therefore, a study must be undertaken to determine if the magnitudes of these coefficients, polynomials, or products of the coefficients and polynomials would violate the overflow and underflow boundaries of the computer. Similarly, the harmonic coefficients, Hansen coefficients, and Jacobi polynomials must be investigated in the SST orbit generator. If the machine boundaries are exceeded, than a switch to normalized components is in order.

Currently, Draper Laboratory's version of GTDS is available in FORTRAN source code for IBM Mainframes, VAX Stations, Sun Workstations, and Silicon Graphics Workstations. The present approximate numerical boundaries for these computer systems are compared in Table 1.4 (information taken from references 42 and 46):

Table 1.4 Current Numerical Boundaries for Computer Systems

System	Underflow Boundary	Overflow Boundary
IBM	10^{-77}	10^{+77}
VAX -- REAL*4	10^{-38}	10^{+38}
VAX -- D-Floating	10^{-38}	10^{+38}
VAX -- G-Floating	10^{-308}	10^{+308}
VAX -- Q-Floating	10^{-4932}	10^{+4932}
Sun Workstation	10^{-308}	10^{+308}
Silicon Graphics	10^{-308}	10^{+308}

where the values in this table represent REAL*8 (double precision) variables with the exception of the Q-Floating option on the VAX (REAL*16--double precision) and the VAX

REAL*4 entry. The difference between REAL*4 and REAL*8 (D-floating implementation) on the VAX is the number of decimal digits in the degree of precision; the REAL*4 option typically has 7 decimal digits, while the REAL*8 (D-floating) option typically has 16 decimal digits [46]. The G-Floating compiler option (11 bit exponent) extends the dynamical range of default double precision (REAL*8, D-Floating) variables (8 bit exponent) on the VAX.

1.2 Thesis Overview

Chapter 2 examines the mathematical principles pertinent to this thesis. Specifically, a general discussion of the non-spherical earth perturbation is given, followed by a description of perturbation techniques, Cowell methods, and SST methods. Derivations for the potential in terms of spherical harmonics, Keplerian elements, and singularity-free equinoctial elements are presented. In addition, the specific effects of zonal and tesseral harmonics are given. The chapter also derives a generic form for the VOP equations, with specific details added for the Lagrangian and Gaussian forms. The generalized method of averaging is described.

Chapter 3 describes stability testing of the necessary components of the potential for the expanded gravity field. This chapter lists the formulae used in R&D GTDS to compute the Legendre polynomials, associated Legendre polynomials, Jacobi polynomials, and Hansen coefficients. Results of stability testing are given, to include comparisons with "truth" values.

Chapter 4 explains the code architecture of R&D GTDS which stems from the mathematical techniques given in Chapter 2, as well as the various modifications that were needed in

order to expand the gravity field model. Flow diagrams are presented where applicable. Details of the structured code modification process are given. Functionality affected by the code modifications are outlined. An explanation of applicable input card decks is presented. A description of the evolution of GTDS from the Goddard Space Flight Center to Draper Laboratory is given, with a focus on the capabilities added at Draper Laboratory.

Chapter 5 outlines the verification testing that was undertaken to ensure that the modifications were correctly implemented and describes the impact of 50 x 50 gravity field models in orbit determination.

Chapter 6 gives a summary, conclusions, and suggestions for further research.

Appendix A describes Keplerian and equinoctial elements.

Appendix B lists the code for HWIRE.FOR, a subroutine which sets options for the averaged equations of motion and short periodics. This listing was provided so that a point of reference would be available when the results of testing for the Semianalytic orbit generator are described in Chapter 5.

Appendix C depicts radial error, cross track error, along track error, element history, and element difference plots for test runs established to analyze the impact of 50x50 gravity field models in orbit determination. These output plots correspond to testing described in Chapter 5.

Appendix D depicts software tree plots for routines associated to the zonal short periodic model associated to the Semianalytical Theory in GTDS. These plots augment other plots given in Chapter 4.

Appendix E lists the various software tools that were developed as part of this thesis.

Chapter 2

Mathematical Techniques

2.1 Non-Spherical Earth Gravitational Attraction

Newton formulated the law of gravity by stating that any two point masses attract one another with a force (magnitude) proportional to the product of their masses and inversely proportional to the square of the distance between them [2]:

$$F_g = \frac{G M m}{d^2} \quad \text{or} \quad F_g = - \frac{G M m}{r^2} \frac{\mathbf{r}}{r} \quad (2.1)$$

where M and m represent the point masses, G is the universal gravitational constant (6.670×10^{-8} dyne cm^2/gm^2), and d (r) is the magnitude of the distance between the two masses (\mathbf{r} is vector distance). Restricting this equation to point masses allows treatment of the mass of the bodies as if it was concentrated at the center of the bodies. However, when considering the effects of perturbations on an earth satellite's orbit, the mass of the bodies can no longer be treated in this fashion. In actuality, the earth is not a spherically symmetric body but is bulged at the equator, flattened at the poles and is generally asymmetric [2]. This irregular distribution of mass leads to the most dominant perturbation on a near-earth satellite--the perturbation which stems from forces arising from the earth's gravity field. Section 2.1 will analyze the central-body gravitational perturbation. First, mathematical expressions for the non-spherical gravitational perturbation will be given, followed by a discussion of spherical harmonics. Then, the specific perturbative effects of

both zonal harmonics and tesseral harmonics will be discussed. Section 2.2 will discuss perturbation techniques, with an emphasis on Cowell and Variation of Parameter methods. Section 2.3 will highlight semianalytic methods, to include a discussion on the generalized method of averaging.

2.1.1 Geopotential and Spherical Harmonics

Kreyszig [32] states that the gradient operator, ∇ , can be used to transform some scalar functions into vector fields.

$$\nabla = \frac{\partial}{\partial x} \hat{i} + \frac{\partial}{\partial y} \hat{j} + \frac{\partial}{\partial z} \hat{k} \quad (2.2)$$

A scalar function which can be transformed to a vector field via the gradient operator is referred to as a potential function or the potential of the corresponding vector field. A gravity field is one such vector field that can be derived as the (negative) gradient of a gravity potential function. If a body exists in this gravity field (i.e., a satellite), it will experience a force due to gravity. A vector field, such as a gravity field, can be thought of as an acceleration; a mass coupled with this acceleration produces a force. Mathematically, this gravitational field can be expressed in the following manner:

$$\text{Field}_{\text{gravity}} = \frac{\mathbf{F}_{\text{grav}}}{m} = - \nabla V(x,y,z) \quad (2.3)$$

where V is the gravity potential function which, for the earth, is referred to as the geopotential. McClain [39] states that the particular form of this gravity potential function associated with the gravitational force exerted by the attracting body depends on the mass

distribution of that body. Several theorems from calculus can be used to derive the geopotential.

The flux through an area a_j is defined in the following manner:

$$\phi = \text{Field}_j \cdot a_j \quad (2.4)$$

where Field_j is the magnitude of the vector field in that area. The total flux through a surface comprised of all areas a_j is, then:

$$\phi_{\text{total}} = \int_{\text{entire surface}} \text{Field} \cdot da \quad (2.5)$$

If the mass of one of the bodies (m) is divided out of both sides of Newton's expression for the force of gravity in (2.1), an expression for the gravity field results (remember, the gravity field can be thought of as an acceleration):

$$\text{Field}_{\text{gravity}} = -\frac{GM}{r^2} \frac{\mathbf{r}}{r} \quad (2.6)$$

in which $-\frac{GM}{r^2}$ is the magnitude and $\frac{\mathbf{r}}{r}$ is the direction of the gravity field. If the surface of interest is considered to be a sphere (with area $4\pi r^2$), then the expression for total gravity flux through this surface can be expressed as:

$$\phi_{\text{total gravity}} = \int_{\text{entire surface}} \text{Field}_{\text{gravity}} \cdot da = -\frac{GM}{r^2} \cdot 4\pi r^2 = -4\pi GM \quad (2.7)$$

The mass of the large, attracting body (M--for example, the earth) can be re-expressed as a summation of mass densities per unit volume at specific points within the mass body, $\rho(x,y,z)$:

$$M = \int \rho(x,y,z) dv = \int \rho dv \quad (2.8)$$

where the function of x, y, and z will be left off for notational convenience. Substituting (2.8) into (2.7) provides an alternative expression for the total gravity flux through the surface of interest:

$$\Phi_{\text{total gravity}} = \int \text{Field}_{\text{gravity}} \cdot da = - \int 4\pi G \rho dv \quad (2.9)$$

This expression can be simplified through the use of Gauss' divergence theorem:

$$\int \text{Field} \cdot da = \int (\nabla \cdot \text{Field}) dv \quad (2.10)$$

where $\nabla \cdot$ is the divergence, defined for a vector F with x, y, and z components as:

$$\nabla \cdot = \frac{\partial F_x}{\partial x} + \frac{\partial F_y}{\partial y} + \frac{\partial F_z}{\partial z} \quad (2.11)$$

by which a vector is transformed into a scalar.

With the use of Gauss' divergence theorem, equation (2.9) can now be re-expressed:

$$\Phi_{\text{total gravity}} = \int (\nabla \cdot \text{Field}) dv = - \int 4\pi G \rho dv \quad (2.12)$$

As stated in equation (2.3), the gravity field is the gradient of the gravity potential function (with a negative sign added by definition):

$$\text{Field}_{\text{gravity}} = - \nabla V(x,y,z) \quad (2.13)$$

Substituting (2.13) into (2.12), as well as canceling the minus signs, leads to the following relationship:

$$\int \nabla^2 V(x,y,z) \cdot dv = \int 4\pi G \rho dv \quad (2.14)$$

The expression in (2.14) implies that the potential function must satisfy Poisson's equation:

$$\nabla^2 V(x,y,z) = 4\pi G \rho(x,y,z) \quad (2.15)$$

At all points outside the attracting body, the density per unit volume vanishes, and (2.15) reduces to Laplace's equation:

$$\nabla^2 V(x,y,z) = 0 \quad (2.16)$$

The general solution to (2.16) yields the geopotential for the gravitational force exerted on a satellite of mass m at the position (x,y,z) by an attracting body of arbitrary mass, M . Specifying appropriate boundary conditions to this general solution leads to the solution for a given mass configuration within the attracting body. McClain [39] uses the separation of variables technique to arrive at the geopotential (which will be referred to as ψ in order to differentiate it from some general potential function, V):

$$\psi = -\frac{\mu}{r} \sum_{n=0}^{\infty} \sum_{m=0}^n G_{n,m} \quad (2.17)$$

where

$$G_{n,m} = \left(\frac{R_e}{r}\right)^n P_{n,m}(\sin \phi) (C_{n,m} \cos m\lambda + S_{n,m} \sin m\lambda) \quad (2.18)$$

and

μ is the gravitational parameter

R_e is the mean equatorial radius of the earth

r is the distance of the satellite from the origin of the coordinate system

reference frame

$P_{n,m}(x)$ is an associated Legendre polynomial of degree n , order m , and

argument x

ϕ is the satellite's latitude measured relative to the same coordinate system

reference frame of r

$C_{n,m}, S_{n,m}$ are the spherical harmonic coefficients which are determined

empirically for a given body

λ the body-fixed longitude of the satellite (measured positive eastward from

the Greenwich Meridian)

The term $\psi_{0,0}$ corresponds to the two-body potential, and can be derived from the equation governing two body motion:

$$\ddot{\mathbf{r}} = -\frac{\mu}{r^2} \frac{\mathbf{r}}{r} \quad (2.19)$$

in which $-\frac{\mu}{r^2}$ is the magnitude of the two-body acceleration with direction $\frac{\mathbf{r}}{r}$. As stated earlier in this chapter, a vector field (which can be thought of as an acceleration) is the (negative) gradient of a potential. Therefore, if this two-body acceleration is integrated (with the inclusion of the negative sign), the two-body potential is found:

$$V_{0,0} = - \int -\frac{\mu}{r^2} dr = -\frac{\mu}{r} \quad (2.20)$$

McClain [39] states that if the origin of the coordinate system is placed at the center of mass of the attracting body, then the following can be proved:

$$\psi_{1,0} = 0 \quad (2.21)$$

$$\psi_{1,1} = 0$$

which leads to an alternate form for the geopotential:

$$\psi = -\frac{\mu}{r} \left[1 + \sum_{n=2}^{\infty} \sum_{m=0}^n \left(\frac{R_e}{r}\right)^n P_{n,m}(\sin \phi) (C_{n,m} \cos m\lambda + S_{n,m} \sin m\lambda) \right] \quad (2.22)$$

It should be noted that this derivation is not solely limited to spherical surfaces as was assumed in (2.7); Purcell [52] extends a similar derivation for the flux of an electric field to all surfaces and obtains the same result as for spherical surfaces. By analogy, this gravitational derivation can be extended to all surfaces.

The terms $P_{n,m}(\sin \phi) K \begin{pmatrix} \cos \\ \sin \end{pmatrix} m\lambda$ are called spherical harmonics of degree n and order m , where K represents the particular spherical harmonic coefficient $C_{n,m}$ or $S_{n,m}$. These spherical harmonics are used to describe the variation of the actual, pear-shaped earth from the spherically symmetric earth of the two-body problem. The indices n and m are used to differentiate between zonal harmonics ($m = 0$), sectorial harmonics ($n = m, m \neq 0$), and tesseral harmonics ($n \neq m, m \neq 0$). The specific perturbative effects of both zonal and tesseral harmonics will be discussed in the following sections (the sectorial harmonics are a subset of the tesseral harmonics and will not be discussed independently); however, it is first desirable to convert the spherical harmonic form of the potential given in (2.22) to a form expressed in orbital elements. This conversion is useful if Variation of Parameter (VOP) equations are used to describe the motion in the non spherical gravity field, as in semianalytic theory. This formulation requires the partial derivatives of the potential with respect to the orbital elements. In the subsequent paragraphs, this conversion will be analyzed for two different sets of elements: Keplerian and equinoctial.

For Keplerian elements, the latitude (ϕ) and longitude (λ) are first converted to the argument of latitude ($u = \omega + f$, where f is the true anomaly), inclination (i), longitude of the ascending node (Ω), and Greenwich hour angle (θ , the angle measured westwardly in the equatorial plane from Greenwich to the Vernal Equinox). This conversion corresponds to a rotation of the spherical harmonics from the geocentric-equatorial frame to the geocentric-orbital frame (in which the \hat{x} axis points towards perigee and the orbit plane is the "equatorial" plane after the rotation). Specifically, this conversion consists of the following three rotations: (1) the \hat{x} axis is rotated through the ascending node Ω , (2) the plane is rotated about the line of nodes through the inclination (to the orbital plane), and (3) the resulting axis, \hat{x}' , is rotated in the orbital plane through the argument of perigee ω .

Due to the complicated nature of these rotations, Kaula [31] takes a brute force approach to transforming the spherical harmonics. He substitutes expressions for the latitude and longitude in terms of the orbital elements and expands. One such expression, the inclination function, is determined in the following fashion [31]:

$$F_{nmp}(i) = \sum_t \frac{(2n-2t)!}{t! (n-t)! (n-m-2t)! 2^{2n-2t}} \sin^{n-m-2t} i \times \sum_{s=0}^m \binom{m}{s} \cos^s i \sum_c \binom{n-m-2t+s}{c} \binom{m-s}{p-t-c} (-1)^{c-k} \quad (2.23)$$

where k is the integer part of $(n-m)/2$, t is summed from 0 to the lesser of p or k , and c is summed over all values making the binomial coefficients non zero.

Since this expression is quite involved, Kaula recommends its use solely for computer algorithms. For hand calculations, he presents several values for this function--a few of which are listed in Table 2.1 [31]:

Table 2.1 Inclination Function Values

n	m	p	$F_{nmp}(i)$
2	0	0	$\frac{-3 \sin^2 i}{8}$
2	0	1	$\frac{3 \sin^2 i}{4} - \frac{1}{2}$
2	0	2	$\frac{-3 \sin^2 i}{8}$
2	1	0	$\frac{3 \sin i (1 + \cos i)}{4}$

where p is the inclination function index.

Second, the position (r) and the true anomaly (f) are replaced with the semi-major axis (a), mean anomaly (M), and the eccentricity (e). This replacement facilitates a simple

relationship with the time and the isolation of terms which contribute to resonance. However, it does require the introduction of the eccentricity function, $G_{npq}(e)$ [31]:

$$G_{np(2p-n)}(e) = \frac{1}{(1-e^2)^{n-(1/2)}} \sum_{d=0}^{p'-1} \binom{n-1}{2d+n-2p'} \binom{2d+n-2p'}{d} \left(\frac{e}{2}\right)^{2d+n-2p'} \quad (2.24)$$

in which

$$\begin{aligned} p' &= p & \text{for } p \leq n/2 \\ p' &= n-p & \text{for } p \geq n/2 \end{aligned} \quad (2.25)$$

The analogous expression for short period terms $(n-2p+q) \neq 0$ is much more difficult and can be found in Kaula. Table 2.2 [31] lists a few representative values for the eccentricity function:

Table 2.2 Eccentricity Function Values

n	p	q	$G_{npq}(e)$
2	0	0	$1 - \frac{5e^2}{2} + \frac{13e^4}{16} + \dots$
2	0	1	$\frac{7e}{2} - \frac{123e^3}{16} + \dots$
2	0	-1	$-\frac{e}{2} + \frac{e^3}{16} + \dots$
3	2	1	$e(1-e^2)^{-5/2}$

where q is the eccentricity function index.

The final form for the potential in terms of the Keplerian elements is given in classical form by Kaula [31]:

$$\Psi = \frac{\mu}{a} \sum_{n=2}^N \left(\frac{R_e}{a}\right)^n \sum_{m=0}^n \sum_{p=0}^n F_{n,m,p} (i) \sum_{q=-\infty}^{\infty} G_{n,p,q} (e) S_{n,m,p,q} (\omega, M, \Omega, \theta) \quad (2.26)$$

where

$$S_{n,m,p,q} = C_{n,m} \cos [(n - 2p)\omega + (n - 2p + q)M + m(\Omega - \theta)] \\ + S_{n,m} \sin [(n - 2p)\omega + (n - 2p + q)M + m(\Omega - \theta)] \quad (2.27)$$

for $(n - m)$ even, and

$$S_{n,m,p,q} = -S_{n,m} \cos [(n - 2p)\omega + (n - 2p + q)M + m(\Omega - \theta)] \\ + C_{n,m} \sin [(n - 2p)\omega + (n - 2p + q)M + m(\Omega - \theta)] \quad (2.28)$$

for $(n - m)$ odd.

When using the Keplerian form of the gravitational potential in the Variation of Parameters equations of motion, singularity problems arise for small eccentricities and small and near-180 degree inclinations. These singularity conditions cause rapid oscillation in either the longitude of the ascending node or the argument of perigee [5]. For this reason, efforts were directed to develop a non-singular formulation for the gravitational potential. One such singularity-free formulation, which is expressed in terms of equinoctial elements, can be found in the work of Cefola [7]. Cefola's derivation starts with an expression for the disturbing potential in terms of radial distance, latitude, and longitude relative to an earth-fixed frame (i.e., geocentric equatorial). This disturbing function is derived by taking the negative of the potential function given by (2.22) and removing the two body contribution μ/r :

$$U = \frac{\mu}{r} \sum_{n=2}^{\infty} \sum_{m=0}^n \left(\frac{R_e}{r} \right)^n P_{n,m}(\sin \phi) (C_{n,m} \cos m\lambda + S_{n,m} \sin m\lambda) \quad (2.29)$$

which can be re-expressed in complex form for a particular degree and order pair through the use of Euler identities:

$$U_{n,m}^* = \frac{\mu}{r} \left(\frac{R_e}{r} \right)^n C_{n,m}^* P_{n,m}(\sin \phi) \exp^{jm\lambda} \quad (2.30)$$

in which $C_{n,m}^*$ is defined in the following manner:

$$C_{n,m}^* = C_{n,m} - j S_{n,m} \quad (2.31)$$

such that

$$U_{n,m} = \text{Real} \{ U_{n,m}^* \} \quad (2.32)$$

where aforementioned definitions apply and j is the imaginary unit variable. If the longitude is expressed as the difference between the inertial right ascension and the Greenwich Hour Angle:

$$\lambda = \alpha - \theta \quad (2.33)$$

equation (2.30) can be re-written in the following manner:

$$U_{n,m}^* = \frac{\mu}{r} \left(\frac{R_e}{r} \right)^n C_{n,m}^* \exp^{-jm\theta} P_{n,m}(\sin \phi) \exp^{jm\alpha} \quad (2.34)$$

Next, it is desirable to perform a rotational transformation of the spherical harmonics present in equations (2.29) through (2.34) to the equinoctial orbital frame (Courant and Hilbert [17] provide the details of this rotation). The first step of this transformation re-expresses the spherical harmonics in terms of a Fourier sum of functions of the equinoctial elements p and q and the true longitude (L):

$$P_{n,m}(\sin \phi) \exp^{jm\alpha} = \sum_{r=-n}^n \frac{(n-r)!}{(n-m)!} P_{n,r}(0) S_{2n}^{(m,r)}(p,q) \exp^{jrL} \quad (2.35)$$

in which $P_{n,r}(0)$ is an associated Legendre function of argument zero [39]:

$$P_{n,r}(0) = (-1)^{(n-r)/2} \frac{(n+r)!}{2^n \left(\frac{n+r}{2}\right)! \left(\frac{n-r}{2}\right)!} \quad (2.36)$$

and for $m \geq 0$:

$$S_{2n}^{(m,r)}(p,q) = (1+p^2+q^2)^r (p-jq)^{m-r} P_{n+r}^{(m-r, -m-r)}(\gamma) \quad (2.37)$$

$r \leq -m$

$$S_{2n}^{(m,r)}(p,q) = \frac{(n+m)! (n-m)!}{(n+r)! (n-r)!} (1+p^2+q^2)^{-m} (p-jq)^{m-r} P_{n-m}^{(m-r, r+m)}(\gamma) \quad (2.38)$$

$-m \leq r \leq +m$

$$S_{2n}^{(m,r)}(p,q) = (-1)^{m-r} (1+p^2+q^2)^{-r} (p+jq)^{r-m} P_{n-r}^{(r-m, r+m)}(\gamma) \quad (2.39)$$

$r \geq m$

where $P_n^{a,b}$ are the well known Jacobi polynomials [39]

$$P_n^{a,b}(\gamma) = \frac{\Gamma(a+n+1)}{n! \Gamma(a+b+n+1)} \sum_{m=0}^n \binom{n}{m} \frac{\Gamma(a+b+n+m+1)}{2^m \Gamma(a+m+1)} (\gamma-1)^m \quad (2.40)$$

of argument γ :

$$\gamma = \frac{1-p^2-q^2}{1+p^2+q^2} = \cos i \quad (2.41)$$

If (2.35) is substituted into (2.34), the following expression results:

$$U_{n,m}^* = \frac{\mu}{r} \left(\frac{R_e}{r}\right)^n C_{n,m}^* \exp^{-jm\theta} \sum_{s=-n}^n \frac{(n-s)!}{(n-m)!} P_{n,s}(0) S_{2n}^{(m,s)}(p,q) \exp^{jsL} \quad (2.42)$$

which can be re-arranged to produce:

$$U_{n,m}^* = \frac{\mu}{a} \left(\frac{R_e}{a}\right)^n C_{n,m}^* \exp^{-jm\theta} \sum_{s=-n}^n V_{n,s}^m S_{2n}^{(m,s)}(p,q) \left(\frac{a}{r}\right)^{n+1} \exp^{jsL} \quad (2.43)$$

if the following definition is made:

$$V_{n,s}^m = \frac{(n-s)!}{(n-m)!} P_{n,s}(0) \quad (2.44)$$

This definition allows the analogous relationship between Kaula's inclination function and the "S" function to be presented [66]:

$$F_{nmp}(i) = V_{n,(n-2p)}^m S_{2n}^{(m,n-2p)}\left(0, \tan\left(\frac{i}{2}\right)\right) \quad (2.45)$$

for (n-m) even, and

$$F_{nmp}(i) = j V_{n,(n-2p)}^m S_{2n}^{(m,n-2p)}\left(0, \tan\left(\frac{i}{2}\right)\right) \quad (2.46)$$

for (n-m) odd.

Next, the product $\left(\frac{r}{a}\right)^n \exp^{jsL}$ can be re-expressed in terms of a Fourier series of functions of the equinoctial elements h, k , and the mean longitude (λ):

$$\left(\frac{r}{a}\right)^n \exp^{jsL} = \sum_{t=-\infty}^{+\infty} Y_t^{n,s} \exp^{jt\lambda} \quad (2.47)$$

This relationship between (2.43) and (2.47) may not be evident without explanation; the key lies in the indices. With the correct implementation of indices

$$\left(\frac{a}{r}\right)^{n''+1} = \left(\frac{r}{a}\right)^n, \text{ if } n = -n''-1 \quad (2.48)$$

It should also be noted that (2.47) contains both L and λ , which are defined in the following manner:

$$\lambda = M + \omega + \Omega \quad (2.49)$$

$$L = f + \omega + \Omega \quad (2.50)$$

which can be inserted into (2.47):

$$\left(\frac{r}{a}\right)^n \exp^{jsf} = \sum_{t=-\infty}^{+\infty} Y_t^{n,s} \exp^{[j(t-s)(\omega + \Omega)]} \exp^{jtM} \quad (2.51)$$

Cefola points out that the left hand side of (2.51) is the generating function for the Hansen Coefficients:

$$\left(\frac{r}{a}\right)^n \exp^{jsf} = \sum_{t=-\infty}^{+\infty} X_t^{n,s} \exp^{jtM} \quad (2.52)$$

Therefore

$$\sum_{t=-\infty}^{+\infty} X_t^{n,s} \exp^{jtM} = \sum_{t=-\infty}^{+\infty} Y_t^{n,s} \exp^{j(t-s)(\omega+\Omega)} \exp^{jtM} \quad (2.53)$$

or, equivalently:

$$\sum_{t=-\infty}^{+\infty} X_t^{n,s} = \sum_{t=-\infty}^{+\infty} Y_t^{n,s} \exp^{j(t-s)(\omega+\Omega)} \quad (2.54)$$

which provides an expression for $Y_t^{n,s}$ in terms of the Hansen coefficients, $X_t^{n,s}$:

$$Y_t^{n,s} = X_t^{n,s} \exp^{j(s-t)(\omega+\Omega)} \quad (2.55)$$

where the Hansen coefficients are functions of rational numbers and the orbital eccentricity ($e^2 = h^2 + k^2$). The Newcomb-Poincare power series representation for the Hansen coefficients takes the following form:

$$X_t^{n,s} = e^{|t-s|} \sum_{i=0}^{\infty} X_{i+a,i+b}^{n,s} e^{2i} \quad (2.56)$$

This expression can be factored into a form which offers much better convergence for high eccentricity cases with no penalty for low eccentricity cases [48]:

$$X_t^{n,s} = (1 - e^2)^{n+3/2} e^{|t-s|} \sum_{i=0}^{\infty} Y_{i+a,i+b}^{n,s} e^{2i} \quad (2.57)$$

where

$$\begin{aligned} a &= \frac{|t-s| + (t-s)}{2} \\ b &= \frac{|t-s| - (t-s)}{2} \end{aligned} \quad (2.58)$$

Substituting either (2.56) or (2.57) into (2.55) provides the solution for the $Y_t^{n,s}$ terms, which are referred to as modified Hansen coefficients in terms of equinoctial variables. The $X_{i+a,i+b}^{n,s}$ and $Y_{i+a,i+b}^{n,s}$ terms are coefficients which result from the Newcomb operator (for simplicity, these terms will hereafter be referred to as Newcomb operators). Recursions for these Newcomb operators can be found in the work of McClain and Proulx [39,48]. It is interesting to note is that the Hansen coefficients *are* Kaula's eccentricity functions described previously in the Keplerian expression of the gravitational potential.

Substituting (2.47) into (2.43) provides an expression for the gravitational potential in terms of the equinoctial elements for a particular degree and order pair:

$$U_{n,m}^* = \frac{\mu}{a} \left(\frac{R_e}{a} \right)^n C_{n,m}^* \sum_{s=-n}^n V_{n,s}^m S_{2n}^{(m,s)}(p,q) \sum_{t=-\infty}^{+\infty} Y_t^{-n-1,s}(k,h) \exp^{j(\lambda - m\theta)} \quad (2.59)$$

2.1.2 Zonal Harmonics (order $m = 0$)

If the order (m) is set equal to zero in equation (2.22), the following expression results:

$$\psi = -\frac{\mu}{r} \left[1 + \sum_{n=2}^{\infty} \left(\frac{R_e}{r} \right)^n C_{n,0} P_{n,0}(\sin \phi) \right] \quad (2.60)$$

which, since $J_{n,0} = J_n = -C_{n,0} = -C_n$, leads to:

$$\psi = -\frac{\mu}{r} \left[1 - \sum_{n=2}^{\infty} \left(\frac{R_e}{r} \right)^n J_n P_n (\sin \phi) \right] \quad (2.61)$$

Similarly, if the order (m) is set equal to zero in equations (2.26), (2.27), and (2.28), an expression for the zonal potential in terms of Keplerian elements results:

$$\psi = \frac{\mu}{a} \sum_{n=2}^N \left(\frac{R_e}{a} \right)^n \sum_{p=0}^n F_{n,0,p} (i) \sum_{q=-\infty}^{\infty} G_{n,p,q} (e) S_{n,0,p,q} (\omega, M, \Omega, \theta) \quad (2.62)$$

where

$$S_{n,0,p,q} = C_{n,0} \cos [(n - 2p)\omega + (n - 2p + q)M] \quad (2.63)$$

for n even, and

$$S_{n,0,p,q} = C_{n,0} \sin [(n - 2p)\omega + (n - 2p + q)M] \quad (2.64)$$

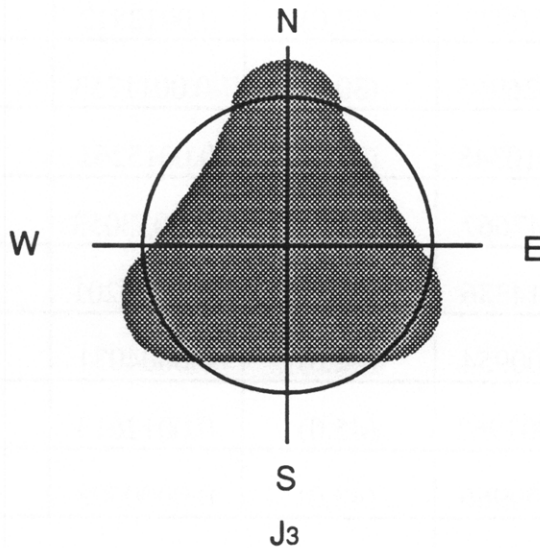
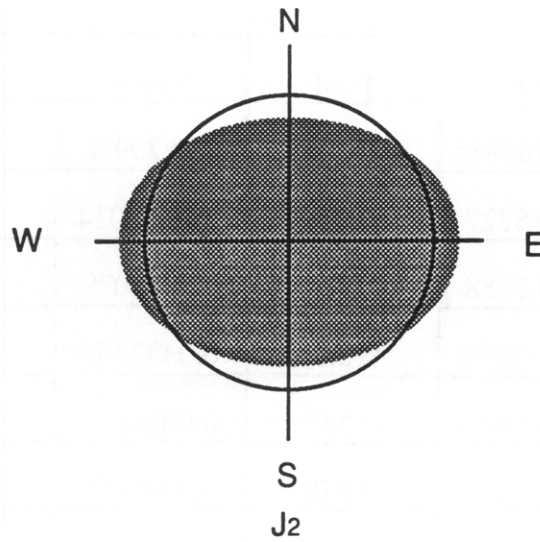
for n odd (the coefficients $S_{n,0}$ are, by definition, zero). It should be noted that the effects of the zonal harmonics can ably be described in terms of any of the three forms of the potential: spherical harmonic form, Keplerian element form, or equinoctial element form. In this discussion, they will be described in terms of this simplified Keplerian formulation of the gravitational potential.

The zonal harmonic coefficients of the geopotential, J_n , can be found in numerous references. Table 2.3 [35] lists values for normalized GEMT3 harmonic coefficients in units of 10^{-6} :

Table 2.3 Normalized GEMT3 Zonal Harmonic Coefficient Values

(n,m)	Value	(n,m)	Value	(n,m)	Value
(2,0)	-484.164885	(3,0)	0.9570928	(4,0)	0.5388446
(5,0)	0.0685727	(6,0)	-0.1483014	(7,0)	0.0903888
(8,0)	0.0467358	(9,0)	0.0281079	(10,0)	0.0560775
(11,0)	-0.0513932	(12,0)	0.0332468	(13,0)	0.0423347
(14,0)	-0.0208865	(15,0)	0.0015621	(16,0)	-0.0077271
(17,0)	0.0201231	(18,0)	0.0095858	(19,0)	-0.0042338
(20,0)	0.0171279	(21,0)	0.0085040	(22,0)	-0.0075970
(23,0)	-0.0243201	(24,0)	-0.0016892	(25,0)	0.0065304
(26,0)	0.0020972	(27,0)	0.0012812	(28,0)	-0.0063334
(29,0)	-0.0026965	(30,0)	-0.0011753	(31,0)	0.0055504
(32,0)	-0.0010348	(33,0)	0.0015261	(34,0)	-0.0053579
(35,0)	0.0047667	(36,0)	-0.0033053	(37,0)	0.0004951
(38,0)	0.0014386	(39,0)	-0.0020201	(40,0)	0.0012413
(41,0)	0.0000954	(42,0)	0.0004031	(43,0)	0.0012005
(44,0)	-0.0001962	(45,0)	0.0012613	(46,0)	-0.0004856
(47,0)	0.0000966	(48,0)	0.0000508	(49,0)	-0.0003145
(50,0)	0.0004076				

These coefficients are related to equipotential surfaces; any position along one of these surfaces possesses an equal value for the potential even though the positions may be at differing distances from the origin of the reference frame--refer to Figure 2.1 [43]).



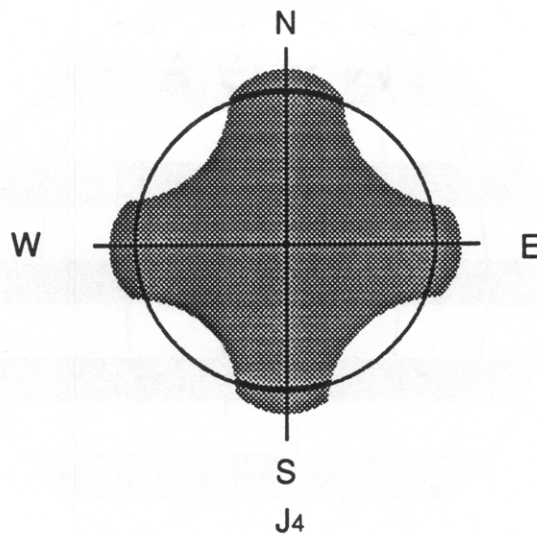


Figure 2.1 Zonal Harmonics / Equipotential Surfaces

where the surfaces shown in this figure are for positive values of the J_n coefficients.

As is evident in equation (2.61), zonal harmonics are dependent solely upon a satellite's latitude and radial distance. The zonal harmonics describe how the actual shape of the earth deviates from the symmetrical Kepler earth in terms of latitude. For example, the density of the earth at one particular line of latitude may be different (either higher or lower) than at another line of latitude. Figure 2.2 depicts this relationship [43]:

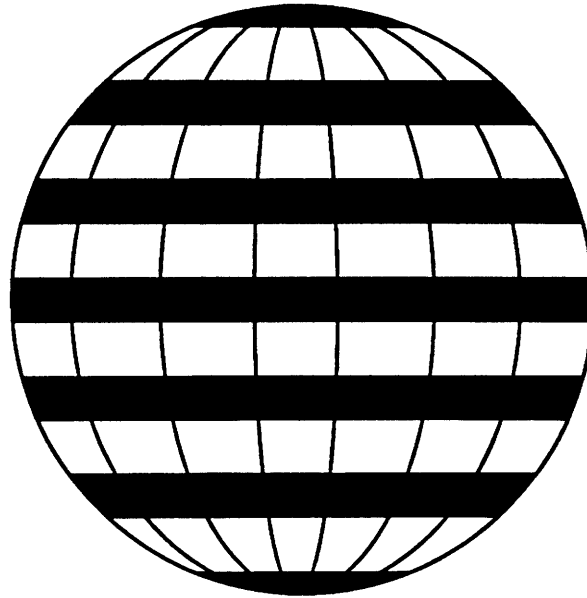


Figure 2.2 Zonal Harmonics

where the alternating dark and light "bands" represent lines of latitude which have densities lower and higher than the two-body earth's density. These zonal harmonics represent the dominant perturbation on a near-earth satellite. The physical effects which arise due to the zonal harmonics are nicely summarized by Blitzer [3]:

1. Secular perturbations in the longitude of ascending node, the argument of perigee, and the mean anomaly are induced by *even* zonal harmonics. These secular variations are the principal long-term effects of the non-spherical earth perturbation. The bulge at the equator produces a torque which tends to turn the satellite's orbit plane towards the equator; the satellite for the aspherical earth will cross the equator short of the crossing point for the unperturbed, two-body satellite. This phenomena, which is referred to as the regression of the node, is depicted in Figure 2.3 [3] (for direct orbits; an advancement of the node occurs for retrograde orbits).

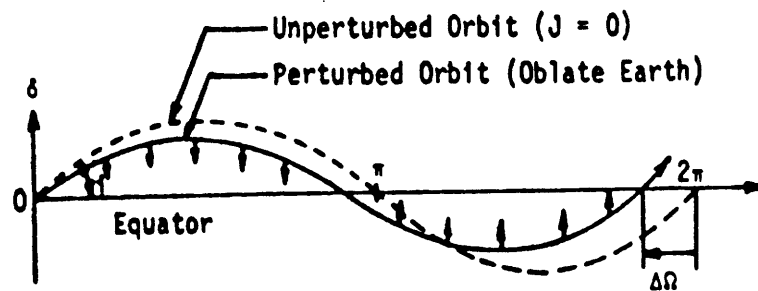


Figure 2.3 Nodal Regression

The non-spherical earth perturbation also causes the apsidal line to precess. This effect is exhibited in Figure 2.4 [3].

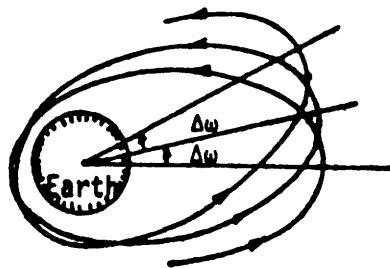


Figure 2.4 Apsidal Line Precession

By letting $(n - 2p) = (n - 2p + q) = 0$ in equations (2.62) through (2.64), the secular effects can be viewed in a mathematical sense:

$$\psi = \frac{\mu}{a} \sum_{n=2}^N \left(\frac{R_e}{a}\right)^n F_{n,0,n/2} (i) G_{n,n/2,0} (e) S_{n,0,n/2,0} (\omega, M, \Omega, \theta) \quad (2.65)$$

with

$$S_{n,0,n/2,0} = C_{n,0} \quad (2.66)$$

for n even, and

$$S_{n,0,n/2,0} = 0 \quad (2.67)$$

for n odd.

Hence, only even zonal harmonics give rise to secular effects (odd $n-m$ would reduce this equation to zero).

2. The zonal harmonics also contribute periodic (both long and short periodic) effects to the motion. Equations (2.62) through (2.64) can again be used to determine the periodic effects of the zonal harmonics. Short-period effects are caused by the terms containing M (the fast variable), while the long-period variations are induced by the term containing ω (slow variable). In order to remove short-period variations, the coefficient of the fast variable $(n - 2p + q)$ in (2.63) and (2.64) must be set equal to zero (to meet this condition,

$q = 2p - n$). Similarly, to remove long-period effects, the coefficient for ω would have to be set to zero ($n = 2p$).

The long-period and secular effects caused by zonal terms of high degree are not insignificant. Cefola [12] points out that neglecting the long periodic and secular terms with degree greater than 5 (actually, J_6 through J_{18}) may cause position errors on the order of 500 or 1000 meters after just 10 revolutions of a 16 rev/day satellite. It is not sensible to utilize a gravitational model with errors of this order if sensor data is more accurate.

3. The magnitude of the secular and periodic variations decreases as altitude (semi-major axis) increases, while the magnitude of the effect increases with increasing eccentricity.

4. The dominance of the J_2 term in the secular rate equation ensures that the node always regresses (again, for direct orbits):

$$\dot{\Omega}_{\text{sec}} = -\frac{3n \cos i}{2} \left\{ \frac{J_2}{p^2} - \frac{J_2^2}{16 p^4} [(12 - 80 I) - (4 + 15 I)e^2] \pm \dots \right\} \quad (2.68)$$

where $I = \sin^2 i$ and $p = \frac{a}{R_e} (1 - e^2)$.

In contrast, the motion of perigee is dependent on the term $(4 - 5 \sin^2 i)$ in the secular rate equation:

$$\dot{\omega}_{\text{sec}} = \frac{3 n J_2}{4 p^2} (4 - 5 \sin^2 i) \pm \dots \quad (2.69)$$

If the inclination is equal to 63.43 degrees (a value referred to as the critical inclination--for retrograde orbits, the critical inclination is equal to 116.57), perigee exhibits no secular variation. If the inclination is less than the value for the critical inclination, the apsidal line will advance; if the inclination is greater than the critical inclination, the apsidal line will regress. Deprit *et al.* have done much work with critical inclination type orbits [14].

Blitzer [3] also gives the equation for the secular element rate for the mean anomaly due to the non-spherical earth perturbation. It is important to note that element rate equations can be derived by inserting into the VOP equations the disturbing function for the non-spherical earth perturbation, which is defined as the negative of the geopotential. For simplicity, only the final results have been included.

5. For polar orbits (inclination equal to 90 degrees), the node exhibits no secular variation--refer to equation (2.68); the cosine of 90 degrees is zero.

6. The term $(4 - 5 \sin^2 i)$ exists in the denominator of the periodic element rate equations for the e , i , Ω , and ω (Blitzer [3] presents the element rate equations for periodic variations due to the non-spherical earth perturbation). For this reason, special techniques must be used for values of inclination near the critical inclination to avoid small divisor problems.

2.1.3 Tesseral Harmonics (order $m \neq 0$)

The physical effects which arise from the tesseral harmonics can be determined by an analysis of equation (2.59). Similar to the zonal harmonics, both short-period and long-period effects are present. These effects are best described through analysis of tesseral m -

daily, tesseral resonance, and tesseral linear combination terms. These terms must not be neglected since they serve to introduce errors on the order of the neglected zonals described above.

The key to understanding the effects of tesseral harmonic terms lies in the interaction between a satellite's orbit and the mass distribution of the earth. It is of interest to note that the mass distribution of the earth is not static; the rotation of the earth causes this mass distribution to rotate. Therefore, when studying the effects of harmonic terms, it is important to understand the relationship prescribed by a satellite's orbit about the rotating mass distribution of the earth. An understanding of this relationship can be mathematically viewed with the aid of the following expression:

$$\dot{\Phi} = t \dot{\lambda} - m \dot{\theta} \quad (2.70)$$

which is the time derivative of the phase angle in (2.59).

The conditions for tesseral resonance can now be given:

$$m \neq 0 \quad (2.71)$$
$$t \dot{\lambda} - m \dot{\theta} \approx 0$$

Shallow resonance occurs if the magnitude of (2.71) is small; if this quantity is very close to zero, deep resonance results. The tolerances which distinguish between deep and shallow resonance are determined by the implementors of the differing theories.

As an example, consider a typical low altitude satellite completing approximately 14 revolutions in one day (a quantity known as the satellite's mean motion), which can be stated mathematically in the following manner:

$$\dot{\lambda} = 14 \omega_e + \varepsilon \quad (2.72)$$

since $\dot{\lambda}$ resulted from a combination of $\dot{\Omega}$, $\dot{\omega}$, and \dot{M} . Inserting (2.72) into (2.71) and rearranging leads to the resonant condition:

$$(14 t - m) \omega_e + t \varepsilon \approx 0 \quad (2.73)$$

where $\dot{\theta}$ is approximately the rotation rate of the earth, ω_e . For combinations like ($t = 1$, $m = 14$) and ($t = 2$, $m = 28$), deep resonance occurs. Combinations like ($t = 1$, $m = 15$) produce the shallow resonance effects described previously. In other words, resonance occurs when the satellite mean motion is some multiple of the earth's rotation rate, causing the satellite to periodically encounter the same set of gravitational forces--a condition which results when repeat ground track orbits are used. Tesseral resonance contributes long-periodic effects to a satellite's motion.

Tesseral linear combination terms which satisfy the following conditions:

$$m \neq 0 \quad (2.74)$$

$$t \dot{\lambda} - m \dot{\theta} \gg 0$$

contribute high frequency, short-periodic effects to a satellite's motion.

Viewed in a slightly different manner, linear combination terms arise from combinations of the variables λ and θ . Tesseral resonance can be seen as a special linear combination term which meets the criteria defined in (2.71). The remaining linear combination terms (i.e., excluding the tesseral resonance terms) satisfy the conditions given in (2.74). In this fashion, tesseral resonance terms provide the long-periodic contribution of the linear combination terms; the remainder of the linear combination terms provide the short-periodic contribution.

Tesseral m-dailies, which provide additional short-period variations, result when the following conditions are met :

$$\begin{aligned}
 m &\neq 0 \\
 t &= 0
 \end{aligned}
 \tag{2.75}$$

These variations, which result from the presence of the $m\theta$ or $m\dot{\theta}$ term, repeat m times per day. At a given latitude, the tesseral m-dailies account for variations in a satellite's motion due to changes in the earth's gravitational attraction caused by the motion of longitudinal irregularities in the earth's mass distribution resulting from the earth's rotation.

The sectorial harmonics, which can be considered a subset of the tesseral harmonics, superimpose bands of mass density upon the spherical earth of the two-body problem (similar to the sections of an orange. Refer to Figure 2.5 [43]):

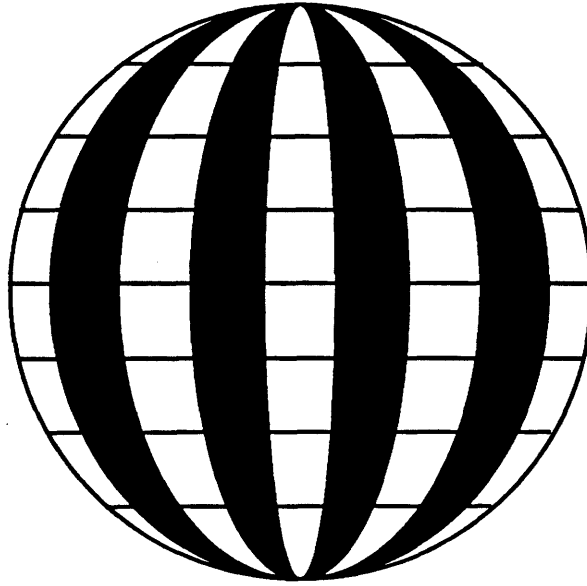


Figure 2.5 Sectorial Harmonics

In this manner, the sectorial harmonics represent the longitude dependent terms of the geopotential. The tesseral harmonics represent the "latitude and longitude dependent" deviations from a regular distribution of mass (much like that of a checker board--refer to Figure 2.6 [43]):

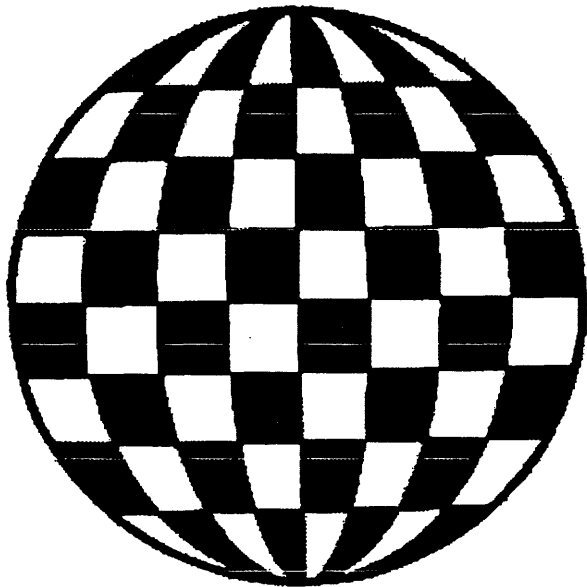


Figure 2.6 Tesseral Harmonics

where the alternating dark and light bands represent belts of mass density which increase or decrease the local density. It should not be inferred that the tesseral harmonics are a direct superposition of the zonal and sectorial harmonics. The bands or belts of mass density which the zonal and sectorial harmonics superimpose upon the spherical, uniformly dense earth are concentric along a line of latitude or longitude, respectively (in other words, these bands form spherical cross-sections). The tesseral harmonics, on the other hand, do not necessarily form spherical cross-sections along a particular line of latitude or longitude. Rather, each "square" in the checker-board configuration can be at differing "heights" or "depths."

2.2 Perturbation Techniques

Perturbation techniques are techniques which account for the various perturbative effects in the determination of a satellite's motion. Since this thesis focused on the effect of the non-spherical earth perturbation, an understanding of perturbation techniques was vital. Classically, two main perturbation techniques have been recognized: special and general perturbation techniques. More recently, semianalytic theories, which combine the advantages of the two classical techniques, have been recognized. Section 2.2 will re-emphasize some of the points expressed in Chapter 1 concerning these three perturbative techniques.

One class of perturbation techniques is special perturbations. Bate, Mueller, and White define special perturbations as techniques which deal with the direct numerical integration of the equations of motion including all necessary perturbing accelerations [2]. These techniques offer both advantages and disadvantages to other perturbation techniques, some of which can be attributed to the numerical integration method implemented. The selection

of an appropriate integration method is vital to optimize the trade-off between result precision and computation time. Numerical integration can provide precise results at the expense of computational time through the use of small step sizes (adequate modeling of high frequency perturbations requires small steps sizes to obtain desired precision). These small step sizes, however, contribute greatly to computer round-off and truncation errors, which can eventually build up and corrupt results. It should be noted that the advent of computers has made the use of special perturbation techniques more convenient for modern applications. Sections 2.2.1 and 2.2.2 of this thesis will describe Cowell's Method and the VOP Method, respectively. These two methods are the special perturbative techniques analyzed in this thesis.

In contrast to special perturbation techniques, general perturbation techniques provide analytical formulae which are used to predict a satellite's motion, usually with the aid of series approximations to model the effect of various perturbations. These techniques are advantageous in that the formulae can be applied to a variety of individual cases; special perturbation techniques are specific to one set of initial conditions; they take a set of given initial conditions and numerically integrate through multiple time steps to arrive at a desired solution. If new initial conditions are prescribed, each of the time steps in the numerical integration process must be re-accomplished to arrive at the desired solution. General perturbation techniques, however, use a system of analytic equations to compute a desired solution directly from any given set of initial conditions; no multiple time steps are needed to transform the initial conditions to desired solutions. In other words, general perturbation techniques provide a savings in computational time as compared to special perturbation techniques. However, these increased efficiencies are gained at the expense of accuracy; the assumptions that go into developing the theory reduce the accuracy of the results. Furthermore, the development of the actual theory itself has classically been time-consuming, negating some of the benefits of the increased efficiency described above. It

should be mentioned that modern symbolic manipulators, such as *Mathematica* [64], can potentially reduce the development time of these theories by significant amounts. As one final note, increased accuracy could be obtained if the integrations required in the expansions could be exactly determined. Since these integrations are often difficult or tedious to determine exactly, simplifying assumptions are made and, in turn, reduce accuracy.

Semianalytic methods, which combine the advantageous aspects of both special and general perturbative methods, comprise a third class of perturbation techniques. These techniques provide accurate results in a manner that is computationally efficient. The basic philosophy for one such semianalytic orbit determination system, the mean element theory (the theory used in Draper Laboratory's R&D version of GTDS), can be summarized rather simply. First, osculating element equations of motion are established; this is usually accomplished by modeling conservative perturbations through Lagrange's VOP equations and non-conservative perturbations through Gauss's VOP equations. Then, these osculating element equations of motion, which contain secular, long-period, and short-period variations to a satellite's motion, are converted to mean element equations of motion. These mean element equations of motion are comprised of only the secular and long-period contributions to the motion. This removal or "stripping" of the short-period terms, which is accomplished by applying the method of averaging to the equations of motion, is significant because the high frequency nature of the short-period terms drive step size requirements for numeric techniques; in order to preserve accuracy in ephemerides, small step sizes must be used to model the high frequency, short-period terms. However, if the short-period variations are removed, the remaining mean element equations of motion can be propagated with numerical integration techniques using much larger step sizes than if osculating element equations of motion were used. These larger step sizes, which are usually on the order of one day, have sizes which are driven by the nature of the frequency

contained in the long-period terms. The short period contribution to the motion can then be independently constructed using analytic or numeric methods. At a desired output time, the short period contributions are added into the long-period and secular contributions contained in the mean elements to yield an approximation to the osculating elements. This method proves to be both accurate and computationally efficient.

In addition, writing the osculating equations of motion in terms of mean elements does not imply that short period variations have been removed. For example, osculating equations of motion written in terms of mean elements still contain short period variations; short period variations are caused by the fast variable--even if it is a mean fast variable. The averaged equations of motion (which give the mean element rates), however, do imply that short period variations have been removed; the fast variable dependence has been removed from these equations which, in turn, removes the short-period variations.

Section 2.2.3 of this thesis will address the generalized method of averaging and specific Semianalytic Satellite Theory (SST) mathematical techniques.

2.2.1 Cowell Mathematical Techniques

Cowell's method is an excellent example of a special perturbation technique that readily flows from the two-body equation:

$$\ddot{\mathbf{r}} + \frac{\mu}{r^3} \mathbf{r} = 0 \tag{2.76}$$

If the acceleration caused by a desired perturbation was known (\mathbf{a}_p), this two-body equation could be modified to give:

$$\ddot{\mathbf{r}} + \frac{\mu}{r^3} \mathbf{r} = \mathbf{a}_p \quad (2.77)$$

Rearranging this equation produces a more desirable form

$$\ddot{\mathbf{r}} = \mathbf{a}_p - \frac{\mu}{r^3} \mathbf{r} \quad (2.78)$$

since

$$\mathbf{v} = \dot{\mathbf{r}} = \int \ddot{\mathbf{r}} dt \quad (2.79)$$

and

$$\mathbf{r} = \int \mathbf{v} dt = \int \dot{\mathbf{r}} dt \quad (2.80)$$

In other words, the velocity and position of a body can be determined as a function of time by integration of equation (2.78) if the body's initial position and velocity, gravitational parameter, and perturbative acceleration at the desired time are known. For computer systems, this integration is performed via some type of numerical method [26].

This brief explanation of Cowell's method has been developed in vector form. However, in real-world applications, the position and velocity of the body (often times referred to as the state of the body) are broken down into corresponding unit directions (x, y, and z) in terms of body-fixed coordinates. These unit directions lead to a scalar derivation, where:

$$r = \sqrt{x^2 + y^2 + z^2} \quad (2.81)$$

Therefore, equation (2.78) can be rewritten for each of the directions:

$$\begin{aligned}\dot{r}_x &= a_{px} - \frac{\mu}{r^3} x \\ \dot{r}_y &= a_{py} - \frac{\mu}{r^3} y \\ \dot{r}_z &= a_{pz} - \frac{\mu}{r^3} z\end{aligned}\tag{2.82}$$

Then, with expressions for \mathbf{a}_p in each of the directions, the new state can readily be determined through integration. These expressions for the non-spherical earth perturbation are given in the GTDS Math Specification [26]:

$$\begin{aligned}a_{px} &= \left(\frac{1}{r} \frac{\partial \psi}{\partial r} - \frac{z_b}{r^2 \sqrt{x_b^2 + y_b^2}} \frac{\partial \psi}{\partial \phi} \right) x_b - \left(\frac{1}{x_b^2 + y_b^2} \frac{\partial \psi}{\partial \lambda} \right) y_b \\ a_{py} &= \left(\frac{1}{r} \frac{\partial \psi}{\partial r} - \frac{z_b}{r^2 \sqrt{x_b^2 + y_b^2}} \frac{\partial \psi}{\partial \phi} \right) y_b - \left(\frac{1}{x_b^2 + y_b^2} \frac{\partial \psi}{\partial \lambda} \right) x_b \\ a_{pz} &= \left(\frac{1}{r} \frac{\partial \psi}{\partial r} \right) z_b - \frac{\sqrt{x_b^2 + y_b^2}}{r^2} \frac{\partial \psi}{\partial \phi}\end{aligned}\tag{2.83}$$

where x_b , y_b , and z_b are the inertial coordinates of the spacecraft in the body-fixed coordinate system, r is the magnitude of the vector from the body's center of mass to the satellite, and ψ is the disturbing function for the non-spherical earth:

$$\psi = \frac{\mu}{r} \left[\sum_{n=2}^{\infty} \sum_{m=0}^n \left(\frac{R_e}{r} \right)^n P_{n,m}(\sin \phi) (C_{n,m} \cos m\lambda + S_{n,m} \sin m\lambda) \right]\tag{2.84}$$

The partial derivatives in (2.83) are as follows [26]:

$$\begin{aligned} \frac{\partial \psi}{\partial r} &= -\frac{\mu}{r^2} \sum_{n=2}^{\infty} \left(\frac{R_e}{r}\right)^n (n+1) \sum_{m=0}^n P_{n,m}(\sin \phi) (C_{n,m} \cos m\lambda + S_{n,m} \sin m\lambda) \\ \frac{\partial \psi}{\partial \phi} &= \frac{\mu}{r} \left[\sum_{n=2}^{\infty} \left(\frac{R_e}{r}\right)^n \sum_{m=0}^n (C_{n,m} \cos m\lambda + S_{n,m} \sin m\lambda) \right] \\ &\quad \times [P_{n,m+1}(\sin \phi) - (m \tan \phi) P_{n,m}(\sin \phi)] \end{aligned} \quad (2.85)$$

$$\frac{\partial \psi}{\partial \lambda} = \frac{\mu}{r} \sum_{n=2}^{\infty} \left(\frac{R_e}{r}\right)^n \sum_{m=0}^n P_{n,m}(\sin \phi) m (S_{n,m} \cos m\lambda - C_{n,m} \sin m\lambda)$$

2.2.2 Variation of Parameters (VOP)

As described in the preceding section, Cowell's method models a spacecraft's motion as a variation in the position and velocity of the spacecraft. Perturbation techniques prior to Cowell's method dealt with variations in the orbital elements or any other consistent set of parameters which describe an orbit [2]--thus the name, Variation of Parameters. The goal of this derivation will be to provide explicit expressions for parameter rates of change of the form:

$$\frac{dc_j}{dt} = Z(c_j, t) \quad \text{for } j = 1, 2, \dots, 6 \quad (2.86)$$

where Z is an expression involving the parameters and time (Z has been described as an expression involving the parameters and time rather than a function of parameters and time in foresight of matrix expressions in the solution). It is important to note that the

parameters c_j for this solution are time-dependent quantities--as opposed to the "constant" (time-independent) parameters found in the two-body solution.

The VOP derivation which follows is modeled after that of Brouwer and Clemence [4], with much insight provided by McClain [40]. As with most astrodynamic derivations, the starting point is the two-body equation of motion:

$$\ddot{\mathbf{r}} + \frac{\mu}{r^3} \mathbf{r} = 0 \quad (2.87)$$

In the two-body solution (a solution in which six constants of integration arise), functions for position and velocity of the following form result:

$$\begin{aligned} x &= f_1(c_1, c_2, \dots, c_6, t) \\ y &= f_2(c_1, c_2, \dots, c_6, t) \\ z &= f_3(c_1, c_2, \dots, c_6, t) \\ \dot{x} &= g_1(c_1, c_2, \dots, c_6, t) \\ \dot{y} &= g_2(c_1, c_2, \dots, c_6, t) \\ \dot{z} &= g_3(c_1, c_2, \dots, c_6, t) \end{aligned} \quad (2.88)$$

where c_1, c_2, \dots, c_6 represent the chosen set of parameters; t is time; and

$$\mathbf{g}_k = \frac{\partial f_k}{\partial t}, \quad \text{for } k = 1, 2, 3 \quad (2.89)$$

since the chosen set of parameters are considered to be constant in the two body solution. With the introduction of perturbations, the equations of motion for the two-body problem take a form analogous to (2.82):

$$\begin{aligned}\ddot{x} + \frac{\mu x}{r^3} &= P_x \\ \ddot{y} + \frac{\mu y}{r^3} &= P_y \\ \ddot{z} + \frac{\mu z}{r^3} &= P_z\end{aligned}\tag{2.90}$$

where $P_{x,y,z}$ represent the perturbing accelerations (for the corresponding unit directions) due to either conservative or non-conservative perturbing forces. These perturbing accelerations are a function of the corresponding components of position and velocity, as well as time: $P_{x,y,z}(r_{x,y,z}, \dot{r}_{x,y,z}, t)$.

In this perturbed solution, the set of parameters can no longer be considered a constant; they vary slightly with time, which leads to the chain rule of differentiation in order to determine velocity:

$$\dot{x} = \frac{dx}{dt} = \frac{\partial f_1}{\partial t} + \sum \frac{\partial f_1}{\partial c_j} \frac{dc_j}{dt} \quad \text{for } j = 1, 2, \dots, 6\tag{2.91}$$

with the assumption that the two-body expressions for position remain applicable for this perturbed case and that the equations for velocity in the other directions (Y and Z directions) are of the same form as (2.91).

What results for the perturbed case is a set of six first order equations (the first three equations take the form of (2.88) for position and three equations of form (2.91) representing all directions for velocity) in six unknowns (the set of parameters). In order to determine a unique solution for this system of equations, six "initial conditions" or constraints on the chosen parameters or orbital elements (which, in turn, also represent constraints on the position and velocity) must be specified. The expressions offered in (2.92), which represent a common set of constraints placed on the velocity, are three of the six required constraints which aid in the transformation of the perturbed solution to the desired parameter rate expression of form (2.86):

$$\begin{aligned} \sum \frac{\partial f_1}{\partial c_j} \frac{dc_j}{dt} &= 0 \\ \sum \frac{\partial f_2}{\partial c_j} \frac{dc_j}{dt} &= 0 \\ \sum \frac{\partial f_3}{\partial c_j} \frac{dc_j}{dt} &= 0 \end{aligned} \tag{2.92}$$

for $j = 1, 2, \dots, 6$

For perturbed motion, these three conditions constrain the velocity to explicitly equal the time derivative of position, as in the two-body case (which allows the perturbed case to maintain the appearance of the two-body case). However, it should not be inferred that the perturbed elements are a constant (as the elements in the two-body case are); the constraints listed in (2.92) do not imply that $\frac{dc_j}{dt}$ is zero for the perturbed case. Rather, the summation $\frac{\partial f_i}{\partial c_j} \frac{dc_j}{dt}$ is zero, which means $\frac{\partial f_i}{\partial c_j}$ and $\frac{dc_j}{dt}$ could both be zero, both be non-zero, or either one of the two zero while the other non-zero. As a result, McClain [40] states that at any

time t , the perturbed elements always correspond to a set of unperturbed elements, which are referred to as osculating elements. The constraints allow both the position and velocity to be related to the perturbed elements through the formulas for elliptic (two-body) motion.

Due to these constraints, the derivation resumes with equations of the form (2.89):

$$\begin{aligned}\dot{x} &= \frac{dx}{dt} = \frac{\partial f_1}{\partial t} = g_1(c_1, c_2, \dots, c_6, t) \\ \dot{y} &= \frac{dy}{dt} = \frac{\partial f_2}{\partial t} = g_2(c_1, c_2, \dots, c_6, t) \\ \dot{z} &= \frac{dz}{dt} = \frac{\partial f_3}{\partial t} = g_3(c_1, c_2, \dots, c_6, t)\end{aligned}\tag{2.93}$$

By differentiating these equations once more, the following expressions result:

$$\begin{aligned}\ddot{x} &= \frac{\partial^2 f_1}{\partial t^2} + \sum \frac{\partial^2 f_1}{\partial c_j \partial t} \frac{dc_j}{dt} \quad \text{or} \quad \frac{\partial g_1}{\partial t} + \sum \frac{\partial g_1}{\partial c_j} \frac{dc_j}{dt} \\ \ddot{y} &= \frac{\partial^2 f_2}{\partial t^2} + \sum \frac{\partial^2 f_2}{\partial c_j \partial t} \frac{dc_j}{dt} \quad \text{or} \quad \frac{\partial g_2}{\partial t} + \sum \frac{\partial g_2}{\partial c_j} \frac{dc_j}{dt} \\ \ddot{z} &= \frac{\partial^2 f_3}{\partial t^2} + \sum \frac{\partial^2 f_3}{\partial c_j \partial t} \frac{dc_j}{dt} \quad \text{or} \quad \frac{\partial g_3}{\partial t} + \sum \frac{\partial g_3}{\partial c_j} \frac{dc_j}{dt}\end{aligned}\tag{2.94}$$

for $j = 1, 2, \dots, 6$

which can be substituted into (2.90):

$$\frac{\partial^2 f_1}{\partial t^2} + \frac{\mu f_1}{r^3} + \Sigma \frac{\partial^2 f_1}{\partial c_j \partial t} \frac{dc_j}{dt} = P_x (r, \dot{r}, t)$$

$$\frac{\partial^2 f_2}{\partial t^2} + \frac{\mu f_2}{r^3} + \Sigma \frac{\partial^2 f_2}{\partial c_j \partial t} \frac{dc_j}{dt} = P_y (r, \dot{r}, t)$$
(2.95)

$$\frac{\partial^2 f_3}{\partial t^2} + \frac{\mu f_3}{r^3} + \Sigma \frac{\partial^2 f_3}{\partial c_j \partial t} \frac{dc_j}{dt} = P_z (r, \dot{r}, t)$$

for $j = 1, 2, \dots, 6$

If the two body motion is expressed in a similar fashion, the final three constraints on the parameters can be identified as:

$$\frac{\partial^2 f_k}{\partial t^2} + \frac{\mu f_k}{r^3} = 0, \quad k = 1, 2, 3$$
(2.96)

When subtracted out of equations (2.95), a simplified set of expressions can be obtained.

$$\Sigma \frac{\partial^2 f_1}{\partial c_j \partial t} \frac{dc_j}{dt} = \Sigma \frac{\partial g_1}{\partial c_j} \frac{dc_j}{dt} = P_x (r, \dot{r}, t)$$

$$\Sigma \frac{\partial^2 f_2}{\partial c_j \partial t} \frac{dc_j}{dt} = \Sigma \frac{\partial g_2}{\partial c_j} \frac{dc_j}{dt} = P_y (r, \dot{r}, t)$$
(2.97)

$$\Sigma \frac{\partial^2 f_3}{\partial c_j \partial t} \frac{dc_j}{dt} = \Sigma \frac{\partial g_3}{\partial c_j} \frac{dc_j}{dt} = P_z (r, \dot{r}, t)$$

for $j = 1, 2, \dots, 6$

The entire system of six constraints expressed in terms of $x, y, z, \dot{x}, \dot{y},$ and \dot{z} rather than f_k and g_k provides the desired relationship--six equations involving the six parameter rates of change.

$$\frac{\partial x}{\partial c_1} \frac{dc_1}{dt} + \frac{\partial x}{\partial c_2} \frac{dc_2}{dt} + \frac{\partial x}{\partial c_3} \frac{dc_3}{dt} + \frac{\partial x}{\partial c_4} \frac{dc_4}{dt} + \frac{\partial x}{\partial c_5} \frac{dc_5}{dt} + \frac{\partial x}{\partial c_6} \frac{dc_6}{dt} = 0$$

$$\frac{\partial y}{\partial c_1} \frac{dc_1}{dt} + \frac{\partial y}{\partial c_2} \frac{dc_2}{dt} + \frac{\partial y}{\partial c_3} \frac{dc_3}{dt} + \frac{\partial y}{\partial c_4} \frac{dc_4}{dt} + \frac{\partial y}{\partial c_5} \frac{dc_5}{dt} + \frac{\partial y}{\partial c_6} \frac{dc_6}{dt} = 0$$

$$\frac{\partial z}{\partial c_1} \frac{dc_1}{dt} + \frac{\partial z}{\partial c_2} \frac{dc_2}{dt} + \frac{\partial z}{\partial c_3} \frac{dc_3}{dt} + \frac{\partial z}{\partial c_4} \frac{dc_4}{dt} + \frac{\partial z}{\partial c_5} \frac{dc_5}{dt} + \frac{\partial z}{\partial c_6} \frac{dc_6}{dt} = 0$$

(2.98)

$$\frac{\partial \dot{x}}{\partial c_1} \frac{dc_1}{dt} + \frac{\partial \dot{x}}{\partial c_2} \frac{dc_2}{dt} + \frac{\partial \dot{x}}{\partial c_3} \frac{dc_3}{dt} + \frac{\partial \dot{x}}{\partial c_4} \frac{dc_4}{dt} + \frac{\partial \dot{x}}{\partial c_5} \frac{dc_5}{dt} + \frac{\partial \dot{x}}{\partial c_6} \frac{dc_6}{dt} = P_x(r, \dot{r}, t)$$

$$\frac{\partial \dot{y}}{\partial c_1} \frac{dc_1}{dt} + \frac{\partial \dot{y}}{\partial c_2} \frac{dc_2}{dt} + \frac{\partial \dot{y}}{\partial c_3} \frac{dc_3}{dt} + \frac{\partial \dot{y}}{\partial c_4} \frac{dc_4}{dt} + \frac{\partial \dot{y}}{\partial c_5} \frac{dc_5}{dt} + \frac{\partial \dot{y}}{\partial c_6} \frac{dc_6}{dt} = P_y(r, \dot{r}, t)$$

$$\frac{\partial \dot{z}}{\partial c_1} \frac{dc_1}{dt} + \frac{\partial \dot{z}}{\partial c_2} \frac{dc_2}{dt} + \frac{\partial \dot{z}}{\partial c_3} \frac{dc_3}{dt} + \frac{\partial \dot{z}}{\partial c_4} \frac{dc_4}{dt} + \frac{\partial \dot{z}}{\partial c_5} \frac{dc_5}{dt} + \frac{\partial \dot{z}}{\partial c_6} \frac{dc_6}{dt} = P_z(r, \dot{r}, t)$$

The system of equations offered by (2.98) represent six equations with imbedded expressions for parameter rates of change--the crux of the variation of parameter derivation. It would be tedious to solve this system of six equations for the six element rate expressions; a more convenient set of expressions would be useful in astrodynamic applications. Indeed, Lagrange has developed a set for conservative forces, while Gauss has developed a set for both conservative and non-conservative forces.

2.2.2.1 Lagrange's VOP Equations

Lagrange VOP equations (also known as Lagrange's Planetary Equations) deal with conservative forces, or forces that produce no net work upon an object through a round-trip or closed path. In astrodynamics, third body and central body (i.e., non-spherical earth) perturbations are examples of conservative perturbations which could be solved using Lagrange's VOP formulation. For his formulation, Lagrange modeled the perturbing accelerations $P_{x,y,z}(\mathbf{r}_{x,y,z}, \dot{\mathbf{r}}_{x,y,z}, t)$ through partial derivatives of a conservative disturbing function, R , which can be mathematically expressed in the following manner:

$$P_x = \frac{\partial R}{\partial x}, \quad P_y = \frac{\partial R}{\partial y}, \quad P_z = \frac{\partial R}{\partial z} \quad (2.99)$$

Lagrange documented that equations of the form (2.98) can be greatly simplified--six new equations can be derived from the set offered in (2.98) through the use of:

- 1) matrix notation
- 2) Lagrange brackets
- 3) perturbing accelerations of form (2.99)
- 4) successive multiplications by $\frac{-\partial \dot{x}}{\partial c_j}$, $\frac{-\partial \dot{y}}{\partial c_j}$, $\frac{-\partial \dot{z}}{\partial c_j}$, $\frac{+\partial x}{\partial c_j}$, $\frac{+\partial y}{\partial c_j}$ and $\frac{+\partial z}{\partial c_j}$, ($j = 1, 2, \dots, 6$)

and

- 5) addition

Note that the right hand sides for the final three equations of (2.98) become $\frac{\partial R}{\partial x}$, $\frac{\partial R}{\partial y}$, and $\frac{\partial R}{\partial z}$ with the perturbing acceleration assumption of (2.99) above).

Separating the parameter rate expressions $\overline{\frac{dc}{dt}}$ from the Lagrange bracket expressions $[c_j, c_k]$

in this set, the following matrix system results:

$$[[c_j, c_k]] \overline{\frac{dc}{dt}} = \overline{\frac{\partial R}{\partial c}} \quad (2.100)$$

where $[[c_j, c_k]]$ represents a coefficient matrix of Lagrange brackets, $\overline{\frac{dc}{dt}}$ a vector of parameter rate expressions, and $\overline{\frac{\partial R}{\partial c}}$ a vector of partials of the disturbing function with respect to the elements. In order to determine the vector of parameter rate expressions directly, the inverse of the Lagrange bracket matrix is needed. According to proof by de Lafontaine [20], the negative inverse of the Lagrange bracket matrix is the Poisson matrix, \mathbf{P} , which leads to the following expressions:

$$\overline{\frac{dc}{dt}} = [[c_j, c_k]]^{-1} \overline{\frac{\partial R}{\partial c}} \quad (2.101)$$

and

$$\overline{\frac{dc}{dt}} = -\mathbf{P} \overline{\frac{\partial R}{\partial c}} \quad (2.102)$$

as long as conditions for invertability exist for the Lagrange bracket matrix (i.e., a non-zero determinant, etc...). Since this Poisson matrix is skew-symmetric, another form can be given:

$$\overline{\frac{dc}{dt}} = \mathbf{P}^T \overline{\frac{\partial R}{dc}} \quad (2.103)$$

The Poisson brackets of equinoctial elements are given by Cefola [8]:

$$(a, \lambda_0) = -2a s_1$$

$$(\lambda_0, h) = -h s_4$$

$$(\lambda_0, k) = -k s_4$$

$$(\lambda_0, p) = -p s_5$$

$$(\lambda_0, q) = -q s_5$$

$$(h, k) = -s_1 s_3 \quad (2.104)$$

$$(h, p) = -kp s_5$$

$$(h, q) = -kq s_5$$

$$(k, p) = hp s_5$$

$$(k, q) = hq s_5$$

$$(p, q) = \frac{1}{2} s_3 s_5 I$$

where

$$s_1 = \frac{1}{na^2}$$

$$s_2 = 1 + p^2 + q^2$$

$$s_3 = \sqrt{1 - h^2 - k^2} \quad (2.105)$$

$$s_4 = \frac{s_1 s_3}{1 + s_3}$$

$$s_5 = \frac{s_1 s_2}{2 s_3}$$

with the retrograde factor, I.

2.2.2.2 Gauss' VOP Equations

Gauss' VOP equations, which are used for perturbations which can not be expressed by some disturbing function R, are equally acceptable for non-conservative and conservative forces. Gauss' derivation flows nicely from the equations offered in (2.92) and (2.97), which will be restated as (2.106):

$$\Sigma \frac{\partial f_1}{\partial c_j} \frac{dc_j}{dt} = \Sigma \frac{\partial x}{\partial c_j} \dot{c}_j = 0$$

$$\Sigma \frac{\partial f_2}{\partial c_j} \frac{dc_j}{dt} = \Sigma \frac{\partial y}{\partial c_j} \dot{c}_j = 0$$

$$\Sigma \frac{\partial f_3}{\partial c_j} \frac{dc_j}{dt} = \Sigma \frac{\partial z}{\partial c_j} \dot{c}_j = 0$$

(2.106)

$$\Sigma \frac{\partial g_1}{\partial c_j} \frac{dc_j}{dt} = \Sigma \frac{\partial \dot{x}}{\partial c_j} \dot{c}_j = P_x (r, \dot{r}, t)$$

$$\Sigma \frac{\partial g_2}{\partial c_j} \frac{dc_j}{dt} = \Sigma \frac{\partial \dot{y}}{\partial c_j} \dot{c}_j = P_y (r, \dot{r}, t)$$

$$\Sigma \frac{\partial g_3}{\partial c_j} \frac{dc_j}{dt} = \Sigma \frac{\partial \dot{z}}{\partial c_j} \dot{c}_j = P_z (r, \dot{r}, t)$$

for $j = 1, 2, \dots, 6$

In order to simplify the expressions which follow, the components of position (x , y , and z) and the components of velocity (\dot{x} , \dot{y} , and \dot{z}) will be replaced by r_i and v_i , where $i = 1, 2$, and 3 . This notation reduces the set of equations listed in (2.106) to the following two double summations:

$$\sum_{i=1}^3 \sum_{j=1}^6 \frac{\partial r_i}{\partial c_j} \dot{c}_j = 0$$

(2.107)

$$\sum_{i=1}^3 \sum_{j=1}^6 \frac{\partial v_i}{\partial c_j} \dot{c}_j = \sum_{i=1}^3 P_i (r, \dot{r}, t)$$

Multiplying both sides of the first three equations of (2.107) by $\frac{\partial c_k}{\partial r_i}$, the last three by $\frac{\partial c_k}{\partial v_i}$,

and summing the results, the following equation results:

$$\sum_{i=1}^3 \sum_{j=1}^6 \left(\frac{\partial c_k}{\partial v_i} \frac{\partial v_i}{\partial c_j} + \frac{\partial c_k}{\partial r_i} \frac{\partial r_i}{\partial c_j} \right) \dot{c}_j = \sum_{i=1}^3 \frac{\partial c_k}{\partial v_i} P_i(r, \dot{r}, t) \quad (2.108)$$

for $k = 1, 2, \dots, 6$

Noting that the elements are mutually independent leads to the Kronecker delta function:

$$\sum_{i=1}^3 \left(\frac{\partial c_k}{\partial v_i} \frac{\partial v_i}{\partial c_j} + \frac{\partial c_k}{\partial r_i} \frac{\partial r_i}{\partial c_j} \right) = \delta_{j,k} \quad (2.109)$$

for $j, k = 1, 2, \dots, 6$

which reduces equation (2.108) to the following form:

$$\sum_{j=1}^6 \delta_{j,k} \dot{c}_j = \sum_{i=1}^3 \frac{\partial c_k}{\partial v_i} P_i(r, \dot{r}, t) \quad (2.110)$$

But since the Kronecker delta function is unity for $j = k$ (otherwise zero), the final form is readily obtained:

$$\dot{c}_j = \sum_{i=1}^3 \frac{\partial c_j}{\partial v_i} P_i(r, \dot{r}, t) \quad (2.111)$$

Jablonski presents a summary of the equations [30] in terms of the singularity free equinoctial elements a , h , k , p , q , and λ :

$$\begin{aligned}\frac{da}{dt} &= \frac{2v}{n^2 a} \mathbf{a}_d \\ \frac{dh}{dt} &= \left[\frac{1}{\mu} [(2\dot{X}_1 Y_1 - X_1 \dot{Y}_1) \hat{f} - X_1 \dot{X}_1 \hat{g}] + \frac{k}{G} (qI Y_1 - p X_1) \hat{w} \right] \mathbf{a}_d \\ \frac{dk}{dt} &= \left[-\frac{1}{\mu} [Y_1 \dot{Y}_1 \hat{f} - (2X_1 \dot{Y}_1 - \dot{X}_1 Y_1) \hat{g}] - \frac{h}{G} (qI Y_1 - p X_1) \hat{w} \right] \mathbf{a}_d \\ \frac{dp}{dt} &= \left[\frac{1+p^2+q^2}{2G} Y_1 \hat{w} \right] \mathbf{a}_d \\ \frac{dq}{dt} &= \left[\frac{I(1+p^2+q^2)}{2G} X_1 \hat{w} \right] \mathbf{a}_d \\ \frac{d\lambda}{dt} &= \left[n - \frac{2}{na^3} r + \beta \left(k \frac{\partial h}{\partial v} - h \frac{\partial k}{\partial v} \right) + \frac{1}{na^2} (qI Y_1 - p X_1) \hat{w} \right] \mathbf{a}_d\end{aligned}\tag{2.112}$$

where \mathbf{a}_d is the perturbing acceleration acting on the satellite, I is the retrograde factor, r and v are the position and velocity of the satellite, n is the mean motion, and X_1 , Y_1 , \dot{X}_1 , and \dot{Y}_1 are the position and velocity coordinates of the satellite in the equinoctial orbital frame. The parameters G and B are defined in the following manner:

$$G = n a^2 \sqrt{1 - h^2 - k^2}\tag{2.113}$$

$$\beta = \frac{1}{1 + \sqrt{1 - h^2 - k^2}}\tag{2.114}$$

Atmospheric drag, solar radiation pressure, and thrust are examples of non-conservative perturbations which require Gauss' VOP formulation.

2.2.3 Implementation of VOP Formulations with Numerical Methods

It is now convenient to establish steps for the implementation of a VOP formulation as part of a numerical method. This description, which indicates a very simple process, does not reflect the more elaborate process used by the Goddard Trajectory Determination System (GTDS):

1. At some desired time, record/obtain a desired set of orbital elements or parameters (usually a "given").
2. Compute the desired perturbing accelerations.
3. Compute the element rates of change from the appropriate VOP formulation.
4. Numerically integrate these rates through the desired time step.
5. Add the result of step (4) to the elements used in step (1).
6. Continue to step through time until the final time is obtained, making sure to replace the elements of step (1) in successive iterations with the perturbed set from step (5).

2.3 Semianalytic Methods

As mentioned in Section 2.2, special perturbation techniques provide extremely accurate results at the expense of computation efficiency. General perturbation techniques, on the other hand, are much more efficient, but provide less accurate results due to simplifying assumptions made in the analytic development of these techniques. The current trend in the design of orbit propagators has been to use semianalytic methods. These methods, which

provide accurate results in a manner that is computationally efficient, will be analyzed in this section.

2.3.1 Semianalytic Equations of Motion and the Generalized Method of Averaging

Since both Lagrangian and Gaussian VOP equations can be used to model the perturbations in semianalytic theory, a generic equation representing either VOP form shall be the starting point for the semianalytic equations of motion. Again, the derivation follows that of McClain [38] (an additional reference is the work of Morrison [44]):

$$\frac{dc_i}{dt} = \varepsilon F_i(\hat{c}, f) , \text{ for } i = 1, 2, \dots, 5 \tag{2.115}$$

$$\frac{df}{dt} = n(c_1) + \varepsilon F_6(\hat{c}, f)$$

where \hat{c} is a vector of the five slowly varying elements, ε is a small parameter related to the perturbations, and f is the fast element. For effects of the geopotential, the small parameter usually takes the form of small coefficients such as harmonic coefficients ($J_2, J_3, \text{etc.}$).

These expressions represent osculating equations of motion in terms of osculating elements (they include secular, long-period, and short-period variations). The goal of the method of averaging is to separate the short period variations from the long-period and secular contributions to motion. To accomplish this goal, it is first necessary to express equations (2.115) in terms of mean elements. These equations will remain osculating equations of motion, however, since the mean fast variable will still be present in the equations to contribute short-period variations. Representing these osculating equations of motion in terms of mean elements is desirable in that it provides a form which can be readily stripped of its fast variable dependence and the resulting short-period variations. The near identity

transformation will be used to convert the left hand sides of equations (2.115), while a Taylor series expansion of the perturbing functions ($F_{1,2,3,4,5,6}$) about the mean elements will be used to transform the right hand sides. In this derivation, the terms "rates" and "equations of motion" will be used interchangeably.

An important concept in semianalytic theory is that of the near identity transform. This transformation expresses the osculating elements in terms of the mean elements:

$$c_i = \bar{c}_i + \varepsilon \eta_{i,1} + \varepsilon^2 \eta_{i,2} + \dots, \text{ for } i = 1, 2, \dots, 5 \quad (2.116)$$

$$f = \bar{f} + \varepsilon \eta_{6,1} + \varepsilon^2 \eta_{6,2} + \dots$$

where the overbar notation is used to signify mean elements (and to distinguish them from osculating elements) and $\eta_{i,\text{order}}$ are functions of the mean elements ($\eta = \eta(\bar{c}, \bar{f})$) that are 2π periodic in \bar{f} . These functions represent the short-period terms. The expressions in (2.116) can be differentiated with respect to time to produce the following relationships:

$$\frac{dc_i}{dt} = \frac{d\bar{c}_i}{dt} + \varepsilon \frac{\partial \eta_{i,1}}{\partial \bar{c}_k} \dot{\bar{c}}_k + \varepsilon^2 \frac{\partial \eta_{i,2}}{\partial \bar{c}_k} \dot{\bar{c}}_k + \dots$$

for $i = 1, 2, \dots, 5; \quad k = 1, 2, \dots, 6 \quad (2.117)$

$$\frac{df}{dt} = \frac{d\bar{f}}{dt} + \varepsilon \frac{\partial \eta_{6,1}}{\partial \bar{c}_k} \dot{\bar{c}}_k + \varepsilon^2 \frac{\partial \eta_{6,2}}{\partial \bar{c}_k} \dot{\bar{c}}_k + \dots$$

where a summation is implied for the terms involving dot products of partial derivatives with rate vectors.

It can be assumed that expressions for the mean element equations of motion $\left(\frac{d\bar{c}_i}{dt} \text{ and } \frac{d\bar{f}}{dt}\right)$ can be expressed as power series in terms of the same small parameter given in (2.116), ϵ .

$$\frac{d\bar{c}_i}{dt} = \epsilon A_{i,1}(\hat{c}) + \epsilon^2 A_{i,2}(\hat{c}) + \dots, \text{ for } i = 1, 2, \dots, 5 \quad (2.118)$$

$$\frac{d\bar{f}}{dt} = \bar{n}(\bar{c}_1) + \epsilon A_{6,1}(\hat{c}) + \epsilon^2 A_{6,2}(\hat{c}) + \dots$$

where \hat{c} represents a vector of the five slow, mean elements, \bar{n} represents the mean motion, and $A_{w,x}$ represent the x^{th} order contribution to the mean element rates for the w^{th} element ($w = 1, 2, \dots, 6$). Note that these expressions are for contributions to the mean element rates. For this reason, the terms $A_{w,x}$ are assumed to represent only long-period and secular contributions--not short-period contributions and, therefore, do not contain the fast variable. Since \bar{n} is a function of the mean semi-major axis alone, it can also be thought of as a "mean" element--the mean mean motion.

Now, the assumed form for the mean element equations of motion (equations (2.118) above) can be substituted into equations (2.117) to produce expressions for the osculating equations of motion in terms of the mean elements:

$$\frac{dc_i}{dt} = \left[\epsilon A_{i,1}(\hat{c}) + \epsilon^2 A_{i,2}(\hat{c}) + \dots \right] + \epsilon \frac{\partial \eta_{i,1}}{\partial \bar{c}_k} \dot{\bar{c}}_k + \epsilon^2 \frac{\partial \eta_{i,2}}{\partial \bar{c}_k} \dot{\bar{c}}_k + \dots$$

for $i = 1, 2, \dots, 5; \quad k = 1, 2, \dots, 6$ (2.119)

$$\frac{df}{dt} = \left[\bar{n} + \epsilon A_{6,1}(\hat{c}) + \epsilon^2 A_{6,2}(\hat{c}) + \dots \right] + \epsilon \frac{\partial \eta_{6,1}}{\partial \bar{c}_k} \dot{\bar{c}}_k + \epsilon^2 \frac{\partial \eta_{6,2}}{\partial \bar{c}_k} \dot{\bar{c}}_k + \dots$$

The right hand sides of these expressions, which contain only the mean elements or functions of the mean elements, will later be substituted into the left hand sides of equations (2.115).

The perturbing functions on the right hand sides of (2.115), which are expressed in terms of osculating elements, can be expanded in a Taylor series about the mean elements:

$$F_i(\hat{c}, f) = F_i(\hat{c}, \bar{f}) + \sum_{k=1}^6 \left[\frac{\partial F_i}{\partial \bar{c}_k} \right]_{\text{mean elements}} \Delta c + \dots, \text{ for } i = 1, 2, \dots, 6 \quad (2.120)$$

where Δc can be thought of as the difference between the mean elements and the osculating elements (in other words, how far away the mean elements are from the osculating elements). If the near identity transformation in (2.116) above is re-arranged (to first order), the following expression for Δc is obtained:

$$c_i - \bar{c}_i = \Delta c = \varepsilon \eta_{i,1}, \text{ for } i = 1, 2, \dots, 5 \quad (2.121)$$

or, when $i = 6$,

$$f - \bar{f} = \Delta c = \varepsilon \eta_{6,1} \quad (2.122)$$

These expressions can be substituted into (2.120).

$$F_i(\hat{c}, f) = F_i(\hat{c}, \bar{f}) + \varepsilon \sum_{k=1}^6 \left[\frac{\partial F_i}{\partial \bar{c}_k} \right]_{\text{mean elements}} \eta_{i,1} + \text{HOT}(\varepsilon^2) \quad (2.123)$$

for $i = 1, 2, \dots, 6$

In order to expand the entire right hand side of the second equation of (2.115) in a Taylor series about the mean elements, the mean motion also must be expanded and expressed in a power series of the small parameter:

$$n(c_1) = n_0 + \varepsilon n_1 + \varepsilon^2 n_2 + \dots \quad (2.124)$$

where McClain [38] presents the values for n_x :

$$n_0 = \bar{n}$$

$$n_1 = -\frac{3}{2} \frac{\bar{n}}{c_1} \eta_{1,1} \quad (2.125)$$

$$n_2 = \frac{15}{8} \frac{\bar{n}}{c_1^2} \eta_{1,1}^2 - \frac{3}{2} \frac{\bar{n}}{c_1} \eta_{1,2}$$

Substituting these expressions into (2.124), a series representation for the mean motion (in terms of mean elements) is obtained:

$$n(c_1) = \bar{n} - \varepsilon \frac{3}{2} \frac{\bar{n}}{c_1} \eta_{1,1} + \varepsilon^2 \left(\frac{15}{8} \frac{\bar{n}}{c_1^2} \eta_{1,1}^2 - \frac{3}{2} \frac{\bar{n}}{c_1} \eta_{1,2} \right) + \dots \quad (2.126)$$

Now, equations (2.119) can be plugged into the left hand sides and equations (2.123) and (2.126) into the right hand sides of equation (2.115). Expressions for the osculating equations of motion in terms of mean elements result:

$$\begin{aligned} & \left[\varepsilon A_{i,1}(\hat{c}) + \varepsilon^2 A_{i,2}(\hat{c}) + \dots \right] + \varepsilon \frac{\partial \eta_{i,1}}{\partial \bar{c}_k} \dot{\bar{c}}_k + \varepsilon^2 \frac{\partial \eta_{i,2}}{\partial \bar{c}_k} \dot{\bar{c}}_k + \dots = \\ & \varepsilon F_i(\hat{c}, \bar{f}) + \varepsilon^2 \sum_{k=1}^6 \left[\frac{\partial F_i}{\partial \bar{c}_k} \right]_{\text{mean elements}} \eta_{i,1} + \dots \end{aligned}$$

$$\text{for } i = 1, 2, \dots, 5; \quad k = 1, 2, \dots, 6 \quad (2.127)$$

$$\begin{aligned} & \left[\bar{n} + \varepsilon A_{6,1}(\hat{c}) + \varepsilon^2 A_{6,2}(\hat{c}) + \dots \right] + \varepsilon \frac{\partial \eta_{6,1}}{\partial \bar{c}_k} \dot{\bar{c}}_k + \varepsilon^2 \frac{\partial \eta_{6,2}}{\partial \bar{c}_k} \dot{\bar{c}}_k + \dots = \\ & \bar{n} - \varepsilon \frac{3}{2} \frac{\bar{n}}{\bar{c}_1} \eta_{1,1} + \varepsilon^2 \left(\frac{15}{8} \frac{\bar{n}}{\bar{c}_1^2} \eta_{1,1}^2 - \frac{3}{2} \frac{\bar{n}}{\bar{c}_1} \eta_{1,2} \right) + \dots \\ & + \varepsilon F_6(\hat{c}, \bar{f}) + \varepsilon^2 \sum_{k=1}^6 \left[\frac{\partial F_6}{\partial \bar{c}_k} \right]_{\text{mean elements}} \eta_{6,1} + \dots \end{aligned}$$

It is of importance to analyze the term $\left(\varepsilon \frac{\partial \eta_{i,1}}{\partial \bar{c}_k} \dot{\bar{c}}_k \right)$ with the understanding that $\left(\dot{\bar{c}}_k = \frac{d\bar{c}_k}{dt} \right)$.

When $k = 1, 2, \dots, 5$, these terms are on the order of ε^2 or higher, since each term in the first equation of (2.118) contains powers of ε . When $k = 6$, a term of the order of ε results, since the leading term in the second equation of (2.118) does not contain a power of ε (refer to equations (2.128) for detail):

$$\varepsilon \frac{\partial \eta_{i,1}}{\partial \bar{c}_k} \dot{\bar{c}}_k = \varepsilon \frac{\partial \eta_{i,1}}{\partial \bar{c}_k} \frac{d\bar{c}_k}{dt} = \varepsilon \left(\varepsilon A_{i,1}(\hat{c}) + \varepsilon^2 A_{i,2}(\hat{c}) + \dots \right) \frac{\partial \eta_{i,1}}{\partial \bar{c}_k}$$

for $k = 1, 2, \dots, 5$

for $i = 1, 2, \dots, 5$

(2.128)

$$\varepsilon \frac{\partial \eta_{i,1}}{\partial \bar{c}_6} \dot{\bar{c}}_6 = \varepsilon \frac{\partial \eta_{i,1}}{\partial \bar{f}} \frac{d\bar{f}}{dt} = \varepsilon \left(\bar{n} + \varepsilon A_{6,1}(\hat{c}) + \varepsilon^2 A_{6,2}(\hat{c}) + \dots \right) \frac{\partial \eta_{i,1}}{\partial \bar{f}}$$

for $k = 6$

The term $\left(\varepsilon \frac{\partial \eta_{i,1}}{\partial \bar{f}} \bar{n} \right)$ is, obviously, on the order of ε . This detail is extremely important in the next step of this derivation--equating like powers of ε in equations (2.127):

$$A_{i,1}(\hat{c}) + \frac{\partial \eta_{i,1}}{\partial \bar{f}} \bar{n} = F_i(\hat{c}, \bar{f})$$

for $i = 1, 2, \dots, 5$

(2.129)

$$A_{6,1}(\hat{c}) + \frac{\partial \eta_{6,1}}{\partial \bar{f}} \bar{n} = F_6(\hat{c}, \bar{f}) - \frac{3}{2} \frac{\bar{n}}{\bar{c}_1} \eta_{1,1}$$

Re-arranging these equations provides a clean form for the first order contributions to the osculating element equations of motion in terms of mean elements; the osculating equations of motion in terms of osculating elements in (2.115) have been transformed to osculating equations of motion in terms of mean elements:

$$F_{\text{osc EOM}_i}(\hat{c}, \bar{f}) = A_{i,1}(\hat{c}) + \frac{\partial \eta_{i,1}}{\partial \bar{f}} \bar{n}$$

$$\text{for } i = 1, 2, \dots, 5 \quad (2.130)$$

$$F_{\text{osc EOM}_6}(\hat{c}, \bar{f}) = A_{6,1}(\hat{c}) + \frac{\partial \eta_{6,1}}{\partial \bar{f}} \bar{n} + \frac{3}{2} \frac{\bar{n}}{c_1} \eta_{1,1}$$

Intuitively, these equations seem correct; the osculating rates (to first order) are equal to the mean contributions (the "A" terms) plus the short period contributions (the "η" terms). These equations can again be re-arranged to yield expressions for the mean element rates (to first order):

$$A_{i,1}(\hat{c}) = F_{\text{osc EOM}_i}(\hat{c}, \bar{f}) - \frac{\partial \eta_{i,1}}{\partial \bar{f}} \bar{n}$$

$$\text{for } i = 1, 2, \dots, 5 \quad (2.131)$$

$$A_{6,1}(\hat{c}) = F_{\text{osc EOM}_6}(\hat{c}, \bar{f}) - \frac{\partial \eta_{6,1}}{\partial \bar{f}} \bar{n} - \frac{3}{2} \frac{\bar{n}}{c_1} \eta_{1,1}$$

Once again, these equations seem intuitively correct; the mean rates (to first order) are equal to the osculating rates minus the short period contributions.

The mean fast variable that remains in these equations still contributes short-period variations to the motion. The next step is to use the averaging operation to remove the fast variable dependence in these equations, which removes short-period variations from the long-period and secular variations to the motion. What results is an expression for the

mean element rates in terms of mean elements. If these mean element rates are then subtracted from the osculating element rates, equations of motion for the short-period variations in terms of the mean elements result.

As stated earlier in the chapter, the $A_{w,x}$ terms in (2.130) and (2.131) contain no short-period contributions (when the forms for the mean element equations of motion were given in (2.118), it was assumed that the $A_{w,x}$ terms did not contain the fast variable). The $F_{oscEOMi}$ (for $i = 1, 2, \dots, 6$) are functions of the mean elements (including the mean fast variable); therefore, these functions will contribute short period variations. Similarly, the η terms will contribute short period variations (remember, $\eta_{i,order}$ are functions representing the short-period terms that are 2π periodic in \bar{f}). The averaging operation is used to "strip" these short period contributions.

The averaging operation for some function can be defined as follows:

$$\langle \text{Function}(\hat{c}, \bar{f}) \rangle_{\bar{f}} = \frac{1}{2\pi} \int_0^{2\pi} \text{Function}(\hat{c}, \bar{f}) d\bar{f} \quad (2.132)$$

With this definition, the averaging operation is a definite integral over the fast variable.

Term-by-term averaging of equations (2.131) can now be performed:

$$\left\langle A_{i,1}(\hat{C}) \right\rangle_{\bar{f}} = \left\langle F_{\text{osc EOM}_i}(\hat{C}, \bar{f}) \right\rangle_{\bar{f}} - \left\langle \frac{\partial \eta_{i,1}}{\partial \bar{f}} \bar{n} \right\rangle_{\bar{f}}$$

$$\text{for } i = 1, 2, \dots, 5 \quad (2.133)$$

$$\left\langle A_{6,1}(\hat{C}) \right\rangle_{\bar{f}} = \left\langle F_{\text{osc EOM}_6}(\hat{C}, \bar{f}) \right\rangle_{\bar{f}} - \left\langle \frac{3}{2} \frac{\bar{n}}{c_1} \eta_{1,1} \right\rangle_{\bar{f}} - \left\langle \frac{\partial \eta_{6,1}}{\partial \bar{f}} \bar{n} \right\rangle_{\bar{f}}$$

Both expressions in (2.133) can be simplified through the use of properties of the averaging operation (given by McClain [38]). Two such properties that will help in eliminating the short period contributions are:

$$\left\langle \rho \text{ Function}(\hat{C}, \bar{f}) \right\rangle_{\bar{f}} = \rho \left\langle \text{Function}(\hat{C}, \bar{f}) \right\rangle_{\bar{f}}$$

$$(2.134)$$

$$\left\langle \frac{\partial \text{Function}(\hat{C}, \bar{f})}{\partial \bar{c}_k} \right\rangle_{\bar{f}} = \frac{\partial}{\partial \bar{c}_k} \left\langle \text{Function}(\hat{C}, \bar{f}) \right\rangle_{\bar{f}} \quad \text{for } k = 1, 2, \dots, 6$$

where ρ is any function independent of \bar{f} . Using these two properties and knowing the functions $\eta_{i,\text{order}}$ are 2π periodic in \bar{f} , the following can be shown:

$$\left\langle \frac{\partial \eta_{i,1}}{\partial \bar{f}} \bar{n} \right\rangle_{\bar{f}} = 0 \quad (2.135)$$

Using the same reasoning, it can also be shown that:

$$\left\langle \frac{3}{2} \frac{\bar{n}}{c_1} \eta_{1,1} \right\rangle_{\bar{f}} = 0 \quad (2.136)$$

The relations in (2.135) and (2.136) hold due to the fact that the "η" terms are 2π periodic in \bar{f} . In effect, only enough is assumed about these terms to make them vanish. If these terms are assumed to be centered about the mean element trajectory (similar to a generic sine wave being symmetric about the "X" axis), they will go to zero if they are 2π periodic.

Furthermore, when the functions containing the fast variable are averaged over the fast variable, the dependence upon the fast variable is removed. Take, for example, the hypothetical situation in which:

$$F_i(\hat{c}, \bar{f}) = \bar{\omega} \cos \bar{f} \quad (2.137)$$

then

$$\langle F_i(\hat{c}, \bar{f}) \rangle_{\bar{f}} = \frac{1}{2\pi} \int_0^{2\pi} \bar{\omega} \cos \bar{f} \, d\bar{f} = 0 \quad (2.138)$$

since the cosine function is 2π periodic. However, this derivation does not need to be limited to pure sines and cosines; whenever a definite integral with respect to a certain variable is performed, the certain variable in these equations is replaced by the limits of integration. In other words, the definite integral is performed, and the certain variable is removed. This is the heart of the method of averaging. Whenever a function is averaged with respect to the fast variable, a definite integral is performed and the fast variable is replaced with the limits of integration. The function now represents its "average value" over the averaging interval. In this fashion, the fast variable has been removed (or, replaced), as well as the short-period variations.

Substituting (2.135) and (2.136) into (2.133), and using the argument just described, expressions for the mean element equations of motion in terms of the mean elements result:

$$A_{i,1}(\hat{\mathbf{c}}) = \left\langle F_{\text{osc EOM}_i}(\hat{\mathbf{c}}, \bar{f}) \right\rangle_{\bar{f}} = F_{\text{mean EOM}_i}(\hat{\mathbf{c}}) \quad , \quad \text{for } i = 1, 2, \dots, 5$$

(2.139)

$$A_{6,1}(\hat{\mathbf{c}}) = \left\langle F_{\text{osc EOM}_6}(\hat{\mathbf{c}}, \bar{f}) \right\rangle_{\bar{f}} = F_{\text{mean EOM}_6}(\hat{\mathbf{c}})$$

In which $\left\langle A_{i,1}(\hat{\mathbf{c}}) \right\rangle_{\bar{f}} = A_{i,1}(\hat{\mathbf{c}})$ and $\left\langle A_{6,1}(\hat{\mathbf{c}}) \right\rangle_{\bar{f}} = A_{6,1}(\hat{\mathbf{c}})$ since the $A_{i,1}$ terms are not functions of the fast variable.

If the expressions in (2.139) are subtracted out of the osculating element equations of motion given in (2.130), the short period equations of motion in terms of the mean elements are obtained:

$$F_{\text{osc EOM}_i}(\hat{\mathbf{c}}, \bar{f}) - A_{i,1}(\hat{\mathbf{c}}) = \frac{\partial \eta_{i,1}}{\partial \bar{f}} \bar{n} \quad , \quad \text{for } i = 1, 2, \dots, 5$$

(2.140)

$$F_{\text{osc EOM}_6}(\hat{\mathbf{c}}, \bar{f}) - A_{6,1}(\hat{\mathbf{c}}) = \frac{\partial \eta_{6,1}}{\partial \bar{f}} \bar{n} + \frac{3}{2} \frac{\bar{n}}{\bar{c}_1} \eta_{1,1}$$

or, for consistent notation:

$$F_{\text{SP EOM}_i}(\hat{\mathbf{c}}, \bar{f}) = \frac{\partial \eta_{i,1}}{\partial \bar{f}} \bar{n} \quad , \quad \text{for } i = 1, 2, \dots, 5$$

(2.141)

$$F_{\text{SP EOM}_6}(\hat{\mathbf{c}}, \bar{f}) = \frac{\partial \eta_{6,1}}{\partial \bar{f}} \bar{n} + \frac{3}{2} \frac{\bar{n}}{\bar{c}_1} \eta_{1,1}$$

The equations in (2.139) and (2.141) represent the first order mean element rates and the short period rates, respectively (both in terms of the mean elements). A semianalytic propagator would independently propagate each set of these equations. The mean element equation of motion propagation is usually accomplished through the use of numeric techniques, since complex force models can be used and the accurate results inherent in these techniques can be obtained in an efficient manner. The short-period terms, which drive step size requirements in numeric techniques, have been removed in the mean element equations of motion. Therefore, step size requirements will be driven by the much lower frequency long-period variations. These larger step sizes allow for an efficient propagation in terms of computational time.

The short-period equations of motion can be propagated either analytically or numerically. Often times, these short-period variations are reconstructed analytically through the use of Fourier series representation (all computational benefits are lost if numerical integration is used); the Fourier series models the short-period equations of motion as a series potentially containing a constant plus sine and cosine waves, the integration of which is trivial. The coefficients of this Fourier series are slowly varying. At a desired output time, the short period contributions are added into the mean elements which arise from the propagation of the mean element equations of motion. In this manner, all of the secular, short-period, and

long-period contributions to the motion can be accounted for in the determination of satellite ephemerides.

As an example, an expression for the gravitational potential in terms of equinoctial elements averaged over λ with the other variables held constant during the integration can be given [7]:

$$U_{n,m}^* = \frac{\mu}{a} \left(\frac{R_e}{a} \right)^n C_{n,m}^* e^{-jm\theta} \sum_{s=-n}^n V_{n,s}^m S_{2n}^{(m,s)}(p,q) Y_0^{-n-1,s}(k,h) \quad (2.142)$$

where

$$Y_0^{n,m} = \frac{1}{2\pi} \int_0^{2\pi} \left(\frac{r}{a} \right)^n e^{jmL} d\lambda \quad (2.143)$$

2.3.2 Semianalytic Propagators and Orbit Determination

Semianalytic propagators play a major role in orbit determination (OD). A semianalytic propagator can be thought of as an estimation tool which propagates a set of elements through a desired time period--either forward or backward in time; all contributions to the motion from perturbations are accounted for to produce an estimate of the satellite state at the end of the desired time period. An OD system relates these estimates to actual observations made with satellite tracking hardware. The OD system can then minimize the difference between these observed and estimated values (this difference is often referred to as the state residual) through the use of a differential correction process (in actuality, the weighted least square of this difference is minimized). Within this differential correction process, an iteration is performed to produce estimates which match the observations (or,

minimizes the difference between the two). This iteration consists of the following (assuming a satellite state is available at the specified epoch):

1. Estimate the satellite's trajectory over the desired time period with the orbit propagator. Output can consist of state estimates at the end of the desired time period or at multiple intervals within this time period.
2. Obtain actual observations at the same output times as in Step 1 with the OD system using tracking hardware.
3. Compare predicted state with the actual observations at a given time.
4. Compute the state residual.
5. If the residual is large, adjust the initial state (i.e., elements) and input these to Step 1 to find new state estimates.
6. Repeat until the state residual is within some acceptable tolerance.

In this manner, an OD system can potentially make several calls to an orbit propagator in an attempt to accurately determine an orbit.

[This page intentionally left blank.]

Chapter 3

Stability Testing

3.1 Background

One of the primary tasks of this study was to investigate the Legendre polynomials, associated Legendre polynomials, Jacobi polynomials, Hansen coefficients, and harmonic coefficients. This investigation was undertaken to determine whether the computation of these components (or their products) in the expansion to the 50x50 gravity field would cause a violation of machine boundary limits or a loss of accuracy for high degree and order. If a violation occurred with this expansion, then a switch to normalized components of the potential would be in order. As an example, Cowell theory contains a product of Legendre or associated Legendre polynomials and the harmonic coefficients. This product is evident in the spherical harmonic form of the geopotential:

$$\Psi = -\frac{\mu}{r} \left[1 + \sum_{n=2}^{\infty} \sum_{m=0}^n \left(\frac{R_e}{r} \right)^n P_{n,m}(\sin \phi) (C_{n,m} \cos m\lambda + S_{n,m} \sin m\lambda) \right] \quad (3.1)$$

where

μ is the gravitational parameter

R_e is the mean equatorial radius of the earth

r is the distance to the satellite from the origin of the coordinate system

reference frame

$P_{n,m}(x)$ is an associated Legendre polynomial of degree n , order m , and argument x

ϕ is the satellite's latitude measured relative to the coordinate system reference frame

$C_{n,m}, S_{n,m}$ are the spherical harmonic coefficients which are determined empirically for a given body

λ the body-fixed longitude of the satellite (measured positive eastward from the Greenwich Meridian)

Normalized components possess sizes that are much better conditioned than the corresponding un-normalized components; hence, they avoid the limits prescribed by machine boundaries. Lundberg and Schutz [36] provide one typical set of expressions which govern the transformation process from un-normalized to normalized values:

$$N_{n,m} = \left[\frac{(n-m)! (2n+1) (2-\delta_{0,m})}{(n+m)!} \right]^{1/2} \quad (3.2)$$

with

$$\bar{P}_{n,m} = N_{n,m} P_{n,m}, \quad \bar{C}_{n,m} = \frac{C_{n,m}}{N_{n,m}}, \quad \bar{S}_{n,m} = \frac{S_{n,m}}{N_{n,m}} \quad (3.3)$$

such that

$$\bar{P}_{n,m} \bar{C}_{n,m} = P_{n,m} C_{n,m}, \quad \bar{P}_{n,m} \bar{S}_{n,m} = P_{n,m} S_{n,m} \quad (3.4)$$

where the Kronecker delta function is non-zero only when the order m is equal to zero.

This chapter highlights the formulae used to compute the Legendre polynomials, associated Legendre polynomials, Jacobi polynomials, and Hansen coefficients in the Cowell and SST (mean element and short-periodic) branches of GTDS. The test tools and techniques for this study will be described, as well as the results stemming from the computation of these components. This testing will include a comparison of these components with "truth" values.

3.2 Cowell Truth Model Description and Test Set-Up

For this study, normalized recursions for Legendre and associated Legendre polynomials were built into a Q-floating standalone routine to compute Cowell accelerations. These normalized recursions are given by Lundberg and Schutz [36]:

$$\bar{P}_{n,m}(\sin \phi) = \cos^m \phi A_{n,m}(\sin \phi) \quad (3.5)$$

where $\bar{P}_{n,m}$ are the normalized polynomials and ϕ is the geocentric latitude. If the degree and order combination (n,m) indicates a sectorial term or a term in which the order m equals $(n-1)$, $A_{n,m}$ takes the corresponding form:

$$A_{n,n} = \frac{(2n-1)!}{2^{n-1} (n-1)!} \quad (3.6)$$

$$A_{n,n-1} = \sin \phi \left| \frac{(2n-1)!}{2^{n-1} (n-1)!} \right| \quad (3.7)$$

For the zonal harmonics and remaining tesseral harmonics (i.e., with the exception of the aforementioned condition of $m = [n-1]$), $A_{n,m}$ is computed with the following equation:

$$A_{n,m} = \frac{\bar{A}_{n,m}}{N_{n,m}} \quad (3.8)$$

where $N_{n,m}$ is the normalization factor described in the preceding section and $\bar{A}_{n,m}$ is as follows:

$$\bar{A}_{n,m} = \sin \phi \left[\frac{(2n+1)(2n-1)}{(n-m)(n+m)} \right]^{1/2} \bar{A}_{n-1,m} - \left[\frac{(2n+1)(n-m-1)(n+m-1)}{(2n-3)(n+m)(n-m)} \right]^{1/2} \bar{A}_{n-2,m} \quad (3.9)$$

It should be noted that the recursion for $\bar{A}_{n,m}$ in (3.9) is one of six given by Lundberg and Schutz. In the other recursions, the onset of instability occurs sooner and increases more quickly than for the recursion given here. For this reason, Lundberg and Schutz recommend the use of (3.9) for studies involving large values of degree and order.

The first step in utilizing the standalone truth model was to verify that it was coded correctly. This truth model contains an independent coding of the equations given in Section 2.2.1, *Cowell Mathematical Techniques*. In this manner, the truth model is analogous to subroutine SPART within GTDS in that they both compute Cowell accelerations. The differences between the truth model and SPART are two-fold: (1) the truth model uses the Lundberg recursions, while GTDS uses the recursions outlined in the GTDS Math Specification [26] and (2) the truth model contains an independent coding of the equations offered in 2.2.1--not a "cut" and "paste" copy of what is inside of SPART. Results produced from the Cowell functionality within GTDS are accepted as truth for the 21x21 class models GTDS is configured to implement. For this reason, if the Legendre polynomials, associated Legendre polynomials, and Cowell accelerations obtained from the truth model match the corresponding components from SPART, they can also be accepted as truth.

To this end, values for the polynomials were outputted from subroutine SPART in a DEBUG run of the un-modified version of GTDS on the VAX. It should be noted that the un-modified version of GTDS represents the previously tested 21x21 un-normalized capability. In addition, polynomials outputted from the truth model needed to be un-normalized for comparison purposes. Table 3.1 offers comparison results for four representative degree and order pairs (one zonal, one sectorial, and two tesseral terms; one tesseral term matches the condition where $m = n - 1$ as in (3.7) above):

**Table 3.1 Un-Normalized Polynomial Validation
GTDS vs. Lundberg Truth**

(n,m)	GTDS Value	Truth Value
(21,0)	0.385389365005720	0.385389365005720017620934469614764
(21,21)	405012060.632803	405012060.632780532468925736115058
(21,5)	354542.107743601	354542.107743597065734097685187394
(21,20)	-2442182686.11423	-2442182686.11409981594492291939271

The results presented in Table 3.1, which are representative of results for several other test cases and for other degree and order pairs, indicate that the recursions for the Legendre and associated Legendre polynomials were coded correctly for the truth model.

The initial conditions for this test are summarized in Table 3.2:

Table 3.2 Initial Condition Summary

Initial Condition	Value
Inertial S/C Coordinate, X	180.295260378399 km
Inertial S/C Coordinate, Y	-1145.13224944286 km
Inertial S/C Coordinate, Z	-6990.09446227757 km
Geocentric Longitude	-4.09449590512370 rad
Geocentric Latitude	-1.40645188850273 rad
Radius of Earth, R_e (GEM10B)	6378.138 km
Gravitational Parameter, μ (GEM10B)	398600.44 km ³ /sec ²
Truth Model Precision	Q-floating, REAL*16, VAX
GTDS Precision	G-floating, REAL*8, VAX (standard)

Similarly, results for Cowell accelerations are presented in Table 3.3:

**Table 3.3 Cowell Acceleration Validation
GTDS vs. Lundberg Truth (21x21 GEM10B)**

	GTDS Value	Lundberg Truth Value
ax_b	8.653210294968294E-7	8.653210294968288481236474144803601E-7
ay_b	-6.515584998975128E-6	-6.515584998975091510625442206439533E-6
az_b	-1.931032474628621E-5	-1.931032474628616528394963271551205E-5

It is of importance to note that GEM10B coefficients were used for this test since the unmodified version of GTDS (21x21 field capability, un-normalized coefficients and polynomials) is not configured to implement GEMT3 class coefficients. Furthermore, the

test case described here represents only one discrete point along the Cowell integration; for full validation and calibration, several points needed to be tested. The results of the other points were in accordance with this test and, for the sake of brevity, are not documented herein. After this testing, the truth model was determined to be properly implemented.

The next step was to isolate the recursions used for the polynomials in the Cowell portion of GTDS and attempt to push them to the 50x50 capability in the un-normalized manner. If this process was successful, then comparisons of the new version of GTDS (50x50 field capability, un-normalized coefficients and polynomials) could be made against the truth model. If this process was not successful, then modifications to implement normalized recursions for the polynomials and normalized coefficients would have to be accomplished before comparisons could be made to the truth model. It should be noted that the truth model explained in this section applies solely to Legendre polynomials, associated Legendre polynomials, and Cowell accelerations; the validation of a 50x50 field for orbit determination purposes is discussed in Chapter 5.

3.3 Cowell Testing for 50x50 Fields

The recursions used by GTDS for the Legendre and associated Legendre polynomials in the Cowell orbit generator are found in the GTDS Math Specification [26]:

$$P_{n,0}(\sin \phi) = \frac{(2n-1)(\sin \phi) P_{n-1,0}(\sin \phi) - (n-1) P_{n-2,0}(\sin \phi)}{n} \quad (3.10)$$

$$P_{n,m}(\sin \phi) = P_{n-2,m}(\sin \phi) + (2n-1)(\cos \phi) P_{n-1,m-1}(\sin \phi) \quad (3.11)$$

$$P_{n,n}(\sin \phi) = (2n-1)(\cos \phi) P_{n-1,n-1}(\sin \phi) \quad (3.12)$$

which represent recursions for the zonal, tesseral, and sectorial harmonic terms, respectively. The following initial conditions apply:

$$P_{0,0}(\sin \phi) = 1 \quad (3.13)$$

$$P_{1,0}(\sin \phi) = \sin \phi \quad (3.14)$$

$$P_{1,1}(\sin \phi) = \cos \phi \quad (3.15)$$

It was found to be somewhat tedious to run GTDS on the VAX under the DEBUG option in order to simply test the recursions or obtain Cowell accelerations. For this reason, a VAX standalone version of subroutine SPART was developed to emulate the actual GTDS version. The use of the GTDS emulation provided the capability to test the stability of the recursions and product of the polynomials and harmonic coefficients without modifying the actual GTDS code. If the stability was found to be insufficient in this manner, time would not have been wasted in (1) modifying a large program (GTDS with 1000 subroutines and approximately 125,000 lines of code) to use 50x50 coefficients in an un-normalized fashion, (2) getting the program to compile, link, and run, (3) having the underflow or overflow boundaries violated, and (4) re-modifying the code for a 50x50, normalized gravity field model. In other words, this method was chosen in an attempt to maximize efficiency and to eliminate non-productive efforts.

For verification and calibration of the GTDS emulation, a 21x21 GEM10B run was established and compared against the un-modified version of GTDS (21x21 capability, un-normalized coefficients and polynomials). Results for this validation test for polynomials are included in Table 3.4 and for Cowell accelerations in Table 3.5:

**Table 3.4 Un-Normalized Polynomial Validation
GTDS Emulation vs. Actual GTDS**

Degree and Order	GTDS Emulation Value	GTDS Value
n = 21, m = 0, zonal	0.385389365005720	0.385389365005720
n = 21, m = 21, sectorial	405012060.632779	405012060.632803
n = 21, m = 5, tesseral	354542.107743596	354542.107743601
n = 21, m = 20, m = n-1	-2442182686.11409	-2442182686.11423

**Table 3.5 Cowell Acceleration Validation
GTDS Emulation vs. Actual GTDS (21x21 GEM10B)**

	GTDS Emulation Value	GTDS Value
ax_b	8.653210294968284E ⁻⁷	8.653210294968294E ⁻⁷
ay_b	-6.515584998975087E ⁻⁶	-6.515584998975128E ⁻⁶
az_b	-1.931032474628619E ⁻⁵	-1.931032474628621E ⁻⁵

Again, the initial conditions presented in Table 3.2 hold, as well as the consistency of results with other degree and order pairs and other points along the Cowell integration. The accuracy of the standalone GTDS emulation is sufficient for test purposes.

A brute force approach using GEMT3 harmonic coefficients was chosen to initially test the ability of recursions (3.10) through (3.12) to handle the 50x50 capability on the VAX. In other words, the loops controlling the computation of the polynomials and the Cowell accelerations were increased to handle the 50x50 capability; during the execution of the run, if an error message was delivered stating that an underflow or overflow error occurred, then it would be obvious that a switch to normalized coefficients would be in order.

When this test was executed, no error message was received. Results comparing the 50x50 un-normalized polynomials (GTDS emulation) with Lundberg truth values are presented in Table 3.6 (again, the truth polynomials needed to be un-normalized for comparison purposes):

**Table 3.6 Un-Normalized Polynomial Validation
GTDS Emulation vs. Lundberg Truth**

(n,m)	GTDS Emulation Value	Lundberg Truth
(50,0)	9.634780379822722E-002	9.634780379823085161812315709569356E-0002
(50,50)	1.334572710963763E+039	1.334572710963775698820557920992278E+0039
(50,21)	-1.443200082785759E+028	-14432000827857661203015450149.6553
(50,49)	-8.047341511222794E+039	-8.047341511222872817916340126813171E+0039

Similarly, Cowell accelerations between the GTDS emulation and Lundberg truth for a 50x50 field could be compared to ensure that the Cowell accelerations were correct (remember, Chapter 5 will discuss the impact upon orbit determination of 50x50 fields within the modified version of GTDS).

**Table 3.7 Cowell Acceleration Validation
GTDS Emulation vs. Lundberg Truth (50x50 GEMT3)**

	GTDS Emulation Value	Lundberg Truth Value
ax_b	8.683465146150188E-007	8.683465146150193614319424992827359E-0007
ay_b	-6.519678538340073E-006	-6.519678538340080232354478851469384E-0006
az_b	-1.931876804829165E-005	-1.931876804829163932564593223959640E-0005

Again, the initial conditions of Table 3.2 hold, with the exception of GEMT3 values for the gravitational parameter and radius of the earth ($398600.436 \text{ km}^3/\text{sec}^2$ and 6378.137 km , respectively).

The GTDS emulation also serves to simulate the Sun Workstation (REAL*8 precision) and Silicon Graphics (REAL*8 precision) environments. Both of these environments are in accordance with the VAX G-floating GTDS emulation described in this section (refer to Chapter 1, Table 1.3). Therefore, the VAX, Sun Workstation, and Silicon Graphics environments will all support the 50x50 field with un-normalized harmonic coefficients and un-normalized polynomials in their Cowell orbit generators.

Initial testing shows that a switch to normalized coefficients and normalized polynomials is in order for the IBM mainframe. Even though the IBM system may be able to support 50x50 gravity fields, the machine limits are nearly violated with fields of this size; any future modifications to further increase the size of the gravity field will require the use of normalized polynomials and harmonic coefficients. Therefore, action to modify the IBM code to support larger gravity field models in a normalized fashion should be made as soon as possible. To this end, work has been done at Goddard to implement normalized coefficients and polynomials in their version of GTDS [27]. Specifically, Goddard's version of GTDS has been configured to implement 50x50, normalized GEMT3 coefficients.

3.4 Stability Testing for Semianalytic Theory

In Chapter 2, the equinoctial form of the potential used by the semianalytic orbit generator of GTDS was derived:

$$U = \sum_{n=2}^{\infty} \sum_{m=0}^n \sum_{s=-n}^n \sum_{t=-\infty}^{\infty} U_{n,m,s,t} \quad (3.16)$$

in which

$$U_{n,m,s,t} = \text{Real} \left\{ U_{n,m,s,t}^* \right\} \quad (3.17)$$

and

$$U_{n,m,s,t}^* = \frac{\mu}{a} \left(\frac{R_e}{a} \right)^n C_{n,m}^* \sum_{s=-n}^n V_{n,s}^m S_{2n}^{(m,s)}(p,q) \sum_{t=-\infty}^{+\infty} Y_t^{-n-1,s}(k,h) e^{j(t\lambda - m\theta)} \quad (3.18)$$

where the $Y_t^{-n-1,s}(k,h)$ terms are modified Hansen coefficients and the $S_{2n}^{(m,s)}(p,q)$ terms contain embedded expressions for the Jacobi polynomials, $P_u^{v,w}(\gamma)$. As mentioned in the introduction to this chapter, the stability of the Hansen coefficients and Jacobi polynomials required investigation. Specifically, it was desirable to determine if a loss of accuracy would occur in the computation of these quantities at the higher values of degree and order characteristic of this thesis. Proulx *et al* [47] provide recursions which are representative of those used in the semianalytic orbit generator of GTDS. Sections 3.4.1 and 3.4.2 describe the stability testing of these representative recursions for the Jacobi polynomials and Hansen coefficients, respectively.

3.4.1 Jacobi Polynomial Stability Testing

In Chapter 2, the following analytic expression was given to compute the Jacobi polynomials:

$$P_n^{a,b}(\gamma) = \frac{\Gamma(a+n+1)}{n! \Gamma(a+b+n+1)} \sum_{m=0}^n \binom{n}{m} \frac{\Gamma(a+b+n+m+1)}{2^m \Gamma(a+m+1)} (\gamma-1)^m \quad (3.19)$$

In order to enhance efficiency, GTDS computes these polynomials recursively [47]:

$$\begin{aligned} & 2u(u+v+w)(2u+v+w-2) P_u^{v,w}(\gamma) = \\ & (2u+v+w-1) [(2u+v+w)(2u+v+w-2)\gamma + v^2 - w^2] P_{u-1}^{v,w}(\gamma) \\ & - 2(u+v-1)(u+w-1)(2u+v+w) P_{u-2}^{v,w}(\gamma) \end{aligned} \quad (3.20)$$

subject to the initial conditions

$$\begin{aligned} P_{-1}(\gamma) &= 0 \\ P_0(\gamma) &= 1 \end{aligned} \quad (3.21)$$

where

$$\gamma = \frac{1-p^2-q^2}{1+p^2+q^2} = \cos i \quad (3.22)$$

This recursion can be re-expressed as a function of the indices given in (3.16):

$$\begin{aligned} (n-m+1)(n+m+1)(n) P_{n-m+1}^{\alpha, \beta} &= (2n+1)[(n+1)(n)\gamma - m|s|] P_{n-m}^{\alpha, \beta} \\ - (n-|s|)(n+|s|)(n+1) P_{n-m-1}^{\alpha, \beta} \end{aligned} \quad (3.23)$$

for the polynomial $P_{n-m+1}^{m-|s|, m+|s|}$ with $|s| \leq m$, $s \geq 0$, or:

$$\begin{aligned} (n-m+1)(n+m+1)(n) P_{n-m+1}^{\alpha, \beta} &= (2n+1)[(n+1)(n)\gamma + m|s|] P_{n-m}^{\alpha, \beta} \\ - (n-|s|)(n+|s|)(n+1) P_{n-m-1}^{\alpha, \beta} \end{aligned} \quad (3.24)$$

for the polynomial $P_{n-m+1}^{m+|s|, m-|s|}$ with $|s| \leq m$, $s < 0$, or:

$$\begin{aligned} (n-|s|+1)(n+|s|+1)(n) P_{n-|s|+1}^{\alpha, \beta} &= (2n+1)[(n+1)(n)\gamma - m|s|] P_{n-|s|}^{\alpha, \beta} \\ - (n-m)(n+m)(n+1) P_{n-|s|-1}^{\alpha, \beta} \end{aligned} \quad (3.25)$$

for the polynomial $P_{n-|s|+1}^{|s|-m, |s|+m}$ with $|s| > m$, $s \geq 0$, and finally:

$$\begin{aligned} (n-|s|+1)(n+|s|+1)(n) P_{n-|s|+1}^{\alpha, \beta} &= (2n+1)[(n+1)(n)\gamma + m|s|] P_{n-|s|}^{\alpha, \beta} \\ - (n-m)(n+m)(n+1) P_{n-|s|-1}^{\alpha, \beta} \end{aligned} \quad (3.26)$$

for the polynomial $P_{n-|s|+1}^{|s|+m, |s|-m}$ with $|s| > m$, $s < 0$.

Inherent in equations (3.23) through (3.26) are four distinct branches--the relationship between $|s|$ and m establishes two branches, each of which has a sub-branch dependent upon the sign of s .

The methodology used to test stability was as follows:

- (1) Compute the Jacobi polynomials using REAL*8 precision
- (2) Compute the Jacobi polynomials using REAL*16 precision
- (3) Sanity check results of (1) & (2) with *Mathematica*
- (4) Determine relative error between REAL*8 and REAL*16 implementations

The relative error was determined in the following way:

$$\frac{\text{REAL*16 polynomial} - \text{REAL*8 polynomial}}{\text{REAL*16 polynomial}} \quad (3.27)$$

A standalone routine was built to compute the polynomials. Within this routine, the following ranges were established for the indices of interest:

$$\begin{aligned} \text{range of } s &= -n \Rightarrow n \text{ or } -50 \Rightarrow 50 \\ \text{range of } m &= 0 \Rightarrow n \text{ or } 0 \Rightarrow 50 \end{aligned} \quad (3.28)$$

The range for the degree n was dependent upon the relationship between the absolute value of s and m . If $|s| \leq m$, the degree loop began at the value of m ; if $|s| > m$, the degree loop began at $|s|$. These definitions avoided the singularities inherent in the recursion for the Jacobi polynomials. In addition, these ranges ensured that all realistic cases for the 50x50 gravity field model would be tested. In other words, these ranges test all cases that GTDS would encounter.

An inclination of 98 degrees was used for the Jacobi polynomial testing. This value for inclination is characteristic of satellites in sun-synchronous orbits. Since the majority of Draper's recent work has focused on satellites in sun-synchronous, repeat groundtrack, frozen type orbits [30], this choice for inclination seemed logical. Specifically, the RADARSAT program [18] was particularly interested in modeling the high degree and order effects of the non-spherical earth perturbation.

The output of the standalone routine consisted of (1) a description of the polynomial pairs whose relative error was greater than 1.0D-13 and (2) variables containing the number of relative errors within the following ranges:

$$\begin{aligned}
& \text{relative error} > 1.0\text{D}-10 \\
& 1.0\text{D}-10 \leq \text{relative error} \leq 1.0\text{D}-11 \\
& 1.0\text{D}-11 < \text{relative error} \leq 1.0\text{D}-12 \\
& 1.0\text{D}-12 < \text{relative error} \leq 1.0\text{D}-13 \\
& 1.0\text{D}-13 < \text{relative error} \leq 1.0\text{D}-14 \\
& 1.0\text{D}-14 < \text{relative error} \leq 1.0\text{D}-15 \\
& 1.0\text{D}-15 < \text{relative error} \leq 1.0\text{D}-16 \\
& 1.0\text{D}-16 < \text{relative error} \leq 1.0\text{D}-17 \\
& 1.0\text{D}-17 < \text{relative error} \leq 1.0\text{D}-18 \\
& 1.0\text{D}-18 < \text{relative error} \leq 1.0\text{D}-19 \\
& \text{relative error} < 1.0\text{D}-19
\end{aligned} \tag{3.29}$$

Table 3.8 describes the four largest errors which were outputted from the standalone routine:

Table 3.8 Maximum Jacobi Polynomial Relative Errors

n	m	s	Relative Errors
30	7	26	7.446533373947289220519607685322614E-0013
30	26	7	7.446533373947289220519607685322614E-0013
48	17	32	5.511849112982165177465394764316413E-0011
48	32	17	5.511849112982165177465394764316413E-0011

In the relative errors listed in this table, the symmetry between s and m in (3.23) through (3.26) is evident.

The other relative errors listed in the output of the standalone routine were on the order of the first two entries in Table 3.8 and, in order to avoid unnecessary repetition, were not given here. It should also be re-emphasized that the values for the polynomials used to construct the relative errors listed in this table (as well as the values for several other

polynomials not listed in this table) were verified against polynomials generated with the intrinsic function **JacobiP** in *Mathematica*. This intrinsic function computes Jacobi polynomials for a given set of indices.

In all, a total of 82,075 polynomial pairs were analyzed (i.e. 82,075 REAL*8 values and 82,075 REAL*16 values). This total, however, does not account for the trivial cases in which the values of both the REAL*8 and the REAL*16 polynomials are zero. The error distribution is given in the following table:

Table 3.9 Jacobi Polynomial Relative Error Distribution

Error Range	Number of Errors
relative error > 1.0D-10	0
1.0D-10 ≤ relative error ≤ 1.0D-11	2
1.0D-11 < relative error ≤ 1.0D-12	0
1.0D-12 < relative error ≤ 1.0D-13	35
1.0D-13 < relative error ≤ 1.0D-14	483
1.0D-14 < relative error ≤ 1.0D-15	3753
1.0D-15 < relative error ≤ 1.0D-16	15804
1.0D-16 < relative error ≤ 1.0D-17	7324
1.0D-17 < relative error ≤ 1.0D-18	847
1.0D-18 < relative error ≤ 1.0D-19	58
relative error < 1.0D-19	53759

This table indicates that almost 54,000 of the errors are beyond the 1.0D-19 range. Of the remaining errors, the majority falls into the 1.0D-15 to 1.0D-16 range, which can be expected since this range encompasses the boundary of computed digits for REAL*8

variables. A total of 37 out of 82,075 errors (0.045 %) were larger than the output criteria of 1.0D-13. It should be noted that the two largest errors were for a polynomial (n=45, m=32, s=17 or n=45,m=17,s=32) with a relatively small value:

Table 3.10 Jacobi Polynomials for Maximum Relative Errors

Precision	Polynomial Value
REAL*8	19.0564826584949109644639975158498
REAL*16	19.0564826595452755348997439053899
<i>Mathematica</i>	19.05648265954527553489974390588687

where the value of the REAL*8 polynomial was extended to REAL*16 precision to ensure consistent mode operations for computational purposes (using the QEXTD intrinsic function on the VAX). This means that 8 significant decimal places of accuracy have been preserved for these entries. It is worth noting that all the Jacobi polynomial pairs listed in the output of the standalone routine retained at least this many significant decimal digits of accuracy.

The GEMT3 harmonic coefficients contain errors on the order of 1.0D-9 [35]. Since the relative errors in the Jacobi polynomials (as determined on the VAX) are smaller than the relative errors in the harmonic coefficients, the stability of the Jacobi polynomials can be considered sufficient. This stability can be extended to include Sun Workstations and Silicon Graphics Stations since the numerical boundaries for these environments are similar (reference Table 1.4).

3.4.2 Hansen Coefficient Stability Testing

In Chapter 2, the following expression for the Hansen coefficients was derived:

$$X_t^{-n-1,s} = (1 - e^2)^{(-n-1)+3/2} e^{|t-s|} \sum_{i=0}^{\infty} X_{i+a,i+b}^{(-n-1)s} e^{2i} \quad (3.30)$$

where $X_{i+a,i+b}^{(-n-1)s}$ are modified Newcomb operators, e is the orbital eccentricity, and $|t-s|$ is the D'Alembert characteristic. This expression represents a factored form of the Newcomb-Poincare power series representation given by (2.56). Both (2.56) and (3.30) contain Newcomb operator terms. The difference between the two sets of Newcomb operators stems from the factored term given in (3.30). For clarity, the coefficients in (2.56) are referred to as Newcomb operators, while the coefficients in (3.30) are referred to as *modified* Newcomb operators.

The factored form for the Hansen coefficients given by (3.30) offers much better convergence for high eccentricity cases (with no penalty for low eccentricity cases) than the classical form given by (2.56) [48]. For this reason, recursive formulae representing the factored form were used exclusively within GTDS. A power series representation of this factored form was also used in a standalone program to generate Hansen coefficients at Draper Laboratory [51]. Since this standalone program was readily available, it was chosen to generate truth values for the stability testing of the Hansen coefficients.

The philosophy used to test the stability of the Hansen coefficients is similar to the philosophy used to test the stability of the Jacobi polynomials:

- (1) Compute the Hansen coefficients recursively using REAL*8 precision
- (2) Compute the "truth" Hansen coefficients using REAL*16 precision with the standalone Hansen coefficient generator
- (3) Determine relative error between REAL*8 and REAL*16 implementations

The relative error was determined in the following way:

$$\frac{\text{REAL*16 coefficient} - \text{REAL*8 coefficient}}{\text{REAL*16 coefficient}} \quad (3.31)$$

The standalone program used to generate the truth Hansen coefficients for this thesis was developed in the early 1980's. This program computes two separate quantities: Hansen coefficients and Hansen coefficient kernels. The stability testing described in this section focuses on the kernels of the Hansen coefficients, which are defined in the following way:

$$K_t^{-n-1,s} = (1 - e^2)^{(-n-1)+3/2} \sum_{i=0}^{\infty} X_{i+a,i+b}^{(-n-1)s} e^{2i} \quad (3.32)$$

In this manner, the difference between the kernel and the actual Hansen coefficient is the $e^{|t-s|}$ term.

For computational purposes, the standalone program accepts an input value for a convergence criterion. Additional terms in the series representation are accumulated until successive values of the sum meet the convergence criterion. This converged sum of the series is multiplied by the $(1 - e^2)^{(-n-1)+3/2}$ term to provide Hansen coefficient kernels.

For this thesis, an input convergence criterion of 1.0Q-25 and an eccentricity of 0.1Q0 were used for the testing of the Hansen coefficients. To optimally test the sun-synchronous, repeat groundtrack, frozen type orbit class of satellites described in the

previous section, an eccentricity on the order of 0.001 would seem more logical. However, the number of terms kept in the power series representation for the Hansen coefficients is directly proportional to the value for the eccentricity; the number of terms kept in the series decreases with decreasing eccentricity. The behavior of the Newcomb operators is such that the power series expansion has the potential to rapidly oscillate before converging [51]. Choosing a value of 0.1 for the eccentricity ensures that (1) the sun-synchronous, repeat ground track, frozen type orbit class of satellites is adequately addressed as well as (2) moderately testing the ability of the power series expansion to converge.

The REAL*8 values for the kernels used in the stability testing were generated by a separate standalone subroutine which implements the following recursion [47]:

$$K_t^{-n-1,s} = \frac{x^2}{(3-n)(1-n+s)(1-n-s)} \left\{ (3-n)(1-n)(3-2n) K_t^{-n,s} - (2-n) \left[(3-n)(1-n) + \frac{2ts}{x} \right] K_t^{-n+1,s} + t^2 (1-n) K_t^{-n+3,s} \right\} \quad (3.33)$$

in which $x = \frac{1}{\sqrt{1-e^2}}$. This recursion is representative of what can be found in GTDS. The question which arises is how to properly initialize this recursion with the necessary "back" values. GTDS computes the required back values using the power series representation. For this thesis, the truth values generated by the standalone program were used as seeds for the recursion. The subroutine built to implement (3.33) is called by the standalone Hansen coefficient generator after the desired REAL*16 kernels are computed via the power series representation. The REAL*16 values are then converted to REAL*8 values using the DBLEQ intrinsic function on the VAX. With the required REAL*8 back values available, the recursion in the standalone subroutine can be used to provide Hansen coefficients which are representative of those computed in GTDS.

The values of the modified Newcomb operators become very large for increasing values of the index t . These large Newcomb operator provide for a poor initialization of the Hansen coefficient recursion. For this reason, stability test cases were chosen to avoid these extremities. Specifically, test cases were chosen for small values of the index t which correspond to physical cases of interest. Small values of t lead to resonant effects for the following combinations of indices:

$$\begin{aligned} & (t=1, m=14), (t=2, m=28), (t=3, m=42), \dots, \\ & (t=t_{\text{upper limit}}, m=14*t_{\text{upper limit}}) \end{aligned} \quad (3.34)$$

for satellites completing approximately 14 revolutions per day. RADARSAT and LANDSAT are two satellites which meet this criteria. A satellite theory implementing a 50x50 gravity field model would capture the first three combinations given in (3.34). Since 50x50 fields were being studied in this thesis, the following ranges for the indices were established for the stability testing:

$$\begin{aligned} \text{range of } t &= 1 \Rightarrow 3 \\ \text{range of } s &= -50 \Rightarrow 50 \end{aligned} \quad (3.35)$$

The range for the degree n was constrained to begin at the maximum of m and the absolute value of s . The value for m was explicitly set using the resonant conditions given in (3.34):

$$\begin{aligned} & \text{if } t = 1, m = 14 \\ & \text{if } t = 2, m = 28 \\ & \text{if } t = 3, m = 42 \end{aligned} \quad (3.36)$$

Defining the constraints on the n index in this fashion avoided the singularities inherent in (3.33).

The output of the standalone routine consisted of a description of the Hansen coefficient pairs whose relative error was greater than 1.0D-10. Table 3.11 describes the two largest errors which were outputted from the standalone routine:

Table 3.11 Maximum Hansen Coefficient Relative Errors

t	s	n	Relative Errors
1	-20	30	2.350551813300362360406304315194285E-0010
1	-20	31	2.350550581159087195163119706345606E-0010

In all, a total of 375 non-zero Hansen coefficient pairs (375 REAL*8 values and 375 REAL*16) had relative errors greater than 1.0D-10. Each of these errors, however, was on the order of the errors listed in Table 3.11. For the sake of brevity, only these two relative errors were given.

The magnitude of the Hansen coefficients producing the relative errors listed in Table 3.11 is given next:

Table 3.12 Hansen Coefficients for Maximum Relative Errors

t	s	n	Precision	Polynomial Value
1	-20	30	REAL*8	18.5058791457064302221624529920518
1	-20	30	REAL*16	18.5058791500563330014506812052115
1	-20	31	REAL*8	56.7617696662896449311119795311242
1	-20	31	REAL*16	56.7617696796317860019196544494950

Again, it should be noted that the REAL*8 values have been extended to REAL*16 precision to ensure consistent mode operations for computational purposes (using the

QEXTD intrinsic function on the VAX). This means that at least 7 decimal places of accuracy have been preserved for these entries.

The Hansen coefficients with the maximum relative errors represent the resonant combination ($t=1, m=14$). Inspection of (3.33) shows that the recursion for the Hansen coefficients is based on the index n . The case ($t=1, m=14$) provides for the greatest range on n (n ranges from 14 to 50 in this case). Since each value in the recursion is dependent upon several back values, the relative error is dependent on the number of computations. Therefore, it can be expected that the cases in which ($t=1, m=14$) should have the maximum relative errors.

For some combinations of indices on the output report, a smaller number of significant decimal digits was preserved. However, the magnitudes of the Hansen coefficients for these cases were significantly larger. The Hansen coefficient pairs with the fewest number of matching decimal digits is given in Table 3.13:

Table 3.13 Hansen Coefficients with the Minimum Number of Significant Digits of Decimal Accuracy

t	s	n	Precision	Polynomial Value
1	-21	50	REAL*8	58136644.6921029016375541687011719
1	-21	50	REAL*16	58136644.7051783832809533162959757
Relative Error				
2.249094647568210998385838268176701E-0010				

For this combination of indices, only one significant decimal digit of accuracy has been preserved. However, a total of 9 places (non-decimal plus decimal) of accuracy has been preserved. This total number of places is consistent with the other Hansen coefficient

results on the output report. Again, since these relative errors are no worse than the errors in the harmonic coefficients, the stability of the Hansen coefficients was deemed acceptable. This stability holds for the VAX, Sun Workstations, and Silicon Graphics Workstations.

[This page intentionally left blank.]

Chapter 4

Draper R&D GTDS Description

4.1 Chapter Introduction

The purpose of this chapter is to describe the Goddard Trajectory Determination System (GTDS), the orbit determination system that is the focal point of this thesis. First, an overview of GTDS will be given, to include the various programs which comprise this multipurpose computer system. Then, the developmental history of GTDS will be described. This description will highlight the evolution of GTDS from the original version built at the NASA Goddard Space Flight Center. Next, the various functions within GTDS that are associated to gravity modeling will be outlined. This functionality includes numerical, analytic, and semianalytic theories. Following this, the input processing and database management pertinent to gravity modeling will be discussed. Finally, the code modifications that were made to GTDS in support of the larger gravity field model will be presented.

4.1.1 GTDS Overview

Draper Laboratory's version of GTDS (Draper R&D GTDS, hereafter referred to as GTDS), is a descendant of the Goddard Trajectory Determination System developed for the NASA/Goddard Space Flight Center. NASA's Operational GTDS Math Specification [26] describes GTDS as a multipurpose computer system designed to provide operational

support for individual Earth, lunar, and planetary space missions and for the research and development of the various space related projects. This orbit determination system, which combines the disciplines of orbital dynamics, measurement modeling, and estimation theory, includes the following programs [26]:

- Differential Correction Program
- Ephemeris Generation Program
- Ephemeris Comparison Program
- Filter Program
- Early Orbit Determination Program
- Data Simulation Program
- Error Analysis Program
- Data Management Program
- Permanent File Report Generation Program

The program descriptions which follow are taken from NASA's previously referenced Operational GTDS Math Specification:

The primary purpose of the **Differential Correction Program (DC)** is to estimate the satellite orbit and associated parameters. The estimation algorithm used in the DC is called the weighted least-squares with a priori covariance or the Bayesian weighted least-squares algorithm. It minimizes the sum of the squares of the weighted residuals between the actual and computed measurements, while simultaneously constraining the model parameters to satisfy the a priori conditions to within a specified uncertainty. Both first and second order statistics (i.e., the mean and covariance matrices) are determined for the estimated variables. The DC is a batch processing method.

The function of the **Ephemeris Generation Program** is to compute, from prescribed initial conditions, the value at a specified time of the vehicle state and, optionally, the state partial derivatives. Several orbital generator options have been incorporated into GTDS, including time regularized Cowell, Cowell, Brouwer, Brouwer-Lyddane, and Variation of Parameter methods.

The **Ephemeris Comparison Program** compares two input ephemerides. The comparison can be specified over a particular arc or over the arc of overlap between the ephemerides. The radial, along-track, and cross-track differences are computed and output.

The **Filter Program** provides an alternative to the DC for estimating the satellite orbit and parameters. The Filter Program contains Kalman (sequential) and Extended Kalman (extended sequential) estimation algorithms. Sequential filters update the satellite state recursively at each measurement point processed.

The **Early Orbit Determination Program** is designed to determine approximately an initial estimate of a satellite orbit when there is no a priori estimate available to start a differential correction process. This program provides three methods for achieving this: (1) the Gauss Method, (2) the Double R-Iteration Method, and (3) the Range and Angles Method.

The **Data Simulation Program** computes simulated tracking measurements of a spacecraft from specified ground sites. The simulated data are generated for specified measurement intervals and sampling frequencies. The program also has the capability to simulate onboard attitude sensor measurements. Optionally, random and bias errors can be added to the measurements. Measurements can also be modified to account for the effects

of atmospheric refraction, antenna mount errors, transponder delays, and signal propagation time delays.

The **GTDS Error Analysis Program** provides the capability of analyzing the effect of tracking error uncertainties, solve-for vector uncertainties, and consider parameter uncertainties associated with a specified orbit and station-dependent tracking schedule.

The primary function of the **Data Management Program** is to create working files of data to be used by other programs in GTDS.

The **Permanent File Report Generation Program** outputs a report of the specified permanent file.

In addition, there is a separate program to test, report, and maintain the physical model data bases used by GTDS. This program is known as **TRAMP** [56,57,58].

4.1.2 GTDS Developmental History

As stated in Section 4.1.1, Draper Laboratory's version of GTDS is a descendant of the original version developed at the NASA/Goddard Space Flight Center (GSFC). This original version of GTDS was developed through the efforts of several individuals [16,45] in the 1970-1976 time frame. It should be noted that Draper's version of GTDS is not the only offspring of NASA/GSFC's original version. An operational version and a distinct R&D version of GTDS at NASA/GSFC were also derived from the original version. Draper's version, in turn, has spawned various other versions of GTDS. Figure 4.1 depicts the relationship among the various versions of GTDS:

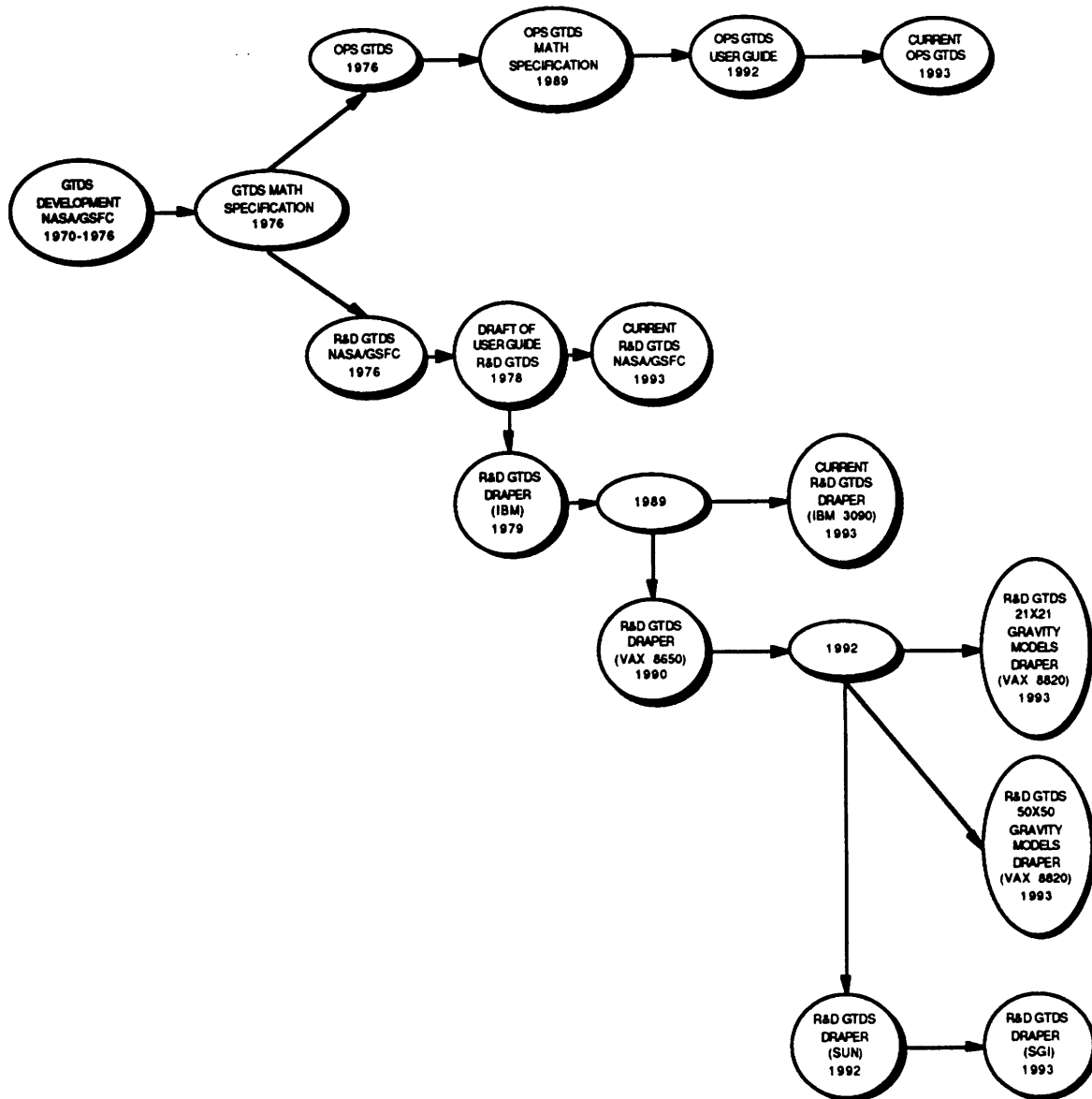


Figure 4.1 Tree Structure of GTDS Developmental History

As evident in Figure 4.1, Draper Laboratory has played a major role in the expansion of GTDS. During the 1979 to 1989 time period, the majority of these expansion efforts involved the capabilities of the Semianalytic Satellite Theory. Cefola [11,34] summarizes the major modifications and functionality added to the system during this time frame:

- comprehensive short periodic models including zonal and tesseral harmonics, third body point masses, atmospheric drag, solar radiation pressure, and certain second order coupling terms
- second order coupling terms for the mean element equations of motion (emphasis on coupling of atmospheric drag and oblateness)
- enhanced tesseral resonance capabilities for the mean element equations of motion (both in terms of the number of allowable resonant terms and the extension to high eccentricity cases)
- third body point mass double averaging theory for the mean element equations of motion
- semianalytic theory for the partial derivatives including both the mean element state transition matrix and the short periodic partials
- comprehensive interpolation strategy including the mean elements, short periodic expansion Fourier coefficients, and perturbed position and velocity (and associated partial derivatives)
- batch least squares estimator that can estimate the mean elements directly from tracking data.
- Kalman Filters including an innovative hybrid linear/extended filter that can recursively estimate the mean elements directly from the tracking data

- additional sources and coordinate systems for Precise Conversion of Element (PCE) observation data.
- maintained and upgraded the data bases employed by the physical models (geopotential models, solar activity/geomagnetic index file supporting the Jacchia-Roberts density model, solar/lunar/planetary (SLP) ephemeris and timing coefficient files)
- included NORAD General Perturbation Theories SGP, GP4, DP4, HANDE, and SALT
- replacement of assembly language routines with equivalent FORTRAN 77 routines
- conversion of the source code to well structured FORTRAN 77 (partially completed)

This work was accomplished on Draper's CCF IBM Mainframe computers.

In 1989, the IBM version of GTDS was ported to Draper's CCF VAX 8650. This port established a baseline VAX version of GTDS at Draper Laboratory. Initially, it was desirable to possess a VAX version of GTDS to support the LANDSAT 6 program. This program led to a version of GTDS on the DECKER VAX 8530 (located first at Princeton, New Jersey and then at Lanham, Maryland). At the completion of the LANDSAT effort, a BIGSIM VAX 8820 version was established at Draper to replace the CCF VAX 8650 version as Draper's baseline VAX version of GTDS. Currently, this BIGSIM version is used to support the RADARSAT program at Draper Laboratory. This program initially

planned to use gravity field models characteristic of those studied in this thesis. In fact, the work for this thesis was funded by the RADARSAT program. Therefore, all work for this thesis was carried out on the BIGSIM VAX.

In 1992, a Sun Workstation version of GTDS was created. This version resulted from a port of the BIGSIM version to the "Earth" Sparcstation 1 at Draper Laboratory. In 1993, this Sun Workstation version was ported, in turn, to a Silicon Graphics Station (SGI 220). A description of these UNIX Workstation versions of GTDS (which are identical) is given by Cefola [13]. Validation of the UNIX Workstation versions of GTDS against standard benchmark cases is documented by Metzinger [41].

One tedious feature of the VAX and IBM versions of GTDS is the process used to invoke portions of the Semianalytic Satellite Theory (SST) developed at Draper Laboratory; this process involves setting various switches in three subroutines (HWIRE, ESTSET, and SKFSET) and one block data (ESTFLG#). Changing the desired semianalytic capabilities required (1) editing the appropriate subroutine or block data, (2) compiling the modified code, (3) linking the resulting R&D GTDS program, and (4) execution. Recently, a SST input processor has been developed in the Sun and SGI environments [11]. This input processor eliminates the inefficiency of setting desired semianalytic capabilities. It is planned to transfer this capability to the VAX system.

4.2 R&D GTDS Functionality Associated to Gravity Modeling

Within GTDS, much functionality is associated to the gravity model. This functionality, for the most part, can be distinguished as stemming from numerical, analytical, or semianalytical theories. This section will briefly outline the various functionality associated

to the gravity model for each of these three theories. In addition, a description of the input processing pertinent to this functionality will be given. The database maintenance of the permanent earth and lunar potential files will also be discussed.

One functionality that is distinct from a specific type of theory is the Permanent Report Generation Program. This program is used to output a report on the harmonic coefficients and related data for the various gravity models within the GTDS permanent earth or lunar files.

4.2.1 Numerical Theories

The basis for the numerical theory within GTDS is the Cowell Orbit Generator (OG). As described in Section 2.2.1, the equations of motion are expressed in terms of the total acceleration vector (i.e., point-mass central body effects plus perturbing accelerations) and solved directly for the position and velocity vectors [26]. Specifically, the position vector is obtained using Stormer-Cowell numerical integration formulas, while the velocity vector is obtained using Adams numerical integration formulas [26].

The variational equations comprise another subset of the numerical theory within GTDS which is associated to the gravity model. In the differential correction process, the partial derivatives of the current state vector with respect to the initial state vector are required. These partial derivatives, which constitute the state transition matrix, can be obtained by numerically integrating the system of variational equations in conjunction with the Cowell orbit generator [26].

4.2.2 Analytical Theories

GTDS also possesses several classical analytical theories which are associated to the gravity model. These analytical theories are summarized in Table 4.1 [26]:

Table 4.1 Analytical Theories in GTDS Associated to the Gravity Model

Orbit Generator	Limitations	Comments
Brouwer	<ul style="list-style-type: none"> •Singularities for $e=0$ •Singularities for $i=0$ deg •Singularities for $i=63.4$ deg •Elliptic motion only 	•Solution includes only J_2 through J_5 effects
Brouwer-Lyddane	<ul style="list-style-type: none"> •Singularities for $i=63.4$ deg •Elliptic motion only 	•Solution includes only J_2 through J_5 effects
Vinti	<ul style="list-style-type: none"> •Elliptic motion only 	•Solution includes only J_2 through J_4 effects

4.2.3 Semianalytical Theory

The Semianalytic theory can be viewed as having two distinct branches: mean element (averaged) equations of motion and short-periodic equations of motion. These two branches result from applying the generalized method of averaging to the Variation of Parameters (VOP) equations of motion. To summarize what was presented in Chapter 2, the zonal harmonic (including J_2^2) and tesseral resonance terms contribute to the mean motion, while the zonal harmonic (including J_2^2), tesseral m-daily, tesseral linear combination, and J_2/m -daily coupling terms contribute to the short-periodic motion. When running the semianalytic theory in GTDS, the averaged equations of motion are always

(automatically by default) used in the determination of a satellite's motion. On the contrary, it is up to the user's discretion which short-periodic contributions to include. Again, the implementation of the short-periodic option is currently system dependent. The UNIX versions of GTDS use the Semianalytic Theory input processor, while the IBM and VAX versions uses several "hardwired" switches which must explicitly be set within block data ESTFLG# and the subroutines HWIRE, ESTSET, and SKFSET. It is planned to port the Semianalytic Theory input processor to the IBM and VAX environments.

The gravity model related software in the Semianalytic Theory is separated according to functionality. Figure 4.2 depicts the routines associated to the averaged orbit generator, while Figure 4.3 depicts the routines associated to the short-periodic orbit generator (it should be noted that the ordering of subroutines in this plot, as well as all the other software tree plots in this thesis, has no significance; the ordering that is presented was chosen out of convenience from the application in which these plots were generated):

[This space intentionally left blank.]

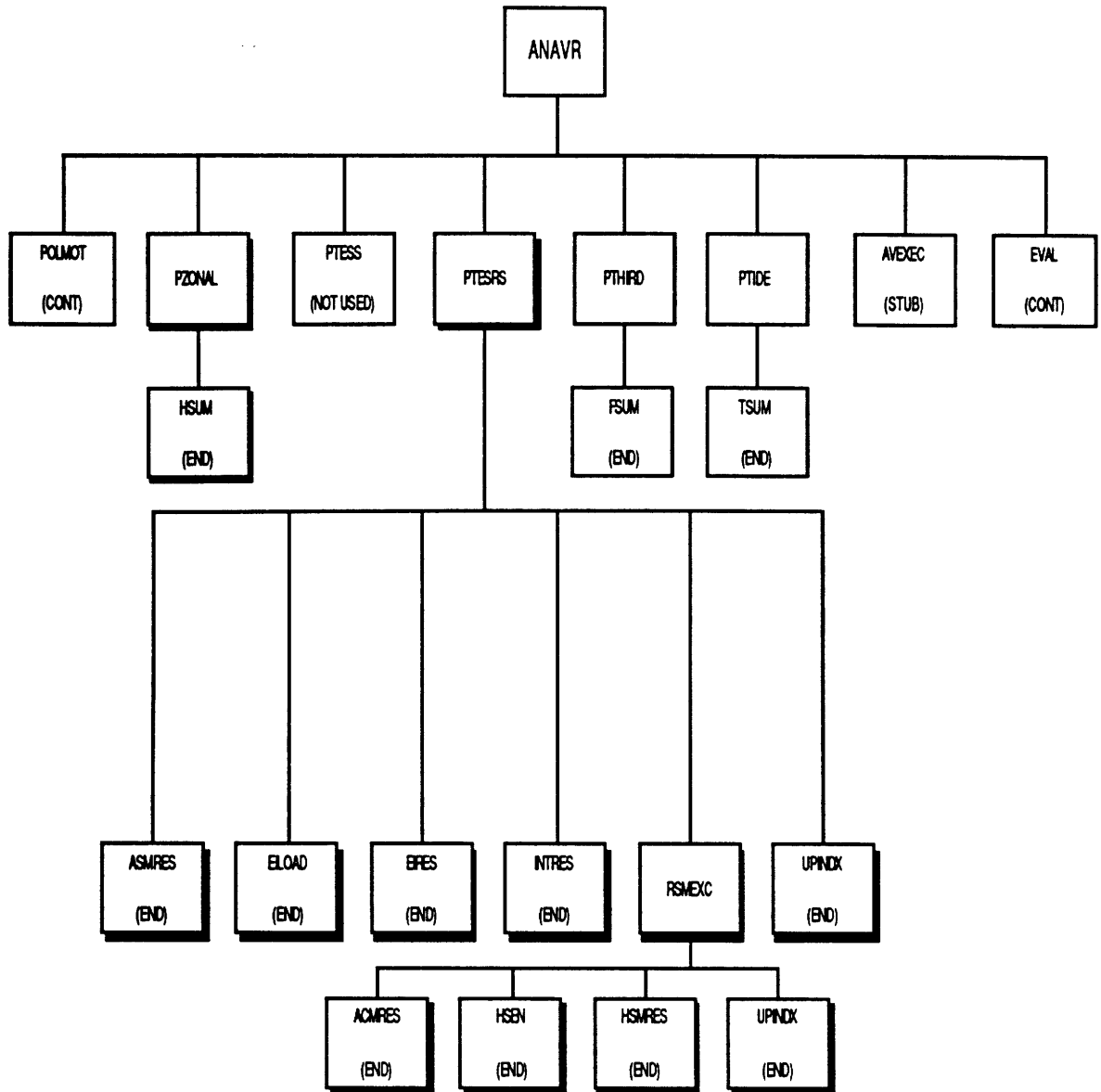


Figure 4.2 Routines Associated to the Averaged Orbit Generator

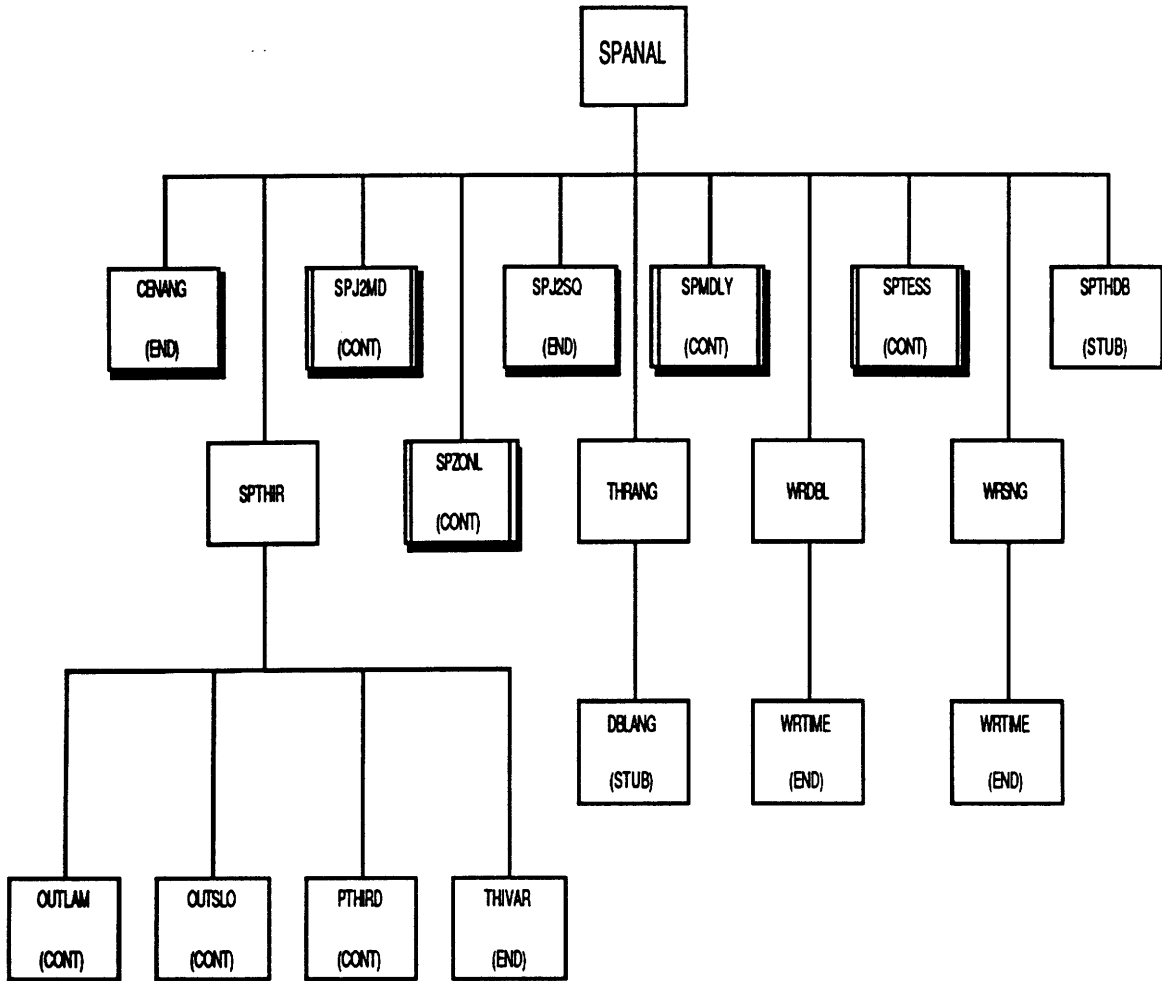


Figure 4.3 Routines Associated to the Short-Periodic Orbit Generator

The "shadowed" boxes represent subroutines which are devoted solely to the gravity model. The "END" qualifier signifies subroutines which do not call other subroutines, while the "CONT" qualifier signifies subroutines which do call other subroutines. The "STUB" qualifier signifies subroutines which belong to Collins's double averaging software [15,21]--software which is present only in the IBM version of GTDS. PTESS, which is a residual routine remaining from the initial tesseral averaging capability, is no longer used. PTERES is a routine built at Draper Laboratory to replace PTXRES, the original routine designed to handle resonant effects. The work of Proulx [49,50] describes the tesseral resonance capability in GTDS associated to PTERES. The boxes which

contain vertical lines on the left and right edges represent gravity model related subroutines which are depicted in greater detail in separate figures. These figures are given next:

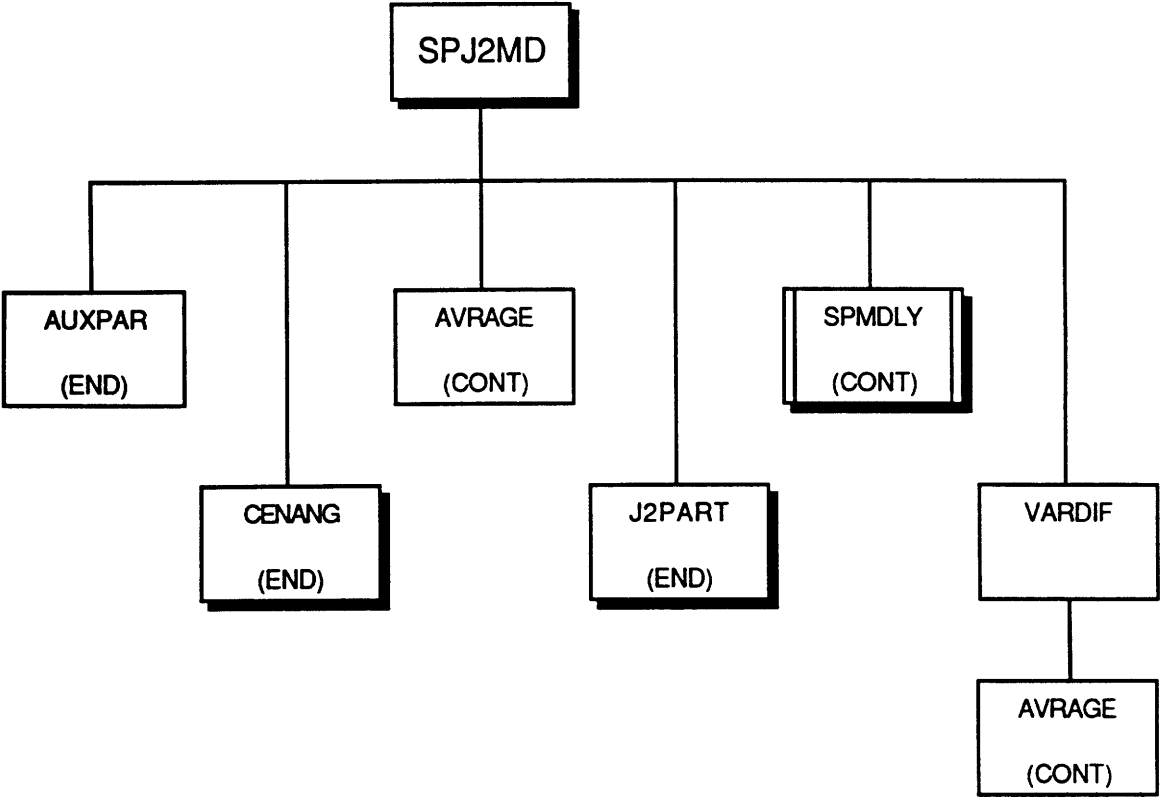


Figure 4.4 J₂/M-Daily Coupling Short Periodic (SPJ2MD) Software Tree

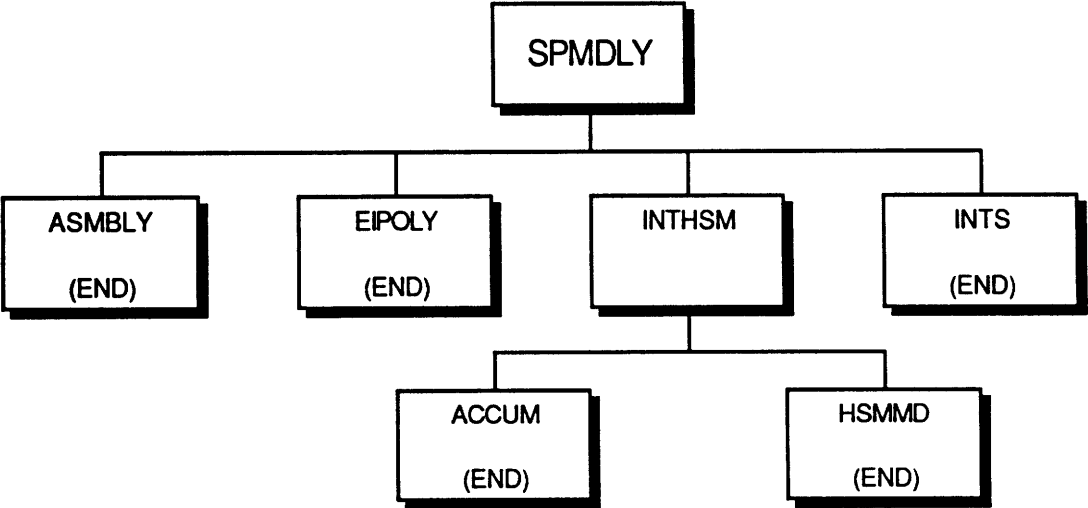


Figure 4.5 Tesseral M-Daily Short Periodic (SPMDLY) Software Tree

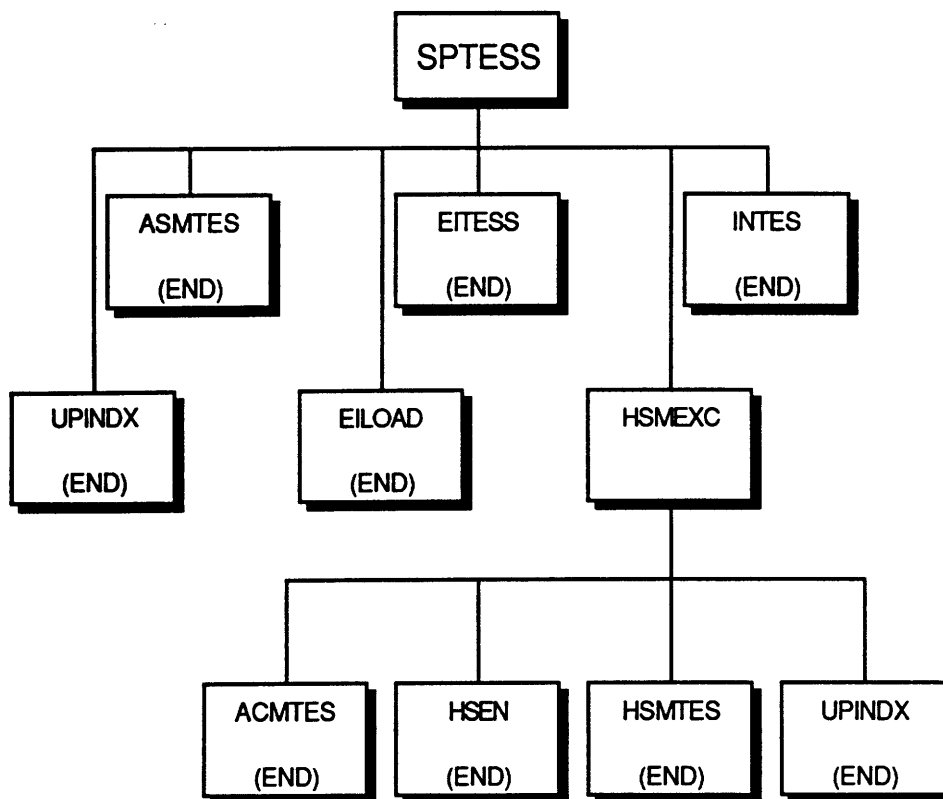


Figure 4.6 Tesselal Linear Combination Short Periodic (SPTESS) Software Tree

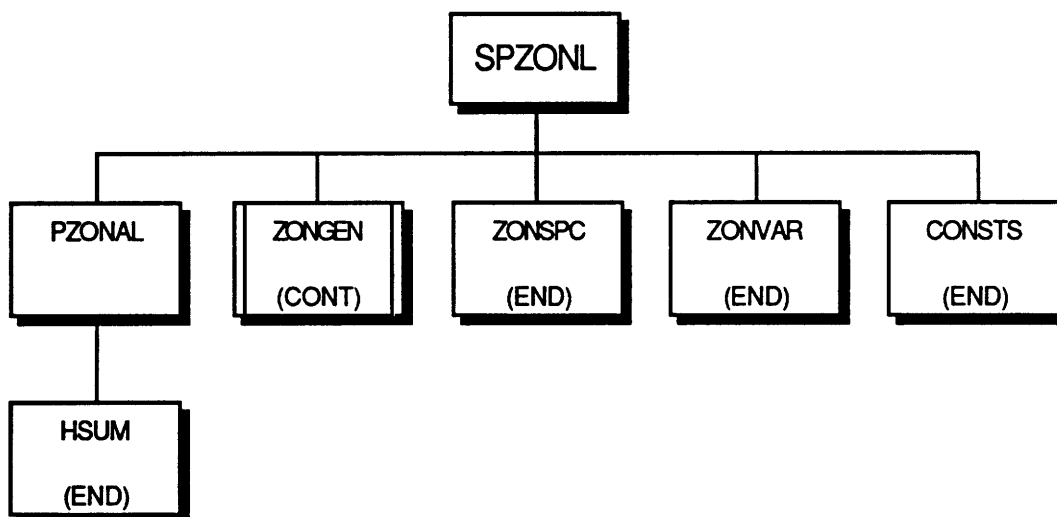


Figure 4.7 Zonal Short Periodic (SPZONL) Software Tree

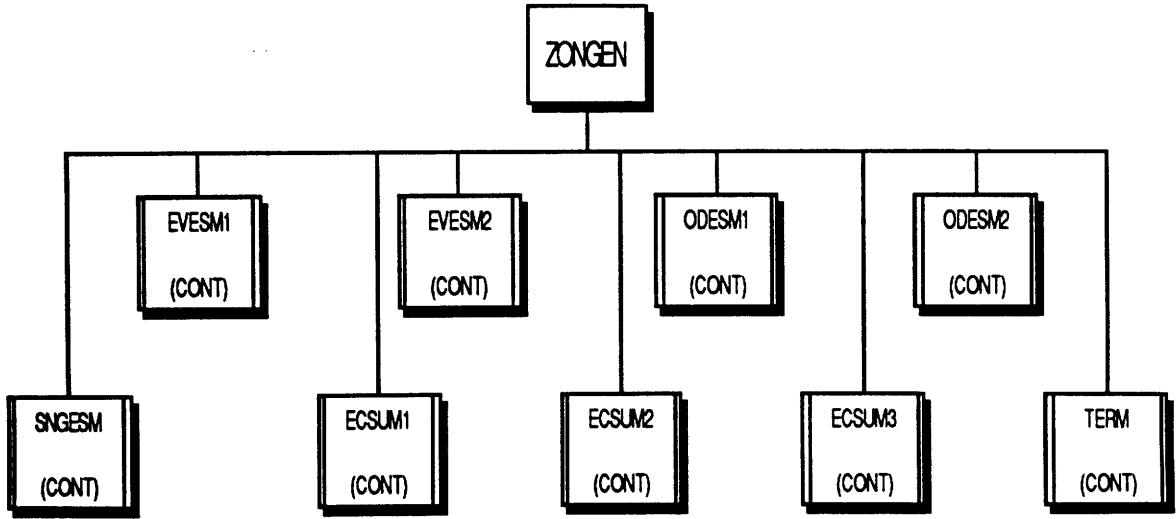


Figure 4.8 Zonal Short Periodic Software Tree for Routines Under ZONGEN

Plots for routines under EVESM1, EVESM2, ODESM1, ODESM2, SNGESM, ECSUM1, ECSUM2, ECSUM3, and TERM can be found in Appendix D.

Mean element partial derivatives comprise another subset of the Semianalytical Theory within GTDS which is associated to the gravity model. These partial derivatives, which are used in the solution of "solve-for" quantities [26], are discussed in the work of Green [67] and Taylor [68].

4.2.4 Gravity-Related Input Processing

When running GTDS, "card decks" are used to describe input parameters. Typically, these card decks contain keywords, three column dependent integer fields, and three column dependent real fields. The keywords are used to identify program options or quantities related to the program options. The integer and real fields are used to specify numerical values related to the keywords. The sample card deck given in Figure 4.9 is set up to (1)

generate a Cowell ephemeris listing and an associated ORB1 file containing time-tagged values of position and velocity, (2) use the Differential Correction Program to perform a Precise Conversion of Elements to obtain a set of mean elements which correspond to the osculating elements used by the Cowell orbit generator, (3) generate a Semianalytic ephemeris listing with the computed mean elements and an associated ORB1 file containing time-tagged values of position and velocity, and (4) use the Ephemeris Comparison Program to compare the two ORB1 files.

Several gravity related key words from Figure 4.9 require additional explanation:

(1) The DATAMGT keyword provides for a global setting of parameters. In this example, DATAMGT provides for a global setting of the POTFIELD keyword. The POTFIELD keyword establishes gravity field model related parameters. The first and second integer fields specify the earth as the central body and model number thirteen as the desired gravity field model, respectively. It should be noted that having an OGOPT subdeck in a CONTROL DATAMGT step is a capability developed at Draper Laboratory.

(2) The ORBTYPE keyword designates the desired orbit propagator. In this example, the difference between the two usages of ORBTYPE stems from the first integer field. In the first usage, the "2" signifies the Cowell orbit generator, while the "5" in the second usage signifies the Semianalytic orbit generator. The difference in step sizes which can be used by the two theories is also evident in this example.

(3) The MAXDEGEQ keyword specifies the maximum degree of the gravity field model to be used in the evaluation of the equations of motion of the satellite. The work for this thesis extended the limit of MAXDEGEQ from 21 to 50.

```

CONTROL  DATAMGT  LNSAT-4  8207201
OGOPT
POTFIELD 1 13
END
FIN
CONTROL  EPHEM  LNSAT-4  8207201
EPOCH 820224.0 0.0
ELEMENT1 1 2 1 7077.8 0.0011 98.2
ELEMENT2 158.1 89.4 176.0
OUTPUT 1 2 1 820226.0 0.0 43200.
ORBTYPE 2 1 1 10.0
OGOPT
MAXDEGEQ 1 50.
MAXORDEQ 1 50.
OUTOPT 1 820224000000. 820226000000. 3600.
END
FIN
CONTROL  DC  LNSAT-4  8207201
EPOCH 820224.0 0.0
ELEMENT1 1 6 1 7077.8 0.0011 98.2
ELEMENT2 158.1 89.4 176.0
OBSINPUT 9 820224000000.0 820226000000.0
ORBTYPE 5 1 1 86400.0 1.0
DMOPT
OBSDEV 21 22 23 100. 100. 100.
OBSDEV 24 25 26 10. 10. 10.
END
OGOPT
MAXDEGEQ 1 50.
MAXORDEQ 1 50.
STATEPAR 3
STATETAB 1 2 3 4.0 5.0 6.0
END
DCOPT
PRINTOUT 1 4
CONVERG 30 1 1.D-5
END
FIN
CONTROL  EPHEM  OUTPUT  LNSAT-4  8207201
OUTPUT 1 2 1 820226.0 0.0 43200.
ORBTYPE 5 1 1 86400.0 1.0
OGOPT
MAXDEGEQ 1 50.
MAXORDEQ 1 50.
OUTOPT 21 820224000000.0 820226000000.0 3600.
END
FIN
CONTROL  COMPARE  LNSAT-4  8207201
COMPOPT
CMPEPHEM 1102102 820224000000.0 820226000000.0 480.0
CMPLOT 1 2.0
HISTPLOT 1102102 820224000000.0 820226000000.0 28800.0
END
FIN

```

Figure 4.9 Sample GTDS Card Deck to Fit Semianalytic Theory to Cowell Theory

(4) The MAXORDEQ keyword specifies the maximum order of the gravity field model to be used in the evaluation of the equations of motion of the satellite. The work for this thesis extended the limit of MAXORDEQ from 21 to 50. If the value of MAXORDEQ is input to be greater than the value of MAXDEGEQ, the value for MAXORDEQ is set to equal the value for MAXDEGEQ.

(5) The OUTOPT keyword provides output options. In this example, the value in the first integer field specifies that an ORB1 file should be written. The difference in the two usages of the OUTOPT keyword provides for the first ORB1 file to be written on the primary unit and the second ORB1 file on the secondary unit. It should be noted that the OUTOPT keyword can also be used to provide ORBIT and EPHEM files. For a description of ORBIT and EPHEM files, as well as a description for the other, non-gravity related features of GTDS input processing, refer to the GTDS user's guide [53].

MAXDEGVE, MAXORDVE, RESONPRD, CNM, and SNM are five other keywords related to the gravity field model which are not given in this example. They can be described in the following manner:

(1) The MAXDEGVE keyword specifies the maximum degree of the gravity field model to be used in the variational equations. This value must be less than or equal to the value for MAXDEGEQ. The format for this keyword is similar to what is given for MAXDEGEQ in Figure 4.9.

(2) The MAXORDVE keyword specifies the maximum degree of the gravity field model to be used in the variational equations. This value must be less than or equal to the value for MAXORDEQ. The format for this keyword is similar to what is given for MAXORDEQ in Figure 4.9.

(3) The RESONPRD keyword allows the user to set the minimum resonant perturbation periods for VOP averaging (the default value for GTDS is 10 days). In other words, if the period of the resonance is less than the default value of ten days, the resonant effects will be considered to be short periodic and not included in the computation of mean element rates due to analytically resonant perturbations [53]. For this thesis, the DMSP orbit [6] was analyzed since this satellite completed very close to 14 revolutions per day. In this manner, the effects at the 28th and 42nd orders would be emphasized--orders which can be analyzed with the new 50x50 gravity field model capability. The period of the resonance for the 42nd order was determined to be approximately 8 days. By setting the minimum period of the resonance to 5 days with the RESONPRD keyword, the effects at the 42nd order could be accounted for by the averaged orbit generator.

(4) The CNM keyword allows the user to specify a value for harmonic coefficient, C , of degree n and order m ($C_{n,m}$). For this thesis, the CNM keyword was used to set J_2 to a small value so that its normal magnitude does not dominant the effects of the non-spherical earth perturbation (the way GTDS is configured, a value of zero causes a run-time error; for this reason, J_2 is set to a small value rather than to zero). Specifically, setting J_2 to a small value is a useful procedure for testing the linear high degree and order terms. An example of this procedure can be found in reference [47].

(5) The SNM keyword allows the user to specify a value for harmonic coefficient, S , of degree n and order m ($S_{n,m}$).

It should be noted that the POTFIELD and CNM/SNM keyword cards cannot appear in the same subdeck. For instances in which it is desirable to use these keyword cards together (i.e., in setting J_2 to a small value), the CONTROL DATAMGT option can be used.

4.2.5 Gravity-Related Database Maintenance

When making a run with GTDS, the user specifies on the POTFIELD card a desired potential field model number. Draper's original version of GTDS was configured to implement the following models:

**Table 4.2 Earth Gravity Models, Original GTDS
NEW_EARTHFLD.DAT**

Model Number	Description	Size
1	Update of SAO 1969 Standard Earth Model No 1	15x15
2	Earth Potential for Manned Flight Computations	4x0
3	Goddard Earth Model One (GEM1)	21x21
4	Goddard Earth Model Seven (GEM7)	21x21
5	Goddard Earth Model Nine (GEM9)	21x21
6	Goddard Earth Model Ten B (GEM10B)	21x21
7	World Geodetic System 72 (WGS72)	12x12
8	Goddard Earth Model L2 (GEM L2)	21x21
9	World Geodetic System 84 (WGS84)	12x12

In accordance with the modifications to allow GTDS to handle larger gravity field models, the following field capabilities were added to GTDS:

**Table 4.3 Additional Earth Gravity Models, Modified GTDS
DAN_POTENTIAL.DAT**

Model Number	Description	Size
10	Goddard Earth Model Ten B (GEM10B)	36x36
11	Goddard Earth Model T2 (GEMT2)	50x50
12	Goddard Earth Model T2 Clone (GEMT2 CLONE)	50x50
13	Goddard Earth Model T3 (GEMT3)	50x50
14	Goddard Earth Model T3 Clone (GEMT3 CLONE)	50x50
15	Goddard Earth Model (GEM) T3S (Satellite Only)	50x50
16	World Geodetic System 84 (WGS 84)	41x41
17	Joint Gravitational Model One (JGM-1)	50x50
18	Joint Gravitational Model One Clone (JGM-1 Clone)	50x50
19	Joint Gravitational Model Two (JGM-2)	50x50

Models one through nine for original GTDS are stored on FORTRAN file number eight (FRN 8), which is a direct access file. This file contains nine records which correspond to the nine models used by original GTDS, each comprising 4200 bytes. This standard number of bytes was established to meet the requirement that all records on a direct access file have the same size. Therefore, when the new (larger) models were added to GTDS, an additional permanent earth potential file needed to be built. This file was designated FRN 47 with each record comprising 21368 bytes (the next section will detail how this number of bytes is derived). It should be noted that the same type of standard existed for the permanent lunar model file (FRN 9). For this reason, FRN 48 was set aside to house potentially new (larger) lunar filed models.

As mentioned in Section 4.1.1, TRAMP is the program to test, report, and maintain the physical model data bases used by GTDS. However, Draper Laboratory did not possess a version of TRAMP until 1991. For this reason, Leo Early built WRITHARM.FOR, a standalone routine to place 21x21 class gravity field models on FRN 8 [21]. This routine reads the harmonic coefficients from an existing file with the following format:

```

TITLE      GEM 10B Earth potential coefficients.
NORMAL     Normalized spherical harmonic coefficients.
RECTANGL   Rectangular coordinates.
GRAVMASS   398600.440000000000
RADIUS     6378.13800000000000
MODEL      6
MAXDEGREE  21
MAXORDER   21
-----
2  0      -4.8416551325533293D-04      0.0000000000000000D+00
3  0      9.5867438084322601D-07      0.0000000000000000D+00
4  0      5.4111656666666668D-07      0.0000000000000000D+00
...
...
...
21 17     -3.0979709938678087D-09     -1.3313422123388820D-08
18 18      5.2037600952278646D-09     -2.9178848383334230D-08
19 18      3.9148071185871325D-08     -2.5941339431748656D-08
20 18      4.1193894565491756D-09      7.6970610614978906D-09
21 18      1.9984043766283332D-08     -1.3325108719821466D-08
19 19     -6.8537933780577993D-09      8.1594160107248540D-09
20 19      5.4833208757996896D-09      2.3351964186700980D-09
21 19     -1.2835855169466875D-08      6.9449130651534003D-09
20 20      2.2428401436143970D-09     -9.4120038552482564D-09
21 20     -3.8797503612088120D-08      9.4653091390057133D-09
21 21      3.7589143961456210D-10     -1.0478099380488057D-08

```

Figure 4.10 EARTHFLD_GEM10B_21BY21_NORREC.DAT

The name for the files of this form are to be descriptive in nature, where (1) EARTHFLD specifies the earth as the body for the coefficients, (2) GEM10B specifies the particular gravity model, (3) 21by21 is the model size, and (4) NORREC indicates normalized, rectangular coordinate coefficients. As note (4) might indicate, WRITHARM accepts normalized and unnormalized coefficients, as well as coefficients which are expressed in polar or rectangular coordinates.

The top eight lines of Figure 4.10 are referred to as control cards. These control cards describe the model and parameters related to this model. The column on the left side of this figure represents the "C" and the column on the right the "S" coefficients.

It is evident that WRITHARM would require modification to support the 50x50 class gravity models. DANWHARM.FOR, the modified version of WRITHARM built to support these larger gravity field models, is described in the following section, which outlines all the code related changes that resulted from this thesis.

4.3 Code Related Changes for 50x50 Gravity Field Models

When the decision was made to implement 50x50 gravity field models in GTDS, it was obvious that several modifications were necessary to the existing code structure. For this reason, much care was taken to ensure that all changes were documented in such a manner that no question would arise when the new code was reviewed by people other than the author of this thesis. To this end, a VAX CMS (Code Management System) [61] Library System was built to document all changes. The library system was established in the following fashion:

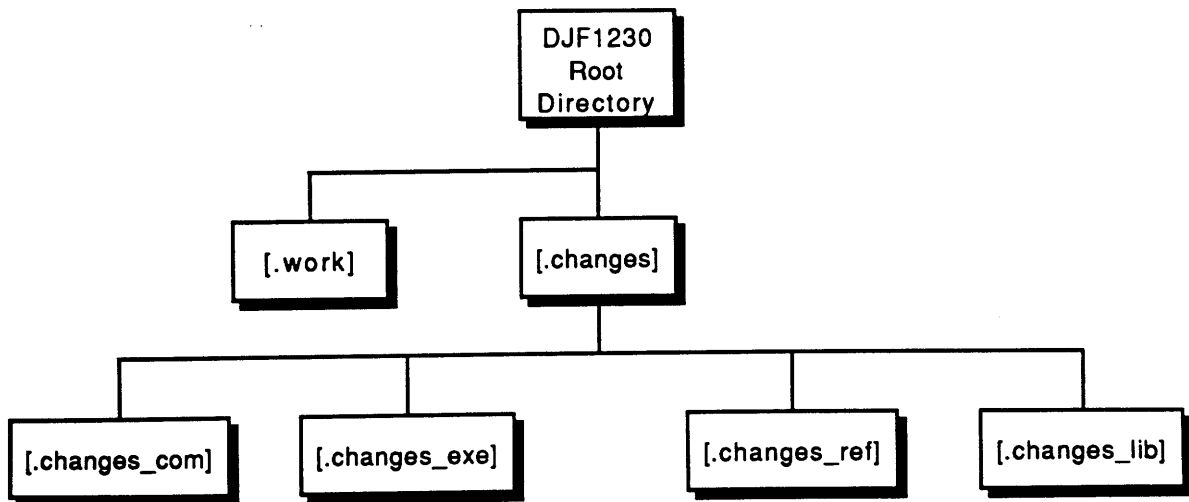


Figure 4.11 CHANGES CMS Library

A system of this type was currently in existence for the baseline, un-modified version of GTDS (previously created through work for the LANDSAT 6 ODEG [33] effort at Draper Laboratory). The use of CMS enables the FETCH, RESERVE, and REPLACE commands. The FETCH and RESERVE commands provide access to a desired routine from an established library. Typically, the FETCH command is used when it is desirable to access a routine for reference purposes, while the RESERVE command is used when it is desired to make modifications to a routine. The REPLACE command returns the RESERVED routine to the appropriate library after modifications are complete (if a routine has been FETCHED, it can simply be deleted from the local directory).

When a particular routine was in need of modification to support the 50x50 gravity field model, it was FETCHED from the previously existing GTDS CMS library into the local work area titled WORK. Then, a new element was created inside of the CHANGES library to house the baseline GTDS version. Next, the particular routine was RESERVED from the CHANGES library [CHANGES_LIB] back into the WORK directory so that the desired modifications could be made. When the modifications were completed, the routine

was REPLACED back into the CHANGES library [CHANGES_LIB]. The RESERVE and REPLACE commands prompted the modifier to comment on the particular modification that was being made, which was added to the routine to produce a CMS version of the FORTRAN code for the particular routine within CHANGES_LIB. In other words, the CHANGES library [CHANGES_LIB] maintains a history of all changes that were made to elements within the library. The CHANGES_REF directory maintains a copy of the most recent version of all elements within CHANGES_LIB.

When modifications were complete, all the elements within the CHANGES library could be compiled and linked. The commands to perform these operations were placed in CHANGES_COM, since the compilation and linking process was accomplished through the use of command files. The executable version of GTDS resulting from the link process was placed in CHANGES_EXE, even though the command procedure to run GTDS was placed within CHANGES_COM. This methodology was established in order to preserve consistency such that all command files would exist in CHANGES_COM. With these tasks complete, GTDS could be executed to produce desired output.

As a final note, it should be mentioned that GTDS was modified in such a manner so that changes of the nature being made for this study would not have to be made again in the future. In the un-modified version of the code, several loops and constants pertinent to the gravity field model were "hard-wired" consistent with the 21x21 field. An easy change would have been to modify the code to "re-hard-wire" these values to be consistent with the 50x50 field; however, this process would need to be re-accomplished each time the field size was to be increased. Therefore, the code was modified in a general manner as to replace all of the "hard-wiring" that existed within the code; PARAMETER statements corresponding to the field size were set in INCLUDE files. In this manner, future modifications to increase the size of the gravity field model would consist of modifying the

INCLUDE files, which are easily identified and easily modified. The specific modifications made to GTDS will be described in the remaining sections of this chapter.

4.3.1 WRITHARM Replacement, DANWHARM.FOR

As was described in Section 4.2, WRITHARM is the standalone utility built to place 21x21 class gravity field models on FRN8, the direct access file designated to store the harmonic coefficients and related parameters. According to the GTDS Data Set Layout manual [19], each record for the 21x21 class gravity field models comprises 4200 bytes. This number of bytes is distributed in the following manner [19]:

Table 4.4 Distribution of Bytes for FRN 8

Bytes	Description
1-4032	CS(I,J,1): I=1,21; J=1,24. Array to store the harmonic coefficients
4033-4040	GM(1): Gravitational constant for the earth
4041-4048	AB(1): Mean radius of the earth
4049-4120	DESCR(I): I=1,9. Model description
4121-4124	IMOD2: Model Number
4125-4128	NDEPF: Maximum degree
4129-4132	NDEFP: Maximum order
4133-4136	MEPDT: Number of earth potential models in Earth Potential File
4137-4140	MAXEP: Total number of records in Earth Potential File
4141-4200	Spare

The first four entries in this table represent real values (8 bytes), while the remainder of the entries represent integer values (4 bytes). The 4032 bytes set aside for the CS array stem from 8 bytes for each of the 504 elements (21 times 24).

Obviously, a lay-out of the form given in Table 4.4 would not be sufficient for the 50x50 class gravity models. Since each record on a direct access file must be the same size, FRN47 was set aside to house the larger earth potential models characteristic of this thesis (FRN48 for lunar models). Table 4.5 describes the distribution of bytes for the 50x50 class gravity field models:

Table 4.5 Distribution of Bytes for FRN 47

Bytes	Description
1-21200	CS(I,J,1): I=1,NUMCOF; J=1,NUMCOF+3. Array to store the harmonic coefficients
21201-21208	GM(1): Gravitational constant for the earth
21209-21216	AB(1): Mean radius of the earth
21217-21288	DESCR(I): I=1,9. Model description
21289-21292	IMOD2: Model Number
21293-21296	NDEPF: Maximum degree
21297-21300	NDEFP: Maximum order
21301-21304	MEPDT: Number of earth potential models in Earth Potential File
21305-21308	MAXEP: Total number of records in Earth Potential File
21309-21368	Spare

Note how the indices for the CS array in Table 4.5 use the generic variable NUMCOF, which represents the maximum degree or order in the gravity field model. This generic parameter was used in DANWHARM, the modified version of WRITHARM built to support the larger gravity field models characteristic of this thesis. WRITHARM's usefulness was limited because several variables and loops were hard-wired consistent with

the 21x21 gravity field model. The use of a generic parameter in DANWHARM made the utility compatible with gravity field models of any size; the user simply needs to (1) change one PARAMETER statement corresponding to the limit of the gravity field model and (2) compile and link the routine in order for the utility to be ready for use.

In DANWHARM, the NUMCOF parameter was first used to generically define the record length variable, LENREC. Then, error checking statements, READ statements, polar/rectangular conversion statements, WRITE statements, normalized/un-normalized conversion statements, and loops for initializing the harmonic coefficients were updated to use the NUMCOF parameter rather than hard-wired values. In addition, new logic was added to ensure proper record and model numbers were placed on FRN47 (or, FRN48). The logic in WRITHARM equivalenced the number of a particular record to its corresponding model number. This logic would be unacceptable for the larger gravity field models since the first record on the new file had to correspond to model number ten. Furthermore, the common area CSHARM, which stored the harmonic coefficients for the file construction process, was changed so that the array storing the harmonic coefficients was dimensioned using NUMCOF.

Like WRITHARM, DANWHARM reads the harmonic coefficients and related data from an existing file of the form given in Figure 4.10. Since most files containing harmonic coefficients are not originally in this form, it is desirable to have a standalone utility which transforms harmonic coefficient files to this required form. The file originally containing the GEMT3 class coefficients was of the following form:

```

RECOEF 2 0 -0.48416510D-03 0.0
RECOEF 3 0 0.95720109D-06 0.0
RECOEF 4 0 0.53952118D-06 0.0
...
...
...
RECOEF5046 -0.19618736D-08 0.21131540D-08
RECOEF4747 0.24329839D-08 -0.34586492D-08
RECOEF4847 0.30067645D-08 0.51068087D-08
RECOEF4947 0.23909876D-08 -0.13928952D-08
RECOEF5047 -0.56725643D-08 -0.81046041D-08
RECOEF4848 0.41555589D-08 -0.19209609D-08
RECOEF4948 0.52270952D-10 0.97919626D-09
RECOEF5048 -0.10698637D-08 -0.19044138D-08
RECOEF4949 0.22865579D-08 0.11050793D-08
RECOEF5049 0.25218088D-08 -0.49950067D-08
RECOEF5050 0.23135159D-08 0.19351819D-08

```

Figure 4.12 Form for Original File Containing GEMT3 Class Harmonic Coefficients

GCSU2.FOR is a standalone utility built as part of the work for this thesis which takes harmonic coefficients from the form given in Figure 4.12 to the required form. Obviously, GCSU2 will require modification for harmonic coefficients which are not originally in the form given by Figure 4.12. This standalone utility calls the function FACTORIAL.FOR:

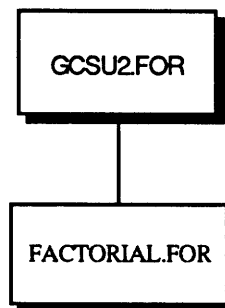


Figure 4.13 GCSU2.FOR Code Diagram

In order to use GCSU2, the following steps are to be performed:

- (1) EDIT GCSU2.FOR
- (2) Check/update the file name in the OPEN statement for the input data file
- (3) Check/update the file name in the OPEN statement for the output data file
- (4) Check/update array dimensions in DIMENSION statements
- (5) Check/update loop values for consistency with field contents
- (6) Check the normalization option; the code assumes that the input must be converted from normalized to un-normalized values.
- (7) Check the READ and WRITE logic

GCSU2 must be compiled with the G_FLOAT option activated. The called function, FACTORIAL.FOR, is a REAL*16 implementation to compute factorials for the un-normalization process. Therefore, it need not be compiled with the G-FLOAT option:

- (8) FORTRAN/G_FLOAT GCSU2 (if necessary)
- (9) FORTRAN FACTORIAL (in necessary)
- (10) LINK GCSU2,FACTORIAL (if necessary)
- (11) RUN GCSU2

Next, the user must simply EDIT one of the existing files of the form in Figure 4.10, CUT and PASTE the control cards into the top of the output which results from the execution of GCSU2, and update the control cards to the desired format.

DANWHARM interacts with the following routines:

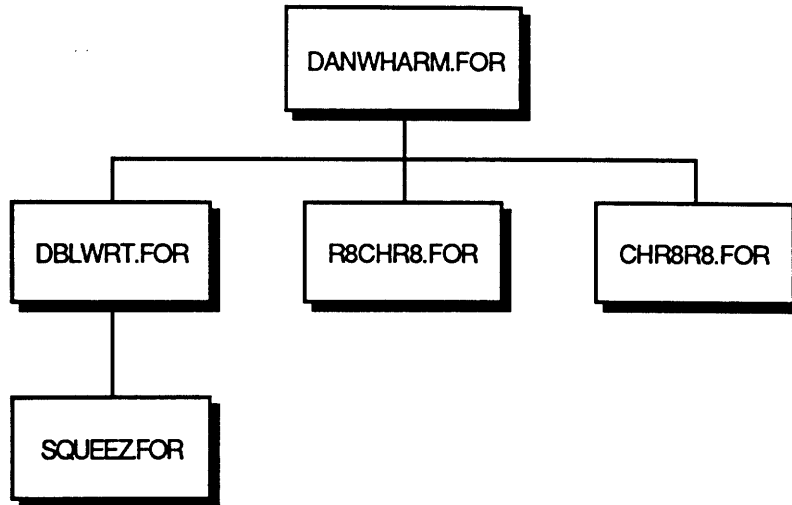


Figure 4.14 DANWHARM.FOR Code Diagram

Before DANWHARM can be executed, a few items specific to the particular field must be checked:

- (1) EDIT DANWHARM.FOR
- (2) Check/update PARAMETER statement concerning field size
- (3) Check/update STATUS of file in OPEN statement. If model is to be added to a currently existing file, set OPEN='OLD'; if model is to be added to a new file, set OPEN='NEW'.

After the modifications to DANWHARM are complete, it must be compiled with the G_FLOAT option. Then, the following command can be given to link the appropriate routines:

```
LINK DANWHARM,DBLWRT,R8CHR8,CHR8R8,  
SQUEEZ,MACHINBD (4.1)
```

where MACHINBD is a block data storing machine related constants. It should be noted that the work for this thesis found an error in the include file MACHIN.CMN. LENINT, a variable representing the number of characters in an integer, was updated to the correct value of four.

With an executable version of DANWHARM in place, the command procedure established to execute DANWHARM.EXE can be updated:

- (1) EDIT DANWHARM.COM
- (2) ASSIGN the augmented file created by GCSU2 to FOR001; this file is the input file for DANWHARM.
- (3) ASSIGN the output text file** to FOR002; this file is a readable imitation of the direct access file described in step 4.
- (4) ASSIGN the output direct access file FOR003; this file is the desired permanent earth/lunar potential file.
- (5) ASSIGN the output data statement file to FOR004; this file contains data statements reflecting the harmonic coefficients.

**Before executing DANWHARM.COM, the user must first set-up the output text file. Specifically, the user must create a file that contains the two control cards describing whether the coefficients are (1) normalized or un-normalized and (2) in polar or rectangular coordinates. Figure 4.15 depicts the control cards for the GEMT3 coefficients:

```
UNNORMAL  Unnormalized spherical harmonic coefficients.  
RECTANGL  Rectangular coordinates.
```

Figure 4.15 OUTPUT_TEXT_GEMT3_50BY50.DAT - Before Execution

The other six control cards can be present, but are not needed. The following command is given to execute DANWHARM:

@DANWHARM (4.2)

The output text file should have the following appearance:

```

TITLE      GEMT3 Earth potential coefficients.
UNNORMAL   Unnormalized spherical harmonic coefficients.
RECTANGL   Rectangular coordinates.
GRAVMASS   398600.435999999999
RADIUS     6378.1369999999997
MODEL      13
MAXDEGREE  50
MAXORDER   50
-----
  2    0    -1.0826260759329829D-03    0.0000000000000000D+00
  3    0     2.5325160388199548D-06    0.0000000000000000D+00
  4    0     1.6185635399999999D-06    0.0000000000000000D+00
...
...
...
 50   46    -1.3717248414582089D-82     1.4774987724116270D-82
 47   47     3.2160895255855009D-81    -4.5718861784472441D-81
 48   47     4.1205061855175162D-82     6.9984319811560448D-82
 49   47     4.7779278981241307D-83    -2.7834326013414670D-83
 50   47    -2.0135366786068120D-83    -2.8768149214169602D-83
 48   48     5.8122593148274060D-83    -2.6867921146405210D-83
 49   48     7.4993187434105878D-86     1.4048538595768350D-84
 50   48    -2.2148019889428671D-85    -3.9424643270074909D-85
 49   49     3.3138326157797472D-85     1.6015548206161991D-85
 50   49     3.7101033978679929D-86    -7.3486900870690090D-86
 50   50     3.4036613725876561D-87     2.8470536476368229D-87

```

Figure 4.16 OUTPUT_TEXT_GEMT3_50BY50.DAT - After Execution

The data statement file should have the following appearance:

```
C
C           Central-body spherical harmonics.
C
DATA  CS ( 1, 1)  /    0.0000000000000000D+00    /
DATA  CS ( 2, 1)  /   -1.0826260759329829D-03    /
DATA  CS ( 3, 1)  /    2.5325160388199548D-06    /
...
...
...
DATA  CS (40, 53) /    0.0000000000000000D+00    /
DATA  CS (41, 53) /    0.0000000000000000D+00    /
DATA  CS (42, 53) /    0.0000000000000000D+00    /
DATA  CS (43, 53) /    0.0000000000000000D+00    /
DATA  CS (44, 53) /    0.0000000000000000D+00    /
DATA  CS (45, 53) /    0.0000000000000000D+00    /
DATA  CS (46, 53) /    0.0000000000000000D+00    /
DATA  CS (47, 53) /    0.0000000000000000D+00    /
DATA  CS (48, 53) /    0.0000000000000000D+00    /
DATA  CS (49, 53) /    0.0000000000000000D+00    /
DATA  CS (50, 53) /    0.0000000000000000D+00    /
```

Figure 4.17 DATA_STATEMENTS_GEMT3_50BY50.DAT

The routines that accompany this permanent potential field file construction process can be found in the following directory:

[DJF1230.50BY50.PASSCOM.GRAVDAT.PROULX] (4.3)

4.3.2 Changes Shared by Cowell and Semianalytic Theory

The changes which were shared by the Cowell and Semianalytic orbit generators could be distinguished by which common area, subroutine, or functionality the change was associated with. For this reason, Section 4.3.2 will be further broken down into the following: HRMCF, GEOVAR, FRCBD, LEGPOL, SETDAF , harmonic coefficient READ logic, LUMPCS, and CSBLNK. This listing adequately addresses the modifications which were shared by the Cowell and Semianalytic orbit generators.

4.3.2.1 HRMCF.CMN

The first and most obvious change within GTDS dealt with the CS array, which stores the harmonic coefficients. For 21x21 class gravity field models, this array is partitioned in such a manner that the C coefficients comprised the lower triangular and the S coefficients the upper triangular portion of a rectangular matrix:

$$C_{N,M} = CS (N, M+1) \quad (4.4)$$

$$S_{N,M} = CS (22-N, 24-M) \quad (4.5)$$

which is DIMENSIONED in the following fashion:

$$\text{DIMENSION} \quad CS (21, 24) \quad (4.6)$$

For 50x50 class gravity field models, this storage arrangement requires modification:

$$C_{N,M} = CS (N, M+1) \quad (4.7)$$

$$S_{N,M} = CS (51-N, 53-M) \quad (4.8)$$

with

$$\text{DIMENSION } CS (50, 53) \quad (4.9)$$

As mentioned in the introduction to Section 4.3, it was desirable to make changes in such a manner that future modifications would not require a re-hash of modifications made in support of this thesis. This meant that the "hard-wired" values related to the maximum degree and order of the gravity model would need to be replaced. For this reason, the general variable NUMCOF was defined to equal the maximum size of the gravity field model:

$$\text{DIMENSION } CS (\text{NUMCOF}, \text{NUMCOF}+3) \quad (4.10)$$

This variable was defined through the use of a PARAMETER statement within HRMCF.CMN, a new include file built to store the array of harmonic coefficients. This new include file needed to be built in order to minimize the modifications resulting from the increased size of the array of harmonic coefficients. In the baseline version of GTDS, the CS array was stored within block data FRC. In all, a total of 504 (21 times 24) locations were reserved for this array. This number of locations would be insufficient for the 50x50 field (50 times 53 or 2650 locations). Therefore, two options existed for the implementation of the new CS array: (1) leave the increased CS array within FRC and "push" the variables stored "under" the CS array to new locations below the CS array or

(2) house the CS array in a new include file and "dummy" out the 504 locations reserved in FRC for the CS array. The first option would require a "re-equivalencing" of variables "under" CS in all the routines that use these elements of FRC. The second option would require the addition of the include file in each of the routines that touch the CS array. The advantage of using the second option and HRMCF.CMN is that if the field size is increased beyond 50x50 in the future, no new "re-equivalencing" would be necessary; rather, the PARAMETER statement in HRMCF.CMN could be updated from 50 to the desired value-- a change which requires only one modification. In addition, the CS array is dimensioned in a general fashion within HRMCF.CMN via (4.10). Since CS is dimensioned within the include file, all DIMENSION statements for CS within GTDS can be removed. Similarly, the NUMCOF variable is used in place of the hard-wired limits for loops or pointers pertinent to the size of the gravity field model within GTDS.

The new include file is accessed in the following manner:

```
INCLUDE 'HRMCF.CMN' (4.11)
```

It should be mentioned that the block data associated with this include file (HRMCF.FOR) is initialized with the same default gravity field that the original version of GTDS was initialized with (GEM1, 21x21). This modification ensures that when no gravity field model is specified on the POTFIELD card, the default gravity field model remains the gravity field model that existed before any modifications were made.

The first step in identifying which routines would need to include HRMCF was to identify which routines accessed the corresponding locations in FRC:

$$CS(1,1) = RFRC(355)$$

(4.12)

$$CS(21,24) = RFRC(858)$$

Any routine which touched one of these 504 locations would need to include HRMCF. To this end, a search was performed for all routines which utilized the common area set aside for FRC. One tool which was extremely helpful in performing this search, as well as many of the other code searches that were required for this thesis, was the GTDS link "map". This map, which is a by-product of the procedure utilized to LINK the baseline set of routines within the GTDS reference library, contains a list of each common area established within the GTDS program along with the routines which access them. Using the information contained in this map, each routine which accessed FRC could easily be identified and analyzed to determine whether HRMCF needed to be included. It should be noted that the development of software trees, such as those given by Figures 4.2 through 4.8, was also extremely helpful in locating routines which required modification.

Another change that accompanies the use of the INCLUDE statement is the removal of all EQUIVALENCE and DIMENSION statements concerning the variables made available through the introduction of the INCLUDE file. The following generic example outlines the standard procedure used to update the reference of the CS array from FRC to HRMCF:

Un-Modified GTDS

```
SUBROUTINE SUB1 (X, Y, Z)
...
...
COMMON /FRC/ RFRC (1300) , IFRC (51)
...
...
EQUIVALENCE ( CS (1, 1) , RFRC (355) )
...
...
DIMENSION CS (21, 24)
```

Modified GTDS

```
SUBROUTINE SUB1 (X, Y, Z)
...
...
INCLUDE 'HRMCF.CMN'
```

Figure 4.18 CS Replacement Example

with locations (355) through (858) replaced by the variable DUMMY1 in FRC:

$$\text{DIMENSION DUMMY1 (21, 24)} \quad (4.13)$$

In other words, the inclusion of HRMCF in the appropriate routines replaces the separate DIMENSION and EQUIVALENCE functions required in the original version of GTDS.

It should also be noted that CS was often times represented as a one-dimensional array in the original version of GTDS:

$$\text{DIMENSION CS (504)} \quad (4.14)$$

This notation required a slightly different modification than the one outlined above; the CS array defined in HRMCF would now need to be equivalenced to a one-dimensional array established in the local routine. The following standard was utilized:

$$\begin{aligned} \text{PARAMETER} & \quad (\text{LIMIT} = \text{NUMCOF} * (\text{NUMCOF}+3)) \\ \text{DIMENSION} & \quad \text{CSLIN (LIMIT)} \\ \text{EQUIVALENCE} & \quad (\text{CSLIN}(1) , \text{CS}(1,1)) \end{aligned} \quad (4.15)$$

Each reference to the CS array in the local routine would be replaced by a reference to CSLIN. This standard provided the functionality required with the generality needed to support potential future modifications to increase the size of the gravity field model.

It should be noted that locations (859) and (860) within FRC are reserved for the CJ2NEG array, which houses the (negative) value of the zonal harmonic J_2 for the earth and moon. These locations were preserved since this array's size need not be increased.

4.3.2.2 GEOVAR.CMN

The second modification that was made to support the larger gravity field model was to move the SINLAM and COSLAM arrays from FRC to a new include file entitled GEOVAR.CMN. These arrays, which store the cosine and sine of the order m times the geocentric longitude of the spacecraft, also have sizes dependent on the limits of the gravity

field model. For the reasons outlined above, the decision was again made to store these variables in a new include file rather than increasing the allocation within FRC. Originally, these arrays were defined in the following manner:

$$\text{DIMENSION SINLAM (22) , COSLAM (22)} \quad (4.16)$$

with

$$\begin{aligned} \text{SINLAM(1)} &= \text{RFRC(1225)} \\ \text{SINLAM(22)} &= \text{RFRC(1246)} \end{aligned} \quad (4.17)$$

and

$$\begin{aligned} \text{COSLAM(1)} &= \text{RFRC(1247)} \\ \text{COSLAM(22)} &= \text{RFRC(1268)} \end{aligned} \quad (4.18)$$

In GEOVAR, they were defined in a general fashion:

$$\begin{aligned} \text{DIMENSION SINLAM (GEONUM+1)} \\ \text{DIMENSION COSLAM (GEONUM+1)} \end{aligned} \quad (4.19)$$

where GEONUM is another generic parameter representing the size of the gravity field model.

The locations in FRC which stored SINLAM and COSLAM were "dummied" out in accordance with the CS array:

$$\begin{aligned} \text{DIMENSION DUMMY2 (22)} \\ \text{DIMENSION DUMMY3 (22)} \end{aligned} \quad (4.20)$$

The search for CS, SINLAM, and COSLAM was conducted concurrently since all of these arrays were stored in FRC.

In the un-modified version of GTDS, block data PASS contained TPSIM, which stored the order m times the tangent of the spacecraft latitude:

$$\begin{aligned} \text{TPSIM}(1) &= \text{RPASS}(45) \\ \text{TPSIM}(22) &= \text{RPASS}(66) \end{aligned} \tag{4.21}$$

with

$$\text{DIMENSION} \quad \text{TPSIM} (22) \tag{4.22}$$

For purposes of consistency, the TPSIM array was also moved to GEOVAR:

$$\text{DIMENSION} \quad \text{TPSIM} (\text{GEONUM}+1) \tag{4.23}$$

In this manner, TPSIM could be stored along side the SINLAM and COSLAM arrays with similar meaning. Inside of PASS, the locations corresponding to TPSIM was "dummied" out:

$$\text{DIMENSION} \quad \text{DUMMY4} (22) \tag{4.24}$$

As with HRMCF, the inclusion of GEOVAR permitted the removal of all DIMENSION and EQUIVALENCE statements in the local routine which referenced the SINLAM, COSLAM, and TPSIM arrays. These three arrays represent variables used by the Cowell orbit generator.

4.3.2.3 LEGPOL.CMN

Block data PASS also stored the array of Legendre or associated Legendre polynomials:

$$\begin{aligned} \text{PMN}(1,1) &= \text{RPASS}(76) \\ \text{PMN}(23,21) &= \text{RPASS}(558) \end{aligned} \quad (4.25)$$

with

$$\text{DIMENSION PMN (23,21)} \quad (4.26)$$

Again, this size of this array needed to be increased in order to support the larger gravity field model. A third include file named LEGPOL.CMN was built to house this array. In keeping with the desire to make the gravity modeling capability general, the PMN array was dimensioned in the following manner:

$$\text{DIMENSION PMN (GEOCS+2, GEOCS)} \quad (4.27)$$

where GEOCS is another generic parameter representing the size of the gravity field model.

Inside of PASS, the locations corresponding to PMN was "dummied" out:

$$\text{DIMENSION DUMMY5 (23,21)} \quad (4.28)$$

Again, the inclusion of LEGPOL permitted the removal of all DIMENSION and EQUIVALENCE statements in the local routine which referenced the PMN array.

4.3.2.4 FRCBD.FOR

Four other variables within FRC also required modification to allow implementation of increased gravity field models: (1) NDEPF, the degree of the earth potential field; (2) NOEPF, the order of the earth potential field; (3) NDMPF, the degree of the lunar potential field; and (4) NOMPF, the order of the lunar potential field. The two variables pertinent to the earth potential field were "hardwired" consistent with the 21x21 models previously used, while the lunar variables were configured for 3x3 models. In order to support the 50x50 gravity field models characteristic of this thesis, these variables have been explicitly set to equal 50. If the limits of the gravity field model are increased in the future, these four variables will have to be updated to support the desired model size.

4.3.2.5 SETDAF.FOR

Subroutine SETDAF.FOR is the routine within GTDS that opens the direct access files. In order to support the new gravity field models stored on FRN 47 and FRN 48, SETDAF needed to be modified. Specifically, two new OPEN statements were added to the code. Conditional statements based on the model number were introduced to distinguish between the "old" and "new" models. In addition, HRMCF was included so that the generic variable NUMCOF could be used to specify record lengths.

4.3.2.6 Harmonic Coefficient READ Logic

Inside of GTDS, there are potentially six routines which could read the harmonic coefficients from the permanent earth file: SETOG1.FOR, SETOG2.FOR, PCWF.FOR,

HARM.FOR, OUTPPC.FOR, and SECUPD.FOR. The READ syntax was of the following form:

```
READ (NEPOT'MODEL_NUMBER,ERR=980)
2  ((CS(J,K),J=1,21),K=1,24), GM(1), AB(1), (HEADER(I,3),I=1,9),
3  IMOD, NDEPF, NOEPF
```

Figure 4.19 "Old" Harmonic Coefficient READ Logic

Obviously, this syntax would require modification for the larger gravity models. First, a conditional loop on the model number would be required. If the model number was less than or equal to nine, a READ statement of form 4.19 would be acceptable. If the model number was greater than nine, a new and general READ statement using the NUMCOF variable would be required. The new READ syntax is depicted in Figure 4.20.

Several items of interest can be noted in the read logic in Figure 4.20. The IF loop checks to see if the model number is indicative of a 21x21 class model GTDS was originally configured to implement (FRN8, referred to as NEPOT). If it is, then the model is read into the OLDCS2 array using 21x21 related logic. Then, OLDCS2 is manipulated so that the values stored in this array are re-arranged to be consistent with the larger, general gravity field limits. These re-arranged values are inserted into the CS array, which is stored in HRMCF. In this manner, model numbers one through nine are read in using the 21x21 field format, but are converted to the larger, general field format for storage purposes.

```

C
  IF (MODEL_NUMBER .LE. 9) THEN
C
    READ (NEPOT, REC=MODEL_NUMBER, ERR=980)
1   ((OLDCS2 (J, K), J=1, 21), K=1, 24), GM (1), AB (1), (HEADER (I, 3), I=1, 9)
2   , IMOD, NDEPF, NOEPF
C
    DO 775 N = 1, 21
C
    DO 776 M = 1, 24
C
    IF ((M-N) .LT. 2) THEN
      CS (N, M) = OLDCS2 (N, M)
    ELSE
      CS (NUMCOF+1-(22-N), NUMCOF+3-(24-M)) = OLDCS2 (N, M)
    ENDIF
C
776    CONTINUE
C
775    CONTINUE
C
  ELSE
C
    MODIFIED_MODEL_NUMBER = MODEL_NUMBER - 9
C
    READ (NEWPOT, REC=MODIFIED_MODEL_NUMBER, ERR=980)
1   ((CS (J, K), J=1, NUMCOF), K=1, NUMCOF+3), GM (1), AB (1), (HEADER (I, 3)
2   , I=1, 9), IMOD, NDEPF, NOEPF
C
  ENDIF
C

```

Figure 4.20 New Harmonic Coefficient READ Statement

The ELSE condition in Figure 4.20 is established to handle the models stored on FRN47. First, the MODIFIED_MODEL_NUMBER variable is defined to equal the model number minus nine. This logic ensures that the correct record number is read from NEWPOT (FRN47). Remember, even though model ten is the first model number stored on FRN47, it corresponds to the first record. Then, the coefficients can be read directly in to the CS array using the NUMCOF variable. The larger, general fields do not require additional manipulation to ensure correct storage in common area HRMCF.

The READ logic outlined in the preceding figure and paragraphs is the logic used in subroutines SETOG1, SETOG2, PCWF, OUTPPC, and SECUPD. The READ statement in subroutine HARM is modeled after the READ statement described in the ELSE condition, above; it directly reads the coefficients into the CS array using the NUMCOF variable.

4.3.2.7 LUMPCS.CMN

It should be noted that SETOG1 has the capability to read in two sets of harmonic coefficients. This stems from the lumped geopotential capability in GTDS. As part of this capability, GTDS computes the difference between the two sets of coefficients. In original GTDS, this difference was stored in the DELCS array within common area STAGEO. The following DIMENSION statement was used:

```
DIMENSION DELCS (21, 24) (4.29)
```

As with the other changes described previously, a new include file was built to store this array of differences. This common area, LUMPCS.CMN, implemented a generic DIMENSION statement for the DELCS array:

DIMENSION DELCS (LUMPNO, LUMPNO+3) (4.30)

where LUMPNO is another generic parameter representing the size of the gravity field model.

The inclusion of this new common area affected only two routines: SETOG1.FOR and SPARTV.FOR.

4.3.2.8 CSBLNK.CMN

Another common area in original GTDS which would not support the increased gravity field models was the blank or unlabeled common. This blank common was essentially a scratch area used by several routines (identifiable with the link map). Two forms of this blank common are of interest for this thesis:

```

COMMON          A1          , RTM(3)      , ITM(3)      , IERROR      ,
2              JC          , LC          , IS          , JS          ,
3              LS          , L          , IDENSW      , IC          ,
4              RS          , RM          , RR          , IM          ,
5              IDUM        , CSSTOR     , ICSTEM      , MODE        ,
6              MODL        , NUMCS

```

Figure 4.21 Blank Common, Version 1

and

```
COMMON PTNTL(21,24)
```

Figure 4.22 Blank Common, Version 2

Both of these forms of the blank common contain variables which are defined using hardwired values reflecting the limits of the gravity field model. In the first version, CSSTOR and ICSTEM are of concern, while PTNTL is of concern in the second. The variables CSSTOR and PTNTL are arrays used to temporarily house the harmonic coefficients. These variables were dimensioned in original GTDS in the following manner:

```

DIMENSION  CSSTOR (21, 24, 2)
DIMENSION  ICSTEM (504, 2)
DIMENSION  PTNTL (21, 24)

```

(4.31)

The include file CSBLNK.CMN was built to store these variables. The DIMENSION statements given in (4.31) were updated in the new include file:

```

DIMENSION  CSSTOR (CSBNUM, CSBNUM+3, 2)
DIMENSION  ICSTEM (CSBNUM*CSBNUM+3, 2)
DIMENSION  PTNTL (CSBNUM, CSBNUM+3)

```

(4.32)

where CSBNUM is another generic parameter representing the size of the gravity field model.

CSBLNK was included in HARM.FOR, OUTPPC.FOR, SETOG1.FOR, SETOG2.FOR, and SETORB.FOR. With the addition of this include file, the location for CSSTOR and ICSTEM were replaced by the dummy variables DAN1 and DAN2, respectively. These dummy variables were dimensioned consistent with the values in (4.31) so that locations "below" these variables could be preserved. With respect to Version 2, the entire line of the form given in Figure 4.22 could be removed, since this variable was now stored in CSBLNK.

4.3.3 Changes Unique to the Semianalytic Theory (SST)

In the preceding section, a standard pattern was described for increasing the size of an array with limits dependent upon the maximum degree and order of the gravity field model. This pattern consisted of the following steps:

- (1) Locate all occurrences of the array in need of modification (usually within a common area)
- (2) Construct a new include file and associated block data to house the array
- (3) Dummy-out the locations in the "old" common area so as to preserve the locations below the array in need of modification
- (4) INCLUDE the new include file in the appropriate routines

In the update of the SST related code, this pattern continued to hold. One new wrinkle that was incorporated into this pattern was the conversion of an *entire* common area to an include file and an associated block data. When analyzing the SST code, it was discovered that most of the common areas did not have a pre-existing block data before execution of the code; rather, the common area was defined during execution of the code. For purposes of consistency, common areas that were identified to contain an array that was in need of modification were converted to an include file and associated block data. A change of this type required heavy reliance on the link map; this map would allow the identification of all routines which would require the inclusion of the new include file. In addition, care would need to be taken to ensure that the addition of the new include files would not introduce a variable which would have a conflicting name with a variable local to the routine in question. Furthermore, it was vital to identify if any of the arrays in question were passed

to other routines through calling sequences. If this type of passage occurred, the potential to update DIMENSION statements in the called routine may exist. The software trees given in Section 4.2.3 were very useful in analyzing the flow of the code for the SST. The paragraphs which follow describe the construction of new include files and associated block datas for the SST related code.

4.3.3.1 ANAV1.CMN

ANAV1 was the first common area identified to be in need of modification. This common area, which is used in routines developed for the initialization of the averaging model [55], was defined in the following manner in the un-modified version of GTDS:

```
COMMON/ANAV1 /  TOLER      ,X          ,XX          ,GAMMA      ,
1              SINISQ     ,FACT(44)   ,EPWR(22)   ,HAFPWR(22) ,
2              XPWR(22)   ,SINPWR(43) ,ONEGPW(43)
```

Figure 4.23 ANAV1 Definition

This common area listing contains several arrays which have sizes dependent upon the degree and order of the potential field model. Table 4.6 lists these variables and their definition:

Table 4.6 ANAV1 Variables

Variable	Definition
FACT	Array of factorials
EPWR	Powers of $\frac{e}{2}$
HAFPWR	Powers of $\frac{1}{2}$
XPWR	$\frac{x}{[2(1-e^2)]^\sigma}$ for $\sigma = 0, 1, \dots, \text{nend}$
SINPWR	Powers of the sine of the inclination
ONEGPW	$(1 + \cos i) \cos^\sigma i$ for $\sigma = 0, 1, \dots, (\text{nend} - 1)$ for lower portion, and $\frac{\cos^\sigma i}{(1 + \cos i)}$ for $\sigma = 0, 1, \dots, (\text{nend} - 1)$ for upper portion of array

The new include file ANAV1.CMN utilized the following, general dimension statements:

$$\begin{aligned}
 \text{DIMENSION} \quad & \text{FACT} (2*\text{POTNUM}+2) \\
 \text{DIMENSION} \quad & \text{EPWR} (\text{POTNUM}+1) \\
 \text{DIMENSION} \quad & \text{HAFPWR} (\text{POTNUM}+1) \\
 \text{DIMENSION} \quad & \text{XPWR} (\text{POTNUM}+1) \\
 \text{DIMENSION} \quad & \text{SINPWR} (2*\text{POTNUM}+1) \\
 \text{DIMENSION} \quad & \text{ONEGPW} (2*\text{POTNUM}+1)
 \end{aligned} \tag{4.33}$$

where POTNUM is another generic parameter representing the size of the gravity field model.

Using the link map, it was determined that ANAV1 needed to be included in the following routines:

ANHARM.FOR

ANTHIR.FOR

AUXTRN.FOR

DBOUND.FOR

RBOUND.FOR

4.3.3.2 AVEPOT.CMN

AVEPOT.CMN is an include file built to hold arrays with sizes dependent upon the limit of the geopotential model in the routines which fall under PZONAL.FOR, PTHIRD.FOR, and PTIDE.FOR. Specifically, the variables XJLAN, ARN, QNM, and GAMMAN were removed from the common area ANAV2 and placed into AVEPOT. These variables are defined in the following manner:

Table 4.7 AVEPOT Variables

Variable	Definition
XJLAN	$J(n) * \left(\frac{R}{a}\right)^n$ for $n = 2, 3, \dots, \text{nend}$
ARN	$\left(\frac{a}{r}\right)^n$ for $n = 2, 3, \dots, \text{nend}$
QNM	$Q(n,m)$ for $n = m, m+2, m+4, \dots, \text{nend}$
GAMMAN	$(2n - 1)\gamma$ for $n = 2, 3, \dots, \text{nend}$

The include file AVEPOT dimensioned these variables in the following way:

```
DIMENSION XJLAN (DEGORD)
DIMENSION ARN (DEGORD)
DIMENSION QNM (DEGORD/2 + 1)
DIMENSION GAMMAN (DEGORD)
```

(4.34)

where DEGORD is another generic parameter representing the size of the gravity field model.

AVEPOT was included in three routines:

FSUM.FOR

HSUM.FOR

TSUM.FOR

4.3.3.3 GRAVITY.CMN

GRAVITY is an include file that was developed to *potentially* provide a set of variables related to the limits of the gravity field model that could be used by all routines within GTDS. This definition of variables could potentially provide a single point of reference for gravity related indices, loop counters, and variables with which to DIMENSION arrays. If the limits of the gravity field model are to be increased in the future, the modifier would simply have to drop the correct values into this common area; no other modifications would be necessary.

Figure 4.24 depicts the current definition of variables in GRAVITY. It should be noted that this listing can augmented as required in the future to support further potential-related work.

```

C   Data Types =====
C
C
C   INTEGER          FIELD_SIZE
C   INTEGER          TWOFS1
C   INTEGER          TWOFS2
C
C
C   Parameter Statements =====
C
C   PARAMETER        (FIELD_SIZE = 50)
C   PARAMETER        (TWOFS1      = (2*FIELD_SIZE) + 1)
C   PARAMETER        (TWOFS2      = (2*FIELD_SIZE) + 2)
C

```

Figure 4.24 GRAVITY Variables

4.3.3.4 MDWRK.CMN

MDWRK, which is related to the m-daily capability in GTDS, is one common area that was entirely converted to an include file and associated block data. This common area contained the arrays SIRE and SICX, which have sizes dependent on the limits of the gravity field model. They are defined in Table 4.8:

Table 4.8 MDWRK Variables

Variable	Definition
SIRE	Array of real parts of $(\alpha + j\beta)$, where alpha and beta are direction cosines
SICX	Array of imaginary parts of $(\alpha + j\beta)$

These variables were dimensioned within MDWRK.CMN in the following manner:

$$\begin{array}{ll} \text{DIMENSION} & \text{SIRE (NUMPOT + 2)} \\ \text{DIMENSION} & \text{SICX (NUMPOT + 2)} \end{array} \quad (4.35)$$

where NUMPOT is another generic parameter representing the size of the gravity field model.

The link map indicated that the following routines needed to include MDWRK:

ACCUM.FOR
 ASMBLY.FOR
 EIPOLY.FOR
 HSMMD.FOR
 INTHSM.FOR
 INTS.FOR
 SPMDLY.FOR

4.3.3.5 NUKES.CMN

NUKES is an include file built to accompany the previously existing block data NUKESBD.FOR. This common area stores the Newcomb operators, which are used to build the Hansen coefficients required in the equinoctial formulation of the potential. In the version of NUKESBD.FOR in the un-modified version of GTDS, the following PARAMETER statement was used to define the total number of Newcomb operators (a number based on the D'Alembert characteristic and loop indices associated to the gravity model):

PARAMETER (NNUKE = 36000)

Figure 4.25 NUKESBD.FOR, Original GTDS

To support the 50x50 class gravity field models, this number required modification:

PARAMETER (NNUKE = 52962)

Figure 4.26 NUKES.CMN, Modified GTDS

This PARAMETER statement was moved to the newly created include file NUKES.CMN, which was included in the new version of NUKESBD.FOR.

4.3.3.6 PTSDAT.CMN

In addition to AVEPOT, the common area ANAV2 in original GTDS led to the development of a second include file and associated block data. PTSDAT was built to store arrays with sizes dependent upon the limits of the gravity model for routines which fall under PTESS.FOR. Table 4.9 describes these variables:

Table 4.9 PTSDAT Variables

Variable	Definition
GLAST	$G(L-RETRG*M-1,L-1,M)(1,+1)$
HLAST	$H(L-RETRG*M-1,L-1,M)(1,+1)$
GLASTX	$G(L+RETRG*M-1,L-1,M)(1,-1)$
HLASTX	$H(L+RETRG*M-1,L-1,M)(1,-1)$
DPDDX	$\frac{DPD}{DX}$ where $PD = \left(\frac{R}{a}\right)^n$ * Modified Hansen Coefficient

It should be noted that the DPDDX array was stored in the common area ANAV3 in original GTDS. Since this array was used in routines which fell under PTESS.FOR, it was also stored in PTSDAT.

These variables were dimensioned in the following way in PTSDAT:

DIMENSION	GLAST (ORDDEG - 1)	
DIMENSION	HLAST (ORDDEG - 1)	
DIMENSION	GLASTX (ORDDEG - 1)	(4.36)
DIMENSION	HLASTX (ORDDEG - 1)	
DIMENSION	DPPDX (ORDDEG)	

where ORDDEG is another generic parameter representing the size of the gravity field model.

PTSDAT was included in five routines:

FINIT.FOR
FNEWM1.FOR
FNEWM2.FOR
PDNEWM.FOR
TSUMN.FOR

4.3.3.7 SPREAL.CMN

SPREAL was another common area that was entirely converted to an include file and an associated block data. This common area contains real variables used by the short-periodic generator, which is used by the semianalytic orbit generator. Table 4.10 defines the arrays that had sizes dependent upon the degree and order of the geopotential model.

Table 4.10 SPREAL Variables

Variable	Definition
CTRUE	C coefficients of the true longitude expansion
STRUE	S coefficients of the true longitude expansion
CECCEN	C coefficients of the eccentric longitude expansion
SECCEN	S coefficients of the eccentric longitude expansion
CLAMDA	C coefficients of the mean longitude expansion
SLAMDA	S coefficients of the mean longitude expansion
CTHETA	C coefficients of the theta expansions
STHETA	S coefficients of the theta expansions
CDOUBL	C coefficients of the lambda-theta double expansions
SDOUBL	S coefficients of the lambda-theta double expansions
CCOEF	C coefficients to be added into one of the single angle expansions
SCOEF	S coefficients to be added into one of the single angle expansions
CFCTRU	C interpolator coefficients for the true longitude expansion
CFSTRU	S interpolator coefficients for the true longitude expansion
CFCECC	C interpolator coefficients for the eccentric longitude expansion
CFSECC	S interpolator coefficients for the eccentric longitude expansion
CFCLAM	C interpolator coefficients for the mean longitude expansion
CFSLAM	S interpolator coefficients for the mean longitude expansion
CFCTHT	C interpolator coefficients for the theta expansions
CFSTHT	S interpolator coefficients for the theta expansions
CFCDL	C interpolator coefficients for the lamda-theta double expansions
CFSDL	S interpolator coefficients for the lamda-theta double expansions

These variables were dimensioned in the following, general way in the include file SPREAL.CMN:

```

DIMENSION      CTRUE  (6,TFDPL2)           ,STRUE  (6,TFDPL2)
DIMENSION      CECCEN (6,TFDPL2)           ,SECCEN (6,TFDPL2)
DIMENSION      CLAMDA (6,FDMIN1)           ,SLAMDA (6,FDMIN1)
DIMENSION      CTHETA (6,TFDMI2)           ,STHETA (6,TFDMI2)
DIMENSION      CDOUBL (6,DUBNUM)           ,SDOUBL (6,DUBNUM)
DIMENSION      CCOEF  (6,TFDPL2)           ,SCOEf  (6,TFDPL2)

C

DIMENSION      CFCTRU (SPINC1)             ,CFSTRU (SPINC1)
DIMENSION      CFCECC (SPINC1)             ,CFSECC (SPINC1)
DIMENSION      CFCLAM (SPINC2)             ,CFSLAM (SPINC2)
DIMENSION      CFCTHT (SPINC3)             ,CFSTHT (SPINC3)
DIMENSION      CFCDBL (SPINC4)             ,CFSDBL (SPINC4)

```

where

```

PARAMETER      (ECCNUM = 4)
PARAMETER      (TFDPL2 = (2 * FLDDIM + 2))
PARAMETER      (FDMIN1 = (FLDDIM - 1))
PARAMETER      (TFDMI2 = (2 * FLDDIM - 2))
PARAMETER      (DUBNUM = (FLDDIM*(2*(FLDDIM+ECCNUM)+1)))

C

PARAMETER      (SPINC1 = (4*6*TFDPL2))
PARAMETER      (SPINC2 = (4*6*FDMIN1))
PARAMETER      (SPINC3 = (4*6*TFDMI2))
PARAMETER      (SPINC4 = (4*6*DUBNUM))

```

Figure 4.27 DIMENSION Statements for SPREAL

where FLDDIM is another generic parameter representing the size of the gravity field model. It should be noted that the definition of DUBNUM has operational implications. This set-up corresponds to low to medium eccentricity orbits utilizing the entire 50x50

field. Specifically, the choice of MTS, LTS, JMINTS, and JMAXTS in HWIRE.FOR (refer to Appendix B) should consider DUBNUM.

The link map indicated that the following routines needed to include SPREAL:

ANLWRT.FOR

HWIRE.FOR

KFHIST.FOR

MEANOSC.FOR

OSCMEAN.FOR

SETSPG.FOR*

SKFPRT.FOR

SPANAL.FOR

SPCOEF.FOR

SPCOTO.FOR

SPDIFF.FOR

SPGENR.FOR

SPINIT.FOR

SPINTP.FOR

SPMOVE.FOR

SPNUM.FOR

SPNUM2.FOR

SPORB.FOR

SPORBP.FOR

SPSKF.FOR

VRSPFD.FOR

*A subroutine which originally was envisioned for use as part of a short-periodic input processor. This subroutine represents a stub, and is not called inside of the IBM and VAX versions of GTDS.

4.3.3.8 SPZONB.CMN

SPZONB was another common area that was entirely converted to an include file and associated block data. This common area, which is related to the zonal short periodic model, was defined in the following manner in original GTDS:

```

COMMON/SPZONB/ XJLAN (21)      ,V (22)      ,D (22)      ,Q (22)      ,
2          CKH (23)      ,SKH (23)      ,CAB (23)      ,SAB (23)      ,
3          XMUNA          ,XMUNA2      ,XCUBE          ,XMUNAK      ,
4          XMNA2K          ,GENCOS (41) ,GENSIN (41) ,GCOSDA (4) ,
5          GSINDA (4)      ,GCOSDH (4) ,GSINDH (4) ,GCOSDK (4) ,
6          GSINDK (4)      ,GCNDAL (4) ,GSNDAL (4) ,GCOSDB (4) ,
7          GSINDB (4)      ,GCOSDG (4) ,GSINDG (4) ,HMSUM          ,
8          HSUMDA          ,HSUMDX          ,HSUMDG          ,HPOLY          ,
9          GPOLY          ,DHDAL          ,DHDB          ,DGDAL          ,
1         DGDB          ,DHDH          ,DHDK          ,DGDH          ,
2         DGDK          ,VCURR          ,QCURR          ,DCURR          ,
3         DDDXCR          ,DQDGR          ,XIPOLY          ,XJPOLY          ,
4         DIDAL          ,DIDB          ,DJDAL          ,DJDB          ,
5         DIDH          ,DIDK          ,DJDH          ,DJDK          ,
6         QNEXT          ,DQDGNX          ,DNEXT          ,DDDXNX          ,
7         XSQR          ,RECIPX

```

Figure 4.28 SPZONB in Original GTDS

In this common area, the variables XJLAN, V, D, Q, CKH, SKH, CAB, SAB, GENCOS, and GENSIN all have sizes dependent on the degree and order of the gravity field model. These variables are defined in the following table.

Table 4.11 SPZONB Variables

Variable	Definition
XJLAN	$J(n) * \left(\frac{R}{a}\right)^n$ for $n = 2, 3, \dots, \text{nend}$
V	$V(I-1, I-1)$ FOR $I=1, \dots, \text{NMAX}$
D	$D(I, I-1)$ FOR $I=1, \dots, \text{NMAX}$
Q	$Q(I-1, I-1)$ FOR $I=1, \dots, \text{NMAX}$
CKH	$RE \left((K+J*H)^{(I-2)} \right)$ FOR $I=2, \dots, \text{NMAX}$
SKH	$IM \left((K+J*H)^{(I-2)} \right)$ FOR $I=2, \dots, \text{NMAX}$
CAB	$RE \left((\text{ALPHA}+J*\text{BETA})^{(I-2)} \right)$ FOR $I=2, \dots, \text{NMAX}$
SAB	$IM \left((\text{ALPHA}+J*\text{BETA})^{(I-2)} \right)$ FOR $I=2, \dots, \text{NMAX}$
GENCOS	Coefficient of $\text{COS}(K*L)$ term in SPG
GENSIN	Coefficient of $\text{SIN}(K*L)$ term in SPG

These variables were defined in the following general way in SPZONB.CMN:

DIMENSION	XJLAN (ZONPOT)	
DIMENSION	V (ZONPOT+1)	
DIMENSION	D (ZONPOT+1)	
DIMENSION	Q (ZONPOT+1)	
DIMENSION	CKH (ZONPOT+2)	
DIMENSION	SKH (ZONPOT+2)	
DIMENSION	CAB (ZONPOT+2)	(4.37)
DIMENSION	SAB (ZONPOT+2)	
DIMENSION	GENCOS (2*ZONPOT - 1)	
DIMENSION	GENSIN (2*ZONPOT - 1)	

where ZONPOT is another generic parameter representing the size of the gravity field model.

The link map indicated that the following routines needed to include SPZONB:

CONSTS.FOR
ECSUM1.FOR
ECSUM2.FOR
ECSUM3.FOR
EVESM1.FOR
EVESM2.FOR
EVHRM1.FOR
EVHRM2.FOR
FNSTEP.FOR
FUNINT.FOR
GHPOLY.FOR
HRMSM1.FOR
HRMSM2.FOR
HRMSM3.FOR
JPOLY.FOR
ODESM1.FOR
ODESM2.FOR
SNGESM.FOR
SPZONL.FOR
TERM.FOR
ZONGEN.FOR

ZONSPC.FOR
 ZONVAR.FOR

4.3.3.9 TESS.CMN

TESS is yet another example of a common area which was entirely converted to an include file and associated block data. This common area was built to store variables which fall under the routines SPTESS, PTESRS, and RESPRT. SPTESS and PTESRS have been described previously. Routine RESPRT provides an SST tesseral resonant solve-for option [49]. Table 4.12 describes the variables in this common area with sizes dependent on the limits of the gravity field model:

Table 4.12 TESS Variables

Variable	Definition
H13	Hansen coefficient kernel, quadrant 1 and 3
P13	Partial derivative of Hansen coefficient kernel with respect to the eccentricity squared, quadrant 1 and 3
H24	Hansen coefficient kernel, quadrant 2 and 4
P24	Partial derivative of Hansen coefficient kernel with respect to the eccentricity squared, quadrant 2 and 4

These variables were dimensioned in the following, general way in TESS.CMN:

DIMENSION H13 (NUMCS+2)
 DIMENSION P13 (NUMCS+2)
 DIMENSION H24 (NUMCS+2)
 DIMENSION P24 (NUMCS+2)

(4.38)

where NUMCS is another generic parameter representing the size of the gravity field model.

The link map indicated that the following routines needed to include TESS:

ACMRES.FOR
ACMTES.FOR
ASMPRT.FOR
ASMRES.FOR
ASMTES.FOR
EIRES.FOR
EITESS.FOR
HSEN.FOR
HSMEXC.FOR
HSMPRT.FOR
HSMRES.FOR
HSMTES.FOR
INTES.FOR
INTPRT.FOR
INTRES.FOR
PTESRS.FOR
RESPRT.FOR
RSMEXC.FOR
RSMINT.FOR
SPTESS.FOR

4.3.3.10 TSRES.CMN

TSRES is the last common area that was converted to an include file and an associated block data. This common area contains the following three arrays with sizes dependent on the degree and order of the gravity field model:

Table 4.13 TSRES Variables

Variable	Definition
JRES	Array to indicate resonant indices
MRES	Array to indicate resonant orders
NRES	Array to indicate resonant degrees

These arrays were dimensioned in the following way in TSRES.CMN:

```
DIMENSION JRES (GRAVNO)
DIMENSION MRES (GRAVNO)
DIMENSION NRES (((1+GRAVNO)*GRAVNO)/2)
```

(4.39)

where GRAVNO is another generic parameter representing the size of the gravity field model. It should be noted that NRES is sized so that the software could support geosynchronous cases in which every harmonic is potentially resonant--a scenario which is, more than likely, not practical.

The link map indicated that the following routines needed to include TSRES:

ANAVR.FOR

ANRES.FOR
 AVRINT.FOR
 SELRES.FOR
 SETAVR.FOR
 SPANAL.FOR
 VARANL.FOR

4.3.4 Summary of Modifications to GTDS

Sections 4.3.2 and 4.3.3 described the various modifications that were made to GTDS. This section will list and describe every routine that was modified. In addition, a listing and description of all new routines will be given.

Table 4.14 Summary of Modifications to Original GTDS

Routine	Change Description
ACCUM.FOR	•Included MDWRK
ACMRES.FOR	•Included TESS
ACMTES.FOR	•Included TESS
ANAVR.FOR	•Included TSRES •Added GRAVNO and NUMNRES to call to PTESRS.FOR
ANHARM.FOR	•Included HRMCF •Included ANAV1
ANLHDR.FOR	•Included HRMCF •Made potential-related indices general
ANLWRT.FOR	•Included SPREAL

ANRES.FOR	•Included TSRES
ANTHIR.FOR	•Included ANAV1
ASMBLY.FOR	•Removed erroneous reference to CS, SIRE, and SICX (comment line fix) •Included MDWRK
AUXTRN.FOR	•Included ANAV1 •Made potential-related indices general
AVRINT.FOR	•Included HRMCF •Included TSRES •Made potential-related indices general
BROLYD.FOR	•Included HRMCF
BROUWR.FOR	•Included HRMCF
CHETO.FOR	•Included HRMCF
CMPMEL.FOR	•Included HRMCF
CMPOEL.FOR	•Included HRMCF
COMORB.FOR	•Included HRMCF
CONSTS.FOR	•Included SPZONB •Updated DIMENSION statements with "*" logic
COREST.FOR	•Included HRMCF •Made potential-related loop indices general
DBOUND.FOR	•Included ANAV1
DCBUG.FOR	•Included HRMCF
DRAGJ2.FOR	•Included HRMCF
ECSUM1.FOR	•Included SPZONB
ECSUM2.FOR	•Included SPZONB

ECSUM3.FOR	•Included SPZONB
EILOAD.FOR	•Included GRAVITY
EIPOLY.FOR	•Removed erroneous reference to CS (comment line fix) •Included MDWRK
EIRES.FOR	•Included TESS •Included GRAVITY
EITESS.FOR	•Included TESS
EITRY.FOR	•Included GRAVITY
ELEMGN.FOR	•Included HRMCF
EPHEM.FOR	•Included HRMCF •Made potential-related loop indices general
EQINT.FOR	•Included HRMCF
EVESM1.FOR	•Included SPZONB
EVESM2.FOR	•Included SPZONB
EVHRM1.FOR	•Included SPZONB
EVHRM2.FOR	•Included SPZONB
FILESBD.FOR	•Assigned FORTRAN reference numbers for new earth and lunar permanent gravity files (FRN47 and FRN48)
FINIT.FOR	•Included PTSDAT
FNEWM1.FOR	•Included PTSDAT
FNEWM2.FOR	•Included PTSDAT
FNSTEP.FOR	•Included SPZONB

FRCBD.FOR	<ul style="list-style-type: none"> •Dummied out old locations for CS, SINLAM, and COSLAM arrays •Updated hardwired values for NDEPF, NOEPF, NDMPF, and NOMPF
FSUM.FOR	<ul style="list-style-type: none"> •Included AVEPOT
FUNINT.FOR	<ul style="list-style-type: none"> •Included SPZONB
FZERO.FOR	<ul style="list-style-type: none"> •Included PTSDAT
GHPOLY.FOR	<ul style="list-style-type: none"> •Included SPZONB
HARM.FOR	<ul style="list-style-type: none"> •Included HRMCF •Included CSBLNK •Updated READ logic •Made potential-related loop indices general
HRMSM1.FOR	<ul style="list-style-type: none"> •Included SPZONB
HRMSM2.FOR	<ul style="list-style-type: none"> •Included SPZONB
HRMSM3.FOR	<ul style="list-style-type: none"> •Included SPZONB
HSEN.FOR	<ul style="list-style-type: none"> •Included TESS •Included NUKES •Renamed local variable FACTOR to avoid conflict with TESS
HSMEXC.FOR	<ul style="list-style-type: none"> •Included TESS
HSMMD.FOR	<ul style="list-style-type: none"> •Included HRMCF •Made potential-related loop indices general •Included MDWRK

HSMprt.FOR	<ul style="list-style-type: none"> • Included TESS • Removed erroneous reference to CS (comment line fix) • Removed erroneous reference to NRES (comment line fix)
HSMRES.FOR	<ul style="list-style-type: none"> • Included TESS • Included HRMCF • Made potential-related indices general • Added NUMNRES to argument call list (to DIMENSION NRES)
HSMTES.FOR	<ul style="list-style-type: none"> • Included TESS • Included HRMCF • Made potential-related indices general
HSUM.FOR	<ul style="list-style-type: none"> • Included HRMCF • Included AVEPOT
HWIRE.FOR	<ul style="list-style-type: none"> • Included SPREAL • Updated comment lines to be consistent with increased gravity field capability
IJPOLY.FOR	<ul style="list-style-type: none"> • Included SPZONB
INREAD.FOR	<ul style="list-style-type: none"> • Included NUKES
INTES.FOR	<ul style="list-style-type: none"> • Included TESS
INTHSM.FOR	<ul style="list-style-type: none"> • Included MDWRK • Removed erroneous reference to FRC (comment line fix)
INTOGV.FOR	<ul style="list-style-type: none"> • Included HRMCF
INTPRT.FOR	<ul style="list-style-type: none"> • Included TESS
INTRES.FOR	<ul style="list-style-type: none"> • Included TESS
INTS.FOR	<ul style="list-style-type: none"> • Included MDWRK • Removed erroneous reference to CS (comment line fix)

J2PART.FOR	•Included HRMCF
J2SOR.FOR	•Included HRMCF
KFHIST.FOR	•Included SPREAL
MEANOSC.FOR	•Included SPREAL
MUKON.FOR	•Included HRMCF
NKREAD.FOR	•Included NUKES
NUKESBD.FOR	•Modified existing code to be compatible with NUKES.CMN
ODESM1.FOR	•Included SPZONB
ODESM2.FOR	•Included SPZONB
OGBUG.FOR	•Included HRMCF •Included GEOVAR •Included LEGPOL
OSM1OR.FOR	•Removed erroneous reference to CS (comment line fix)
OSCMEAN.FOR	•Included SPREAL
OSMEAN.FOR	•Included HRMCF
OSMKEP.FOR	•Included HRMCF
OUTPPC.FOR	•Included HRMCF •Included CSBLNK •Added pointer to FRN47 and FRN48 •Updated READ logic •Added CLOSE capability for FRN47 and FRN48 •Made potential-related indices general
PASSBD.FOR	•Dummied out old locations for PMN and TPSIM arrays

PCWF.FOR	<ul style="list-style-type: none"> •Included HRMCF •Added pointer to FRN47 and FRN48 •Updated harmonic coefficient READ logic •Added CLOSE capability for FRN47 and FRN48 •Made potential-related indices general
PDNEWM.FOR	<ul style="list-style-type: none"> •Included PTSDAT
PSET.FOR	<ul style="list-style-type: none"> •Included HRMCF •Made potential-related indices general
PTESRS.FOR	<ul style="list-style-type: none"> •Included TESS •Included GRAVITY •Made potential-related indices general •Removed erroneous reference to FRC (comment line fix) •Added GRAVNO and NUMNRES to argument call list •Added NUMNRES to call to RSMEXC.FOR
PTESS.FOR	<ul style="list-style-type: none"> •Included HRMCF •Made potential-related indices general
RBOUND.FOR	<ul style="list-style-type: none"> •Included ANAV1 •Made potential-related indices general
RESNJV.FOR	<ul style="list-style-type: none"> •Included HRMCF
RESPAR.FOR	<ul style="list-style-type: none"> •Included HRMCF •Included GEOVAR •Included LEGPOL •Made potential-related indices general

RESPRT.FOR	<ul style="list-style-type: none"> •Included TESS •Included GRAVITY •Added GRAVNO and NUMNRES to argument call list
RESPV.FOR	<ul style="list-style-type: none"> •Included HRMCF •Included GEOVAR •Included LEGPOL •Made potential-related indices general
RPTEST.FOR	<ul style="list-style-type: none"> •Included HRMCF
RSMEXC.FOR	<ul style="list-style-type: none"> •Included TESS •Added NUMNRES to argument call list (to DIMENSION NRES) •Added NUMNRES to call to HSMRES.FOR
RSMINT.FOR	<ul style="list-style-type: none"> •Included TESS
SECULR.FOR	<ul style="list-style-type: none"> •Included HRMCF
SECUPD.FOR	<ul style="list-style-type: none"> •Included HRMCF •Updated harmonic coefficient READ logic •Made potential-related indices general
SELRES.FOR	<ul style="list-style-type: none"> •Included TSRES •Removed erroneous reference to CS (comment line fix) •Made potential-related indices general
SETAVR.FOR	<ul style="list-style-type: none"> •Included TSRES •Updated hardwired limit for degree and order •Made potential-related indices general
SETDAF.FOR	<ul style="list-style-type: none"> •Added capability to OPEN FRN47 and FRN48

SETOG1.FOR	<ul style="list-style-type: none"> •Included HRMCF •Included CSBLNK •Included LUMPCS •Added pointer to FRN47 and FRN48 •Updated harmonic coefficient READ logic •Made potential-related indices general
SETOG2.FOR	<ul style="list-style-type: none"> •Included HRMCF •Included CSBLNK •Added pointer to FRN47 and FRN48 •Updated harmonic coefficient READ logic •Made potential-related indices general
SETORB.FOR	<ul style="list-style-type: none"> •Included HRMCF •Included CSBLNK •Updated hardwired limit for MAXDEGEQ and MAXORDEQ •Made potential-related indices general
SETSPG.FOR	<ul style="list-style-type: none"> •Included SPREAL
SHORTP.FOR	<ul style="list-style-type: none"> •Included HRMCF
SKFPRT.FOR	<ul style="list-style-type: none"> •Included SPREAL
SNGESM.FOR	<ul style="list-style-type: none"> •Included SPZONE
SOLTAB.FOR	<ul style="list-style-type: none"> •Included HRMCF •Made potential-related indices general
SPANAL.FOR	<ul style="list-style-type: none"> •Included TSRES •Included SPREAL •Added GRAVNO to call to SPTESS.FOR •Added TFDPL2 to call to SPTHIR.FOR

SPART.FOR	<ul style="list-style-type: none"> •Included HRMCF •Included GEOVAR •Included LEGPOL •Made potential-related indices general
SPARTV.FOR	<ul style="list-style-type: none"> •Included HRMCF •Included GEOVAR •Included LEGPOL •Included LUMPCS •Made potential-related indices general
SPCOEF.FOR	•Included SPREAL
SPCOTO.FOR	•Included SPREAL
SPDIFF.FOR	•Included SPREAL
SPGENR.FOR	•Included SPREAL
SPINIT.FOR	•Included SPREAL
SPINTGBD.FOR	•Updated comments concerning number of short-periodic coefficients
SPINTP.FOR	•Included SPREAL
SPJ2MD.FOR	•Included SPREAL
SPJ2PR.FOR	•Included HRMCF
SPJ2SQ.FOR	•Included HRMCF
SPMDLY.FOR	<ul style="list-style-type: none"> •Included MDWRK •Removed erroneous reference to FRC (comment line fix)
SPMOVE.FOR	•Included SPREAL

SPNUM.FOR	<ul style="list-style-type: none"> •Included SPREAL •Renamed local variable XLAMDA to XXLAMDA to avoid conflict with SPREAL
SPNUM2.FOR	<ul style="list-style-type: none"> •Included SPREAL •Renamed local variable XLAMDA to XXLAMDA to avoid conflict with SPREAL
SPORB.FOR	<ul style="list-style-type: none"> •Included SPREAL
SPORBP.FOR	<ul style="list-style-type: none"> •Included SPREAL
SPSKF.FOR	<ul style="list-style-type: none"> •Included SPREAL
SPTESS.FOR	<ul style="list-style-type: none"> •Included TESS •Included GRAVITY •Added GRAVNO to argument call list
SPTHIR.FOR	<ul style="list-style-type: none"> •Added TFDPL2 to argument call list •Dimensioned short-periodic coefficients with TFDPL2
SPZONL.FOR	<ul style="list-style-type: none"> •Included HRMCF •Included SPZONB
TERM.FOR	<ul style="list-style-type: none"> •Included SPZONB
THIVAR.FOR	<ul style="list-style-type: none"> •Updated DIMENSION statements with "*" logic
TSROUT.FOR	<ul style="list-style-type: none"> •Included HRMCF •Made potential-related indices general
TSUM.FOR	<ul style="list-style-type: none"> •Included AVEPOT
TSUMN.FOR	<ul style="list-style-type: none"> •Included HRMCF •Included PTSDAT •Made potential-related indices general

VARANL.FOR	<ul style="list-style-type: none"> •Included TSRES •Added GRAVNO and NUMNRES to call to RESPRT.FOR
VRSPFD.FOR	<ul style="list-style-type: none"> •Included SPREAL
VNMEAN.FOR	<ul style="list-style-type: none"> •Included HRMCF
ZONGEN.FOR	<ul style="list-style-type: none"> •Included SPZONB
ZONSPC.FOR	<ul style="list-style-type: none"> •Included SPZONB
ZONVAR.FOR	<ul style="list-style-type: none"> •Updated DIMENSION statements with "*" logic

In all, a total of 144 routines and approximately 2900 lines of code were modified in support of the work for this thesis.

Table 4.15 Summary of New Routines Added to GTDS

Routine	Lines	Description
HRMCF.CMN	40	•Establishes common area for harmonic coefficients
HRMCF.FOR	2719	•Stores the harmonic coefficients
LEGPOL.CMN	41	•Establishes common area for Legendre and associated Legendre polynomials
LEGPOL.FOR	18	•Stores the Legendre and associated Legendre polynomials
GEOVAR.CMN	42	•Establishes common area for SINLAM, COSLAM, and TPSIM arrays
GEOVAR.FOR	21	•Stores the SINLAM, COSLAM, and TPSIM arrays

LUMPCS.CMN	40	•Establishes common area for DELCS array
LUMPCS.FOR	20	•Stores the DELCS array
CSBLNK.CMN	46	•Establishes common area for CSSTOR, ICSTEM, and PTNTL arrays
CSBLNK.FOR	19	•Stores the CSSTOR, ICSTEM, and PTNTL arrays
NUKES.CMN	43	•Establishes common area for the Newcomb operators
ANAV1.CMN	48	•Establishes common area for FACT, EPWR, HAFPWR, XPWR, SINPWR, and ONEGPW arrays
ANAV1.FOR	12	•Stores the FACT, EPWR, HAFPWR, XPWR, SINPWR, and ONEGPW arrays
AVEPOT.CMN	44	•Establishes common area for XJLAN, ARN, QNM, and GAMMAN arrays
AVEPOT.FOR	10	•Stores the XJLAN, ARN, QNM, and GAMMAN arrays
GRAVITY.CMN	32	•Establishes common area for FIELD_SIZE, TWOFS1, and TWOFS2 parameters
MDWRK.CMN	350	•Establishes common area for all variables in this entirely converted version of MDWRK
MDWRK.FOR	19	•Stores all variables used in this entirely converted version of MDWRK
PTSDAT.CMN	44	•Establishes common area for GLAST, HLAST, GLASTX, HLASTX, and DPDDX arrays
PTSDAT.FOR	10	•Stores the GLAST, HLAST, GLASTX, HLASTX, and DPDDX arrays

SPREAL.CMN	336	•Establishes common area for all variables in this entirely converted version of SPREAL
SPREAL.FOR	27	•Stores all variables used in this entirely converted version of SPREAL
SPZONB.CMN	222	•Establishes common area for all variables in this entirely converted version of SPZONB
SPZONB.FOR	10	•Stores all variables used in this entirely converted version of SPZONB
TESS.CMN	603	•Establishes common area for all variables in this entirely converted version of TESS
TESS.FOR	32	•Stores all variables used in this entirely converted version of TESS
TSRES.CMN	57	•Establishes common area for all variables in this entirely converted version of TSRES
TSRES.FOR	53	•Stores all variables used in this entirely converted version of TSRES
TOTAL NEW LINES OF CODE: 4990		

In all, a total of 28 new routines encompassing 4990 lines of code were added to GTDS. This table indicates that all the new routines were include files or associated block datas which store arrays and variables related to the gravity modeling capability within GTDS. It should be noted that the new executable image of GTDS (16,060 blocks) is 4845 blocks larger than executable image that existed before any of the modifications to support the work in this thesis were made (11,215 blocks).

If it was desired to increase the size of the gravity field model beyond the current standard of 50x50, the user would simply need to make the following modifications:

Table 4.16 Summary of Actions to Increase Limits of Gravity Field Model Beyond 50x50

Routine	Action
HRMCF.CMN	•Update value of NUMCOF to desired field size
HRMCF.FOR	•Update lay-out of default harmonic coefficients
LEGPOL.CMN	•Update value of GEOCS to desired field size
GEOVAR.CMN	•Update value of GEONUM to desired field size
ANAV1.CMN	•Update value of POTNUM to desired field size
MDWRK.CMN	•Update value of NUMPOT to desired field size
TSRES.CMN	•Update value of GRAVNO to desired field size
TESS.CMN	•Update value of NUMCS to desired field size
LUMPCS.CMN	•Update value of LUMPNO to desired field size
CSBLNK.CMN	•Update value of CSBNUM to desired field size
AVEPOT.CMN	•Update value of DEGORD to desired field size
PTSDAT.CMN	•Update value of ORDDEG to desired field size
SPZONB.CMN	•Update value of ZONPOT to desired field size
SPREAL.CMN	•Update value of FLDDIM to desired field size
GRAVITY.CMN	•Update value of FIELD_SIZE to desired field size

FRCBD.FOR	<ul style="list-style-type: none"> •Update value of NDEPF to desired field size •Update value of NOEPF to desired field size •Update value of NDMPF to desired field size •Update value of NOMPF to desired field size
NUKES.CMN	<ul style="list-style-type: none"> •Update value of NNUKE to reflect the number of Newcomb operators built by WRITE_NUKES.FOR (refer to Appendix E)
SETDAF.FOR	<ul style="list-style-type: none"> •Open new FRN files corresponding to appropriate permanent earth/lunar potential files
DANWHARM.FOR	<ul style="list-style-type: none"> •Update value of NUMCOF to desired field size •Build new permanent earth/lunar potential files

If so desired, the user can attempt to INCLUDE GRAVITY.CMN into each of the other common areas containing a generic parameter representing the limits of the gravity field model. Then, the generic parameter can be equated or equivalenced to the variable FIELD_SIZE, which lives in GRAVITY.CMN. This modification would provide for a single modification point concerning the generic parameters representing the limits of the gravity field model.

4.3.5 Modifications to "Original" GTDS

During testing of the modified version of GTDS, it was discovered that a discrepancy existed for a Semianalytic run between un-modified and modified versions of GTDS for the limiting 21x21 field case. Using the DEBUG capability of the VAX, it was discovered that the SIRE and SICX arrays used in the routines EILOAD, EIRES, EITESS, EITRY, PTESSRS, RESPRT, and SPTESS were dimensioned incorrectly in the un-modified

version of GTDS. These arrays, which have definitions similar to those for the SIRE and SICX arrays which are stored in the common area MDWRK, were dimensioned in the following way in original GTDS:

DIMENSION	SIRE (43)	(4.40)
DIMENSION	SICX (43)	

For correct implementation, these arrays should be dimensioned slightly larger:

DIMENSION	SIRE (44)	(4.41)
DIMENSION	SICX (44)	

Testing shows that this modification provides exact agreement between original and modified GTDS. It should be noted that the impact of this bug is small in nature; the slight change in the aforementioned DIMENSION statements is a trivial task. The next chapter of this thesis will describe the testing of GTDS in more detail.

[This page intentionally left blank.]

Chapter 5

50X50 Gravity Field Model Results

5.1 Chapter Introduction

Chapter 4 described in detail the various modifications that were made to GTDS as part of the work for this thesis. In summary, 144 routines were modified and 28 new routines were added to the previously existing version of GTDS in order to support the 50x50 class gravity field models (for the remainder of this chapter, the version of GTDS which existed prior to the work for this thesis will be referred to as "old" GTDS, while the version containing all of the work accomplished as part of this thesis will be referred to as "new" GTDS). Since GTDS was significantly modified as part of this thesis, it was necessary to develop a logical validation philosophy to ensure that (1) none of the capabilities of old GTDS were disabled and (2) that the new capabilities added to GTDS were implemented correctly. This Chapter describes the validation philosophy that was implemented for the Cowell and Semianalytic orbit generators.

Chapter 5 is organized in the following fashion:

- Section 5.2 Validation of Permanent File Report Function.
- Section 5.3 Unit testing of Cowell Accelerations
- Section 5.4 Testing of the Cowell Orbit Generator
- Section 5.5 Testing of Cowell Differential Correction
- Section 5.6 Testing of the Semianalytic Orbit Generator

- Section 5.7 Impact of 50x50 Gravity Models in Orbit Determination

The first step in the validation process was to check that the Permanent File Report Function in GTDS was working properly. This check ensured that correct values for the harmonic coefficients were being obtained. Then, Cowell accelerations computed by new GTDS were checked against values obtained from the standalone routine described in Chapter 3. After successful unit testing of the Cowell accelerations, the step to full-up testing of Cowell integrations was taken. First, 21x21 class gravity field models were compared between old and new GTDS. Then, a gradual increase in field size from 21x21 to 50x50 was taken to check consistency of results. Cowell 50x50 results from new GTDS were compared against results obtained from TRACE [54], a separate orbit determination program [59,60]. In addition, a 50x50 Cowell Differential Correction run was made to test the Differential Correction Program and the use of the variational equations. Validated Cowell results were used, in turn, to validate Semianalytic runs.

Once it was determined that both the Cowell and Semianalytic orbit generators were working successfully, the impact of 50 x 50 gravity field models in orbit determination was analyzed. Specifically, resonant effects captured by 50x50 class models which had been neglected by 21x21 class models were studied.

On the BIGSIM VAX 8820, the following directory system was created to support the testing described in this Chapter:

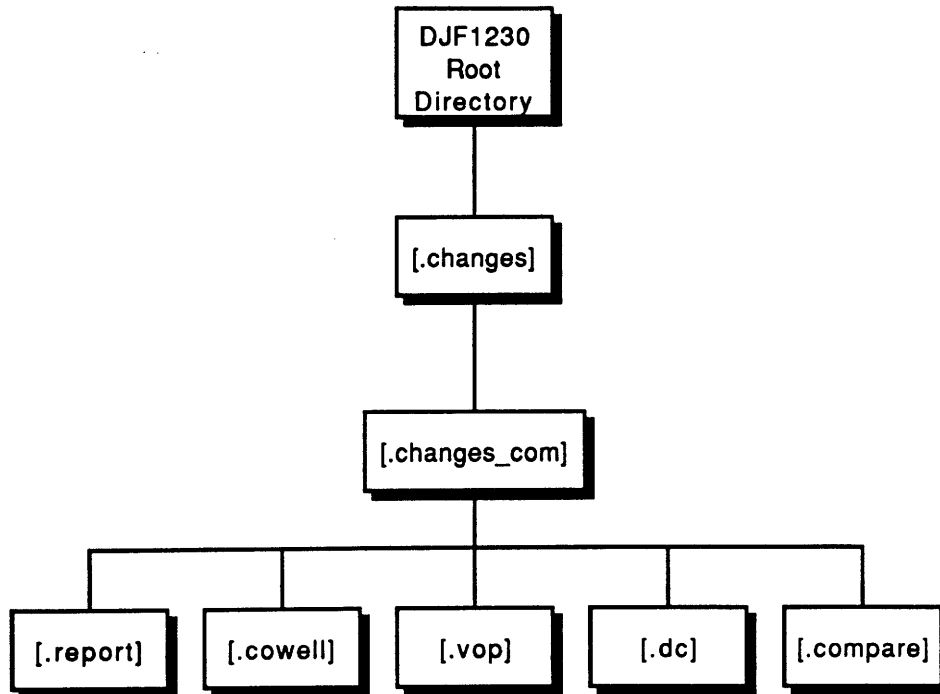


Figure 5.1 Directory System for Testing

This directory system augments the one given in Figure 4.11. These directories were used to store test-related files for the validation of the Permanent File Report Generation Program, Cowell orbit generator, Semianalytic orbit generator, Differential Correction Program, and the Ephemeris Comparison Program.

5.2 Validation of Report Function

The Permanent File Report Function was used to ensure that GTDS was obtaining the correct values for the harmonic coefficients from FRN8 and FRN47. The following input deck was used in this test:

```
CONTROL  FILERPT
PFROPT
EPOTRPT  2  0
END
FIN
```

**Figure 5.2 Sample Input Deck to Validate Report Function
THESIS_REPORT.GTDS**

The output which results from this deck contains a full report on all the models in the permanent earth potential field files (FRN 8 and FRN47). This report consists of (1) the name and model number of the various models, (2) the value used for the gravitational parameter for each of the models, (3) the value used for the radius of the earth for each of the models, and (4) listings of the harmonic coefficients for each of the models. Since the output which corresponds to this input deck is rather large, it is not included here. It can, however, be referenced under the filename

THESIS_REPORT.OUTPUT (5.1)

in the directory

[DJF1230.CHANGES.CHANGES_COM.REPORT] (5.2)

It should be noted that this process provided a second check that DANWHARM.FOR was functioning properly (the output text file described in Section 4.3.1 was the first).

5.3 Unit Testing of Cowell Accelerations

The purpose of the testing in Chapter 3 was to determine the stability of the Legendre and associated Legendre polynomials and to compute Cowell accelerations with a GTDS Emulation routine. A GTDS emulation was used rather than actual GTDS to avoid (1) making numerous modifications to GTDS to support the 50x50 class fields in an un-normalized sense, (2) finding that the polynomials are unstable, and (3) having to re-modify GTDS to support normalized expressions. Normalized recursions for the polynomials given by Lundberg and Schutz [36] were used in a truth model. The results indicated that the Cowell accelerations obtained from un-normalized expressions in the GTDS emulation produced favorable results in the VAX and UNIX environments (refer to Chapter 3).

The first step in testing the Cowell orbit generator in new GTDS was to compare results for Cowell accelerations between the actual GTDS code and the truth model. The LANDSAT 4 initial conditions were used for test purposes since (1) many benchmark test cases have been generated from these initial conditions and (2) the orbit is similar to that of RADARSAT, the satellite for which this work was intended:

```
CONTROL      EPHEM                      LNSAT-4      8207201
EPOCH                820224.0                0.0
ELEMENT1  1  2  1  7077.8                0.0011      98.2
ELEMENT2                158.1                89.4      176.0
OUTPUT  1  2  1  820227.0                0.0      43200.
ORBTYPE  2  1  1  a.0
OGOPT
MAXDEGEQ  1          x.
MAXORDEQ  1          y.
POTFIELD  1  z
END
FIN
```

**Figure 5.3 Standard Cowell Input Deck Format
LANDSAT 4**

In this input deck, several items of interest can be noted. The EPOCH card establishes an epoch date of 24 February 1982 (0.0 hours). The first integer field in the ELEMENT1 card indicates that the mean earth equator and equinox of 1950.0 is the input system orientation. The second integer field indicates a Keplerian input coordinate system. The third integer field indicates that the earth is the input reference body. The actual elements listed on the ELEMENTX cards represent semimajor axis, eccentricity, inclination (degrees), longitude of ascending node (degrees), argument of perigee (degrees), and mean anomaly (degrees), respectively. The first integer field on the OUTPUT card indicates an output coordinate system of mean earth equator and equinox of 1950.0. The second integer field represents a Cartesian, Keplerian, and spherical output reference system. Again, the third integer field represents the earth as the output reference body. The first real field provides a date of 27 February 1982 (0.0 hours) as the end of the print arc. The third real field specifies the print interval on the output report (in seconds). As described in Section 4.2.4, the value for integration step size (a.0), maximum degree (x), maximum order (y), and gravity model number (z) depends on the specific test case. The set-up of this card implies that only central and third body gravitational perturbations are considered (by default, third body effects are turned on in GTDS). It should be noted that the input conditions given in Figure 5.3 hold for *every* Cowell run (unless otherwise stated).

The Cowell accelerations for a GEM10B 21x21 gravity field model, a capability that old GTDS was configured to handle, are given first:

**Table 5.1 Cowell Acceleration Validation
New GTDS vs. Lundberg Truth (21x21 GEM10B)**

	New GTDS Value	Lundberg Truth Value
ax_b	8.653210294968294E-7	8.653210294968288481236474144803601E-7
ay_b	-6.515584998975128E-6	-6.515584998975091510625442206439533E-6
az_b	-1.931032474628621E-5	-1.931032474628616528394963271551205E-5

where the GEM10B values for the gravitational parameter and radius of the earth are $398600.44 \text{ km}^3/\text{sec}^2$ and 6378.138 km , respectively.

Cowell accelerations for GEMT3 21x21, 25x25, 30x30, and 50x50 are given in Table 5.2 through Table 5.5:

**Table 5.2 Cowell Acceleration Validation
New GTDS vs. Lundberg Truth (21x21 GEMT3)**

	New GTDS Value	Lundberg Truth Value
ax_b	8.713973515294979E-007	8.713973515294979223157917187605221E-0007
ay_b	-6.519983675472165E-006	-6.519983675472133076020419311681219E-0006
az_b	-1.931383457156898E-005	-1.931383457156895243203575004719676E-0005

**Table 5.3 Cowell Acceleration Validation
New GTDS vs. Lundberg Truth (25x25 GEMT3)**

	New GTDS Value	Lundberg Truth Value
ax_b	8.688640158899119E-007	8.688640158899117181705904414281339E-0007
ay_b	-6.519810117658732E-006	-6.519810117658698995672096587377993E-0006
az_b	-1.931666723569801E-005	-1.931666723569798341013986223813520E-0005

**Table 5.4 Cowell Acceleration Validation
New GTDS vs. Lundberg Truth (30x30 GEMT3)**

	New GTDS Value	Lundberg Truth Value
ax_b	8.687362166403940E-007	8.687362166403939787963327971153236E-0007
ay_b	-6.519188447356782E-006	-6.519188447356751035844360468187382E-0006
az_b	-1.931896767331529E-005	-1.931896767331525869055067895284881E-0005

**Table 5.5 Cowell Acceleration Validation
New GTDS vs. Lundberg Truth (50x50 GEMT3)**

	New GTDS Value	Lundberg Truth Value
axb	8.683465146150195E-007	8.683465146150193614319424992827359E-0007
ayb	-6.519678538340111E-006	-6.519678538340080232354478851469384E-0006
azb	-1.931876804829167E-005	-1.931876804829163932564593223959640E-0005

The values listed in Table 5.2 through Table 5.5 correspond to a single point along the Cowell integration. The specifics of this point are given in Table 3.2 (these specifics correspond to the first point along the Cowell integration from the inputs given in Figure 5.3). The results for other points along the integration are in accordance with those given here and, for the sake of brevity are not given. GEMT3 values of 398600.436 km³/sec² and 6378.137 km hold for the gravitational parameter and radius of the earth, respectively. In addition, 60 second step-sizes were used for test cases with gravity field models sized less than or equal to the 21x21 standard; 10 second step-sizes were used for test cases with gravity field models larger than the 21x21 standard.

The results given in this section show that the Cowell accelerations produced by new GTDS possessed tight agreement with the truth model. For this reason, they were considered acceptable, and the step to full-up testing of the Cowell orbit generator was made.

5.4 Testing of the Cowell Orbit Generator

With successful unit testing of the Cowell accelerations completed, the next step was to actually perform a Cowell integration over a desired arc and analyze conditions at the end of the arc. For 21x21 class models, comparisons between old and new GTDS could be made. For testing beyond the 21x21 capability of old GTDS, TRACE was used for comparison purposes. As with the Cowell acceleration unit testing, a standalone routine could have been built to simulate the Cowell Orbit Generator. It was determined, however, that using TRACE for comparison purposes would provide a much more rigorous test of the Cowell orbit generator. For this reason, a standalone Cowell orbit generator was not built for test purposes.

The first test case chosen for the full-up Cowell integration was a 21x21 GEM10B run. Since old GTDS was configured to handle a run of this type (the GEM10B model is stored on FRN8), this run would essentially prove that nothing was broken as a result of the work in this thesis. The results of a three day arc corresponding to the initial conditions given in Figure 5.3 are listed in Table 5.6:

**Table 5.6 Cowell Orbit Generator Validation
Old GTDS vs. New GTDS (21x21 GEM10B)**

State	Old GTDS	New GTDS
X	0.3873178650543644D+04	0.3873178650543644D+04
Y	-0.4305621520174543D+03	-0.4305621520174543D+03
Z	0.5925115219741317D+04	0.5925115219741317D+04

Next, a 21x21 GEMT3 run was made; it should be noted that a 21x21 version of the GEMT3 gravity model was built using the DANWHARM utility. The file is in the following directory

[DJF1230.RUNGTDS] (5.3)

and is named

GEMT3_21BY21.DAT (5.4)

This file can be assigned as old GTDS's permanent earth potential file (FRN8). The results of a three-day arc corresponding to the initial conditions given in Figure 5.3 are given in Table 5.7:

**Table 5.7 Cowell Orbit Generator Validation
Old GTDS vs. New GTDS (21x21 GEMT3)**

State	Old GTDS	New GTDS
X	0.3873119522963696D+04	0.3873119522963696D+04
Y	-0.4305267000347166D+03	-0.4305267000347166D+03
Z	0.5925163676253139D+04	0.5925163676253139D+04

The test which produced the results in Table 5.7 differed from the one which produced the results in Table 5.6 in that the test for 5.7 utilized logic associated with FRN47; the test for 5.6 used logic associated with FRN8--logic which old GTDS was configured to handle.

Again, it should be noted that 60 second step-sizes were used in these test cases with gravity field models sized less than or equal to the 21x21 standard.

Testing for fields beyond the 21x21 capability could not use old GTDS for comparison purposes. TRACE, Aerospace Corporation's orbit determination program, was used for fields larger than 21x21. The input decks used for the GTDS/TRACE comparisons were of the following form:

```

CONTROL  DATAMGT                                RADARSAT  8202230
OGOFT
POTFIELD 1 13
END
FIN
CONTROL  EPHEM                                RADARSAT  8202230
ELEMENT1 1 2 1 7077.8                        0.0011    98.2
ELEMENT2                158.1                89.4      176.0
EPOCH                820224.0                000000.0
OUTPUT  1 2 1 82xxxx.0                      000000.0  120.0
ORBTYPE 2 1 1 10.0
OGOFT
NCBODY  1
MAXDEGEQ 1 50.0
MAXORDEQ 1 50.0
GMCON  1 398600.5
OUTOPT  2 2 1 820224000000.0                82xxxx000000.0
END
FIN

```

**Figure 5.4 GTDS/TRACE Input Deck Format
GEMT3 Harmonic Coefficients**

where the time periods of integration and for output to an ORB1 file are case dependent.

The format of this input deck is similar to that of the deck given in Figure 5.3. There are, however, some differences in this deck which are of interest. These differences, which stem from attempts to align results from two distinct orbit determination programs, are described next:

- (1) NCBODY keyword card. The use of this card as depicted in Figure 5.4 turns off the third-body (lunar-solar) effects which are automatically included by default in GTDS if this card is not present.

(2) GMCON keyword card. This card provides for an overwrite of the value for the gravitational parameter stored on the permanent potential file(s).

Other non-input deck related issues which were addressed in order to compare GTDS with TRACE are as follows:

(1) A time standard of UT1=UTC. This standard, which required modification of the time difference polynomials which govern the transformation between the time systems A.1, UTC, and UT1, was implemented in the following manner in the GTDS time conversion file:

$$\begin{aligned} \text{A.1} - \text{UTC} &= 20.0 \text{ sec} \\ \text{A.1} - \text{UT1} &= 20.0 \text{ sec} \end{aligned} \tag{5.5}$$

This definition was consistent with what was used at Aerospace to produce results with TRACE [54]. It should be noted that the time standards used for this test did not include polar motion corrections. The GTDS Math Specification [26] details the various time systems and the transformation between these systems.

(2) GTDS's Solar/Lunar/Planetary (SLP) Ephemeris File contains ephemerides of the sun, moon, and planets in a mean reference frame on a dynamical (ephemeris) time base [26]. Since this file must correspond to the time standards described in (1), a new SLP file had to be constructed to support the GTDS/TRACE comparison testing. TRAMP [56,57,58] was used to build this new SLP file.

The radial, cross-track, and along-track differences between GTDS and TRACE are given in Figure 5.5 through Figure 5.7 for eleven day arcs (note that the time points are not equally spaced). These graphs depict extremely tight agreement between the two orbit

determination programs. A slight secular run-off can be noticed in the cross-track plot. It is believed that this drift can be accredited to either (1) subtle coordinate systems differences or (2) integration scheme differences. It is also believed that the high frequency variations result from a loss of a digit of accuracy in time stamps in TRACE. Further results stemming from comparisons between GTDS and TRACE are expected in future work [24].

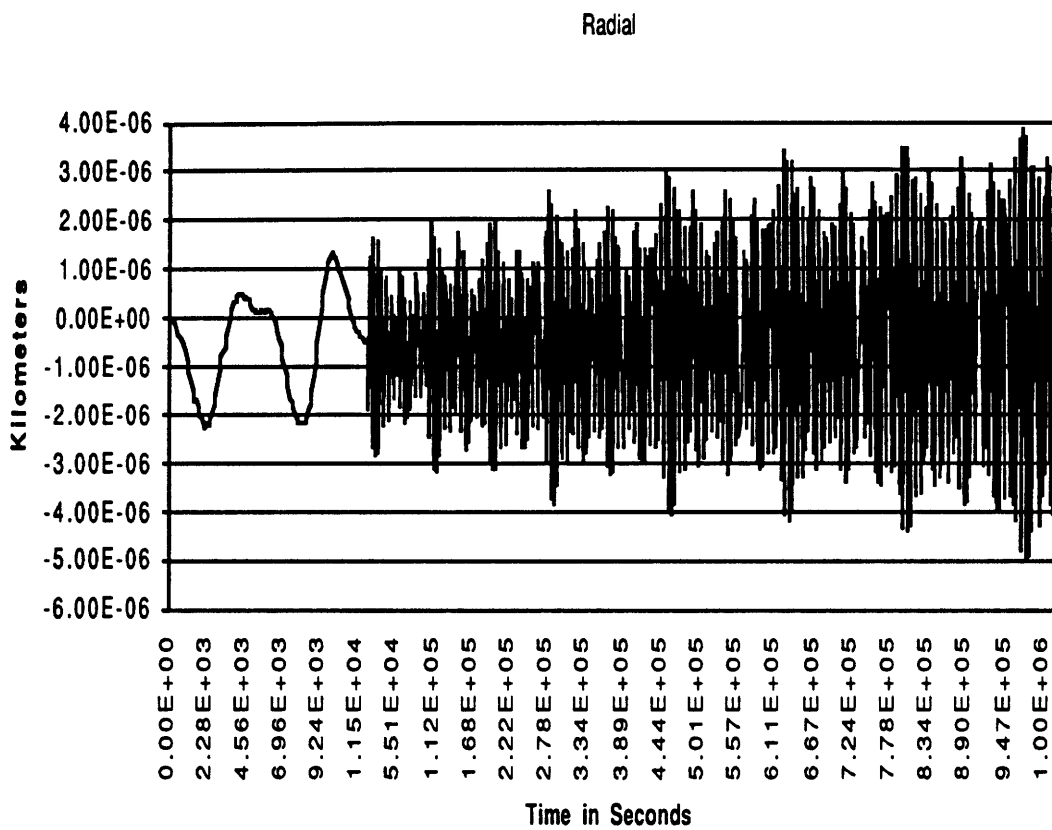


**Figure 5.5 Radial Error Between TRACE and GTDS
11 Day Arc, Cowell 50x50 GEMT3**

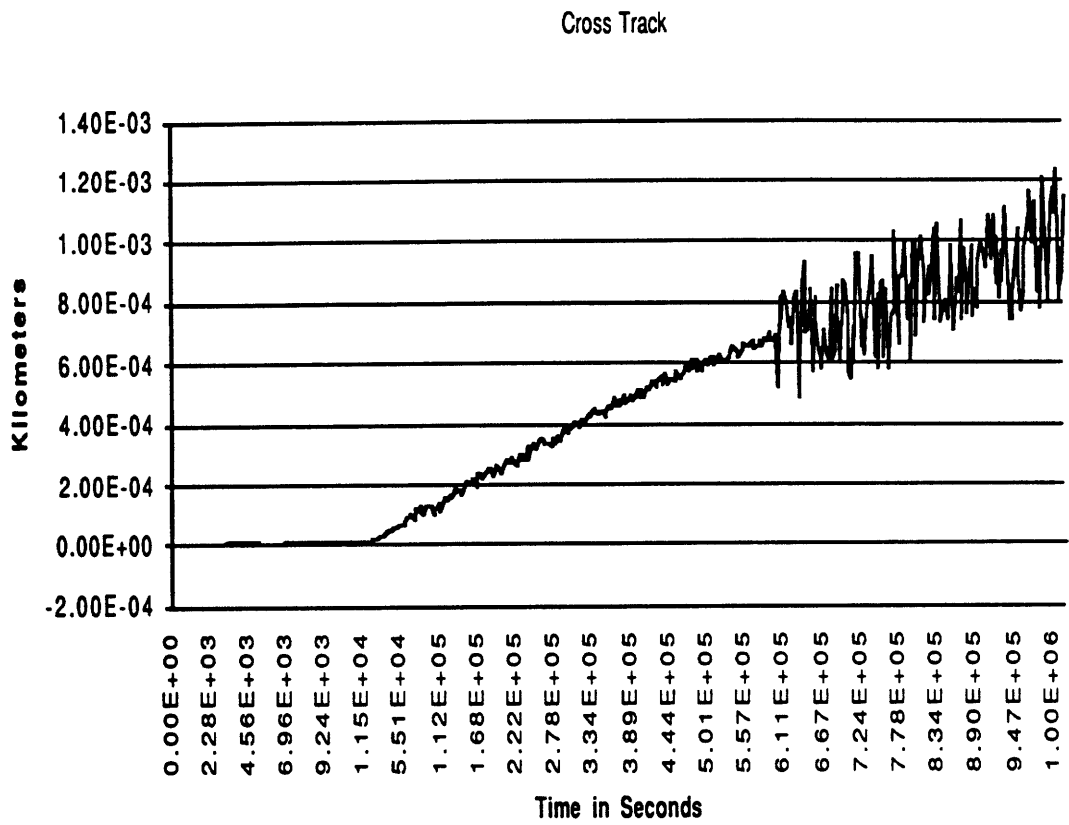


**Figure 5.6 Cross-Track Error Between TRACE and GTDS
11 Day Arc, Cowell 50x50 GEMT3**

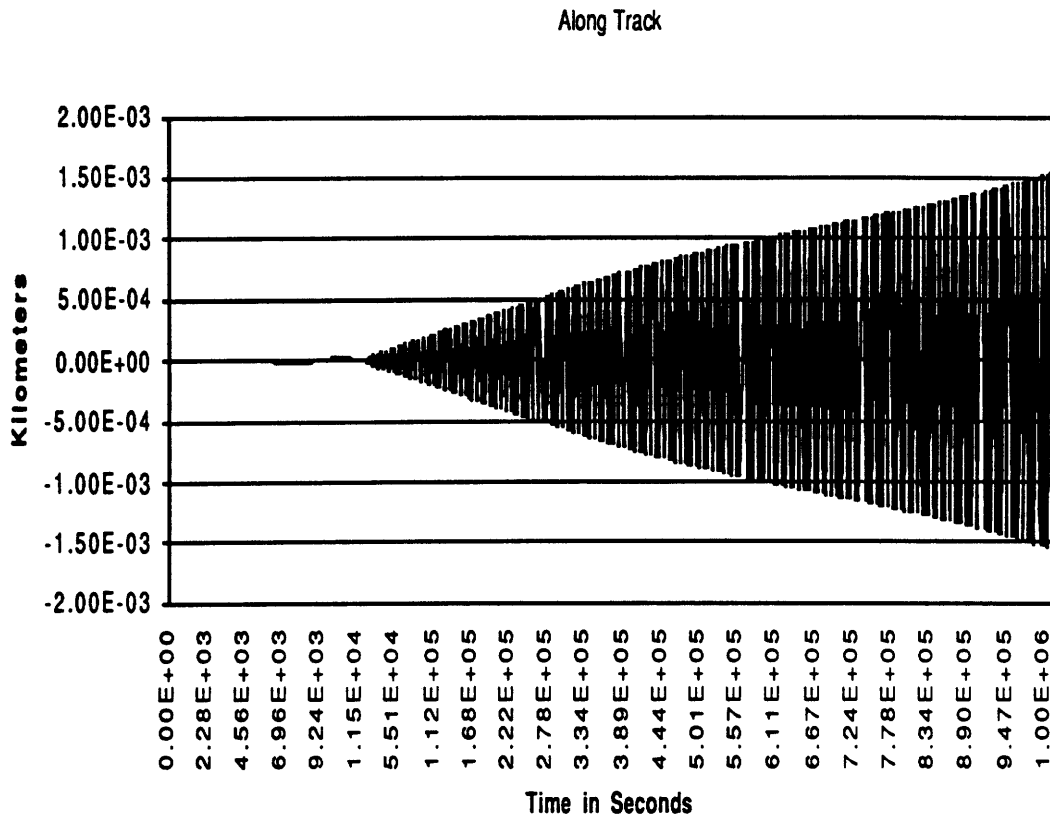


**Figure 5.7 Along-Track Error Between TRACE and GTDS
11 Day Arc, Cowell 50x50 GEMT3**

5.5 Testing of Cowell Differential Correction

Once it was determined that the Cowell orbit generator was functioning properly, a Cowell Differential Correction run was made. This test (1) constructed a truth ORB1 file from a five day Cowell integration, (2) used the Differential Correction Program to solve for the initial state from a set of elements slightly perturbed from the ones used to perform the Cowell integration in step (1), (3) constructed a second ORB1 file from a five day Cowell integration using the "solved-for" state vector from step (2), and (4) compared the two ORB1 files. Executing GTDS in this manner tests the use of the Cowell variational equations in the Differential Correction Program. The input deck used to perform the

Differential Correction, second Cowell integration, and Compare Program is given in

Figure 5.8:

```

CONTROL  DC                                RADARSAT  8202230
ELEMENT1 1 2 1 7173.48434                0.820904343990D-03 98.70378044247322
ELEMENT2                                120.5944241036631 87.9862755708162 250.16721
EPOCH                                820102.0                000240.6
ORBTYPE  2 1 1 10.
OBSINPUT 9                                820102 000340.6    820105 000340.6
DMOPT
OBSDEV  21 22 23 10.                    10.                    10.
OBSDEV  24 25 26 1.                      1.                      1.
END
OGOPT
DRAG      1                                1
ATMOSDEN                                1
DRAGPAR  3 0                                3.0
SOLRAD   1                                1.0
SCPARAM                                14.680D-6                2830.000
MAXDEGEQ 1                                50.0
MAXORDEQ 1                                50.0
POTFIELD 1 13
END
DCOPT
PRINTOUT 1                                4
CONVERG  25 6                                1.D-4
END
FIN
CONTROL  EPHEM                                OUTPUT                RADARSAT  8202230
OUTPUT  1 2 1 820107.0                    003241.0              86400.0
ORBTYPE 2 1 1 10.0
OGOPT
DRAG      1                                1
ATMOSDEN                                1
SOLRAD   1                                1
SCPARAM                                14.680D-6                2830.000
MAXDEGEQ 1                                50.0
MAXORDEQ 1                                50.0
POTFIELD 1 13
OUTOPT  21                                820102000241.0      820107003241.0    1800.
END
FIN
CONTROL  COMPARE                                RADARSAT  8202230
COMPOPT
CMPEPHEM 1102102 820102000241.0          820105003241.0      30.
CMPLOT    3
HISTPLOT 1102102 820102000241.0          820105003241.0      1800.
END
FIN
CONTROL  COMPARE                                RADARSAT  8202230
COMPOPT
CMPEPHEM 1102102 820105000241.0          820107003241.0      30.
CMPLOT    3
HISTPLOT 1102102 820105000241.0          820107003241.0      1800.
END
FIN

```

Figure 5.8 Standard Cowell Differential Correction Input Deck Format RADARSAT

In this deck, the DRAG and SOLRAD keyword cards indicate that this run included the effects of atmospheric drag and solar radiation pressure (ATMOSDEN = 1 specifies the Jacchia-Roberts Density Model). By default, third-body (lunar/solar) effects were also included. The SCPARAM keyword card provided for a specification of the satellite's average cross-sectional area (km²) and mass (kg). The values for area and mass specified in this plot are those of RADARSAT [18].

The results of this test are given in Figure 5.9 and 5.10:

	POSITION RMS	VELOCITY RMS
	(km)	(km/sec)
RADIAL	1.4442D-10	2.3113D-10
CROSS TRACK	1.9252D-11	6.0083D-14
ALONG TRACK	2.2239D-07	2.2946D-13
TOTAL	2.2239D-07	2.3113D-10

**Figure 5.9 50x50 GEMT3 Cowell Differential Correction
First Three Days**

	POSITION RMS	VELOCITY RMS
	(km)	(km/sec)
RADIAL	1.9173D-10	2.0215D-10
CROSS TRACK	2.2519D-11	3.9828D-14
ALONG TRACK	1.9451D-07	2.1681D-13
TOTAL	1.9451D-07	2.0215D-10

**Figure 5.10 50x50 GEMT3 Cowell Differential Correction
Last Two Days**

These results indicate that the Cowell Differential Correction Program functions properly with the default values of the variational equations (degree = 2, order = 0). In other words, the very small errors are consistent with the fact that the same dynamical model is being used for both data generation and the filter.

5.6 Testing of the Semianalytic Orbit Generator

After the Cowell orbit generator and the Cowell Differential Correction process were validated, the next step was to test the semianalytic orbit generator. The input decks used for the initial testing of the Semianalytic orbit generator were similar to those given in Figure 5.3:

```
CONTROL      EPHEM                                LND SAT-4    8207201
EPOCH                820224.0                    0.0
ELEMENT1  1  6  1  7077.8                    0.0011      98.2
ELEMENT2                158.1                    89.4      176.0
OUTPUT    1  2  1  820225.0                    0.0      3600.
ORBTYPE   5  1  1  a.0                        1.0
OGOPT
MAXDEGEQ  1                x.
MAXORDEQ  1                y.
POTFIELD  1  z
END
FIN
```

**Figure 5.11 Standard Semianalytic Input Deck Format
LANDSAT 4**

The differences between this deck and the one given in Figure 5.3 correspond to the differences between the two orbit generators. The second integer field in the ELEMENT1 card indicates an averaged Keplerian input coordinate system. The first integer field in the ORBTYPE card now reflects a Semianalytic (Variation of Parameters) orbit generator. The second real field reflects a 4th order Runge Kutta integrator for state propagation. Again, the value for integration step size (a.0), maximum degree (x), maximum order (y), and gravity model number (z) depends on the specific test case. The set-up of this card implies that only central and third body gravitational perturbations are considered (by default, third body effects are turned on in GTDS). It should be noted that the initial testing for the Semianalytic orbit generator concentrated on one day arcs.

For the Cowell input deck, it was stated that the elements specified on the ELEMENTX cards represent (osculating) Keplerian elements, while the Semianalytic input deck indicates that the elements on these cards are averaged Keplerian. Even though the elements have a different meaning, they have the same value. This configuration is not technically correct, but can be used if physical meaning is of no consequence. It was stated in the introductory paragraph of this section that input decks of form 5.11 were used in the initial testing of the Semianalytic orbit generator. This testing corresponds to cases with gravity field models less than or equal to the 21x21 standard. In these cases, "blind" comparisons are being made between old and new GTDS; both versions of GTDS are using the same inputs--therefore, they should produce the same results (regardless of the physical meaning of the cases). Other testing of the Semianalytic orbit generator did concentrate on physical meaning and, hence, care had to be taken to distinguish between osculating and mean elements.

The first test case analyzed was a 2x0 GEMT3 run. For this run, HWIRE was configured to include short-periodic effects; Appendix B provides a listing with HWIRE configured in this manner.

**Table 5.8 Semianalytic Orbit Generator Validation
Old GTDS vs. New GTDS (2x0 GEMT3)**

State	Old GTDS	New GTDS
X	0.2369421400759936D+04	0.2369421400759936D+04
Y	0.1225725889956325D+03	0.1225725889956325D+03
Z	0.6663929392961351D+04	0.6663929392961351D+04

Following this, a 21x0 GEMT3 run was made (with HWIRE configured as in Appendix B):

**Table 5.9 Semianalytic Orbit Generator Validation
Old GTDS vs. New GTDS (21x0 GEMT3)**

State	Old GTDS	New GTDS
X	0.2369174925655906D+04	0.2369174925655906D+04
Y	0.1225704555654358D+03	0.1225704555654358D+03
Z	0.6663860871035542D+04	0.6663860871035542D+04

This testing confirmed that the zonal portion of GTDS was functioning properly. The next step was to incrementally add the tesseral harmonic terms. The first tesseral harmonic case was a 2x2 GEMT3 run (with HWIRE configured as in Appendix B):

**Table 5.10 Semianalytic Orbit Generator Validation
Old GTDS vs. New GTDS (2x2 GEMT3)**

State	Old GTDS	New GTDS
X	0.2369084341423533D+04	0.2369084341423533D+04
Y	0.1228935326984567D+03	0.1228935326984567D+03
Z	0.6664000865173634D+04	0.6664000865173634D+04

Then, an 8x8 GEMT3 run was executed (with HWIRE configured as in Appendix B):

**Table 5.11 Semianalytic Orbit Generator Validation
Old GTDS vs. New GTDS (8x8 GEMT3)**

State	Old GTDS	New GTDS
X	0.2368712358523536D+04	0.2368712358523536D+04
Y	0.1229598651081748D+03	0.1229598651081748D+03
Z	0.6663903532911122D+04	0.6663903532911122D+04

The final test case comparing the two versions of GTDS was a 21x21 GEMT3 run (with HWIRE configured as in Appendix B). Section 4.3.5 outlined a minor modification that was made to "old" GTDS which affected 21x21 Semianalytic runs; for this reason, there really were two versions of old GTDS for the 21x21 Semianalytic testing. Table 5.12 and Table 5.13 compare new GTDS to un-modified and modified old GTDS:

**Table 5.12 Semianalytic Orbit Generator Validation
Un-Modified Old GTDS vs. New GTDS (21x21 GEMT3)**

State	Un-Modified Old GTDS	New GTDS
X	0.2368701370462711D+04	0.2368719128112088D+04
Y	0.1230491326940926D+03	0.1229402039157586D+03
Z	0.6663910978707961D+04	0.6663871060900344D+04

**Table 5.13 Semianalytic Orbit Generator Validation
Modified Old GTDS vs. New GTDS (21x21 GEMT3)**

State	Modified Old GTDS	New GTDS
X	0.2368719128112088D+04	0.2368719128112088D+04
Y	0.1229402039157586D+03	0.1229402039157586D+03
Z	0.6663871060900344D+04	0.6663871060900344D+04

Figure 5.13 indicates that the modified version of old GTDS and new GTDS provide exact agreement for the 21x21 GEMT3 test case.

All of the test cases described in Table 5.8 through Table 5.13 represented one day arcs with one-quarter day step-sizes (21600 sec). It should be noted that in the debugging

process, numerous runs containing different combinations of short-periodic terms were made to ensure proper functioning of the short-periodic orbit generator. On the BIGSIM VAX, this process required changing various "flags" in subroutine HWIRE for the zonal, m-daily, tesseral, third-body, J_2 / m-daily coupling, and J_2^2 short periodic contributions from the "default" values given in Appendix B. This debugging process will be greatly simplified when the Semianalytic input processor is ported from the UNIX environment to the VAX environment.

Testing of 50x50 class gravity field models for the Semianalytic orbit generator relied heavily on the previously completed testing of the Cowell orbit generator. This testing, which attempts to "fit" the Semianalytic theory to the Cowell Theory, consisted of the following steps: (1) a Cowell ephemeris listing and an associated ORB1 file containing time-tagged values of position and velocity were generated, (2) the Differential Correction Program (DC) was used to perform a Precise Conversion of Elements (PCE) to obtain a set of mean elements which corresponded to the osculating elements used by the Cowell orbit generator, (3) a Semianalytic ephemeris listing and an associated ORB1 file containing time-tagged values of position and velocity were generated with the computed mean elements (including short-periodic contributions), and (4) the Ephemeris Comparison Program was used to compare the two ORB1 files. The input deck required to make this run is given in Figure 5.12:


```

CONTROL  DATAMGT                                LNSAT-4  8207201
OGOPT
POTFIELD 1 13
END
FIN
CONTROL  EPHEM                                LNSAT-4  8207201
EPOCH          820224.0                0.0
ELEMENT1 1 2 1 7077.8                0.0011          98.2
ELEMENT2          158.1                89.4            176.0
OUTPUT 1 2 1 820226.0                0.0            43200.
ORBTYP 2 1 1 10.0
OGOPT
MAXDEGEQ 1          50.
MAXORDEQ 1          50.
OUTOPT 1          820224000000.        820226000000.   3600.
END
FIN
CONTROL  DC                                LNSAT-4  8207201
EPOCH          820224.0                0.0
ELEMENT1 1 6 1 7077.8                0.0011          98.2
ELEMENT2          158.1                89.4            176.0
OBSINPUT 9          820224000000.0    820226000000.0
ORBTYP 5 1 1 86400.0                1.0
DMOPT
OBSDEV 21 22 23 100.                100.            100.
OBSDEV 24 25 26 10.                 10.             10.
END
OGOPT
MAXDEGEQ 1          50.
MAXORDEQ 1          50.
STATEPAR 3
STATETAB 1 2 3 4.0                5.0             6.0
END
DCOPT
PRINTOUT 1          4
CONVERG 30          1 1.D-5
END
FIN
CONTROL  EPHEM                                LNSAT-4  8207201
OUTPUT 1 2 1 820226.0                0.0            43200.
ORBTYP 5 1 1 86400.0                1.0
OGOPT
MAXDEGEQ 1          50.
MAXORDEQ 1          50.
OUTOPT 21          820224000000.0    820226000000.0   3600.
END
FIN
CONTROL  COMPARE                            LNSAT-4  8207201
COMPOPT
CMPEPHEM 1102102 820224000000.0    820226000000.0   480.0
CMPLOT 1
HISTPLOT 1102102 820224000000.0    820226000000.0  28800.0
END
FIN

```

**Figure 5.12 GTDS Card Deck to Fit Semianalytic Theory to Cowell Theory
50x50 GEMT3**

The results are summarized next:

	POSITION RMS	VELOCITY RMS
	(km)	(km/sec)
RADIAL	5.0203D-04	2.0035D-06
CROSS TRACK	1.0954D-03	7.0972D-07
ALONG TRACK	1.9867D-03	6.8605D-07
TOTAL	2.3235D-03	2.2335D-06

Figure 5.13 Two Day 50x50 GEMT3 Fit of Semianalytic Theory to Cowell Theory

These results imply a position RMS error of a little over 2 meters for a two day fit. For comparison purposes, this same type of run for a 21x21 GEMT3 field (60 second Cowell step size) was made with the un-modified and modified versions of old GTDS. The results are summarized in the following figures:

	POSITION RMS	VELOCITY RMS
	(km)	(km/sec)
RADIAL	5.9446D-02	1.2108D-04
CROSS TRACK	6.2275D-02	5.9055D-05
ALONG TRACK	9.0760D-02	4.5775D-05
TOTAL	1.2510D-01	1.4228D-04

Figure 5.14 Two Day 21x21 GEMT3 Fit of Semianalytic Theory to Cowell Theory, Un-Modified Old GTDS

	POSITION RMS	VELOCITY RMS
	(km)	(km/sec)
RADIAL	4.8325D-04	1.5221D-05
CROSS TRACK	1.7147D-03	1.6065D-06
ALONG TRACK	1.4139D-02	7.2171D-07
TOTAL	1.4251D-02	1.5322D-05

Figure 5.15 Two Day 21x21 GEMT3 Fit of Semianalytic Theory to Cowell Theory, Modified Old GTDS

These results show that the 50x50 field provided a fit between the two theories which was as good as the fit with the 21x21 field. A direct comparison of the total RMS errors between the two field sizes was not really of consequence since the differing field sizes captured different dynamics; the 50x50 field captured resonant terms at the 29th order which were obviously not captured by the 21x21 field. In essence, two different problems were being analyzed. However, comparisons to the previously accepted 21x21 fit provided a reasonable sanity check of the 50x50 fit. It was concluded that the results of the Semianalytic orbit generator compared favorably with the results of the Cowell orbit generator. Since the Cowell orbit generator had previously been successfully validated against TRACE, the validation of the Semianalytic orbit generator was considered complete.

5.7 Impact of 50x50 Gravity Models in Orbit Determination

The previous work in this Chapter described the validation of the Cowell and Semianalytic orbit generators of GTDS. Once this validation was complete, some preliminary test cases were run to assess the impact of 50x50 gravity field models in the orbit determination process. It was of particular interest to study the effects of resonant terms which could not be captured by 21x21 class models. For example, a satellite completing approximately 14 revolutions per day experiences resonant effects at the 14th (for degrees greater than 21), 28th, and 42nd order which are not captured by 21x21 models. The resonant effects produced at these orders would be captured by the new 50x50 gravity model.

The test case chosen to study these effects incorporated a two hundred day fit of the 21x21 GEMT3 Averaged Orbit Generator to the 50x50 GEMT3 Averaged Orbit Generator (AOG). Since the DMSP study orbit [6] closely resembles the 14 revolution per day

pattern, it was chosen for use in this test case. As with the LANDSAT and RADARSAT orbits described in Section 3.4.1, this orbit implements sun-synchronous, repeat groundtrack, and frozen orbit constructs. Figure 5.16 depicts the input deck (due to its length, it must be listed over two pages):

```

CONTROL   DATAMGT                               DMS PBL-6   1234567
OGOPT
POTFIELD  1 13
END
FIN
CONTROL   EPHEM                               DMS PBL-6   1234567
EPOCH                    820223.0             0.0
ELEMENT1  a  6  1  7272.0             0.001125   99.0
ELEMENT2                    65.931             90.0       0.0
OUTPUT    1  2  1  820911.0           0.0       864000.
ORBTYPE   5  1  1  43200.             1.0
OGOPT
NCBODY    1
RESONPRD                    432000.0
MAXDEGEQ  1             50.
MAXORDEQ  1             50.
OUTOPT    1             820223000000.0         820911000000.0   14400.
END
FIN
CONTROL   DC                               DMS PBL-6   1234567
EPOCH                    820223.0             0.0
ELEMENT1  a  6  1  7271.99999         0.0011235  98.9999
ELEMENT2                    65.93136          89.66716   0.322
OBSINPUT  9             820223000000.0         820911000000.0
ORBTYPE   5  1  1  43200.             1.0
DMOPT
OBSDEV    21 22 23  100.             100.       100.
OBSDEV    24 25 26  10.             10.        10.
END
OGOPT
NCBODY    1
MAXDEGEQ  1             21.
MAXORDEQ  1             21.
STATEPAR  3
STATETAB  1  2  3  4.0             5.0        6.0
END
DCOPT
PRINTOUT  1             4
CONVERG   30            1  1.D-4
END
FIN
CONTROL   EPHEM                               OUTPUT      DMS PBL-6   1234567
OUTPUT    1  2  1  820911.0           0.0       864000.0
ORBTYPE   5  1  1  43200.             1.0
OGOPT
NCBODY    1
MAXDEGEQ  1             21.
MAXORDEQ  1             21.
OUTOPT    21            820223000000.0         820911000000.0   14400.
END
FIN

```

```

CONTROL   COMPARE                               DMSPBL-6   1234567
COMPOPT
CMPEPHEM  1102102  820223000000.0    820911000000.0    3600.0
CMPLOT    1                                           2.0
HISTPLOT  1102102  820223000000.0    820911000000.0    216000.0
END
FIN
CONTROL   COMPARE                               DMSPBL-6   1234567
COMPOPT
CMPEPHEM  1102102  820223000000.0    820911000000.0    1200.0
CMPLOT    1                                           2.0
HISTPLOT  1102102  820223000000.0    820911000000.0    72000.0
END
FIN

```

Figure 5.16 200 Day Fit of 21x21 GEMT3 AOG to 50x50 GEMT3 AOG

where the value "a" was given for the input coordinate system of the elements on the ELEMENT1 card. This value was not explicitly given since both mean earth equator and equinox of 1950.0 and true of reference, Earth equator and equinox input systems were used. It should be noted that the difference in the results between the two systems was of no consequence.

Note in this figure how the RESONPRD card was used to force the 42nd order resonant effects into the averaged equations of motion for the 50x50 field. The use of this card required knowledge of the expected resonant periods:

$$\text{resonant period} \approx \frac{2\pi}{t\dot{\lambda} - m\dot{\theta}} \text{ where } \dot{\lambda} \approx n + \dot{\omega} + \dot{\Omega} \quad (5.6)$$

in which n is the satellite's mean motion

$$n = \sqrt{\frac{\mu}{a^3}} \quad (5.7)$$

μ is the gravitational parameter, a is the semimajor axis, t and m (order) are geopotential indices, θ is the Greenwich Hour Angle, ω is the argument of perigee, and Ω is the

longitude of the ascending node. For the DMSP study case, the value for $\dot{\Omega}$ was set to equal the sun-synchronous value of 1.991×10^{-7} rad/sec [23]; μ , the GEMT3 value of $398600.436 \text{ km}^3/\text{sec}^2$; a , the input mean semimajor axis value of 7272 km; $\dot{\omega}$, to the frozen orbit value of zero [23]; and $\dot{\theta}$, to the rotational rate of the earth of $0.72921159 \times 10^{-4}$ rad/sec. The combinations of resonant geopotential indices led to the following "expected" periods:

$$\begin{aligned}
 t = 1, m = 14 &\Rightarrow \text{resonant period} \approx 27.94 \text{ days} \\
 t = 2, m = 28 &\Rightarrow \text{resonant period} \approx 13.97 \text{ days} \\
 t = 3, m = 42 &\Rightarrow \text{resonant period} \approx 9.31 \text{ days}
 \end{aligned}
 \tag{5.8}$$

The smallest period of 9.31 days would not have been captured with GTDS's default value of 10 days. Hence, the RESONPRD card was used with a value of 5 days (432000 sec) to force the effects of the 42nd order in to the AOG (refer to Section 4.2.4 for further details on the RESONPRD card).

This card also indicates that the third body effects of the sun and moon were turned-off for this run; this configuration ensured that the output contained geopotential-only related information.

As expected, the results of this test show that significant errors resulted from the 21x21 fit:

	POSITION RMS (km)	VELOCITY RMS (km/sec)
RADIAL	3.3576D-02	1.6680D-03
CROSS TRACK	1.7800D-02	1.6002D-05
ALONG TRACK	1.6392D+00	3.4504D-05
TOTAL	1.6396D+00	1.6684D-03

Figure 5.17 200 Day GEMT3 Fit of 21x21 AOG to 50x50 AOG

Appendix C provides a listing of the plots of these errors, as well as plots of element histories and element differences. In these plots, a 60 day period is highly visible. A period of this length is surprising since it does not match one of the "expected" values given in (5.8). At this point, much conjecture exists over what this result exactly means. A few opinions are noted here:

(1) The calculation of the "expected" resonant periods is flawed since the value for $\dot{\omega}$ was set to zero. For a perfect frozen orbit, the mean rate of perigee is zero--and this value works well for "quick and dirty" calculations. However, if this value is not exactly zero, the $(t\dot{\lambda} - m\dot{\theta})$ divisor may become a value such that the resonant period is really 60 days. Inspection of the plots in Appendix C indicate that one could derive a worst-case value for $\dot{\omega}$ from the perigee history plot which would be valid over certain regions. In addition, these plots show that a better value to use for the mean semimajor axis may be 7272.015 km. However, periods resulting from computations using these updated values are much closer to the values obtained in (5.8) than they are to the visible 60 day period.

This theory can also be tested by solving the equation given in (5.6) for $\dot{\omega}$. For this test case, it is obvious that the 14th order terms provide for larger resonant periods than the 28th and 42nd order terms. Using the conditions for this 14th order resonance (i. e., $t=1$, $m=14$), the updated value of 7272.015 km for semimajor axis, and the 60 day visible period, the value for $\dot{\omega}$ must be approximately 19 deg/day to produce the 60 day signature. 19 deg/day is an unrealistic value of $\dot{\omega}$ for the chosen frozen orbit case.

These arguments tend to refute that the possibility that the calculation of the resonant periods of (5.8) is flawed.

(2) Coupling exists between J_2 and the resonant terms. Evidence to support this opinion stems from the semimajor axis history plot. Due to the nature of the VOP equations, rates in the semimajor axis are caused by either short-periodic effects or resonance terms. Since the short-periodic effects have been turned off in this test case, the variation in semimajor axis must result from resonance. However, using the argument in (1), it can be assumed that the visible 60 day period is not reflective of the actual resonant period. This period must result from some other effect of the resonance. It is known that J_2 introduces rates in perigee and the node. The work of Zeis [66] indicates that a periodic signature of about 60 days can be expected in the plots for eccentricity, inclination, longitude of ascending node, and argument of perigee due to the effects of the zonal harmonics (dominated by J_2). The rates in perigee and the node, in turn, affect the resonant period. Therefore, there is a coupling effect between J_2 and the resonant terms to produce the 60 day signature.

To test this argument, a separate AOG run can be made in which J_2 is set to a small value (in order to reduce the magnitude of the coupling effect). A semimajor axis history plot resulting from a run of this type is also given in Appendix C. Clearly, the 60 day signature is gone. However, it must be noted that this run corresponds to a different problem; setting J_2 to a small value disrupts the frozen orbit geometry, thereby disallowing the assumption that $\dot{\omega}$ is zero.

(3) Linear combinations of the resonant periods result due to their symmetric nature. An analysis of (5.8) shows that the three resonant periods can be expressed as multiples of 28 days (i. e., 3 times the 42nd order period; 2 times the 28th order period; and 1 times the 14th order period). It is of interest to note that 56 days is another multiple of these resonant periods (and approximately equal to the 60 day visible period). In this manner, the three

periods may align at multiples of 28 days to produce an effect which has a period greater than any of the individual contributing periods.

One difficulty with this argument stems from the results of the separate AOG run with a small value for J_2 . As was stated in (2), the 60 day period vanishes in the semimajor axis plot from this run. A small value for J_2 should not disrupt any combinatory effect among the individual contributing periods (if this combinatory effect is realistic). However, it is possible that an effect with a period greater than any of the three individual contributing periods is evident, but not visible due to a selection effect or other graphing phenomenon.

It is clear that interesting results have been obtained, some of which still remain a source of debate and require additional study. Chapter 6 outlines conclusions and suggestions for further research.

[This page intentionally left blank.]

Chapter 6

Conclusions / Future Work

6.1 Summary

The primary objective of this thesis was to improve the gravity modeling capability of Draper Laboratory's version of the Goddard Trajectory Determination System (GTDS). Specifically, the limits of the gravity field model were extended from degree and order twenty-one to degree and order fifty. This extension required (1) a study of the stability of the various recursions used to calculate the Legendre polynomials, associated Legendre polynomials, Jacobi polynomials, and Hansen coefficients, as well as their product with the harmonic coefficients, (2) many modifications to the software, and (3) an extensive validation process to ensure that the modifications were implemented correctly. The BIGSIM VAX 8820 was the sole platform used for the stability testing, code modifications, and the validation process. However, stability conclusions were drawn for the IBM and UNIX environments, which also support operational versions of GTDS. The following paragraphs provide a summary of the results obtained from the various chapters of this thesis:

Chapter One provides top-level introductory material. Three main areas are addressed: (1) the history of gravity modeling, (2) the need for models of high degree and order, and (3) the numerical boundaries for the various operational versions of GTDS. A brief outline of the thesis is also given.

Chapter Two details the various mathematical techniques that are required for the work in this thesis. Spherical harmonic, Keplerian, and Equinoctial formulations of the potential are derived. These derivations are followed by a description of the effects of the zonal and tesseral harmonics. The equations of motion used by the Cowell and Semianalytic orbit generator are also presented. Finally, a description of the generalized method of averaging, the process used to separate averaged equations of motion (containing secular and long periodic equations of motion) from short periodics, is given.

Chapter Three describes the stability testing undertaken to determine if normalized or un-normalized recursions were required to support 50x50 gravity field models. The results indicate that the VAX, Sun Workstation, and Silicon Graphics versions of GTDS will all support 50x50 gravity field models in an un-normalized sense. It is advisable, however, to convert the IBM version to normalized formulae before extending the gravity modeling limits in this environment. It should be noted that the stability study for the Hansen coefficients only analyzed the resonant orders for a 14 rev/day satellite which are captured by a 50x50 field (orders 14, 28, and 42). The testing for the 14th order provided a more rigorous test than the 28th and 42nd orders since more computations are made in a recursive calculation which starts at the lowest order.

Chapter Four focuses on GTDS: (1) an overview of GTDS and its various programs is given, (2) the developmental history of GTDS is described, (3) the various functions in GTDS related to gravity modeling (numerical, analytical, and semianalytical) are outlined, (4) input processing and database maintenance related to the gravity model is discussed, and (5) code modifications are presented. In all, a total of 144 routines and approximately 2900 lines of code were modified in support of the work for this thesis. In addition, 28 new routines encompassing 4990 lines of code were added to GTDS. All of these new routines include files or associated block datas which store arrays and variables related

to the gravity modeling capability within GTDS. These additions provided for the following new gravity models:

- GEM10B (36x36)
- GEMT2 (50x50)
- GEMT2 Clone (50x50)
- GEMT3 (50x50)
- GEMT3 Clone (50x50)
- GEMT3S (50x50)
- WGS84 (41x41)
- JGM-1 (50x50)
- JGM-1 Clone (50x50)
- JGM-2 (50x50)

Chapter 5 describes the validation process that was used to ensure that the 50x50 gravity field model was implemented properly. The testing outlined in this section includes the use of the Differential Correction Program, Ephemeris Generation Program, Ephemeris Comparison Program, Data Simulation Program, Data Management Program, and the Permanent File Report Generation Program. Comparisons of GTDS with TRACE, Aerospace's orbit determination program, demonstrate that less than 2 meter RMS errors for arcs encompassing about two weeks result from the Cowell orbit generator. This comparison between independent orbit determination programs serves to provide a comprehensive test of coordinate systems, force models, integration methods, and time systems. A two-day 50x50 GEMT3 fit of Semianalytic Theory to Cowell Theory provides RMS errors of a little over 2 meters. These results correspond to LANDSAT 6 type orbits (sun synchronous, repeat groundtrack, frozen orbits). Initial testing of the impact of 50x50 gravity field models for 14 rev/day resonant orbits uncovered 60 day periods which appear

to be unrelated to the actual periods of the contributing resonant orders. Several theories are given in Chapter 5 to possibly explain this phenomenon. The strongest explanation is associated with coupling between the J_2 and the resonant terms.

6.2 Conclusions

The 50x50 gravity field model has been accurately incorporated into Draper Laboratory's version of GTDS. The results presented in Chapter Five reflect a rigorous and complete validation process. The coupling of the 50x50 class gravity models with the Draper Semianalytical (Precise Mean Element) Orbit Propagator results in a unique tool for long term orbit prediction. It should be noted that this long term prediction capability is accomplished in a very efficient manner and spans a multitude of computing environments. In short, Draper Laboratory offers a flight dynamics package for astrodynamics applications that is equally well suited for academic environments, laboratory studies, or operational type mission support.

It is not conceived that the work in this thesis will become stagnant. Work has begun to expand GTDS to incorporate 70x70 class gravity field models. Efforts in this area will serve to further improve the capability of GTDS to model the effects of the non-spherical earth perturbation.

6.3 Future Work

The work for this thesis has provided a tool with a variety of applications. This tool creates the potential for much future work, which can generally be organized into three categories:

(1) software related items, (2) analysis related items, and (3) mission related items. Each of these three areas will be addressed in this section.

Software Related Items

(1) The Semianalytic input processor needs to be ported from the UNIX to the VAX and IBM environments. The incorporation of this input processor provides for a simple adjustment of the options for the averaged equations of motion and the short periodics. In other words, the use of this input processor replaces the "tinkering" that had to be done to subroutine HWIRE.FOR. In addition, the input processor provides for a listing of chosen options on the output report, which aids in the identification of stored runs.

(2) Along the same lines, it is desirable to port the 50x50 version of GTDS from the VAX environment to the UNIX environments as soon as possible. Moving the 50x50 version to different environments serves to increase the applicability of the tool.

(3) As explained in Section 4.3.4, it is desirable to tie together all of the new common areas that were introduced as part of the work in this thesis. GRAVITY.CMN is a stub include file built to provide for a single modification point concerning the generic parameters representing the limits of the gravity field model. This file would have to be included in the common areas containing these generic parameters (refer to Table 4.16 for a listing of these common areas). Then, EQUIVALENCE statements could be used to tie the common areas together.

(4) A bug in the small files directory was uncovered. This bug corresponds to the number of models on the permanent earth potential field file. Currently, this value is explicitly set to nine, the number of models GTDS could handle with the 21x21 standard.

For the work in this thesis, the bug could be avoided by running GTDS in DEBUG mode and updating this value to the current number of models. It should be noted that the scope of this error is limited to the Permanent File Report Generation Program.

(5) The output reports generated by GTDS contain a listing of the harmonic coefficients used for a particular run. When the expansion to 50x50 gravity field models was made, the output of coefficients beyond 21x21 became slightly un-formatted. For aesthetic purposes, this output should be improved.

(6) During the final review of the work done in this thesis, a small bug was found in SPREAL.CMN. The dimension of the variables CECCEN and SECCEN was mistakenly related to the limits of the gravity field model. These variables, which are used in the third-body model, need to have their limits reset to (6,44).

Analysis Related Items

(1) Any software related tools which can be used to perform global searches are desirable for significantly modifying large software systems like GTDS. As described in Chapter 4, the link map was an extremely helpful tool in identifying the various subroutines and common areas which required modification. Any tool which further processes this map, or the structure of GTDS, serves to enhance efficiency and thoroughness. For example, this tool could be used to check if the introduction of an include file causes any conflicts with variables in the local routine. One tool of this sort is PERL [63], which is available in the UNIX environment.

(2) A more detailed study of the stability of the Hansen coefficients could be made. As was described in Section 3.4.2, only the resonant orders for a 14 rev/day were analyzed.

This study should be extended to include orders up to and including fifty. In addition, a standalone routine to compute mean element rates could be developed. This routine would provide a capability in the Semianalytical theory analogous to the routine used to compute Cowell accelerations.

(3) A literature search should be made for an alternative expression for calculating resonant periods. The difficulties using the expression given in (5.8) were explained in Section 5.7. A distinct formula might remove some of the uncertainty concerning the sixty day signature described by argument (1) in this section.

(4) Comparisons could be made between results generated from the different gravity models listed in Table 4.3. These comparisons would serve to categorize the accuracy of the various models.

(5) Validation runs need to be made for the analytical theories described in Table 4.1. These theories use the values for the first few zonal harmonics and, thus, must be checked against benchmarked cases to ensure that the work for this thesis did not hamper this functionality.

(6) A test of the variational equations for values other than the default (2x0) standard should be made. Section 5.5 outlined the testing of a Cowell Differential Correction run using the default values of 2x0. This run could be replicated using larger values for the degree and order on the MAXDEGVE and MAXORDVE cards (refer to Section 4.2.4).

(7) Other accuracy improvement issues concerning GTDS require attention. For example, the J2000 coordinate system and a solid earth tides model should be added to

GTDS. These capabilities would allow GTDS to support accuracy levels of five meters or better in orbit determination.

Mission Related Items

Numerous mission related scenarios can be tested using the 50x50 gravity field model. The work for this thesis concentrated on implementing this capability properly within GTDS. Due to time constraints, not much mission related testing could be undertaken with this tool. It would be desirable to determine how the 50x50 class gravity field models affect certain orbit constructs, such as the frozen orbit. Work of this nature could evolve into separate thesis type studies. In addition, the extension of GTDS to 70x70 class gravity field models coupled with a study of the impact of 70x70 class models would make for a nice thesis. This type of effort would allow for comparisons between 50x50 and 70x70 class models.

Appendix A

Element Sets

A.1 Background

When working in satellite theory or astrodynamics, it is often convenient to describe the size, shape, and orientation of a body's orbit. In general, five independent quantities called "orbital elements" are sufficient to carry out this task (a sixth element is used to pinpoint the position of the satellite along the orbit at a particular time) [2]. One well known set of elements is the classical orbital element set, sometimes better known as the Keplerian orbital element set. Another set is the equinoctial element set, which removes singularity problems experienced by the Keplerian orbital elements in the classical orbital element formulation of the Variation of Parameter equations. This appendix will discuss these two element sets since they represent the element sets used in this study.

A.2 Classical Orbital Elements

Most initial courses in astrodynamics focus on the two-body problem, which Escobal [22] defines as the motion of body A with respect to body B, with only the mutual attractions of A and B taken into consideration. In other words, perturbations (effects which cause deviations from the norm) to a body's orbit have been neglected. In addition, the bodies under investigation are assumed to be spherical, which allows the bodies to be treated as

though their masses were concentrated at their centers. The equation governing two-body motion can be derived from Newton's universal law of gravitation [2]:

$$F_g = - \frac{G M m}{r^2} \frac{\mathbf{r}}{r} \quad (\text{A.1})$$

which can be re-written for both the small (m) and large (M) mass:

$$m \ddot{\mathbf{r}}_m = - \frac{G M m}{r^2} \frac{\mathbf{r}}{r} \quad (\text{A.2})$$

$$M \ddot{\mathbf{r}}_M = - \frac{G M m}{r^2} \frac{\mathbf{r}}{r} \quad (\text{A.3})$$

If equation (A.3) is subtracted from equation (A.2), the following form is obtained:

$$\ddot{\mathbf{r}} = - \frac{G (M + m)}{r^2} \frac{\mathbf{r}}{r} \quad (\text{A.4})$$

The quantity $G (M + m)$ is known as the gravitational parameter, μ . For applications in which an artificial satellite is orbiting a planet, the smaller mass body (the satellite) is much less than the larger mass body (the planet), and can be ignored. In these cases, μ is reduced to GM . The final form for the two-body equation of motion is expressed in the following manner:

$$\ddot{\mathbf{r}} + \frac{\mu}{r^3} \mathbf{r} = 0 \quad (\text{A.5})$$

where \mathbf{r} is the position vector of the satellite with magnitude r (dots represent time differentiation) and G is the universal gravitational constant (6.670×10^{-8} dyne cm^2/gm^2). The solution to this differential equation leads to six constants of integration (this equation can be broken down into the unit directions producing three, second order differential

equations--which leads to six constants of integration) These constants (see Table A.1) have traditionally been recognized as the classical orbital elements (also refer to Figure A.1 [2]).

Table A.1 Keplerian Elements

Symbol	Name	Physical Description
a	semimajor axis	describes size of orbit
e	eccentricity	describes shape of orbit
i	inclination	the angle between the K axis and the angular momentum vector, h [2]
Ω	longitude of the ascending node	the angle in the equatorial plane between the vernal equinox and the longitude of the ascending node
ω	argument of perigee	the angle in the orbit plane between the longitude of the ascending node and periapsis
τ	time of periapsis passage	the time the satellite was at periapsis

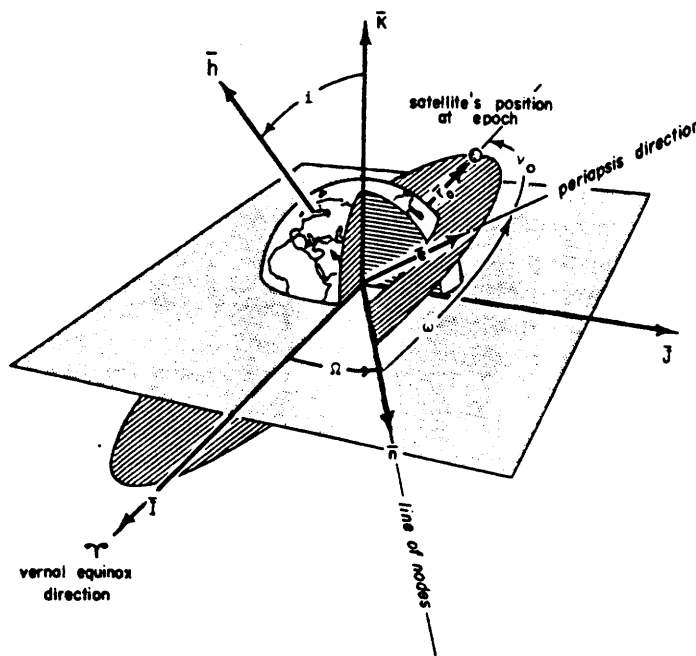


Figure A.1 Classical Orbital Elements

Two other elements of interest when discussing classical orbital elements are true anomaly (ν) and mean anomaly (M). True anomaly is the angle in the orbital plane between periapsis and the satellite's position at a specified time, while mean anomaly is the angle measured from periapsis to the satellite's mean position, as if the satellite had constant velocity throughout the orbit period [30].

Two terms that are frequently encountered when discussing orbital elements are "fast" and "slow" elements. Slow elements represent those that are, for the most part, considered a constant throughout the orbit (a, e, i, Ω, ω). The fast element(s), on the contrary, rapidly change as a function of time throughout the orbit (M).

Specific values for the semimajor axis and eccentricity describe the motion (orbit) of a particular body; Table A.2 (next page) lists the characteristic conic sections for the range of values of semimajor axis and eccentricity.

Table A.2 Semimajor Axis and Eccentricity Ranges for Orbits

Conic Section	Semimajor Axis	Eccentricity
Circle	$a > 0$ ($a = r$)	$e = 0$
Ellipse	$a > 0$	$0 < e < 1$
Parabola	$a = \infty$	$e = 1$
Hyperbola	$a < 0$	$e > 1$

A.3 Equinoctial Element Set

As stated in the introduction of this appendix, singularities arise in the classical orbital element formulation of the Variation of Parameter equations (divide by zero errors occur for values of inclination and eccentricity approaching zero). The equinoctial element set removes such singularities. Table A.3 describes these elements in terms of the classical elements (refer to next page).

Table A.3 Equinoctial Elements

Symbol	Definition
a	$a = a$
h	$h = e \sin (\omega + I\Omega)$
k	$k = e \cos (\omega + I\Omega)$
p	$p = \tan \frac{i}{2} \sin \Omega, I = 1$ $p = \cot \frac{i}{2} \sin \Omega, I = -1$
q	$q = \tan \frac{i}{2} \cos \Omega, I = 1$ $q = \cot \frac{i}{2} \cos \Omega, I = -1$
λ	$\lambda = M + \omega + \Omega$
I	Retrograde Factor +1 (direct equinoctial elements, $0^\circ \leq i < 180^\circ$) -1 (retrograde equinoctial elements, $0^\circ < i \leq 180^\circ$)

Again, a distinction can be made between fast and slow elements. The slow elements are a, h, k, p, and q, while mean longitude (λ) is the fast variable.

Appendix B

HWIRE Listing

B.1 Description

HWIRE.FOR is the subroutine in GTDS which sets the options for the averaged equations of motion and the short periodics. A user must modify this routine to the desired form if no Semianalytic input processor is available (currently, the input processor is not available in the VAX and IBM environments--only the UNIX environments; reference Section 4.1.2 and Section 5.6). As stated in Chapter 5, a listing is provided here as a reference point for the testing that was done to validate the Semianalytic orbit generator (the INCLUDE file SPREAL.CMN is given after HWIRE).

```

SUBROUTINE  HWIRE                                00010000
C                                                    00020000
C                                                    00030000
C                                                    00040000
C          *****                                00050000
C          FUNCTION                                00060000
C          *****                                00070000
C                                                    00080000
C                                                    00090000
C                                                    00100000
C  This subroutine sets options for the averaged equations of motion 00110003
C  and the short-periodics.  These options do not yet have an input 00120003
C  processor.                                          00130003
C                                                    00140000
C                                                    00150000
C                                                    00160000
C  /ANAVIN/ *****                                00170000
C                                                    00180000
C  Third-body averaging options.                      00190003
C                                                    00200000
C          IANGTH  0   Third-body analytical averaging theory.      00210003
C                    1   single averaging                          00220003

```

C		2	double averaging	00230003
C				00240000
C	ITIDE	O	Solid tide model (single-averaged theory	00250003
C			based on NSWC CELEST P2 high-precision	00260003
C			model).	00270003
C		1	analytical averaging	00280003
C		2	off	00290003
C				00300000
C	Double-averaged analytical third-body models.			00310003
C				00320000
C			Maximum and minimum multiples of the phase	00330003
C			angles used in the resonance model.	00340003
C				00350000
C	ISMAX	O	Maximum multiple of lambda' (limit 10)	00360003
C	ISMIN	O	Minimum multiple of lambda' (limit -10)	00370003
C				00380000
C	ITMAX	O	Maximum multiple of lambda (limit 20)	00390003
C	ITMIN	O	Minimum multiple of lambda (limit -20)	00400003
C				00410000
C			Methods of computing third-body potential	00420003
C			expansions.	00430003
C				00440000
C	NENDTH	I/O	Maximum powers of a/r or a/a'	00450003
C	MENDTH	I/O	Maximum powers of e	00460003
C				00470000
C	IRSTAR	O	Maximum powers of e' (if Newcomb operators	00480003
C			are used) or maximum d'Alembert character-	00490003
C			istics (if closed-form) in the expansions	00500003
C			for the third-body potentials.	00510003
C				00520000
C	IRFLAG	O	Method for computing third-body Hansen	00530003
C			coefficients in third-body potentials.	00540003
C		1	closed-form	00550003
C		2	Newcomb operator expansion	00560003
C				00570000
C	IMFLAG	O	Method for computing satellite Hansen	00580003
C			coefficients in third-body potentials.	00590003
C		1	closed-form	00600003
C		2	Newcomb operator expansion	00610003
C				00620000
C	IPOSDL	O	Third-body ephemeris flag.	00630003
C		0	compute position only	00640003
C		2	compute position and velocity	00650003
C				00660000
C	Numerical averaging control switches.			00670003
C				00680000
C	IDRGAV	I	Quadrature control switch for drag in averaged	00690003
C			equations of motion.	00700003
C	ISLRAV	I	Quadrature control switch for solar radiation	00710003
C			pressure in averaged equations of motion.	00720003
C				00730000
C	Second-order averaging options.			00740003
C				00750000
C	IDRDR	O	Second-order drag effects.	00760003
C		0	Iszak's J2 height correction (if on)	00770003
C		1	J2-drag	00780003
C		2	J2-drag, drag-drag	00790003
C		3	J2-drag, drag-drag, numeric drag-J2	00800003
C		4	J2 drag, drag-drag, analytic drag-J2	00810003
C		5	Iszak's J2 height correction (if on),	00820003
C			analytic drag-J2	00830003
C				00840000
C	Second-order averaging short-periodic control switches used in			00850003
C	computing the mean element rates.			00860003

C			00870000
C	JSPJ2	0	Number of coefficients for the J2 short-
C			periodics.
C	JSPDRG	0	Number of coefficients for the drag short-
C			periodics.
C			00920000
C	Output options.		00930003
C			00940000
C	IORBIT	0	Write out a semianalytic orbit file. *
C			00950003
C			00960000
C			00970000
C			00980000
C	/SPINTG/	*****	00990000
C			01000000
C	Position and velocity interpolator.		01010003
C			01020003
C	INTPOS	0	Interpolate for position and velocity.
C	NPTPOS	0	Number of points in the position and velocity
C			interpolator.
C			01050003
C			01060000
C	Short-periodic coefficient interpolator		01070003
C			01080003
C	INTCOF	0	Interpolate for the short-periodic coef-
C			ficients. *
C	NPTCOF	0	Number of points in the interpolator for
C			the short-periodic coefficients.
C			01120003
C			01130000
C	Gravitational perturbation short-periodic options.		01140003
C			01150003
C	ISPBOD	0	List of bodies causing short-periodic
C			effects, including the central body.
C			01160003
C			01170003
C			01180000
C	IZONAL	0	Central body zonal harmonic short-periodic
C			option.
C		1	analytical coefficients
C		2	numerical coefficients
C		3	off
C	IMDALY	0	Central body m-daily tesseral harmonic
C			short-periodic option.
C		1	analytical coefficients
C		3	off
C	ITESS	0	Central body high-frequency tesseral
C			short-periodic option.
C		1	analytical coefficients
C		3	off
C	ITHIRD	0	Third-body short-periodic option.
C		1	analytical coefficients
C		2	numerical coefficients
C		3	off
C	IJ2J2	0	Central body J2-squared short-periodic
C			option.
C		1	analytical coefficients
C		3	off
C	IJ2MD	0	Central body J2 / m-daily short periodic
C			option.
C		1	analytical coefficients
C		3	off
C			01430003
C			01440000
C	Central body zonal harmonic expansion.		01450003
C			01460003
C	NZN	0	Maximum power of r/a
C	LZN	0	Maximum power of e
C	JZN	0	Maximum power of exp(i*L)
C	ITDZN	0	Method of computing time derivatives.
C			01500003

C		1	analytical	01510003
C		2	finite differences	01520003
C	NTDZN	0	Order of the highest time derivative.	01530003
C				01540000
C	Central body m-daily tesseral harmonic expansion.			01550003
C				01560003
C	NMD	0	Maximum power of r/a	01570003
C	MMD	0	Maximum power of exp(i*theta)	01580003
C	LMD	0	Maximum power of e	01590003
C	KMD	0	Maximum power of sin(inclin)	01600003
C	ITDMD	0	Method of computing time derivatives.	01610003
C		1	analytical	01620003
C		2	finite differences	01630003
C	NTDMD	0	Order of the highest time derivative.	01640003
C				01650000
C	Central body J2 / m-daily coupling.			01660003
C				01670003
C	NJ2MD	0	Maximum power of r/a	01680003
C	MJ2MD	0	Maximum power of exp(i*theta)	01690003
C	LJ2MD	0	Maximum power of e	01700003
C	IDRMD	0	Use drag / m-daily coupling?	01710003
C		1	yes	01720003
C		2	no	01730003
C				01740000
C	Central body high-frequency tesseral harmonic expansion.			01750003
C				01760003
C	NTS	0	Maximum power of r/a	01770003
C	MTS	0	Maximum power of exp(i*theta)	01780003
C	LTS	0	Maximum d'Alembert characteristic (maximum power	01790003
C			of e outside Hansen coefficients).	01800003
C	KTS	0	Maximum power of sin(inclin)	01810003
C	LTSHAN	0	Maximum power of e**2 in power series expansion	01820003
C			for Hansen coefficients.	01830003
C	JMINTS	0	Minimum power of exp(i*lambda)	01840003
C	JMAXTS	0	Maximum power of exp(i*lambda)	01850003
C	ITDTS	0	Method of computing time derivatives.	01860003
C		1	analytical	01870003
C		2	finite differences	01880003
C	NTDTS	0	Order of the highest time derivative.	01890003
C				01900000
C	Third body expansions.			01910003
C				01920003
C	NANGTH	0	Type of Fourier series expansion.	01930003
C		1	single expansion in F	01940003
C		2	double expansion in lambda and theta	01950003
C	NTH	0	Maximum power of a/r or a/a'	01960003
C	MMONTH	0	Maximum power of exp(i*theta) in the theta	01970003
C			(m-monthly) expansion.	01980003
C	MTESTH	0	Maximum power of exp(i*theta) in the double	01990003
C			(tesseral) expansion.	02000003
C	LTH	0	Maximum power of e	02010003
C	LEPRTH	0	Maximum power of e'	02020003
C	KTH	0	Maximum power of sin(inclin)	02030003
C	JMINTH	0	Minimum power of exp(i*F) or exp(i*lambda)	02040003
C	JMAXTH	0	Maximum power of exp(i*F) or exp(i*lambda)	02050003
C	ITDTH	0	Method of computing time derivatives.	02060003
C		1	analytical	02070003
C		2	finite differences	02080003
C	NTDTH	0	Order of the highest time derivative.	02090003
C				02100000
C	Numerical short-periodic coefficients.			02110003
C				02120003
C	IGRAV	0	Quadrature control switch for gravitational	02130003
C			perturbations.	02140003

C	IDRAG	O	Quadrature control switch for drag.	02150003
C	ISOLAR	O	Quadrature control switch for solar radiation	02160003
C			pressure.	02170003
C				02180000
C	NGRAV	O	Quadrature order for gravitational perturba-	02190003
C			tions.	02200003
C	NDRAG	O	Quadrature order for drag.	02210003
C	NSOLAR	O	Quadrature order for solar radiation pressure.	02220003
C				02230000
C	LGRAV	O	Short-periodic expansion longitude for gravi-	02240003
C			tational perturbations.	02250003
C	LDRAG	O	Short-periodic expansion longitude for drag.	02260003
C	LSOLAR	O	Short-periodic expansion longitude for solar	02270003
C			radiation pressure.	02280003
C				02290000
C	JGRAV	O	Maximum power of exp(i*lambda) for gravitational	02300003
C			perturbations.	02310003
C	JDRAG	O	Maximum power of exp(i*lambda) for drag.	02320003
C	JSOLAR	O	Maximum power of exp(i*lambda) for solar radia-	02330003
C			tion pressure.	02340003
C				02350000
C	IDGRAV	O	Method of computing time derivatives for gravi-	02360003
C			tational perturbations.	02370003
C	IDDRAG	O	Method of computing time derivatives for drag.	02380003
C	IDSOLR	O	Method of computing time derivatives for solar	02390003
C			radiation pressure.	02400003
C				02410000
C	NDGRAV	O	Order of highest time derivative for gravita-	02420003
C			tional perturbations.	02430003
C	NDDRAG	O	Order of highest time derivative for drag.	02440003
C	NDSOLR	O	Order of highest time derivative for solar	02450003
C			radiation pressure.	02460003
C				02470000
C	Print options.			02480003
C				02490003
C	KINTPV	O	Print coefficients of position and velo-	02500003
C			city interpolator. *	02510003
C	KINTCF	O	Print coefficients of interpolator for	02520003
C			short-periodic coefficients. *	02530003
C	KSP	O	Print short-periodic variations. *	02540003
C	KSPCF	O	Print coefficients of short-periodic vari-	02550003
C			ations. *	02560003
C				02570000
C				02580000
C				02590000
C	/SPREAL/		*****	02600000
C				02610000
C	Position and velocity interpolator.			02620003
C				02630003
C	PVSTEP	O	Nominal interval between interpolator points.	02640003
C				02650000
C	Short-periodic coefficient interpolator.			02660003
C				02670003
C	SPSTEP	O	Nominal interval between interpolator points.	02680003
C				02690000
C	Time steps for numerical time derivatives.			02700003
C				02710003
C	DTCENT	O	Time step for analytical central-body	02720003
C			spherical harmonic model.	02730003
C	DTHIR	O	Time steps for analytical third-body	02740003
C			models.	02750003
C	DTGRAV	O	Time step for numerical gravitational	02760003
C			perturbation model.	02770003
C	DTDRAG	O	Time step for atmospheric drag.	02780003

```

C          DTSOLR  O    Time step for solar radiation pressure.          02790003
C                                                                02800000
C                                                                02810000
C                                                                02820000
C  /SWITCH/ *****02830000
C                                                                02840000
C          IBODY   I    Array of bodies used by averaged equations of    02850003
C                               motion.                                02860003
C          INDEG   I    degree of central body spherical harmonic field.02870003
C          INORD   I    order of central body spherical harmonic field. 02880003
C                                                                02890000
C                                                                02900000
C                                                                02910000
C  /THRRES/ *****02920000
C                                                                02930000
C          ISRES   O    List of double-averaged third-body resonance    02940003
C          ITRES   O    frequencies for each third body.  There can be  02950003
C                               up to 20 frequencies for each of two third 02960003
C                               bodies.                                02970003
C                                                                02980000
C                               ISRES   third-body mean longitude multiple 02990003
C                               ITRES   satellite mean longitude multiple 03000003
C                                                                03010000
C          NUMRES  O    Number of double-averaged third-body resonance 03020003
C                               frequencies for each third body.         03030003
C                                                                03040000
C                                                                03050000
C                                                                03060000
C          *          1 = Yes          2 = No                          03070003
C                                                                03080003
C                                                                03090003
C                                                                03100003
C ***** HISTORY *****03110003
C                                                                03120003
C                                                                03130003
C                                                                03140003
C          VERSION: January 1987                                     03150003
C          Fortran subroutine for the IBM 3090.                    03160003
C                                                                03170003
C          ANALYSIS                                               03180003
C          Andrew J. Green          -- U. S. Army                  03190003
C          (original version)                                             03200003
C          Leo W. Early, Jr.        -- Charles Stark Draper Laboratory 03210003
C          (current version)                                             03220003
C                                                                03230003
C          PROGRAMMER                                             03240003
C          Andrew J. Green          -- U. S. Army                  03250003
C          (original version)                                             03260003
C          Leo W. Early, Jr.        -- Charles Stark Draper Laboratory 03270003
C          (current version)                                             03280003
C                                                                03290000
C          MODIFIER          FEB 1993
C          Daniel J. Fonte, Jr.    -- Charles Stark Draper Laboratory
C
C          1) Included SPREAL.CMN
C
C                                                                03300000
C                                                                03310000
C ***** DECLARATIONS *****03320000
C                                                                03330000
C                                                                03340000
C                                                                03350000
C          IMPLICIT          DOUBLE PRECISION (A-H,O-Z)             03360000
C                                                                03370000

```


C		Coefficient interpolator.		03950003
C				03960000
	EQUIVALENCE	(INTCOF	, ISPINT (6)), 03970000
*		(NPTCOF	, ISPINT (7)), 03980000
				03990000
C		Gravitational perturbations.		04000003
C				04010000
C	EQUIVALENCE	(ISPBOD (1)	, ISPINT (14)), 04020000
	EQUIVALENCE	(IZONAL	, ISPINT (23)), 04030000
*		(IMDALY	, ISPINT (24)), 04040000
*		(ITESS	, ISPINT (25)), 04050000
*		(ITHIRD	, ISPINT (26)), 04060000
*		(IJ2J2	, ISPINT (27)), 04070000
*		(IJ2MD	, ISPINT (174)), 04080000
				04090000
C		Central body zonal harmonics.		04100003
C				04110000
C	EQUIVALENCE	(NZN	, ISPINT (28)), 04120000
*		(LZN	, ISPINT (29)), 04130000
*		(JZN	, ISPINT (30)), 04140000
*		(ITDZN	, ISPINT (31)), 04150000
*		(NTDZN	, ISPINT (32)), 04160000
				04170000
C		Central body m-daily tesseral harmonics.		04180003
C				04190000
C	EQUIVALENCE	(NMD	, ISPINT (33)), 04200000
*		(MMD	, ISPINT (34)), 04210000
*		(LMD	, ISPINT (35)), 04220000
*		(KMD	, ISPINT (36)), 04230000
*		(ITDMD	, ISPINT (37)), 04240000
*		(NTDMD	, ISPINT (38)), 04250000
				04260000
C		Central body J2 / m-daily coupling.		04270003
C				04280000
C	EQUIVALENCE	(NJ2MD	, ISPINT (171)), 04290000
*		(MJ2MD	, ISPINT (172)), 04300000
*		(LJ2MD	, ISPINT (173)), 04310000
*		(IDRMD	, ISPINT (175)), 04320000
				04330003
C		Central body high-frequency tesseral harmonics.		04340003
C				04350000
C	EQUIVALENCE	(NTS	, ISPINT (39)), 04360000
*		(MTS	, ISPINT (40)), 04370000
*		(LTS	, ISPINT (41)), 04380000
*		(LTSHAN	, ISPINT (181)), 04390003
*		(KTS	, ISPINT (42)), 04400000
*		(JMINTS	, ISPINT (43)), 04410000
*		(JMAXTS	, ISPINT (44)), 04420000
*		(ITDTS	, ISPINT (45)), 04430000
*		(NTDTS	, ISPINT (46)), 04440000
				04450000
C		Third bodies.		04460003
C				04470000
C	EQUIVALENCE	(NANGTH (1)	, ISPINT (47)), 04480000
*		(NTH (1)	, ISPINT (55)), 04490000
*		(MMONTH (1)	, ISPINT (63)), 04500000
*		(MTESTH (1)	, ISPINT (71)), 04510000
*		(LTH (1)	, ISPINT (79)), 04520000
*		(LEPRTH (1)	, ISPINT (87)), 04530000
*		(KTH (1)	, ISPINT (95)), 04540000
*		(JMINTH (1)	, ISPINT (103)), 04550000
*		(JMAXTH (1)	, ISPINT (111)), 04560000
*		(ITDTH (1)	, ISPINT (119)), 04570000
*		(NTDTH (1)	, ISPINT (127)), 04580000


```

C
ITIDE (1) = 2 05330000
ITIDE (2) = 2 05340000
ITIDE (3) = 2 05350000
05360000
C 05370000
C 05380000
C 05390000
C ***** THIRD-BODY ***** 05400000
C ***** DOUBLE AVERAGING ***** 05410000
C 05420000
C If both lunar and solar perturbations are on, the 05430003
C first elements of IANGTH, ... ,ISMIN are for 05440003
C the Moon and the second elements are for for the 05450003
C Sun. If the NCBODY card is used in the control 05460003
C deck, care should be exercised in setting these 05470003
C indicators. 05480003
C 05490000
C 05500000
C 05510000
C Third-body analytical averaging theory. 05520003
C 05530000
C IANGTH (1) = 1 05540000
C IANGTH (2) = 1 05550000
C 05560000
C Maximum powers of a/r or a/a'. 05570003
C 05580000
C IF (IANGTH (1) .EQ. 2) NENDTH (1) = 8 05590000
C IF (IANGTH (2) .EQ. 2) NENDTH (2) = 4 05600000
C 05610000
C Maximum powers of e. 05620003
C 05630000
C IF (IANGTH (1) .EQ. 2) MENDTH (1) = 4 05640000
C IF (IANGTH (2) .EQ. 2) MENDTH (2) = 4 05650000
C 05660000
C Maximum powers of e'. 05670003
C 05680000
C IRSTAR (1) = 1 05690000
C IRSTAR (2) = 1 05700000
C 05710000
C Maximum and minimum multiples of lambda for 05720003
C resonance. 05730003
C 05740000
C ITMAX (1) = 0 05750000
C ITMIN (1) = 0 05760000
C 05770000
C ITMAX (2) = 0 05780000
C ITMIN (2) = 0 05790000
C 05800000
C Maximum and minimum multiples of lambda' for 05810003
C resonance. 05820003
C 05830000
C ISMAX (1) = 0 05840000
C ISMIN (1) = 0 05850000
C 05860000
C ISMAX (2) = 0 05870000
C ISMIN (2) = 0 05880000
C 05890000
C Third-body resonance frequencies. 05900003
C 05910000
C NUMRES (1) = 0 05920000
C NUMRES (2) = 0 05930000
C 05940000
C Method for computing third-body Hansen coefficients. 05950004
C 05960000

```

```

C      IRFLAG   =   2                               05970000
C                                                     05980000
C      Method for computing satellite Hansen coefficients. 05990004
C                                                     06000000
C      IMFLAG   =   2                               06010000
C                                                     06020000
C      Third-body emphemeris flag.                    06030003
C                                                     06040000
C      IPOS DL  =   2                               06050000
C                                                     06060000
C                                                     06070000
C                                                     06080000
C      ***** OUTPUT OPTIONS *****                06090000
C                                                     06100000
C      Semianalytic orbit file.                       06110003
C                                                     06120000
C      IORBIT   =   2                               06130000
C                                                     06140000
C                                                     06150000
C                                                     06160000
C      *****
C      SHORT-PERIODIC OPTIONS
C      *****
C                                                     06170000
C                                                     06180000
C                                                     06190000
C                                                     06200000
C                                                     06210000
C                                                     06220000
C      Position and velocity interpolator.            06230003
C                                                     06240000
C      INTPOS   =   2                               06250000
C      NP TPOS  =   3                               06260000
C      PVSTEP   =  120. D0                          06270000
C                                                     06280000
C      Short-periodic coefficient interpolator.        06290003
C                                                     06300000
C      INTCOF   =   1                               06310000
C      NP TCOF  =   3                               06320000
C      SPSTEP   =  86400. D0                          06330000
C                                                     06340000
C      Short-periodic perturbations.                  06350003
C                                                     06360000
C      IZONAL   =   1                               06370000
C      IMDALY   =   1                               06380000
C      I TESS   =   1                               06390000
C      I THIRD  =   1                               06400000
C      I J2 J2  =   1                               06410000
C      I J2 MD  =   1                               06420000
C                                                     06430000
C      Third bodies causing short-periodic perturbations. 06440003
C                                                     06450000
C      ISPBOD (1) = IBODY (1)                       06460000
C      ISPBOD (2) = IBODY (2)                       06470000
C      ISPBOD (3) = IBODY (3)                       06480000
C      ISPBOD (4) = IBODY (4)                       06490000
C      ISPBOD (5) = IBODY (5)                       06500000
C      ISPBOD (6) = IBODY (6)                       06510000
C      ISPBOD (7) = IBODY (7)                       06520000
C      ISPBOD (8) = IBODY (8)                       06530000
C      ISPBOD (9) = IBODY (9)                       06540000
C                                                     06550000
C                                                     06560000
C                                                     06570000
C      *****
C      ANALYTICAL CENTRAL-BODY SHORT-PERIODICS
C      *****
C                                                     06580000
C                                                     06590000
C                                                     06600000

```



```

C          ***** TESSERALS *****                                07250000
C                                                                 07260000
C          ----- WARNING! ----- If the eccentricity of the    07270003
C          satellite orbit is large, then the terms of the power 07280003
C          series expansion for a given Hansen coefficient        07290003
C          increase rapidly for a while, reach a maximum, and    07300003
C          then begin to decrease, eventually becoming smaller   07310003
C          than the Hansen coefficient itself. The first term    07320003
C          in the decreasing part of the expansion which is      07330003
C          smaller than the Hansen coefficient itself marks the  07340003
C          onset of convergence, and the exponent of e**2 in    07350003
C          this term can be called the "convergence index".      07360003
C                                                                 07370003
C          The value of "LTSHAN" must be greater than the       07380003
C          convergence index of each Hansen coefficient in the   07390003
C          high-frequency tesseral short-periodic model. If     07400003
C          "LTSHAN" is smaller than the biggest convergence     07410003
C          index, then the error in the high-frequency tesseral 07420003
C          short-periodic variations will be bigger than the    07430003
C          short-periodics themselves. If "LTSHAN" is           07440003
C          significantly smaller, then the error may be many     07450003
C          orders of magnitude bigger than the short-periodics. 07460003
C          If "LTSHAN" is not significantly bigger, then the    07470003
C          short-periodics will have no significant figures of   07480003
C          accuracy.                                             07490003
C                                                                 07500003
C          NTS          2          to NUMCOF
C          MTS          1          to NTS          07520003
C          LTS          0          to unknown     07530003
C          LTSHAN       0          to unknown     07540003
C          JMINTS       - NTS - LTS to JMAXTS     07550003
C          JMAXTS       JMINTS    to NTS + LTS    07560003
C                                                                 07570003
C                                                                 07580003
C                                                                 07590003
C-----
C          NTS          = INDEG                    07610005
C          MTS          = INORD                    07620005
C          LTS          = 4                       07630005
C          LTSHAN       = 2                       07640005
C          JMINTS       = - NTS - LTS              07650005
C          JMAXTS       = NTS + LTS                07660005
C          ITDTS        = 2                       07670005
C          NTDTS        = 0                       07680005
C-----
C          NTS          = INDEG                    07690005
C          MTS          = INORD                    07700005
C          LTS          = 4                       07710005
C          LTSHAN       = 2                       07720005
C          JMINTS       = - NTS - LTS              07730005
C          JMAXTS       = NTS + LTS                07740005
C          ITDTS        = 2                       07750005
C          NTDTS        = 0                       07760005
C          NTDTS        = 0                       07770005
C                                                                 07780000
C                                                                 07790000
C                                                                 07800000
C          *****
C          ANALYTICAL THIRD-BODY SHORT-PERIODICS 07810000
C          *****                                07820000
C          *****                                07830000
C                                                                 07840000
C                                                                 07850000
C                                                                 07860000
C          ***** MOON *****                    07870000
C                                                                 07880000

```

```

C           Single or double averaging?                                07890003
C                                                                 07900000
C   NANGTH (1) = 1                                                    07910000
C                                                                 07920000
C           ===== Single =====                                07930003
C                                                                 07940000
C           NTH                2   to   20                            07950002
C           JMAXTH             1   to   NTH + 1                        07960001
C           LTH                 0   to   NTH + JMAXTH                 07970001
C                                                                 07980000
C           IF (NANGTH (1) .EQ. 1) THEN                               07990000
C -----
C           NTH (1) = 8                                               08000005
C           JMAXTH (1) = NTH (1) + 1                                  08010005
C           LTH (1) = NTH (1) + JMAXTH (1)                           08020005
C           ITDTH (1) = 2                                             08030005
C           NTDTH (1) = 0                                             08040005
C -----
C           NTH (1) = 8                                               08050005
C           JMAXTH (1) = NTH (1) + 1                                  08060005
C           LTH (1) = NTH (1) + JMAXTH (1)                           08070005
C           ITDTH (1) = 2                                             08080005
C           NTDTH (1) = 0                                             08090005
C           ITDTH (1) = 2                                             08100005
C           NTDTH (1) = 0                                             08110005
C           ITDTH (1) = 2                                             08120000
C           NTDTH (1) = 0                                             08130003
C           ===== Double =====                                08140000
C           NTH      GE  2           NTH      LE  21                    08150000
C           MMONTH   GE  0           MMONTH   LE  NTH                    08160000
C           MTESTH   GE  0           MTESTH   LE  NTH                    08170000
C           LTH      GE  0           LTH      LE  20                    08180000
C           LEPRTH   GE  0           LEPRTH   LE  10                    08190000
C           JMINTH   LE  JMAXTH                                           08200000
C                                                                 08210000
C           ELSE                                                       08220000
C -----
C           NTH (1) = 8                                               08230005
C           LTH (1) = 4                                               08240005
C           MMONTH (1) = NTH (1)                                       08250005
C           MTESTH (1) = NTH (1)                                       08260005
C           LEPRTH (1) = 2                                             08270005
C           JMINTH (1) = - NTH (1) - LTH (1)                            08280005
C           JMAXTH (1) = NTH (1) + LTH (1)                              08290005
C           ITDTH (1) = 2                                             08300005
C           NTDTH (1) = 0                                             08310005
C -----
C           NTH (1) = 8                                               08320005
C           LTH (1) = 4                                               08330005
C           MMONTH (1) = NTH (1)                                       08340005
C           MTESTH (1) = NTH (1)                                       08350005
C           LEPRTH (1) = 2                                             08360005
C           JMINTH (1) = - NTH (1) - LTH (1)                            08370005
C           JMAXTH (1) = NTH (1) + LTH (1)                              08380005
C           ITDTH (1) = 2                                             08390005
C           NTDTH (1) = 0                                             08400005
C           END IF                                                    08410005
C                                                                 08420005
C                                                                 08430000
C                                                                 08440000
C                                                                 08450000
C                                                                 08460000
C           ***** SUN *****                                       08470000
C                                                                 08480000
C           Single or double averaging?                                08490003
C                                                                 08500000
C   NANGTH (2) = 1                                                    08510000
C                                                                 08520000

```

```

C          ===== Single =====
C
C          NTH          2   to   20
C          JMAXTH      1   to   NTH + 1
C          LTH          0   to   NTH + JMAXTH
C
C          IF (NANGTH (2) .EQ. 1) THEN
C-----
C          NTH (2) = 4
C          JMAXTH (2) = NTH (2) + 1
C          LTH (2) = NTH (2) + JMAXTH (2)
C          ITDTH (2) = 2
C          NTDTH (2) = 0
C-----
C          NTH (2) = 4
C          JMAXTH (2) = NTH (2) + 1
C          LTH (2) = NTH (2) + JMAXTH (2)
C          ITDTH (2) = 2
C          NTDTH (2) = 0
C
C          ===== Double =====
C
C          NTH      GE  2          NTH      LE  21
C          MMONTH  GE  0          MMONTH  LE  NTH
C          MTESTH  GE  0          MTESTH  LE  NTH
C          LTH      GE  0          LTH      LE  20
C          LEPRTH  GE  0          LEPRTH  LE  10
C          JMINTH  LE  JMAXTH
C
C          ELSE
C-----
C          NTH (2) = 4
C          LTH (2) = 4
C          MMONTH (2) = NTH (2)
C          MTESTH (2) = NTH (2)
C          LEPRTH (2) = 2
C          JMINTH (2) = - NTH (2) - LTH (2)
C          JMAXTH (2) = NTH (2) + LTH (2)
C          ITDTH (2) = 2
C          NTDTH (2) = 0
C-----
C          NTH (2) = 4
C          LTH (2) = 4
C          MMONTH (2) = NTH (2)
C          MTESTH (2) = NTH (2)
C          LEPRTH (2) = 2
C          JMINTH (2) = - NTH (2) - LTH (2)
C          JMAXTH (2) = NTH (2) + LTH (2)
C          ITDTH (2) = 2
C          NTDTH (2) = 0
C          END IF
C
C
C          ***** PLANETS *****
C
C          ===== Single Averaging =====
C
C          NTH          2   to   20
C          JMAXTH      1   to   NTH + 1
C          LTH          0   to   NTH + JMAXTH
C
C          DO 350 I = 3,8
C-----

```

```

08530003
08540000
08550002
08560001
08570001
08580001
08590000
08600005
08610005
08620005
08630005
08640005
08650005
08660005
08670005
08680005
08690005
08700005
08710005
08720000
08730003
08740000
08750000
08760000
08770000
08780000
08790000
08800000
08810000
08820000
08830005
08840005
08850005
08860005
08870005
08880005
08890005
08900005
08910005
08920005
08930005
08940005
08950005
08960005
08970005
08980005
08990005
09000005
09010005
09020005
09030000
09040000
09050000
09060000
09070000
09080000
09090003
09100000
09110002
09120001
09130001
09140000
09150000
09160005

```

```

C      NANGTH (I) = 1      09170005
C      NTH (I) = 2      09180005
C      JMAXTH (I) = NTH (I) + 1      09190005
C      LTH (I) = NTH (I) + JMAXTH (I)      09200005
C      ITDTH (I) = 2      09210005
C      NTDTH (I) = 0      09220005
C-----
      NANGTH (I) = 1      09240005
      NTH (I) = 2      09250005
      JMAXTH (I) = NTH (I) + 1      09260005
      LTH (I) = NTH (I) + JMAXTH (I)      09270005
      ITDTH (I) = 2      09280005
      NTDTH (I) = 0      09290005
350 CONTINUE      09300000
C      09310000
C      09320000
C      09330000
C      *****      09340000
C      NUMERICAL SHORT-PERIODICS      09350000
C      *****      09360000
C      09370000
C      09380000
C      09390000
C      Quadrature order control switches.      09400003
C      09410000
C-----
C      IDRAG = IDRAGV      09430005
C      ISOLAR = ISLRAV      09440005
C-----
      IDRAG = IDRAGV      09460005
      ISOLAR = ISLRAV      09470005
C      09480000
C      Quadrature order switches.      09490003
C      09500000
C-----
C      NGRAV = 7      09510005
C      NDRAG = 7      09520005
C      NSOLAR = 7      09530005
C-----
      NGRAV = 7      09540005
      NDRAG = 7      09550005
      NSOLAR = 7      09560005
C      09570005
C      09580005
C      09590000
C      Short-periodic expansion longitudes.      09600003
C      09610000
C-----
C      LGRAV = 1      09620005
C      LDRAG = 1      09630005
C      LSOLAR = 1      09640005
C-----
      LGRAV = 1      09650005
      LDRAG = 1      09660005
      LSOLAR = 1      09670005
C      09680005
C      09690005
C      09700000
C      Maximum frequencies.      09710003
C      09720000
C-----
C      JGRAV = 6      09730005
C      JDRAG = 6      09740005
C      JSOLAR = 6      09750005
C-----
      JGRAV = 6      09760005
      JDRAG = 6      09770005
      JSOLAR = 6      09780005
C      09790005
C      09800005

```



```

C      (2-9)                THIRD BODIES
C  ANGVEL  9                ANGULAR VELOCITIES OF PERTURBING BODIES
C                                ABOUT THE ORIGIN OF THE COORDINATE SYSTEM.
C
C      TIME STEPS FOR NUMERICAL TIME DERIVATIVES USED TO COMPUTE
C      TIME-DEPENDENT SHORT-PERIODIC COEFFICIENTS.
C
C  DTCENT  1                TIME STEP FOR ANALYTICAL CENTRAL-BODY
C                                SPHERICAL HARMONIC MODEL.
C  DTTHIR  8                TIME STEPS FOR ANALYTICAL THIRD-BODY
C                                MODELS.
C
C  DTGRAV  1                TIME STEP FOR NUMERICAL GRAVITATIONAL
C                                PERTURBATION MODEL.
C  DTDRAG  1                TIME STEP FOR ATMOSPHERIC DRAG.
C  DTSOLR  1                TIME STEP FOR SOLAR RADIATION PRESSURE.
C
C      SHORT-PERIODIC COEFFICIENTS.
C
C  CTRUE   ***              COEFFICIENTS OF TRUE LONGITUDE EXPANSION.
C  STRUE   ***
C
C  CECCEN  ***              COEFFICIENTS OF ECCENTRIC LONGITUDE EXPAN-
C  SECCEN  ***              SION.
C
C  CLAMDA  ***              COEFFICIENTS OF MEAN LONGITUDE EXPANSION.
C  SLAMDA  ***
C
C  CTHETA  ***              COEFFICIENTS OF THETA EXPANSIONS.
C  STHETA  ***
C
C  CDOUBL  ***              COEFFICIENTS OF LAMBDA-THETA DOUBLE EXPAN-
C  SDOUBL  ***              SIONS.
C
C  CCOEF   ***              COEFFICIENTS TO BE ADDED INTO ONE OF THE
C  SCOEF   ***              SINGLE-ANGLE EXPANSIONS.
C
C      SHORT-PERIODIC COEFFICIENT INTERPOLATOR.
C
C  SPSTEP  1                INTERVAL BETWEEN SUCCESSIVE INTERPOLATOR
C                                POINTS.
C
C  SPBEG   1                BEGINNING OF INTERPOLATION INTERVAL.
C  SPEND   1                END OF INTERPOLATION INTERVAL.
C  SPCEN   1                CENTER OF INTERPOLATION INTERVAL.
C  SPWID   1                HALF-WIDTH OF INTERPOLATION INTERVAL.
C
C  CFCTRU  ***              INTERPOLATOR COEFFICIENTS FOR TRUE LONGI-
C  CFSTRU  ***              TUDE EXPANSION.
C
C  CFCECC  ***              INTERPOLATOR COEFFICIENTS FOR ECCENTRIC
C  CFSECC  ***              LONGITUDE EXPANSION.
C
C  CFCLAM  ***              INTERPOLATOR COEFFICIENTS FOR MEAN LONGI-
C  CFSLAM  ***              TUDE EXPANSION.
C
C  CFCTHT  ***              INTERPOLATOR COEFFICIENTS FOR THETA EXPAN-
C  CFSHT   ***              SIONS.
C
C  CFCDBL  ***              INTERPOLATOR COEFFICIENTS FOR LAMBDA-
C  CFSDBL  ***              THETA DOUBLE EXPANSIONS.
C
C      SHORT-PERIODIC PHASE ANGLE INTERPOLATOR.
C

```

```

C THCOEF 36 INTERPOLATOR COEFFICIENTS FOR PERTURBING-
C BODY PHASE ANGLES.
C
C UNITS ARE KILOMETERS, SECONDS, AND RADIANS.
C
C *** SEE PARAMETER AND DIMENSION STATEMENTS WHICH FOLLOW
C
C Data Types =====
C
C Position and velocity interpolator.
C
C DOUBLE PRECISION PVSTEP
C DOUBLE PRECISION PVBEG
C DOUBLE PRECISION PVEND
C DOUBLE PRECISION PVCEN
C DOUBLE PRECISION PVWID
C DOUBLE PRECISION PCOEF
C DOUBLE PRECISION VCOEF
C
C Short-periodic variations.
C
C DOUBLE PRECISION SPVAR
C DOUBLE PRECISION DA
C DOUBLE PRECISION DH
C DOUBLE PRECISION DK
C DOUBLE PRECISION DP
C DOUBLE PRECISION DQ
C DOUBLE PRECISION DLAM
C
C Short-periodic phase angles.
C
C DOUBLE PRECISION XL
C DOUBLE PRECISION XF
C DOUBLE PRECISION XLAMDA
C DOUBLE PRECISION THETA
C DOUBLE PRECISION ANGVEL
C
C Time steps for numerical time derivatives.
C
C DOUBLE PRECISION DTCENT
C DOUBLE PRECISION DTTHIR
C DOUBLE PRECISION DTGRAV
C DOUBLE PRECISION DTDRAG
C DOUBLE PRECISION DTSOLR
C
C Short-periodic coefficients.
C
C DOUBLE PRECISION CTRUE
C DOUBLE PRECISION STRUE
C DOUBLE PRECISION CECCEN
C DOUBLE PRECISION SECCEN
C DOUBLE PRECISION CLAMDA
C DOUBLE PRECISION SLAMDA
C DOUBLE PRECISION CTHETA
C DOUBLE PRECISION STHETA
C DOUBLE PRECISION CDOUBL
C DOUBLE PRECISION SDOUBL
C DOUBLE PRECISION CCOEF
C DOUBLE PRECISION SCOEF
C

```

```

C           Short-periodic coefficient interpolator.
C
C   DOUBLE PRECISION           SPSTEP
C
C   DOUBLE PRECISION           SPBEG
C   DOUBLE PRECISION           SPEND
C   DOUBLE PRECISION           SPCEN
C   DOUBLE PRECISION           SPWID
C
C   DOUBLE PRECISION           CFCTRU
C   DOUBLE PRECISION           CFSTRU
C   DOUBLE PRECISION           CFCECC
C   DOUBLE PRECISION           CFSECC
C   DOUBLE PRECISION           CFCLAM
C   DOUBLE PRECISION           CFSLAM
C   DOUBLE PRECISION           CFCTHT
C   DOUBLE PRECISION           CFSTHT
C   DOUBLE PRECISION           CFCDBL
C   DOUBLE PRECISION           CFSDBL
C
C           Short-periodic phase angle interpolator.
C
C   DOUBLE PRECISION           THCOEF
C
C
C
C   INTEGER           FLDDIM
C   INTEGER           ECCNUM
C   INTEGER           TFDPL2
C   INTEGER           FDMIN1
C   INTEGER           TFDMI2
C   INTEGER           DUBNUM
C   INTEGER           SPINC1
C   INTEGER           SPINC2
C   INTEGER           SPINC3
C   INTEGER           SPINC4
C
C
C   Parameter Statements =====
C
C   PARAMETER           (FLDDIM = 50)
C   PARAMETER           (ECCNUM = 4)
C   PARAMETER           (TFDPL2 = (2 * FLDDIM + 2))
C   PARAMETER           (FDMIN1 = (FLDDIM - 1))
C   PARAMETER           (TFDMI2 = (2 * FLDDIM - 2))
C   PARAMETER           (DUBNUM = (FLDDIM*(2*(FLDDIM+ECCNUM)+1)))
C   PARAMETER           (SPINC1 = (4*6*TFDPL2))
C   PARAMETER           (SPINC2 = (4*6*FDMIN1))
C   PARAMETER           (SPINC3 = (4*6*TFDMI2))
C   PARAMETER           (SPINC4 = (4*6*DUBNUM))
C
C
C   Dimensions =====
C
C           Short-periodic variations.
C
C   DIMENSION           PCOEF (3, 6) , VCOEF (3, 6) , SPVAR (6) , DTTHIR (8)
C   DIMENSION           THETA (9) , ANGVEL (9) , THCOEF (36)
C
C           Short-periodic coefficients.
C
C   DIMENSION           CTRUE (6, TFDPL2) , STRUE (6, TFDPL2)
C   DIMENSION           CECCEN (6, TFDPL2) , SECCEN (6, TFDPL2)
C   DIMENSION           CLAMDA (6, FDMIN1) , SLAMDA (6, FDMIN1)

```

```

DIMENSION      CTHETA (6,TFDMI2)           ,STHETA (6,TFDMI2)
DIMENSION      CDOUBL (6,DUBNUM)          ,SDOUBL (6,DUBNUM)
DIMENSION      CCOEF  (6,TFDPL2)         ,SCOEF  (6,TFDPL2)

```

C
C
C

Short-periodic coefficient interpolators.

```

DIMENSION      CFCTRU (SPINC1)           ,CFSTRU (SPINC1)
DIMENSION      CFCECC (SPINC1)          ,CFSECC (SPINC1)
DIMENSION      CFCLAM (SPINC2)          ,CFSLAM (SPINC2)
DIMENSION      CFCTHT (SPINC3)          ,CFSTHT (SPINC3)
DIMENSION      CFCDL (SPINC4)           ,CFSDL (SPINC4)

```

C
C
C

Common Block =====

C
C
C
C
C
C
C

Position and velocity interpolator.

```

COMMON /SPREAL/          PVSTEP
COMMON /SPREAL/          PVBEG
COMMON /SPREAL/          PVEND
COMMON /SPREAL/          PVCEN
COMMON /SPREAL/          PVWID
COMMON /SPREAL/          PCOEF
COMMON /SPREAL/          VCOEF

```

C
C
C

Short-periodic variations.

```

COMMON /SPREAL/          SPVAR

```

C
C
C
C

Short-periodic phase angles.

```

COMMON /SPREAL/          XL
COMMON /SPREAL/          XF
COMMON /SPREAL/          XLAMDA
COMMON /SPREAL/          THETA
COMMON /SPREAL/          ANGVEL

```

C
C
C

Time steps for numerical time derivatives.

```

COMMON /SPREAL/          DTCENT
COMMON /SPREAL/          DTHIR
COMMON /SPREAL/          DTGRAV
COMMON /SPREAL/          DTDRA
COMMON /SPREAL/          DTSOLR

```

C
C
C

Short-periodic coefficients.

```

COMMON /SPREAL/          CTRUE
COMMON /SPREAL/          STRUE
COMMON /SPREAL/          CECCEN
COMMON /SPREAL/          SECCEN
COMMON /SPREAL/          CLAMDA
COMMON /SPREAL/          SLAMDA
COMMON /SPREAL/          CTHETA
COMMON /SPREAL/          STHETA
COMMON /SPREAL/          CDOUBL
COMMON /SPREAL/          SDOUBL
COMMON /SPREAL/          CCOEF
COMMON /SPREAL/          SCOEF

```

C

```

C           Short-periodic coefficient interpolator.
C
COMMON /SPREAL/           SPSTEP
C
COMMON /SPREAL/           SPBEG
COMMON /SPREAL/           SPEND
COMMON /SPREAL/           SPCEN
COMMON /SPREAL/           SPWID
C
COMMON /SPREAL/           CFCTRU
COMMON /SPREAL/           CFSTRU
COMMON /SPREAL/           CFCECC
COMMON /SPREAL/           CFSECC
COMMON /SPREAL/           CFCLAM
COMMON /SPREAL/           CFSLAM
COMMON /SPREAL/           CFCTHT
COMMON /SPREAL/           CFSTHT
COMMON /SPREAL/           CFCDBL
COMMON /SPREAL/           CFSDBL
C
C           Short-periodic phase angle interpolator.
C
COMMON /SPREAL/           THCOEF
C
C
C

```

[This page intentionally left blank.]

Appendix C

Output Plots

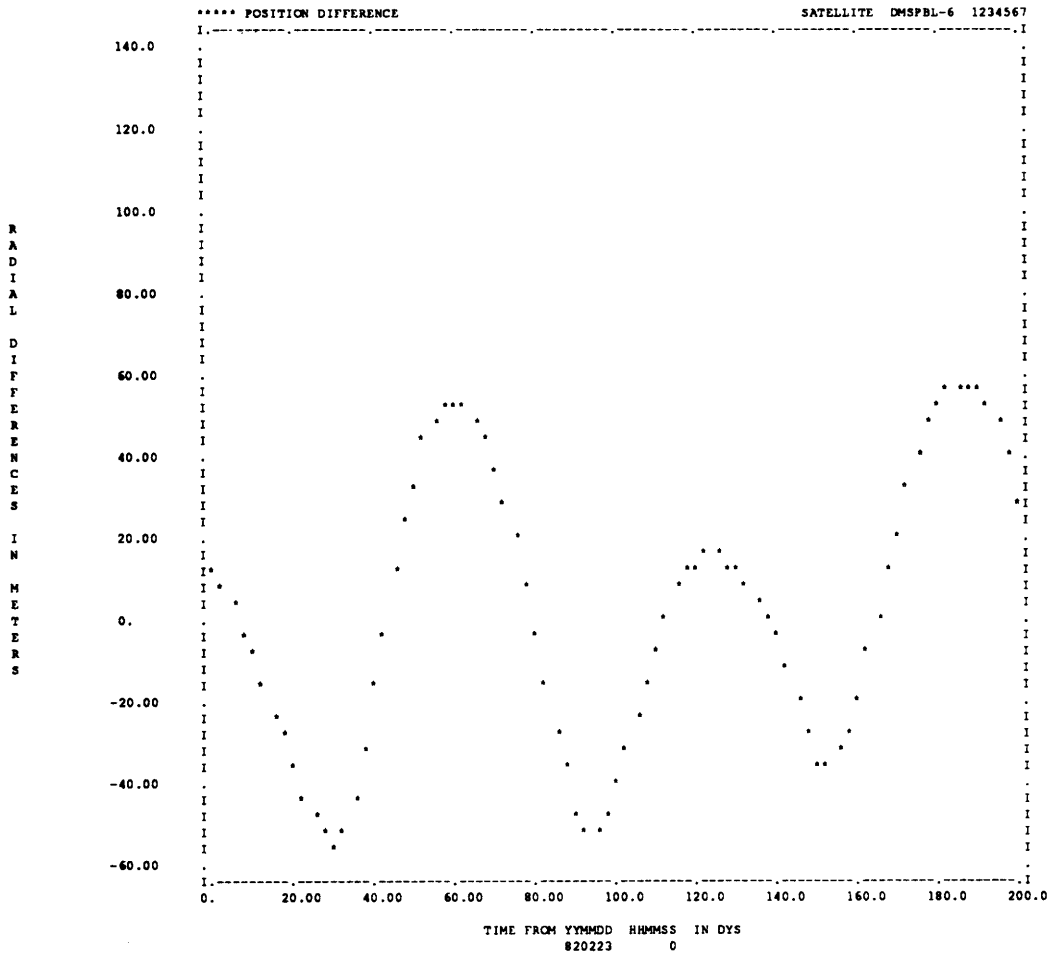
C.1 Description

As described in Chapter 5, Appendix C contains output plots corresponding to a fit of GEMT3 21x21 AOG to 50x50 AOG for the DMSP study orbit. As expected, the results of this test show that significant errors resulted from the 21x21 fit:

	POSITION RMS	VELOCITY RMS
	(km)	(km/sec)
RADIAL	3.3576D-02	1.6680D-03
CROSS TRACK	1.7800D-02	1.6002D-05
ALONG TRACK	1.6392D+00	3.4504D-05
TOTAL	1.6396D+00	1.6684D-03

Figure C.1 Recap of Figure 5.17

The first set of plots, which incorporate a normal value for J_2 , contain a visible 60 day signature:



***** POSITION DIFFERENCE

SATELLITE DMSPBL-6 1234567

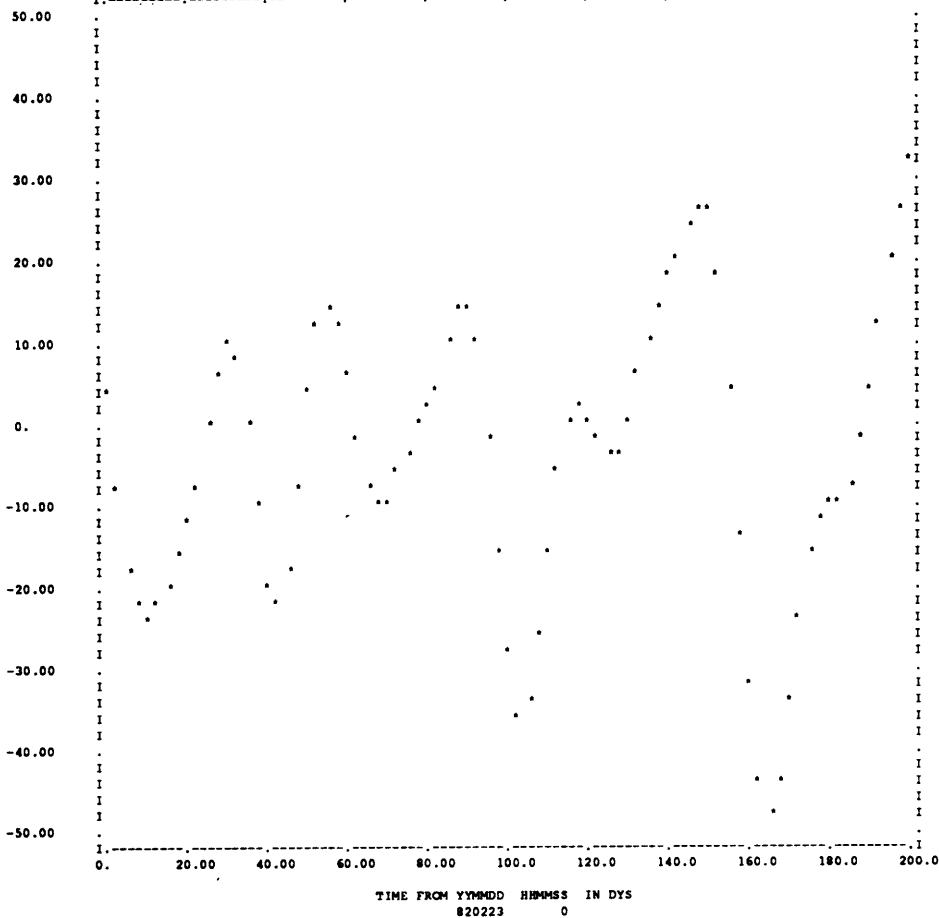
C
R
O
S
S

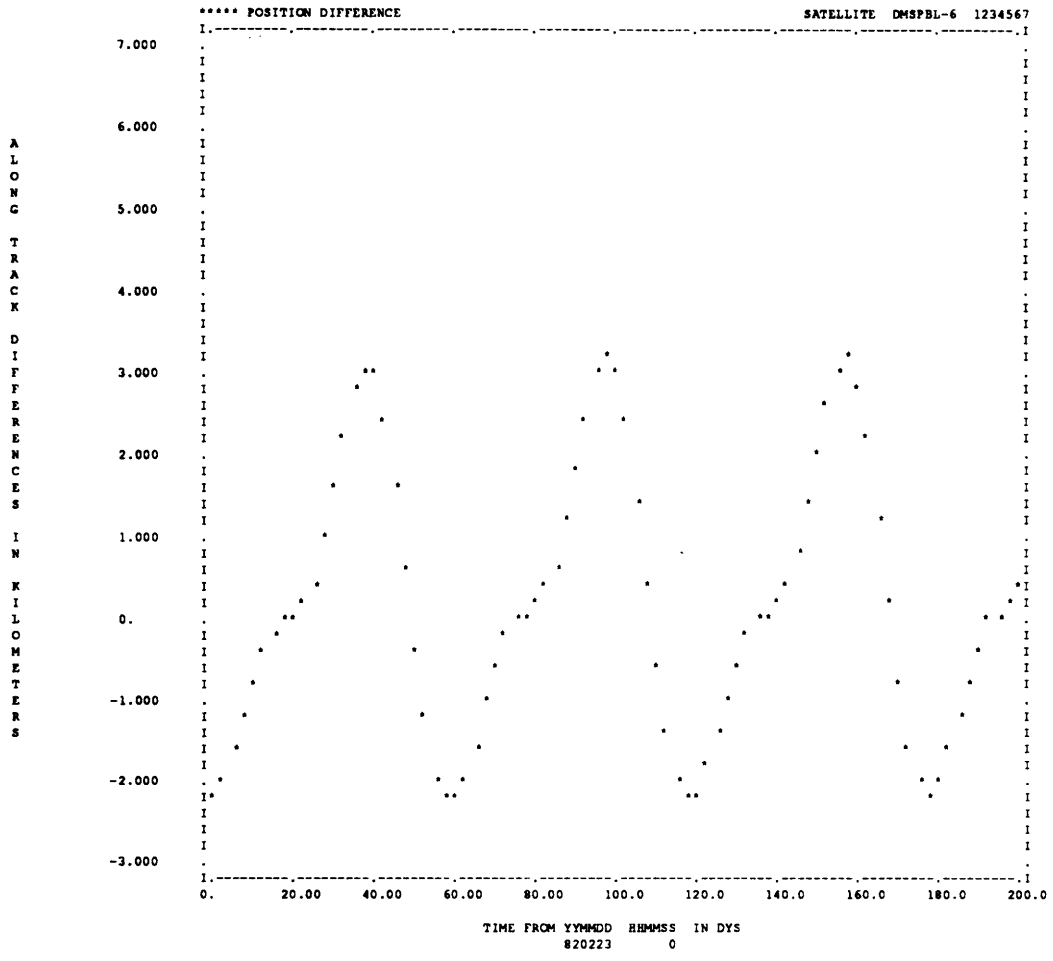
T
R
A
C
K

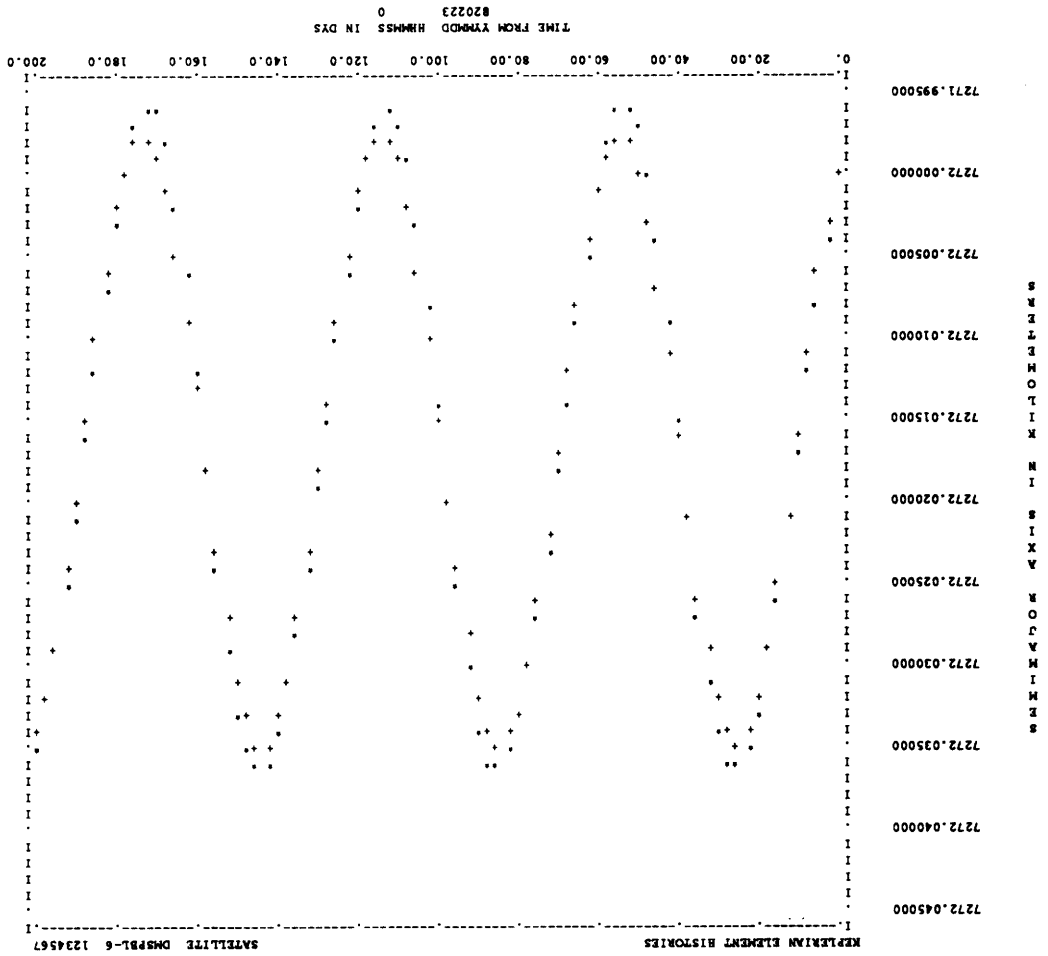
D
I
F
F
E
R
E
N
C
E
S

I
N

M
E
T
E
R
S

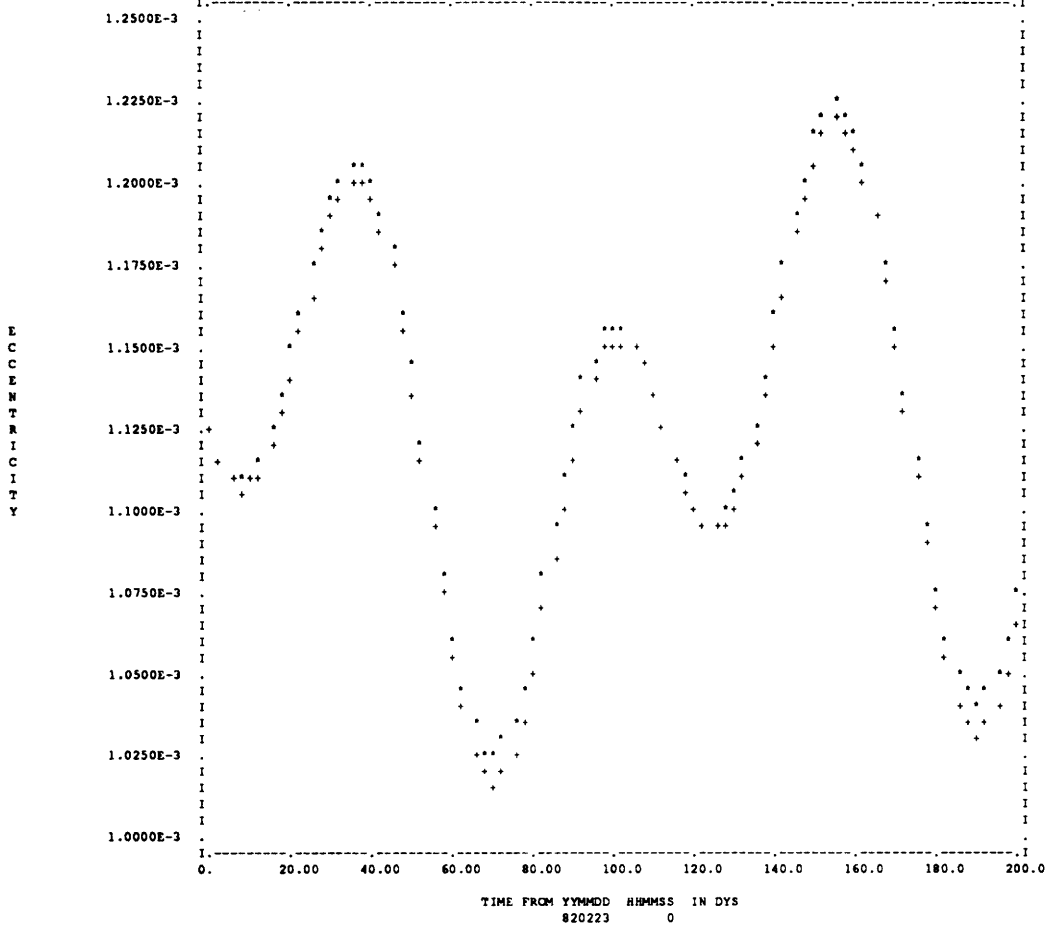


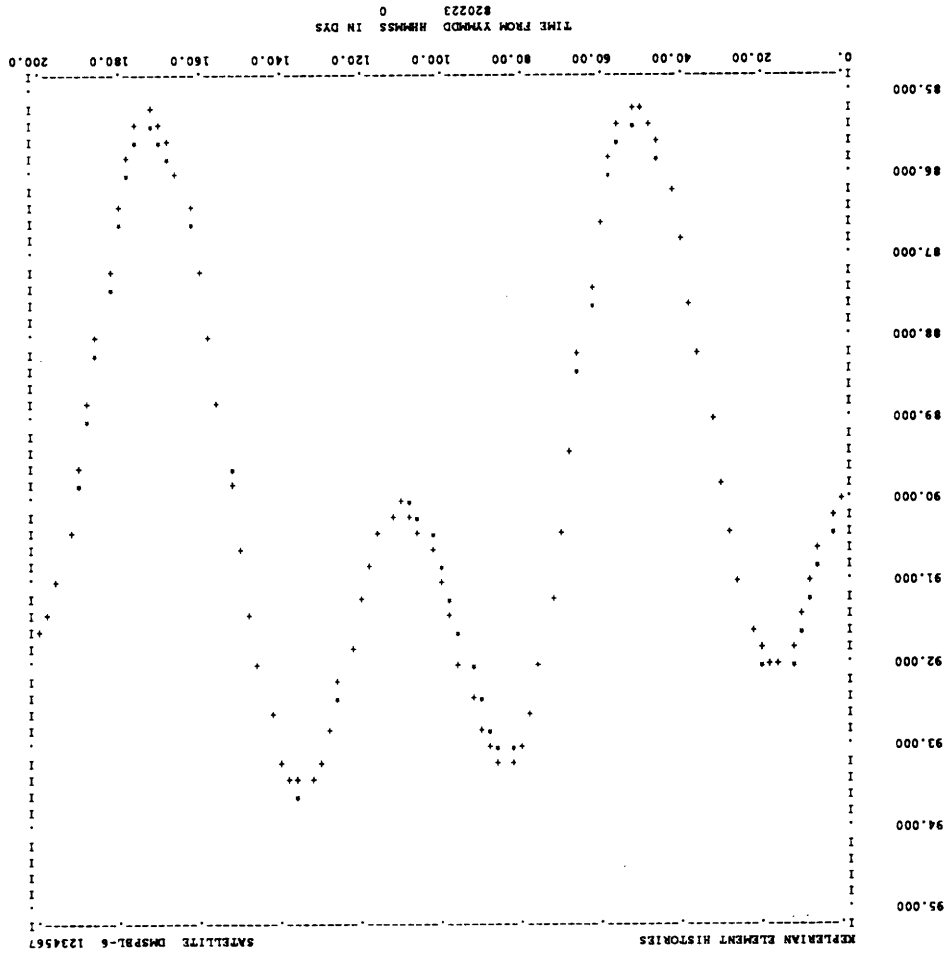




KEPLERIAN ELEMENT HISTORIES

SATELLITE DMSPBL-6 1234567



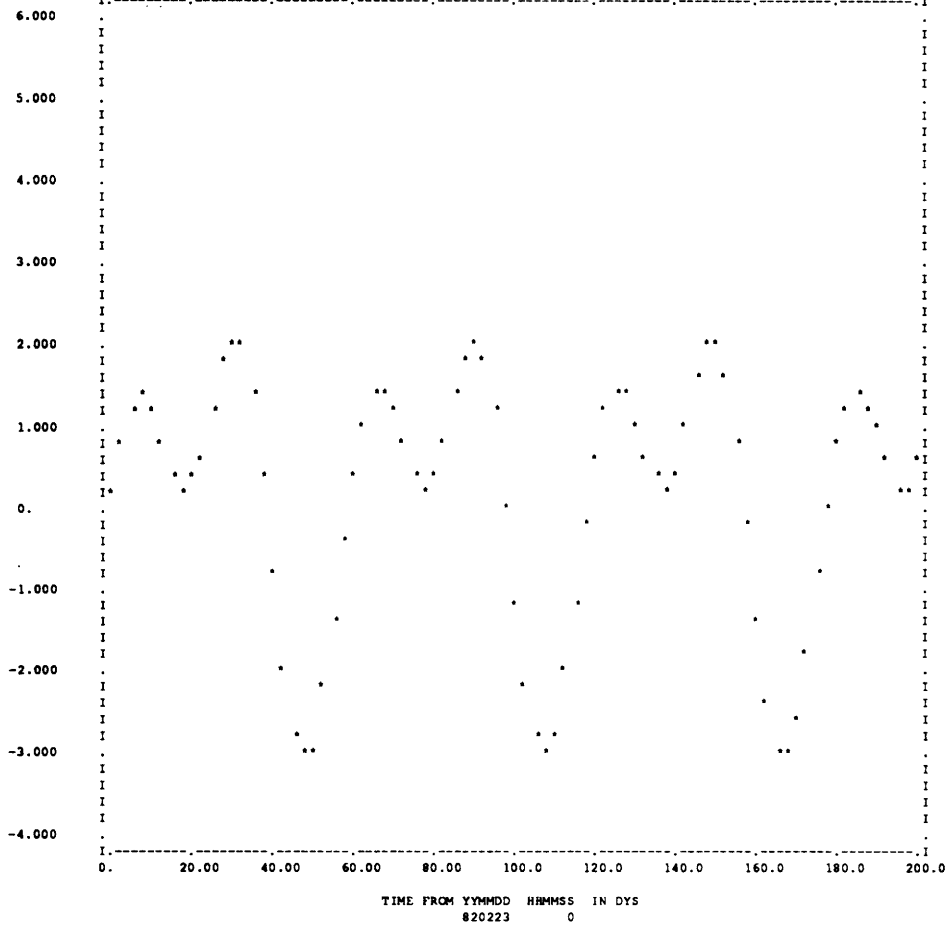


S
E
M
I
M
A
J
O
R
A
X
I
S
(
A
U)

KEPLERIAN ELEMENT DIFFERENCES

SATELLITE DMSPBL-6 1234567

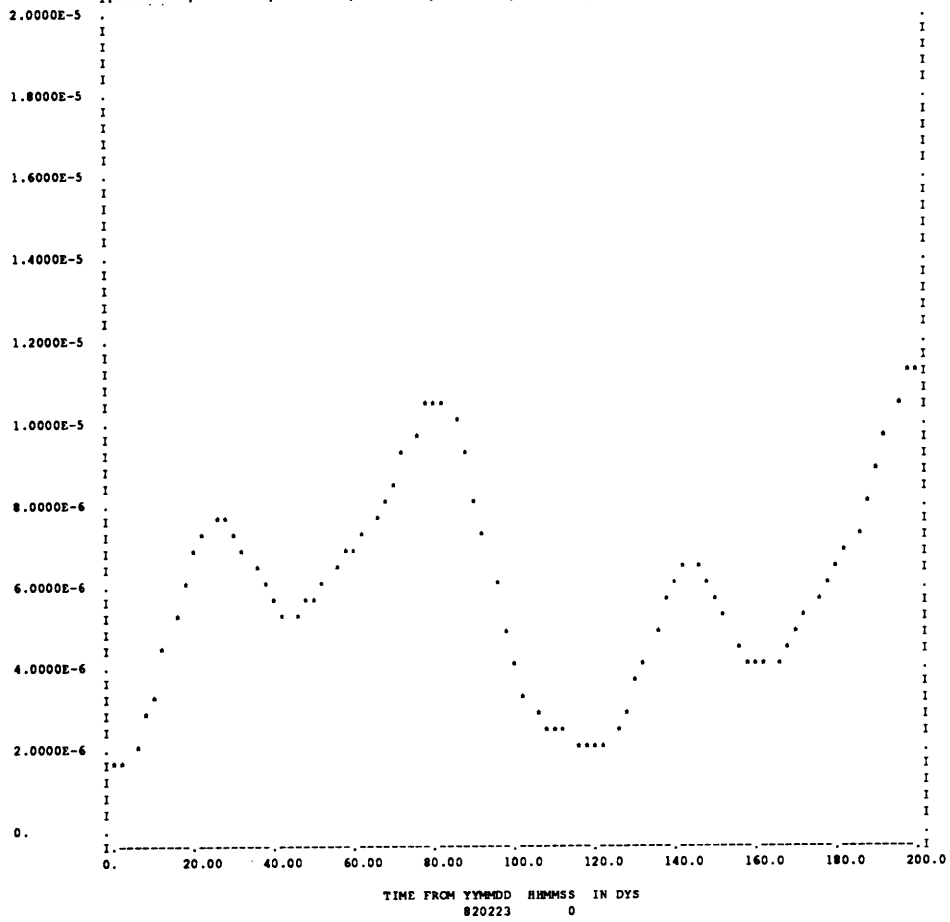
S
E
M
I
M
A
J
O
R
A
X
I
S
I
N
M
E
T
E
R
S



KEPLERIAN ELEMENT DIFFERENCES

SATELLITE DMSPBL-6 1234567

E
C
C
E
N
T
R
I
C
I
T
Y

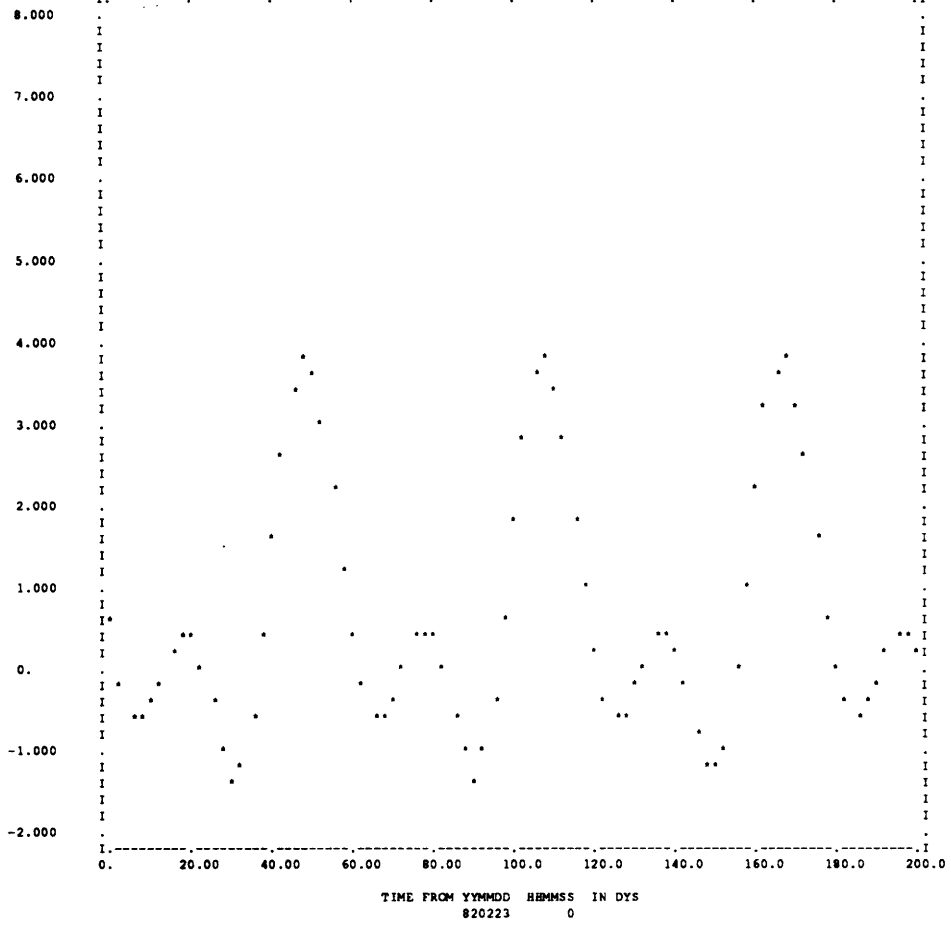


KEPLERIAN ELEMENT DIFFERENCES

SATELLITE DMSPBL-6 1234567

I
N
C
L
I
N
A
T
I
O
N

I
N
M
I
C
R
O
R
A
D
I
A
N
S



KEPLERIAN ELEMENT DIFFERENCES

SATELLITE DMSPBL-6 1234567

L
O
N
G
I
T
U
D
E

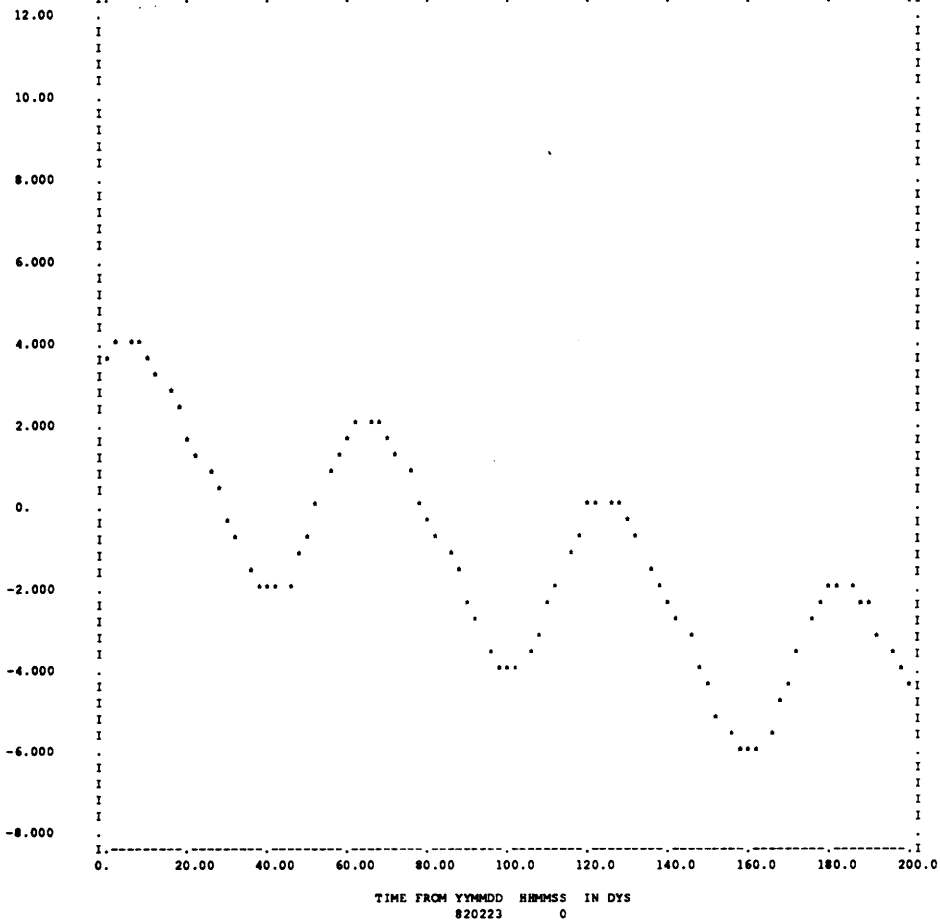
O
F

A
S
C
E
N
D
I
N
G

M
O
D
E

I
N

M
I
C
R
O
R
A
D
S



KEPLERIAN ELEMENT DIFFERENCES

SATELLITE DMSPBL-6 1234567

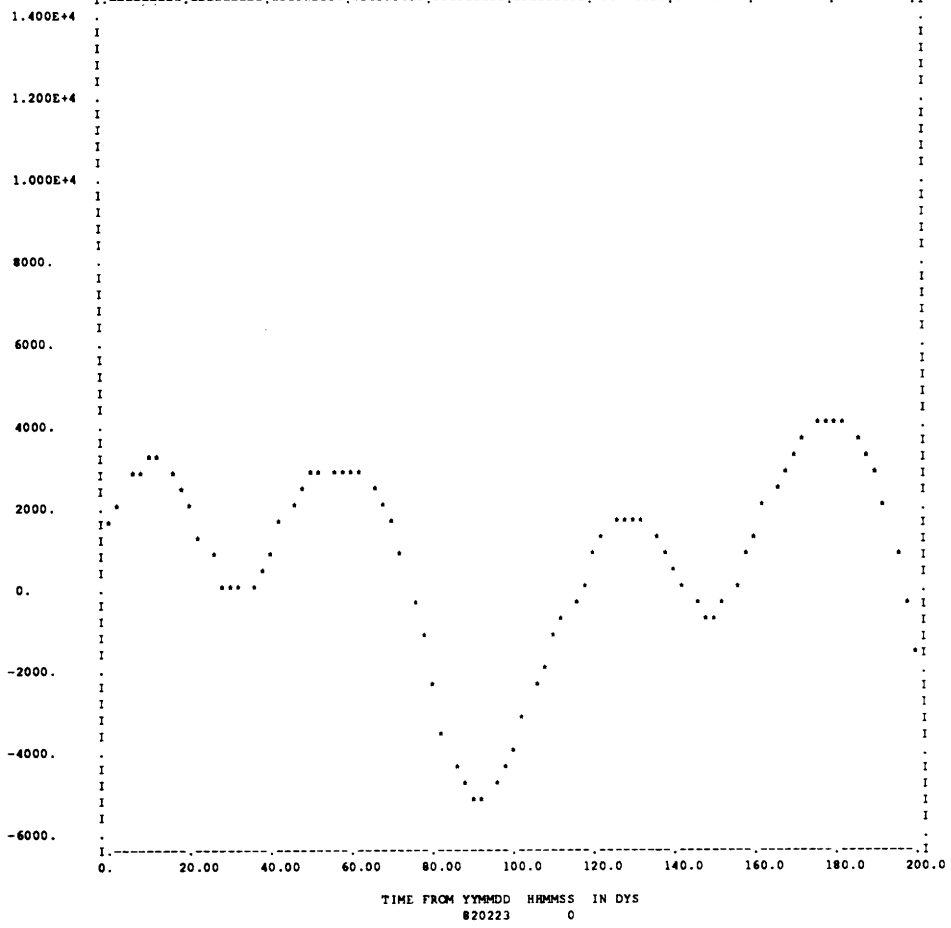
A
R
G
U
M
E
N
T

O
F

P
E
R
I
F
O
C
U
S

I
N

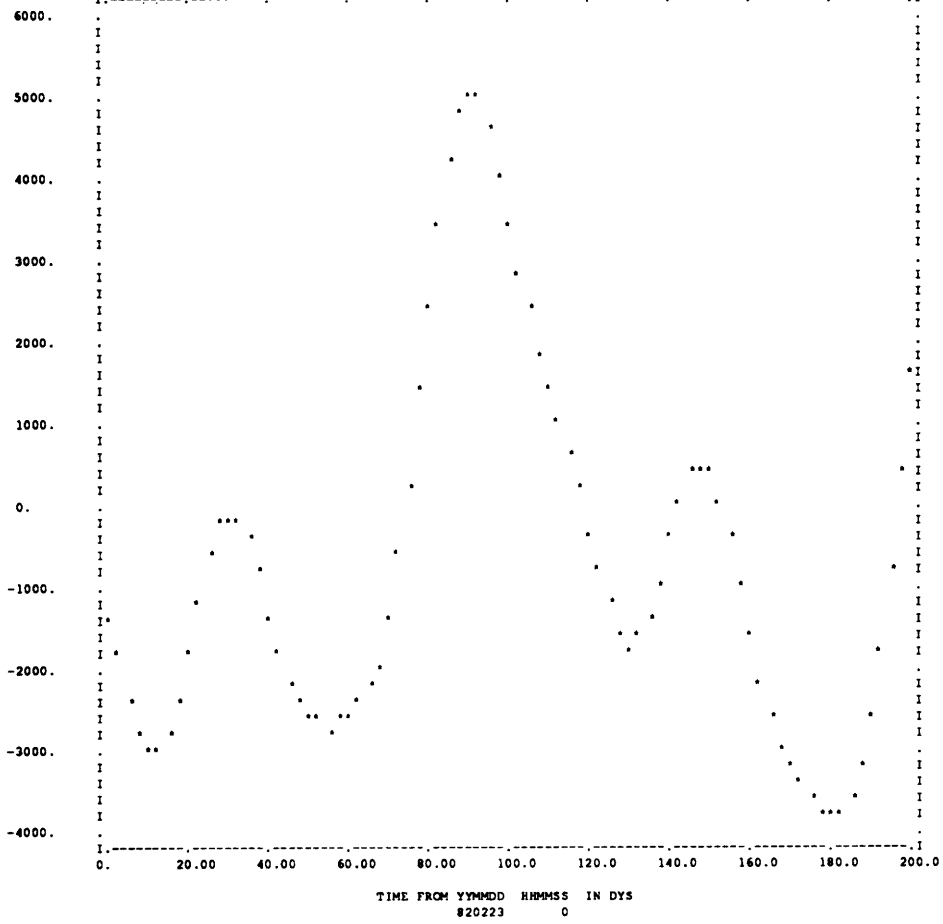
M
I
C
R
O
R
A
D
I
A
N
S



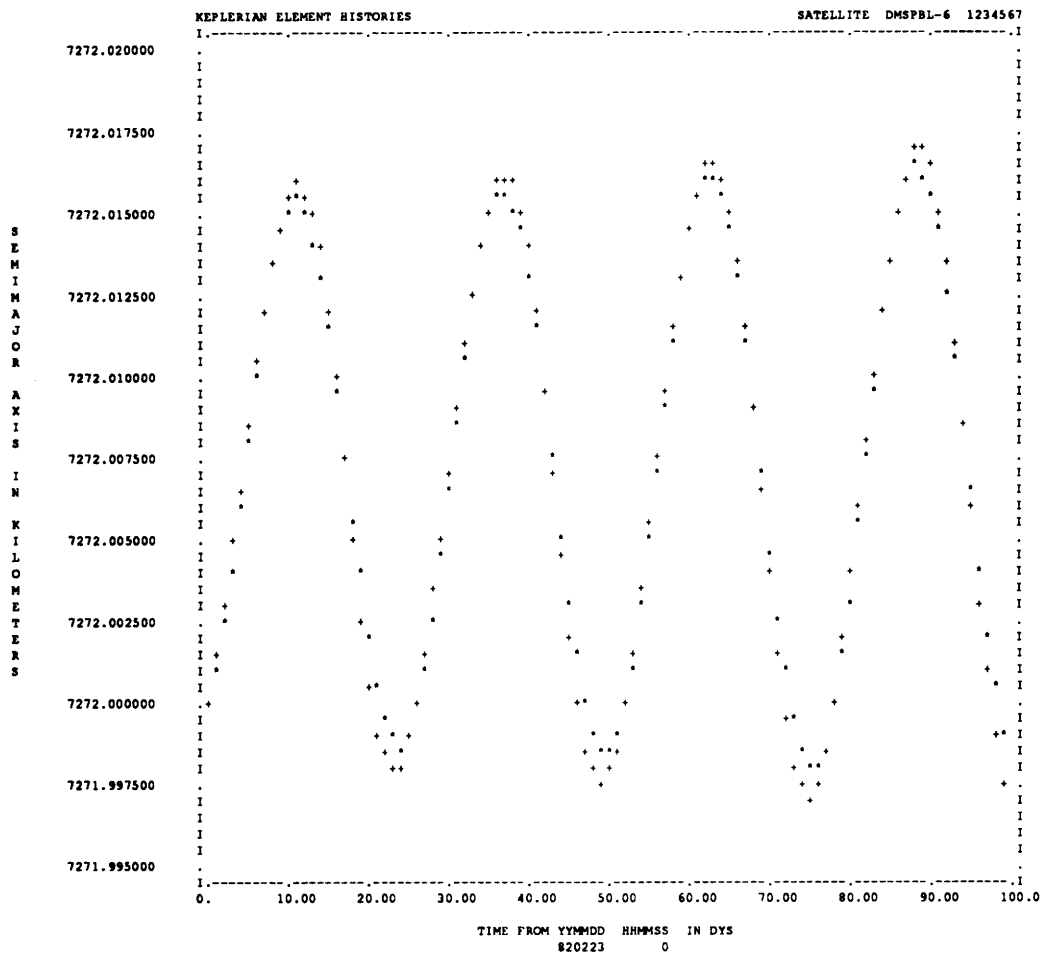
KEPLERIAN ELEMENT DIFFERENCES

SATELLITE DMSPBL-6 1234567

M
E
A
N
A
N
O
M
A
L
Y
I
N
M
I
C
R
O
R
A
D
I
A
N
S



The following plot incorporates a small value for J_2 ($1.0D-5$):



[This page intentionally left blank.]

Appendix D

Additional Software Tree Plots

D.1 Background

As described in Section 4.2.3, this appendix contains plots of routines which fall under ECSUM1, ECSUM2, ECSUM3, SNGESM, TERM, EVESM1, EVESM2, ODESM1, ODESM2. These routines are associated to the zonal short periodic model in GTDS.

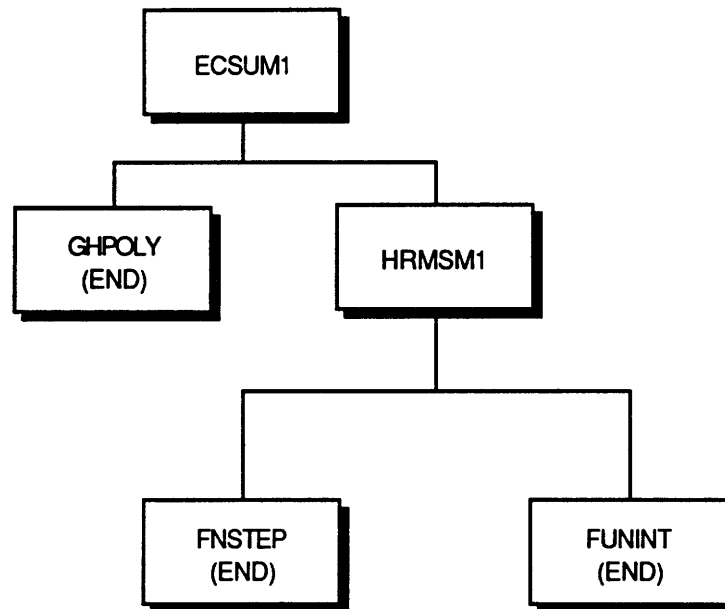


Figure D.1 Software Tree for Routines Under ECSUM1

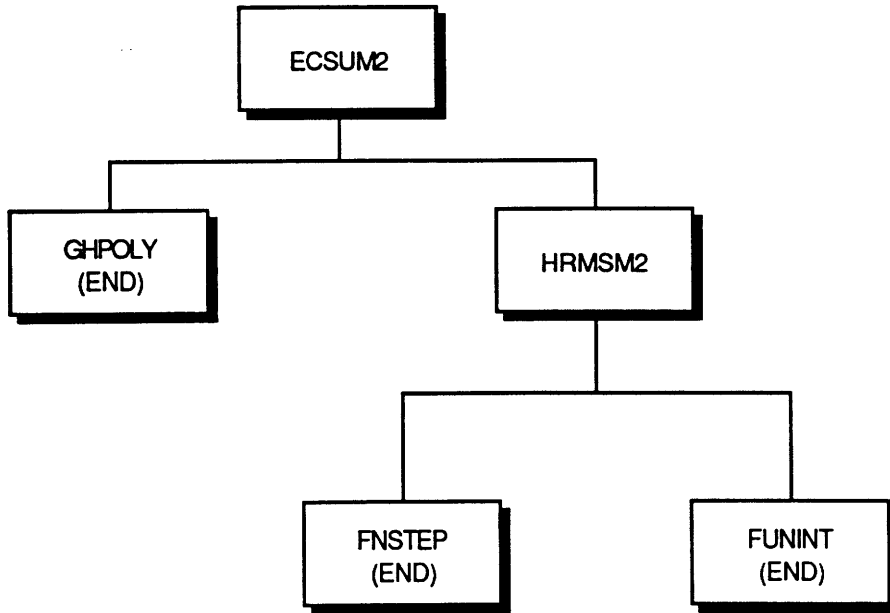


Figure D.2 Software Tree for Routines Under ECSUM2

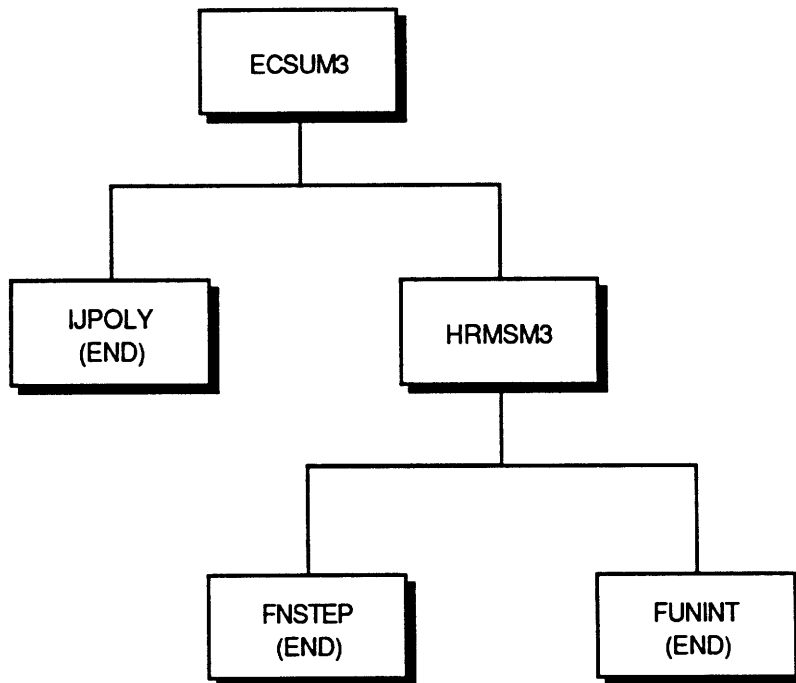


Figure D.3 Software Tree for Routines Under ECSUM3

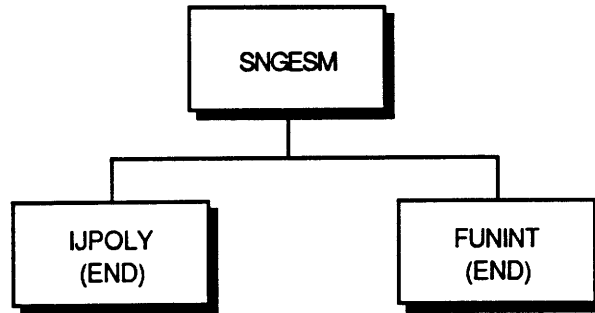


Figure D.4 Software Tree for Routines Under SNGESM

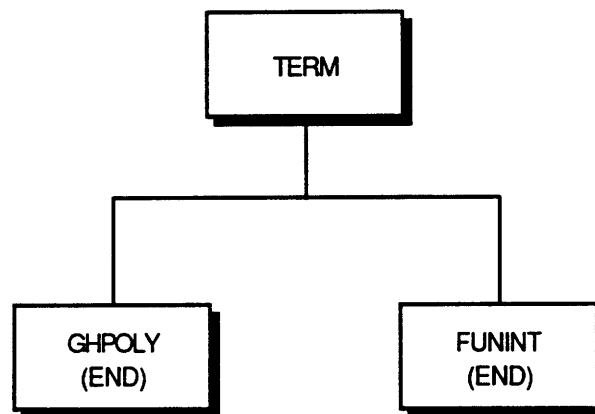


Figure D.5 Software Tree for Routines Under TERM

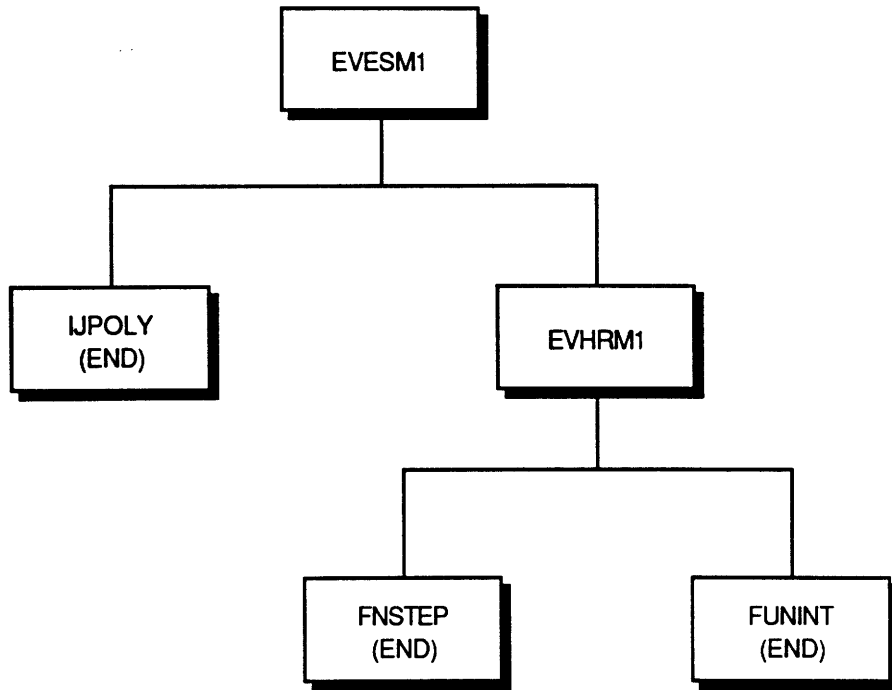


Figure D.6 Software Tree for Routines Under EVESM1

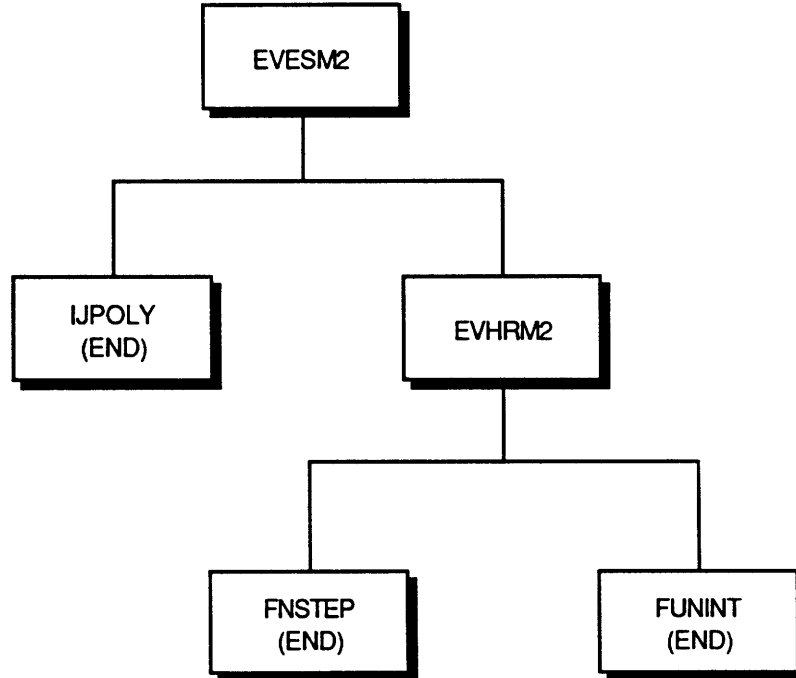


Figure D.7 Software Tree for Routines Under EVESM2

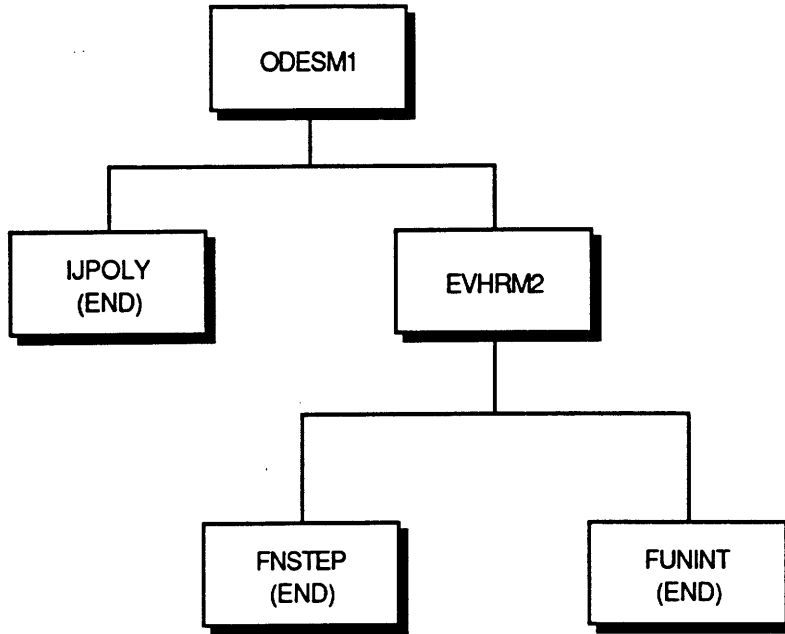


Figure D.8 Software Tree for Routines Under ODESM1

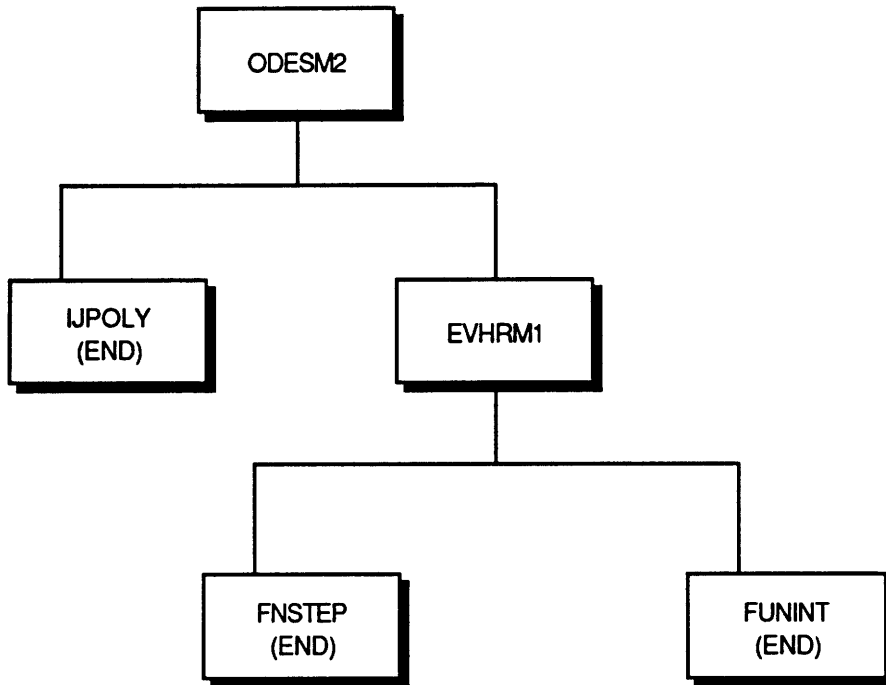


Figure D.9 Software Tree for Routines Under ODESM2

[This page intentionally left blank.]

Appendix E

Software Tools

E.1 Background

For this thesis, several software tools were developed on the BIGSIM VAX 8820. These tools are described in Table E.1:

Table E.1: Software Tools Developed For Thesis

Name	Location	Function
ACCEL.FOR	[DJF1230.GTDSUN]	•GTDS emulation which computes Cowell accelerations
ACCEL.FOR	[DJF1230.LUNN]	•Truth model which computes Cowell accelerations using the recursions from Lundberg and Schutz [36]
GTDS.EXE	[DJF1230.CHANGES.CHANGES_EXE]	•GTDS executable image which supports 50x50 gravity field models

DAN_POTENTIAL.DAT	[DJF1230]	•Permanent earth potential field file for 50x50 class gravity models (FRN47)
MOON.DAT	[DJF1230]	•Stub for permanent lunar potential field file (FRN48)
NEWCOMB.DAT	[RJP9045.NEWCOMB]	•Newcomb operator file which supports 50x50 class gravity models (FRN23)
DANWHARM.FOR	[DJF1230.50BY50. PASSCOM.GRAVDAT. PROULX]	•Places gravity models on the appropriate permanent potential field file
GCSU2.FOR	[DJF1230.50BY50. PASSCOM.GRAVDAT. PROULX]	•Puts GEMT2, GEMT3, and JGM class gravity models into form required by DANWHARM
WGSCS.FOR	[DJF1230.50BY50. PASSCOM.GRAVDAT. PROULX]	•Puts WGS84 class gravity models into form required by DANWHARM
HJAC.FOR	[DJF1230.RECURSIONS]	•Routine to perform stability testing of Jacobi polynomials
TEST.FOR	[DJF1230.RECURSIONS]	•Routine to perform stability testing of Hansen Coefficients
WRITE_NUKES.FOR	[RJP9045.FONTE]	•Routine which builds Newcomb operator file

References

- [1] Arsenault, Jeanine, Chaffee, Lois, and Kuhlman, James. *General Ephemeris Routine Formulation Document*. Technical Documentary Report ESD-TDR-64-522. 496L System Program Office, Electronic System Division, Hanscom Field. Bedford, Massachusetts. Air Force Systems Command, United States Air Force. August 1964. (Copy available from Dr. Paul Cefola, CSDL).

- [2] Bate, Mueller, White. *Fundamentals of Astrodynamics*. New York: Dover Publications, Inc. 1971.

- [3] Blitzer, Leon. *Handbook of Orbital Perturbations*. Professor of Physics, University of Arizona. Partially re-printed and used as course text for Astronautics 422 at the United States Air Force Academy (Spring 1990). Colorado Springs, Colorado. (Copy available from Department of Astronautics at the United States Air Force Academy).

- [4] Brouwer and Clemence. *Methods of Celestial Mechanics*. New York: Academic Press, Inc. 1961.

- [5] Cefola, Paul and Broucke, Roger. *On the Formulation of the Gravitational Potential in Terms of Equinoctial Variables*. AIAA Pre-print #75-9. AIAA 13th Aerospace Sciences Meeting. Pasadena, California. January, 1975.

- [6] Cefola, Paul and Proulx, Ronald. *DMSP Block 6 Autonomous Navigation Concept Verification*. Technical Report. Prepared for Hughes Aircraft Company, Space & Communications Group. Purchase Order S8-534400-XMV. The Charles Stark Draper Laboratory, Inc. May 1989. (Copy available from Dr. Paul Cefola, CSDL).
- [7] Cefola, Paul. *A Recursive Formulation for the Tesseral Disturbing Function in Equinoctial Variables*. AIAA Paper #76-839. AIAA/AAS Astrodynamics Conference. San Diego, California. August 1976.
- [8] Cefola, Paul. *Equinoctial Orbit Elements - Application to Artificial Satellite Orbits*. AIAA Paper #72-937. AIAA/AAS Astrodynamics Conference. Palo Alto, California. September 1972.
- [9] Cefola, Paul. Personal Discussion. Charles Stark Draper Laboratory, Inc. (617) 258-1787. January 1993.
- [10] Cefola, Paul. Personal Discussion. Charles Stark Draper Laboratory, Inc. (617) 258-1787. July 1992.
- [11] Cefola, Paul. *R&D GTDS Semianalytic Satellite Theory Input Processor*. Draper Intralab Memorandum to Rick Metzinger. ESD-92-582. SGI GTDS-92-001. Rev. 1. February 8, 1993.

- [12] Cefola, Paul. *Technical Comments on the Semianalytic Satellite theory and Comparison to Present Applied Methods*. Memorandum to W.G. Denhard. MEMO NO. PL-008-78-PJC. The Charles Stark Draper Laboratory. 1978. (Copy available from Dr. Paul Cefola, CSDL).
- [13] Cefola, Paul. *UNIX Work Station Version of Draper Laboratory R&D GTDS Orbit Determination Program*. Letter to Richard Farrar. ESD-92-558. The Charles Stark Draper Laboratory, Inc. December 1992. (Copy available from Dr. Paul Cefola, CSDL).
- [14] Coffey, Shannon, Deprit, Andre, and Miller, Bruce. *The Critical Inclination in Artificial Satellite Theory*. Celestial Mechanics. 39:365-406. 1986.
- [15] Collins, S.K. *Long Term Prediction of High Altitude Orbits*. Ph.D. Dissertation, Department of Aeronautics and Astronautics, Massachusetts Institute of Technology. CSDL-T--739. March 1981.
- [16] Computer Sciences Corporation. Beltsville, Maryland.
- [17] Courant, R. and Hilbert, D. *Methods of Mathematical Physics*. Volume 1. New York: Interscience Publishers, Inc. 1953.
- [18] Cox, R. P. *et al.* *The RADARSAT System*. IEEE Transactions on Geoscience and Remote Sensing. Vol. 28. No. 4. July 1990.

- [19] *Data Set Layouts for the Goddard Trajectory Determination System (GTDS)*. Prepared for National Aeronautics and Space Administration, Goddard Space Flight Center by Computer Sciences Corporation. Contract NAS 5-24300. Task Assignments 717 and 740. December 1979.
- [20] de Lafontaine, Jean. *Orbital Dynamics in a Stochastic Atmosphere and a Non spherical Gravity Field*. Doctor of Philosophy Thesis. Institute for Aerospace Studies, University of Toronto: Toronto, Canada. 1986.
- [21] Early, Leo. *R&D GTDS User Notes*. CCF IBM Mainframe file MESSAGE.TEXTF. The Charles Stark Draper Laboratory, Inc. 1980-1989. (Copy available through Dr. Paul Cefola, CSDL).
- [22] Escobal, Pedro. *Methods of Orbit Determination*. Malabar, Florida: Robert E. Krieger Publishing Company. 1965.
- [23] Fonte, Daniel. *An Introduction to Perturbation Theory*. Summary of notes made during 16.601, an advanced special topic course at the Massachusetts Institute of Technology. Department of Aeronautics and Astronautics. Spring Term, 1992. (Copy available through Daniel Fonte (216) 488-0698).
- [24] Fonte, Daniel, Proulx, Ronald, and Cefola, Paul. *Implementing a 50x50 Gravity Field Model in an Orbit Determination System*. AAS/AIAA paper to be presented at the Astrodynamics Specialist Conference. Victoria Island, British Columbia. August 1993.

- [25] Gaposchkin, Mike. Personal Discussion. Lincoln Laboratory, Millstone Hill Station. (617) 981-5539. January 1993.
- [26] *Goddard Trajectory Determination System (GTDS) Mathematical Theory*. NASA's Operational GTDS Mathematical Specification. Revision 1. Edited by Computer Sciences Corporation and NASA Goddard Space Flight Center. Contract NAS 5-31500. Task 213. July 1989.
- [27] *Goddard Trajectory Determination System (GTDS) User's Guide*. Revision 2 - Update 4. Prepared for National Aeronautics and Space Administration, Goddard Space Flight Center by Computer Sciences Corporation. Contract NAS 5-31500. Task Assignment 52 337. August 1992.
- [28] Not used.
- [29] Hoots, Felix. *Models for Propagation of Space Command Element Sets*. Spacetrack Report No. 6. USAF Space Command, United States Air Force. July 1986.
- [30] Jablonski, Carole. *Application of Semianalytic Satellite Theory to Maneuver Planning*. Master of Science Thesis, Department of Aeronautics and Astronautics, Massachusetts Institute of Technology. CSDL-T-1086. May 1991.
- [31] Kaula, William. *Theory of Satellite Geodesy*. Professor of Geophysics and Planetary Physics, UCLA. Waltham, Massachusetts: Blaisdell Publishing Company. 1966.

- [32] Kreyszig, Erwin. *Advanced Engineering Mathematics*. 6th edition. New York: John Wiley & Sons, Inc. 1988.
- [33] *LANDSAT 6 Orbit Determination and Ephemeris Generation Critical Design Review, Part 1*. L6/ODEG-91-028. Prepared For Earth Observation Satellite Company by The Charles Stark Draper Laboratory, Inc. November 1991.
- [34] *LANDSAT 6 Orbit Determination and Ephemeris Generation Task*. CSDL Proposal No. 0-823, Enclosure "B". The Charles Stark Draper Laboratory, Inc. March 1990.
- [35] Lerch, F. J. *et al.* *Geopotential Models of the Earth From Satellite Tracking, Altimeter and Surface Gravity Observations: GEM-T3 and GEM-T3S*. NASA Technical Memorandum 104555. Goddard Space Flight Center. Greenbelt, MD. January 1992.
- [36] Lundberg, John B. and Schutz, Bob E. *Recursion Formulas of Legendre Functions for Use With Nonsingular Geopotential Models*. American Institute of Aeronautics and Astronautics. Journal of Guidance, Control, and Dynamics. Volume 11, Number 1. JGCODES 11(1) 1-96(1988). ISSN 0731-5090. January-February 1988.
- [37] Marsh, J. G. *et al.* *A New Gravitational Model for the Earth from Satellite Tracking Data: GEM-T1*. Journal of Geophysical Research. VOL. 93, NO. B6. Pages 6169-6215. June 10, 1988.

- [38] McClain, Wayne. *A Recursively Formulated First-Order Semianalytic Artificial Satellite Theory Based on the Generalized Method of Averaging*. Volume I. Contract NAS 5-24300. Task Assignment 880. June 1978.
- [39] McClain, Wayne. *A Recursively Formulated First-Order Semianalytic Artificial Satellite Theory Based on the Generalized Method of Averaging*. Volume II. Contract NAS 5-24300. Task Assignment 895. May 1978.
- [40] McClain, Wayne. Personal Discussion. Charles Stark Draper Laboratory, Inc. (617) 258-1831. March 1992.
- [41] Metzinger, Richard. *Validation of the Workstation Version of R&D GTDS*. The Charles Stark Draper Laboratory, Inc. February 1993. (Copy available from Dr. Paul Cefola, CSDL).
- [42] Metzinger, Rick. Personal Discussions. Charles Stark Draper Laboratory, Inc. (617) 258-2912. July 1992 - January 1993.
- [43] Meyer, Kurt. *Lifetimes of Lunar Satellite Orbits*. Master of Science Thesis. The George Washington University. August 1991. (Copy available from Wayne McClain, CSDL).
- [44] Morrison, J. A. *Generalized Method of Averaging and the Von Zeipel Method*. Bell Telephone Laboratories, Inc. Murray Hill, N. J. Presented as Reprint 65-687 at the AIAA/ION Astrodynamics Specialist Conference. Monterey, Calif. September, 1965.

- [45] NASA/Goddard Space Flight Center. Greenbelt, Maryland.
- [46] *Programming in VAX FORTRAN*. Manual AA-D034D-TE, Digital Equipment Corporation. Maynard, Massachusetts. Software Version 4.0. September 1984.
- [47] Proulx, R. *et al.* *A Theory for the Short Periodic Motion Due to the Tesseral Harmonic Gravity Field*. AIAA Paper 81-180. AAS/AIAA Astrodynamics Specialist Conference. Lake Tahoe, Nevada. August 3-5, 1981.
- [48] Proulx, Ronald and McClain, Wayne. *Series Representations and Rational Approximations for Hansen Coefficients*. American Institute of Aeronautics and Astronautics. Journal of Guidance, Control, and Dynamics. Volume 11, Number 4. July-August 1988.
- [49] Proulx, Ronald. *Mathematical Description of the Tesseral Resonance and Resonant Harmonic Coefficient Solve-For Capabilities*. NSWC-001-15Z-RJP. The Charles Stark Draper Laboratory, Inc. April 1982.
- [50] Proulx, Ronald. *Numerical Testing of the Generalized Tesseral Resonance Capability in the GTDS R&D Program*. The Charles Stark Draper Laboratory, Inc. April 1982 (Copy available through Dr. Ronald Proulx, CSDL).
- [51] Proulx, Ronald. Personal Discussion. Charles Stark Draper Laboratory, Inc. (617) 258-1144. March 1993.
- [52] Purcell, Edward M. *Electricity and Magnetism*. Berkeley Physics Course, Volume 2. McGraw-Hill, Inc. 1985.

- [53] *Research and Development Goddard Trajectory Determination System (R&D GTDS) User's Guide*. Edited Jointly By Computer Sciences Corporation and Systems Development and Analysis Branch, Goddard Space Flight Center. July 1978.
- [54] Results obtained from Richard Farrar. The Aerospace Corporation. Los Angeles, California. (213) 336-6269. January 1993.
- [55] *System Description and User's Guide for the GTDS R&D Averaged Orbit Generator*. Prepared for NASA/Goddard Space Flight Center by Computer Sciences Corporation. Under Contract No. NAS 5-24300. Task Assignment No. 895. 1978.
- [56] *Testing, Reporting, and Maintenance Program (TRAMP) Data Set Layouts*. Prepared for NASA/Goddard Space Flight Center by Computer Sciences Corporation. May 1984.
- [57] *Testing, Reporting, and Maintenance Program (TRAMP) Maintenance Operations Guide*. Revision 1. Prepared for NASA/Goddard Space Flight Center by Computer Sciences Corporation. Contract NAS 5-27600. Task Assignment 210-751. April 1988.
- [58] *Testing, Reporting, and Maintenance Program (TRAMP) User's Guide*. Revision 1. Prepared for NASA/Goddard Space Flight Center by Computer Sciences Corporation. Contract NAS 5-31500. Task Assignment 51 334. May 1991.

- [59] *TRACE: Trajectory Analysis and Orbit Determination Program*. Volume VII: Usage Guide, Part A: Input Data. Report SAMSO-TR-71-141. Reissue B. Engineering Science Operations. The Aerospace Company. May 1974.
- [60] *TRACE66 Trajectory Analysis and Orbit Determination Program*. Volume I: General Program Objectives, Description, and Summary. Aerospace Report No. TR-0059(9320)-1. Engineering Science Operations. The Aerospace Company. August 1971.
- [61] *VAX DEC/CMS Reference Manual*. Order No. AA-L372B-TE. Operating System and Version VAX/VMS Version 4.0. Software Version VAX DEC/CMS Version 2.0. Digital Equipment Corporation. Maynard, Massachusetts. November 1984.
- [62] Wakker, K. F. *et al.* *Precise Orbit Determination for ERS-1*. ESOC Contract #5227/82/D/IM(SC). Department of Aerospace Engineering, Delft University of Technology: Delf, Netherlands. August 1983.
- [63] Wall, Larry and Schwartz, Randal. *Programming Perl*. Sebastopol, California: O'Reilly & Associates, Inc. 1992.
- [64] Wolfram, Stephen. *Mathematica: A System for Doing Mathematics by Computer*. 2nd Edition. New York: Addison-Wesley Publishing Company. 1991. (User Guide available through Addison-Wesley Publishing Company).
- [65] Wright, James. *Variation of Parameters for Definitive Geocentric Orbits*. AIAA-92-4361-CP. AIAA Conference, Hilton Head, South Carolina. 1992.

- [66] Zeis, Eric. *A Computerized Algebraic Utility for the Construction of Nonsingular Satellite Theories*. Master of Science Thesis, Department of Aeronautics and Astronautics, Massachusetts Institute of Technology. September 1978.
- [67] Green, A.J. *Orbit Determination and Prediction Processes For Low Altitude Satellites*. Ph.D. Dissertation, Department of Aeronautics and Astronautics, Massachusetts Institute of Technology. CSDL-T--703. December 1979.
- [68] Taylor, S.P. *Semianalytic Satellite Theory and Sequential Estimation*. Master of Science Thesis, Department of Aeronautics and Astronautics, Massachusetts Institute of Technology. CSDL-T-757. September 1981.